THE UNIVERSITY OF NEW SOUTH WALES
KENSINGTON, NSW AUSTRALIA 2033

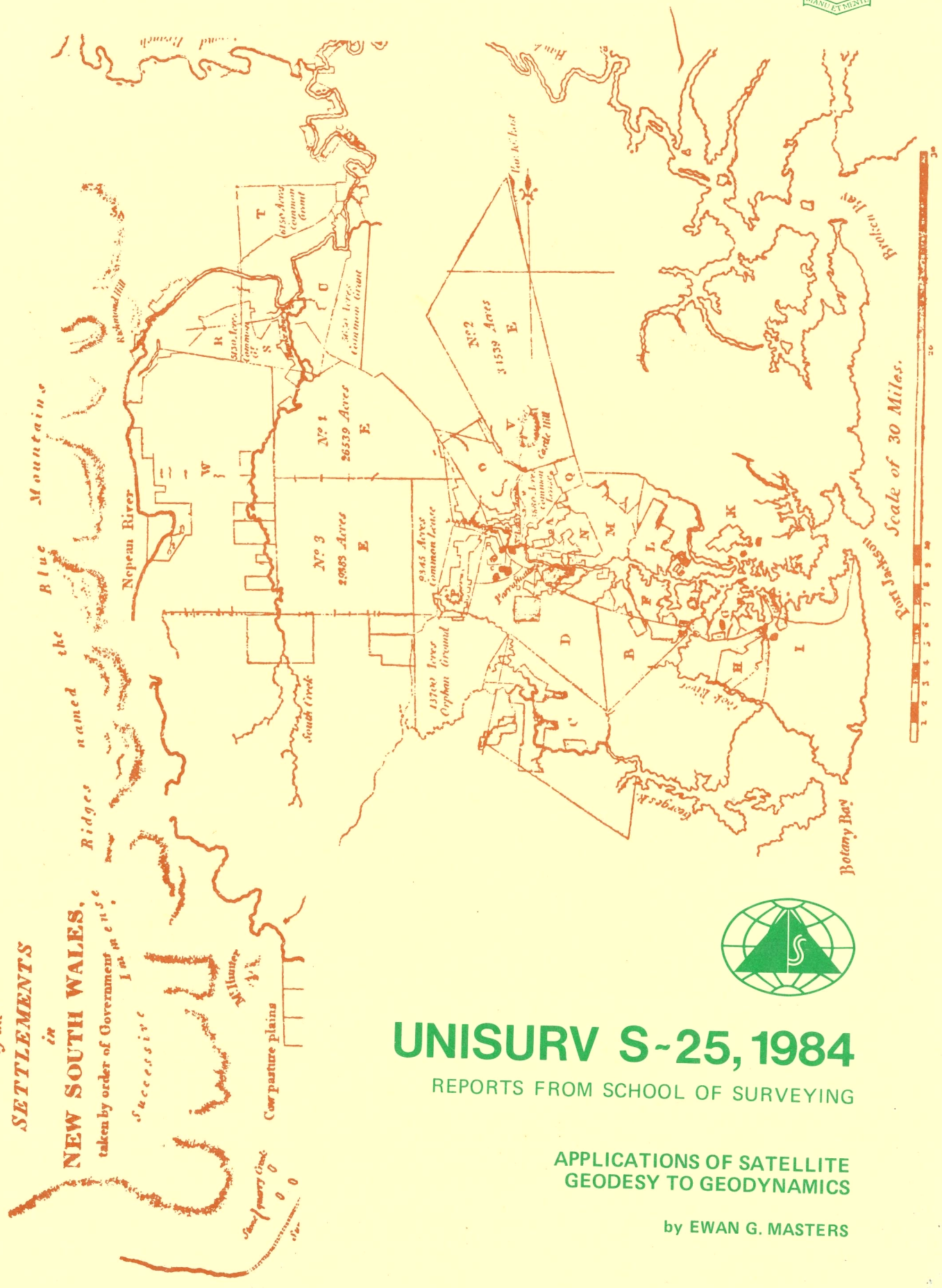

UNISURV S-25, 1984

REPORTS FROM SCHOOL OF SURVEYING

APPLICATIONS OF SATELLITE GEODESY TO GEODYNAMICS

by EWAN G. MASTERS

UNISURV REPORT S25, 1984

APPLICATIONS OF SATELLITE GEODESY TO GEODYNAMICS

by

Ewan G. Masters

Received January, 1984

SCHOOL OF SURVEYING
THE UNIVERSITY OF NEW SOUTH WALES
P.O. BOX 1
KENSINGTON, N.S.W. 2033
AUSTRALIA

National Library of Australia

CARD NO. and ISBN 0 85839 040 X

ABSTRACT

Analyses of satellite laser range data for crustal deformation are presented. These analyses have common theory and error sources with the application of altimetry data to ocean dynamics. Both types of data are examined.

The orbit and geodetic parameter estimation program GEODYN is used for many of the studies. Substantial research effort is expended on the development of expertise with GEODYN. This expertise is applied to both solid-Earth and ocean dynamics investigations.

The ocean tides are usually determined by solving Laplace's tidal equations. Little observational data is available for the tide in the open ocean. GEOS-3 radar altimetry data is a source of information on the complete sea surface height spectrum. However, as yet problems with systematic errors, usually attributed to orbital error, preclude any tidal estimation. Spectral Analysis is used to determine periodic errors in the sea surface height data. Knowledge of these errors can enhance solutions for the M_2 tide. The method reduces the crossover residual variance by 30%. However, this is not enough to allow successful tidal determination. Possible reasons for problems with systematic errors are discussed.

Satellite laser range data can be used to determine accurate orbits and tracking station coordinates. The feasibility of using laser range data from the LAGEOS satellite to determine the crustal movements of the Australasian region are investigated. The GEODYN and ORAN programs are used to determine the effect of errors in dynamic models and solution procedures on estimated geodetic coordinates and baselines. For centimetre accuracy, errors due to force modelling, Earth rotation and solution procedures must be carefully ascertained. Gravity modelling and biases dominate the error budget. Techniques for minimising these errors are examined. Laser range data to LAGEOS are analysed for the baseline distance between the Orroral and Yarragadee tracking stations. The preprocessing software for filtering and compressing the data to normal points is described. Baseline values and variations are discussed and further topics of investigation are suggested.

TABLE OF CONTENTS

ACRONYMS and ABBREVIATIONS

BMR	Bureau of Mineral Resources
BIH	Bureau International de l'Heure
CPU	Central Processing Unit (Computer)
DGFI	Deutsches Geodätisches Forschungsinstitut, West Germany
DMA	Defence Mapping Agency
DPMS	Dahlgren Polar Motion Service
EODAP	Earth and Ocean Dynamics Applications Program
EOPAP	Earth and Ocean Physics Applications Program
GAST	Greenwich Apparent Sidereal Time
GEODYN	Computer program for estimating geodetic and geodynamic parameters
GM	Product of the Gravitational Constant and Mass of the Earth
GPS	Global Positioning System
GSFC	Goddard Space Flight Center
IAU	International Astronomical Union
ICL	Inter-Union Commission on the Lithosphere
IPMS	International Polar Motion Service
LAS79	Sea Surface Height Data Set based on GEOS-3 altimetry and orbits determined by laser ranging
LLR	Lunar Laser Ranging
MOBLAS	Mobile Laser Tracking Station
MSL	Mean Sea Level
NASA	National Aeronautics and Space Administration
NATMAP	Division of National Mapping (Australia)
NAVSAT	Navy Navigation Satellite System
NNSS	Navy Navigation Satellite System (see NAVSAT)
NOAA	National Oceanic and Atmospheric Administration
NGSP	National Geodetic Satellite Program
NSSDC	U.S. National Space Science Data Center
NSWC	Naval Surface Weapons Center
ORAN	Computer program for simulation of geodetic and geodynamic experiments
r.m.s.	Root Mean Square
SLR	Satellite Laser Ranging

SSH	Sea Surface Height
SST	Sea Surface Topography
SPMA	Single-Pass Multi-Arc
SV	Singular Value Decomposition inversion technique
δI	Infinitesimal Bordering inversion technique
TLRS	Transportable Laser Ranging Station
UNSW	University of New South Wales, Australia
VLBI	Very Long Baseline Interferometry
WALLOPS	Wallops Flight Center GEOS-3 altimetry data set
WFC	Wallops Flight Center

CONVENTIONS and DEFINITIONS

In general upper case letters denote matrices, whereas lower case "bold" letters denote vectors. Otherwise the convention will be defined.

The magnitude of a vector **a** is denoted a.

Linear dependence refers to m vectors $\mathbf{a}_i$ satisfying the equation (KREYSZIG,1962):-

$$\sum_i k_i \mathbf{a}_i = 0$$

where k_i are scalars not all equal to zero.

If the vectors do not satisfy this equation they are linearly independent.

The rank of a matrix A is equal to the maximum number of linearly independent rows or columns of the matrix (KREYSZIG,1962). The system of observation equations

$$\mathbf{Ax} + \mathbf{b} = \mathbf{l} + \mathbf{v}$$

are rank deficient if their rank is less than the minimum number of columns or rows.

A is referred to as the design matrix,

x is the vector of parameters,

l is the vector of observations and,

b is the vector of modelled observations.

If the set of observation equations is rank deficient, the rank defect is equal to the number of independent constraint equations necessary to make the system of equations rank full. This set of constraints is referred to as a "**minimal set of constraints**" (BLAHA,1971a).

Pseudo-rank is the rank of a matrix as determined by numerical methods.

The eigenvalues e and eigenvectors y are obtained from solution of the equations:

$$\det(\mathbf{A}-e\mathbf{I}) = 0$$

and

$$\mathbf{Ay} = e\mathbf{y}$$

where I is the identity matrix.

The determinant of A (det A) is equal to the product of the eigenvalues. If A is singular, det A = 0, and there must be at least one zero eigenvalue. If a matrix is singular no inverse A^{-1} exists where:

$$A A^{-1} = I$$

A design matrix is ill-conditioned if small changes to the original matrix result in large changes to the inverse (NOBLE,1973). The **condition** of a matrix is a quantitative estimate of ill-conditioning and its effect on solutions. Methods of determining condition are described in appendix C.

Ill-conditioning implies that several solution vectors nearly satisfy the least squares condition

$$v^T v = \text{minimum}$$

Estimability refers to the parameters, which can be determined from an observation.

The term **geometric**, implies that strictly simultaneous observations have been used to solve for tracking station coordinates in the context of geodetic satellite solutions. The satellite motion is thereby eliminated from the solution.

The term **dynamic**, in the same context as above, implies that observations have been combined into a solution for tracking station coordinates by using a force model to derive the position of the satellite. The satellite motion is therefore also a parameter in the solution.

INDEX OF FIGURES

INDEX OF TABLES

ACKNOWLEDGEMENTS

My thanks must go to the late Associate Professor R.S. Mather, who introduced me to satellite geodesy and helped start this thesis. I greatly appreciate his foresight and inspiration during the early work for this dissertation.

I would also like to express my appreciation to Dr A. Stolz for his supervision, assistance and encouragement with this thesis.

The many discussions with staff and post-graduates at the University of New South Wales will always be remembered. My thanks are extended to Richard Coleman, Chris Rizos, Karl Bretreger and David Close. I would especially like to thank Bernd Hirsch for his computing assistance and keeping GEODYN running.

I am grateful for the support of Professor P. V. Angus-Leppan and the School of Surveying and appreciate the help of Debbie Chesher in typing part of the manuscript.

Dr. David Smith provided the opportunity to work with Geodynamics Branch at Goddard Space Flight Center from January to July 1978. The discussions with members of the Geodynamics Branch greatly improved my insight into satellite geodesy. Assistance was especially provided by Barbara Putney, Frank Lerch of Geodynamics Branch and Steve Klosko of EG&G Washington Analytical Services Center,Inc.

Financial Support for most of this work was provided by a Commonwealth Postgraduate Research Award.

Finally, I would like to express my appreciation for the support over the last three years from my friends at the University Church. My family has also been of great assistance during these years of post-graduate study.

C H A P T E R 1

APPLICATIONS of SATELLITE GEODESY to GEODYNAMICS

1. INTRODUCTION

This dissertation aims to apply satellite geodesy to specific problems in solid-Earth and ocean physics. The problems are:

(1) the analysis of GEOS-3 altimetry data for orbital errors and ocean tides; and

(2) the determination of the crustal deformation from laser ranging measurements to the LAGEOS satellite.

These two topics involve position determinations and are closely related through their dependence on satellite orbital theory and common analysis techniques. The error sources for both applications are dominated by the force models used for orbital calculations.

With the development of precise extra-terrestrial measuring systems since the beginning of the satellite era, the scope of geodesy has broadened to include a much wider field of sciences. Geodynamics is used in this dissertation to refer to both solid-Earth and ocean dynamics. Geodesy has always been closely related to geophysics and hence geodynamics through the study of the size and shape of the Earth (BOMFORD,1962). The geodesist's interests have extended from classical mapping applications to a greater involvment in the Earth sciences. During the last 20 years, measurement accuracy has improved from 1 part in 10^6 to 1 part in 10^8 (NASA,1979; FLINN,1981). Most of this improvement has been obtained through the use of extra-terrestrial measuring techniques. These techniques include tracking of artificial satellites and the Moon and also Very-Long-Baseline-Interferometry (VLBI). Precise tracking of the Moon is accomplished by lunar laser ranging (LLR). Among the artificial satellite tracking techniques are laser ranging (SLR) and Doppler tracking to the Navy Navigation Satellites (NAVSAT or NNSS). The Global Positioning System (GPS) is now being introduced. The measurement of gravity has also achieved an accuracy of 1 part in 10^8 (TANNER & TORGE,1979; DRAGERT et AL,1981). Apart from the improvement in these techniques there has also been an associated improvement in data processing and the measurement of time.

Geodynamic results can be obtained from a multitude of measuring techniques. Two data types are of interest here, SLR and radar

altimetry.

The objectives of SLR are to provide improved information on polar motion, tectonic motion, the Earth's gravity field and to precisely determine orbits (FLINN,1981). Laser tracking stations determine the distance to a spacecraft by measuring the time interval for a light pulse to travel from the tracking station to the spacecraft and back. A travel time accuracy of 1 nsec is equivalent to a one way range accuracy of 15 cm. SLR has been carried out since the mid-1960's. There are now about two dozen SLR observatories around the world with more being constructed or planned. The range accuracies of these stations vary from 3 cm to 1 m. The laser systems at Goddard Space Flight Center (GSFC) and Wetzell, West Germany have a range accuracy of about 3 cm. The NASA Moblas stations operate between the 5 and 10 cm accuracy level, while the SAO stations range to LAGEOS with an accuracy between 10 and 20 cm. Other observatories are at Kootwijk, The Netherlands and Grasse, France. A transportable laser ranging station (TLRS) capable of ranging to LAGEOS with an accuracy of 3 cm has been successfully tested and is being deployed in California for studies of crustal movements (SILVERBERG,1978;1981; SILVERBERG & BYRD,1981). The TLRS was scheduled to visit Australia in 1982 (NASA,1979; FREY,1980). These plans have since been changed. A plan to build a TLRS at the University of Texas or modify a MOBLAS system and deploy it in Antarctica for one season and then move it around Australia was proposed. The Antarctic proposal has now fallen through. Alternative plans for a measuring program in and around the Australian continent are being made.

SLR is the technique of specific interest to this dissertation. Laser range data was used to determine the GEOS-3 ephemeris. This ephemeris was used to reduce altimetry data to sea surface heights and is described in Chapter 6. In Chapter 7 the feasibility of using laser range data to LAGEOS for Australian crustal motion studies is investigated. In Chapter 9 laser range data to LAGEOS is analysed for crustal deformation in Australia.

The other measuring technique of specific interest is radar altimetry. The distance from the satellite to the ocean surface is measured. GEOS-3 altimetry data are internally consistent to about 20-30 cm (STANLEY,1979; COLEMAN,1981). Therefore, they can be used in combination with accurate satellite tracking to determine the geocentric position of the instantaneous ocean surface. These measurements have

been used to improve geopotential models, especially over the oceans. The data have proved useful for investigations of ocean surface features like eddies and the Gulf Stream. The structure of the lithosphere has also been investigated using altimetry in the vicinity of seamounts (LAMBECK,1981b). Further geodetic applications of altimetry data are given in Chapter 2.

Time systems play an important role in extra-terrestrial measuring techniques. A satellite at an altitude of 850 Km has an along-track velocity of approximately 7 km per sec. Therefore, in order to model it's position to an accuracy better than 10 cm, the time must be accurate to the order 10^{-5} sec. The equivalent Universal Time is needed to relate inertial position to position on the Earth's surface. These time systems are maintained by organisations such as the Bureau International de l'Heure (BIH).

Data processing techniques are fundamental to all measuring techniques where observations are used to estimate parameters of geodetic or geophysical interest. The importance of data processing cannot be over-emphasised. Since large amounts of data are collected with extra-terrestrial techniques and also because of the many intricate formulae that are used to model these data any improvement in measuring technology is of little benefit unless it is accompanied by similar improvements in data processing and solution techniques. If this relationship is not maintained the required results will not be obtained. Computational capabilities at GSFC are described by SMITH (1978) and PUTNEY (1980; 1981). These are of interest because the GEODYN computer program was developed at GSFC. GSFC resources are representative of current trends and were used for much of the work in this dissertation (Chapters 6, 7, 8 and 9).

Technological improvement has made a vast field of inter-disciplinary research possible. In order to use the techniques correctly, scientists must have a comprehensive knowledge of a number of distinct topics so that reliable results are obtained. With the present application of geodetic data to new fields of research it is easy to understand the movement of the geodetic community into the field of Earth dynamics. This movement has necessitated an emphasis on inter-disciplinary liaison by the Inter-Union Commission on the Lithosphere (ICL,1980; 1981).

The accuracy of position determination is essentially limited by

either unmodelled or inadequately modelled geodynamic phenomena. At the highest accuracy levels, position fixing and geodynamics cannot be separated. High-precision geodesy is therefore an interdisciplinary science. For example, if satellite techniques are being used to determine tectonic motion, then systematic effects due to the gravity field, Earth-tides and Earth rotation need to be estimated or filtered from the estimated coordinates. Similarly with oceanographic applications of altimetry data, errors in the estimated sea surface height due to orbital errors must be separated from the oceanographic phenomena of interest. The geodesist who provides information on position must both understand and provide information on the multitude of systematic errors that can affect position determinations at the 10 cm accuracy level. This means that reference systems must be uniquely defined and that the data should have all possible errors removed or at least defined. This thesis therefore contains essential error analyses for geodetic calculations. Common error sources exist for applications of both SLR and altimetry to geodynamics.

Earth and ocean phenomena, which can be studied with satellite data are described in Chapters 2 and 3. The application of geodetic techniques to two specific geodynamic investigations are described in Chapters 6, 7, 8 and 9. These investigations could not be made without a thorough understanding of the topics summarised in Chapters 1, 2, 3, 4 and 5.

Applications of satellite geodesy to geodynamics and earthquake research began in 1964 with the National Geodetic Satellite Program (NGSP), which aimed to coordinate the diverse efforts in satellite geodesy and to improve geodetic and geophysical constants. Broad outlines for investigations were formulated in the subsequent research programs. These projects show the global nature of modern geodesy. Results will not be achieved without international cooperation.

Topics in need of investigation for geodynamics are presented in the proceedings of the Williamstown meeting (KAULA,1969), the EOPAP program (NASA,1972), the constitution of the inter-union commission on the Lithosphere (ICL,1980,1981) and NASA's Crustal Dynamics Program (NASA,1979).

The Geodynamic Experimental Ocean Satellite mission (GEOS-3) and Laser Geodynamic Satellite mission (LAGEOS) were developed under EOPAP. These missions are of specific interest to this thesis. Details are

given in Chapter 4.

The application of geodesy to physical oceanography is confined mainly to the GEOS-3 and SEASAT missions. Satellite geodesy can provide information on the dynamics of the sea surface. Ocean dynamics research is now mainly realised through NOAA environmental satellites. Since the malfunction of the SEASAT satellite, analysis of altimetry for oceanography has been confined to the 1975-1978 era. Possible applications of geodesy to oceanography are described further in Chapter 2.

One method of combining fundamental orbit theory with conventional methods for minimising errors in the analysis of altimetry data is investigated in Chapter 6. Essentially similar methods have been independently adopted by other investigators at about the same time as these studies were made (GOAD et AL,1980; MASTERS et AL,1979).

The goals of the NASA research and applications program in crustal dynamics for the period 1980 to 1990 are set out in NASA's Crustal Dynamics Program (NASA,1979). The program involves, amongst other things, testing the postulates and consequences of the plate tectonics theory and global geophysical processes. The program includes searching for fallacies in the theory and development of modifications needed to bring the theory into accord with observations. With the available extra-terrestrial measuring techniques (ie. SLR, LLR, VLBI, GPS and NAVSAT) conditions are conducive to the rapid development of the Earth sciences. However geodetic techniques will need at least ten years to produce significant results. A few geodynamic programs are described in Chapter 3.

The studies presented in Chapters 7, 8 and 9 are part of an ongoing Australian program associated with NASA's Crustal Dynamics Program and the International Lithosphere Program (ICL,1980;1981). The feasibility of pursuing these projects at the University of New South Wales is studied. Work still in progress comprises the processing and analysis of real LAGEOS range data. A few results are presented in Chapter 9. The error analyses for these studies were based on the same theory as used for Chapter 6. GEODYN was used extensively for orbital calculations.

A superficial examination of the different end products of Earth and ocean dynamics in fact obscures the similar procedures used to process and interpret geodetic data from satellites. Earth and ocean dynamics are the end products of systems involving data processing,

satellite dynamics, statistics and geophysics. In fact many of the errors for both applications emanate from the same source, that is the satellite orbit. Laser range and radar altimetry data are similar data types. The same basic theory and procedures can therefore be applied to ascertain the sensitivity of the observations to geodetic and geodynamic parameters. Therefore a thorough understanding of satellite geodesy and geodynamics is necessary to obtain the best geodynamic results from any geodetic data type.

One specific aim of this dissertation is to apply an inter-disciplinary and comprehensive approach to solving geodynamic problems. This approach includes understanding the theory used in GEODYN (MARTIN et AL,1976) and investigating how the theory would effect determinations of crustal deformation and ocean tides. Although not specifically stated elsewhere, similar methods and theory are used in Chapters 6, 7, 8 and 9. GEODYN is used in each chapter and orbital errors are common to the analysis of both altimetry and range data.

The GEODYN Program (MARTIN et AL,1976) has been operational on the University of New South Wales FACOM computer for many years. This program is used internationally for geodynamic applications. It has provided an important tool for Australian geodetic research.

The structuring of satellite geodesy theory in a program like GEODYN involved tens of man-years of development. This program development is also a never-ending procedure as the dynamic models are continually improved and updated. Keeping GEODYN up to date with the continual improvements in technology is itself a daunting task. This is especially so if GEODYN's 40 000 Fortran statements are considered. It is obviously important for the users of this type of software to be aware of its capabilities and especially its limitations. It is important to know the theories adopted and also to some extent how they have been programmed. If this is not done the interpretation of any estimated parameters may be of dubious value.

Essential preparation for the work presented in this dissertation has involved detailed study of the theories and models used in GEODYN. These models and their inter-relation are briefly described in Chapter 5. The analysis and results in Chapters 6, 7, 8 and 9 include investigation of the effects of models and model errors on geodynamic calculations.

The estimated accuracy of measurements and computational techniques implies that they are sensitive to many geodynamic phenomena.

In the past the following three steps of investigation were usually separated.

(i) the analytical and statistical theory used to model the observations must be continually refined, in order to obtain position consistent with the accuracy of the tracking data.
(ii) Computer software used to process the observations using the analytical theory in (i) need to be refined.
(iii) Geophysical phenomena can be analysed using these highly accurate measurements.

However with new data types geodynamic models are needed for the analytical theory used to model the observations. The three distinct steps can no longer be considered to be independent and need to be included in any geodetic investigation. In order to complete this thesis it has been necessary to study the latest developments and interaction between the three steps. The early chapters therefore give an overview of Earth dynamics, ocean dynamics and satellite geodesy with reference to many publications in the area. The later chapters use this knowledge to investigate a few specific topics. A brief synopsis of the chapters is given below.

Chapters 2 and 3 outline the principles of Earth and ocean dynamics. These sections are intended to be introductory rather than comprehensive and give a summary of the areas where satellite altimetry and laser ranging can contribute.

Chapter 4 describes the GEOS-3 and LAGEOS missions.

Chapter 5 is a summary of satellite geodesy theory.

Chapter 6 deals with the effect of data distribution and error sources for the GEOS-3 radar altimetry. These data are analysed with an aim to determining the ocean tides and also removing systematic errors for oceanographic applications. Preliminary results for the determination of the M2 tide in the Sargasso sea region are given. These results are derived from an updated version (in 1979) of GEOS-3 altimetry data set.

Chapter 7 is a feasibility study for the determination of crustal strain in the Australian region using laser tracking data fro. the LAGEOS satellite. This Chapter investigates the available computer resources and a few of the possible systematic errors which could affect position determinations in the Australian region. Possible alternative

methods for processing the LAGEOS range data are looked into and further research topics are suggested.

Chapter 8 analyses the dynamic satellite solution process. The constraints needed to obtain solutions and also the implied reference systems are investigated. The implications of these problems for geodynamic calculations are discussed. Possible errors are especially relevant to the feasibility study in Chapter 6 and analysis of range data in Chapter 9.

Chapter 9 comprises an analysis of laser range data to LAGEOS for the baseline distance between the Orroral and Yarragadee tracking stations. Preprocessing methods for filtering and compressing the data to normal points are described. Baseline results are compared with error analyses and other measurements.

The appendices describe some of the theory and principles of the numerical methods, which have not been elaborated upon in the main text. These include spectral analysis and spherical harmonic theory.

C H A P T E R 2

OCEAN DYNAMICS

2.1 INTRODUCTION

The dynamics of the oceans are concerned with the circulation of the oceans and the physical state of the ocean surface. These are of direct concern to the general global community. Ocean dynamics is also intimately related to climate of the world.

Ocean dynamics is described here in general terms. The GEOS-3 altimetry as used in this dissertation have also been used to analyse many parts of the sea surface height spectrum. Common problems with the propagation of errors occur in all these applications. However these problems are more critical for some parts of the spectrum than others. Specifically, problems with determining the tides have been investigated in Chapter 6. Knowledge of ocean dynamics (tides) and satellite geodesy is used to minimise errors.

A number of satellite techniques, which can globally map oceanographic features within a short time span, have now been developed. Satellite remote sensing technology provides distinct advantages over the often sporadic, conventional oceanographic ship surveys. The GEOS-3 satellite orbit, for example, traces out a 1°x 1° grid sampled between latitudes 65°N and 65°S every 25 days.

Radar altimetry data provides information on the height of the sea surface and is of specific interest to this dissertation. Apart from the global coverage, an important advantage of using radar altimetry to obtain the sea surface height is that the height is determined in absolute space (COLEMAN,1981). The datum problem associated with the dynamic height technique used by oceanographers to determine global geostrophic currents is therefore avoided. This datum problem however is not critical for regional work (COLEMAN,private communication,1981).

Microwave, infra-red and visible radiometers, scatterometers and synthetic aperture radar are also used for oceanographic research. Application of these techniques are given by NAGLER & McCANDLESS (1975), MATHER (1976), COLEMAN (1981), and literature on the SEASAT mission.

The satellite orbit, altimetry measurement and sea surface height are related as follows (Figure 2.1)

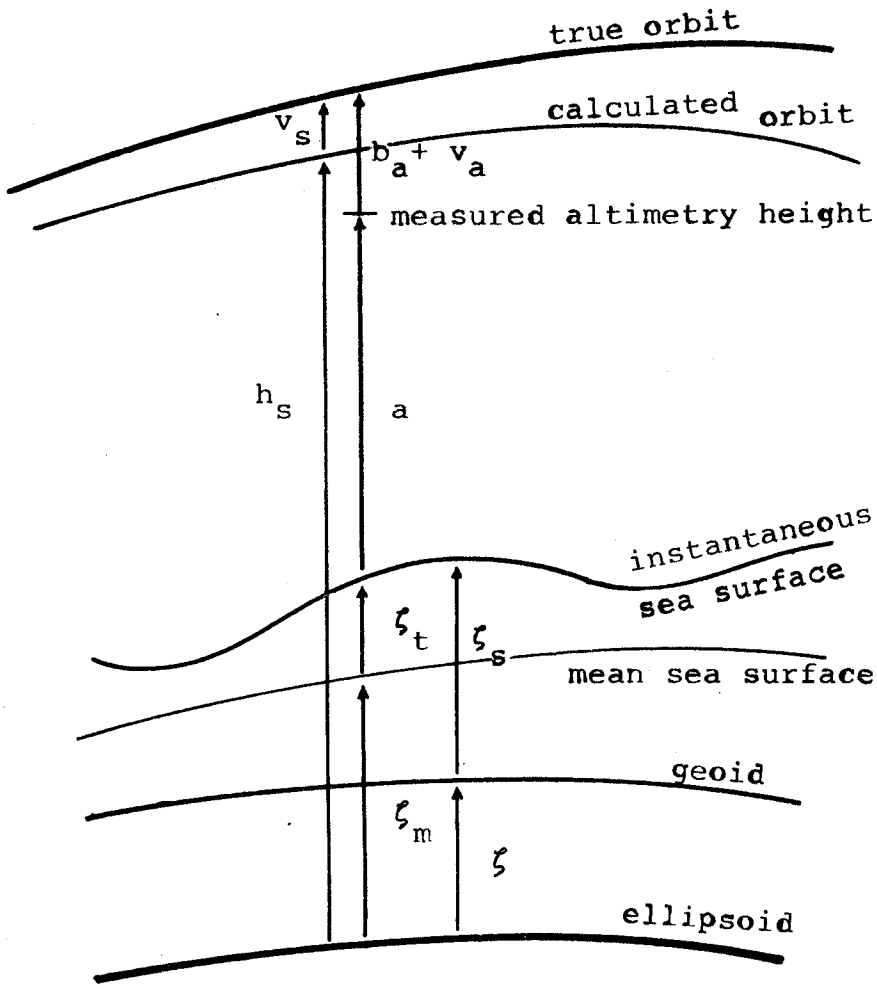

Figure 2.1
Relationship between Altimetry, Satellite Orbit, Geoid and Sea Surface Height.

$$h_s + v_s = \zeta_M + \zeta_t + (a + v_A + b_A) \qquad (2.1)$$

where h_s O(850 Km) is the height of the satellite above the reference ellipsoid as derived from the ephemeris,

v_s O(5 m) is the systematic orbital noise,

ζ_M O(100 m) is the mean sea surface height above the reference ellipsoid,

ζ_t is the time dependent sea surface height referred to the mean sea surface height,

a O(850 Km) is the altimetry measurement corrected for refraction,

v_A O(0.5 m) is the altimeter noise and,

b_A O(5 m) is the altimeter bias.

ζ_t contains the tide signal as well as any periodic and secular time varying features. v_s is a function of the force model used to derive the motion of the satellite, tracking station distribution as well as ranging quality and quantity. Equation 2.1 is used to reduce the measured altimetry and calculated satellite height to instantaneous sea surface heights.

Radar altimetry data is potentially sensitive to the whole sea surface height spectrum. The sensitivity to specific frequencies and spatial wavelengths depends on the magnitude of the phenomena, the accuracy of the altimeter, the accuracy of the ephemeris and the sampling characteristics of the satellite orbit. Different analysis techniques are more suitable for some parts of the spectrum than others (MATHER et AL,1979). For example, an absolute datum is necessary for the global dynamic Sea Surface Topography but not the detection of eddies and temporal features (COLEMAN,1981; CHENEY & MARSH,1981). This means that orbital errors can be separated from temporal variations by differencing passes of data in the same region.

The four broad spectral ranges into which the sea surface height can be divided are shown in Table 2.1. The spectrum is of interest here to put the application of altimetry data into context. Specifically relevant to this dissertation are the short-period ocean tides. However, the same data were analysed by RIZOS (1980a) and COLEMAN (1981) for the applications of satellite geodesy to physical oceanography and other associated geodetic investigations.

TABLE 2.1
SPECTRUM of the SEA SURFACE
(after MATHER,1978b)

spectral band	period
short-period	< 1 d
intermediate-period	1 - 100 d
long-period	100 d - 2 yrs
quasi-stationary	constant

2.2 SHORT PERIOD PHENOMENA

The largest short-period phenomena are the ocean tides. Other short-period phenomena include swell, storm surges and so forth. The dominant tidal constituents have periods less than one day, spatial wavelengths from 500 to 10000 Km and magnitudes of 10 to 100 cm. Tides are caused by gravitational forces exerted on the Earth by celestial bodies. The tidal potential may be calculated from formulae originally developed by LAPLACE (1775). Information on the tides can be found among many treatise including MELCHIOR (1966; 1978), BRETREGER (1978), LAMBECK (1980) and SCHWIDERSKI (1980).

The tide in the open ocean is not expected to exceed 1 m (LISITZIN,1974). Nevertheless anomalies in tidal amplitudes and phases do occur and 5 metre high tides have been recorded along continental coastlines. Reliable measurements of the true ocean tides were possible only at mid-ocean islands, where the topography rose steeply from the ocean floor. This problem has been overcome with the deployment of deep sea tide gauges. The gauges are sensitive to pressure and temperature fluctuations on the ocean floor. An improved knowledge of the tidal amplitudes at the regional level has been obtained through their deployment (ZETLER et AL,1975; CARTWRIGHT et AL,1980). Their geographic distribution is however too sparse to define the tides globally.

The ocean tides load and deform the Earth's surface causing temporal variations of the gravity field. A knowledge of these loads permits the determination of the hydrodynamic structure of the ocean as well as the elastic parameters defining the structure of the solid Earth (LAMBECK,1980). Moreover the tidal signal could be filtered from

altimetry data and orbit perturbations. For example, ocean tidal perturbations are evident in the LAGEOS orbit and corrupt the analyses for other phenomena such as Earth rotation (CHRISTODOULIDIS & SEIFFERT,1980). Tidal dissipation is also responsible for the acceleration of the lunar orbit (LAMBECK,1980). Apart from their purely oceanographic relevance the ocean tides need to be accurately known for other geodynamic and astrodynamic studies.

The tidal potential at a point P can be expressed by a potential of degree two (LAMBECK,1980), that is, (Figure 2.2)

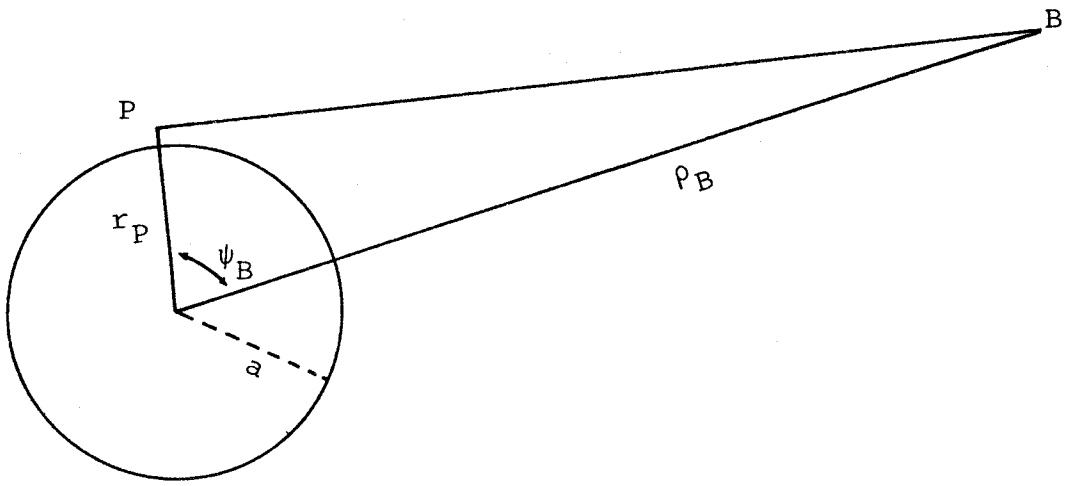

Figure 2.2

The Tide Producing Potential

$$U_B(P) = GM_B/\rho_B \, |r_P/\rho_B|^2 \, P_{20}(\cos\psi_B) \qquad (2.2)$$

where M_b is the mass of the tide producing body B,
G is the gravitational constant,
ρ_B is the geocentric position vector of the body B,
r_P is the geocentric position vector to the point P,
ψ_B is the geocentric angle between r_P and ρ_B and
P_{20} is the Legendre polynomial of degree 2, order 0.

The tidal spectrum for the Sun and Moon has a wide band of frequencies (LAMBECK,1980). Equation 2.2 can be expanded in terms of orbital elements for the Sun and Moon. The main tidal periods can then be separated into long-period, diurnal and semi-diurnal constituents (MELCHIOR,1978). These periods are critical to the determination of the tides using satellite altimetry data. The sampling distribution of the altimetry data with respect to time is not ideal for determining the diurnal or semi-diurnal tides (see section 6.6)

Ocean tide models are commonly obtained by solving Laplace's Tidal Equations (LTE), which can be written as follows (HENDERSHOTT, 1972):

$$\frac{\partial u}{\partial t} - (2w \sin\phi)v = \frac{-g}{R\cos\phi}\frac{\partial(\zeta_u - \Gamma/g)}{\partial\lambda} + \frac{F_\lambda}{\rho_w D_o}$$

$$\frac{\partial v}{\partial t} + (2w \sin\phi)u = \frac{-g}{R}\frac{\partial(\zeta_u - \Gamma/g)}{\partial\phi} + \frac{F_\phi}{\rho_w D_o}$$

$$\frac{\partial\zeta_u}{\partial t} - \frac{\partial\delta_E}{\partial t} + \left[\frac{\partial(uD_o)}{\partial\lambda} + \frac{\partial(v D_o \cos\phi)}{\partial\phi}\right] /R\cos\phi = 0 \quad (2.3)$$

where R is the Earth's mean radius,

(ϕ,λ) are the latitude and longitude,

(u,v) are the eastward and northward components of fluid velocity,

w is the Earth's angular velocity,

D_o is the undisturbed ocean depth,

ζ_u is the deviation of the sea surface from its undisturbed level,

δ_E is the geocentric solid Earth tide height,

F_λ and F_ϕ are the zonal and meridional components of the bottom stress,

ρ_w is the density of water,

g is the downward acceleration of gravity at the Earth's surface and,

Γ is the potential of all the tide generating forces.

Early tide models were obtained by neglecting eddy dissipation, bottom friction and loading effects. Present day models include constraints to account for: land-sea distribution and ocean depth, energy dissipation (usually assumed to occur in shallow seas and along coastlines); solid Earth tides; ocean loading deformation; and tide gauge observations (LAMBECK,1980; SCHWIDERSKI,1980). These models are believed to be very accurate. However the prediction of the tides in the open ocean is still based on theory and not observation. Satellite altimeter data facilitates the modelling of ocean tides on a global scale. It has the potential to provide the information needed to

overcome the deficiencies of existing tide measurements. However, all attempts to resolve this information have been unsuccessful. Problems of determining the ocean tides with altimetry data are investigated in Chapter 6.

A suitable method for analysing altimetry derived SSH data for the tides is described by BRETREGER (1979). COLEMAN (1981) gives the formulae for a global solution using a spherical harmonic series instead of the Fourier series. The development presented below follows BRETREGER (1979).

The ocean tide signal, ζ_T at any point on the globe is expressed as the sum of many tidal constituents, ζ_{Ti}

$$\zeta_T = \sum_i \zeta_{Ti} \qquad (2.4)$$

Tidal constituents can be expressed as

$$\zeta_{Ti} = \zeta_{Ai}(\phi,\lambda)\cos(\theta_i - \alpha_i(\phi,\lambda)) \qquad (2.5)$$

where ζ_{Ai} is the constituent amplitude,

θ_i is the time dependent argument of the i-th tidal constituent (see MELCHIOR,1978, p27 for a listing of these arguments), and

α_i is the phase lag at a particular epoch.

Equation 2.5 can be expressed as

$$\zeta_{Ti} = \zeta_{Ai}(\phi,\lambda)\cos\alpha_i(\phi,\lambda)\cos\theta_i + \zeta_{Ai}(\phi,\lambda)\sin\alpha_i(\phi,\lambda)\sin\theta_i \qquad (2.6)$$

Equation 2.6 relates SSH observations taken at a specific latitude and longitude to the tide. It does not take into consideration the correlation between adjacent observations. In order to overcome this limitation and to allow all observations taken within a finite region to be simultaneously analysed, the Equation 2.6 can be modelled as a 2-dimensional Fourier model. Thus

$$\zeta_{Ti}(\phi,\lambda,t) = \cos\theta_i \sum_{k=1}^{8} \sum_{n}^{nk} F_{kn} C_{kn} + \sin\theta_i \sum_{k=1}^{8} \sum_{n}^{nk} F_{kn} C'_{kn} \qquad (2.7)$$

where

C_{kn} and C'_{kn} are the fourier coefficients to be estimated,

F_{kn} are the position dependent functions, given below

$F_{1n} = \cos n a_\phi \qquad n=0,\ldots\ldots n1$

$F_{2n} = \sin n a_\phi \qquad n=1,\ldots\ldots n2$

$F_{3n} = \cos n a_\lambda \qquad n=1,\ldots\ldots n3$

$F_{4n} = \sin n a_\lambda \qquad n=1,\ldots\ldots n4$

$F_{5n} = \cos n a_{\phi J} \cos m a_{\lambda J}$ n=1,.....n5, m=1,....n5

$F_{6n} = \cos n a_{\phi J} \sin m a_{\lambda J}$ n=1,.....n6, m=1,....n6

$F_{7n} = \cos n a_{\lambda J} \sin m a_{\phi J}$ n=1,.....n7, m=1,....n7

$F_{8n} = \sin n a_{\lambda J} \sin m a_{\phi J}$ n=1,.....n8, m=1,....n8

(2.8)

$a_{\phi J} = \Pi(\phi_J - \phi_0)/(\phi_M - \phi_0)$ and, (2.9)

$a_{\lambda J} = \Pi(\lambda_J - \lambda_0)/(\lambda_M - \lambda_0)$ (2.10)

Note that (ϕ_0, λ_0) is the south-east corner of the region and (ϕ_M, λ_M) the north east corner.

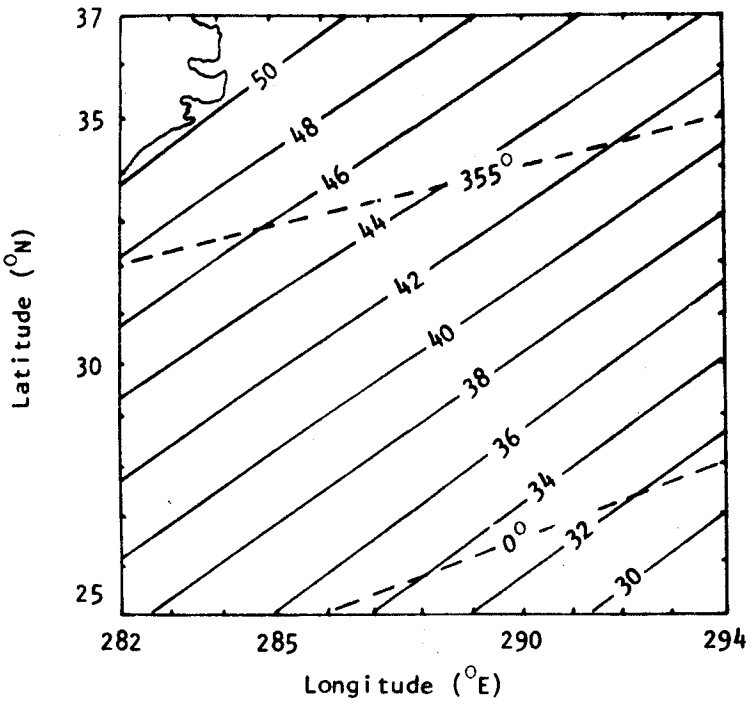

Figure 2.3
Mofjeld M_2 Tide Model

Several analytical global tide models have been developed in recent years. For the North Atlantic Ocean an empirical tidal prediction model developed by MOFJELD (1975) is available. This model agrees with deep sea tide gauge data to ±3 cm. The amplitude of the ocean tide in this area is about 60 cm, which predominantly comes from the M_2, N_2, S_2, K_1, O_1 and P_1 tidal constituents. The cotidal-corange chart for the M_2 tide constituent is shown in Figure 2.3. The significant estimated

Fourier coefficients are (BRETREGER,1979):

$C_{10} = 0.403$	$C'_{10} = -0.029$
$C_{11} = -0.064$	$C'_{11} = 0.028$
$C_{31} = 0.043$	$C'_{31} = -0.009$

These coefficients reproduce the M_2 Mofjeld tidal signal to ±2 cm. The first degree coefficients correspond to an average amplitude of 40 cm and a phase of 356 degrees with respect to Greenwich. However, this SSH model is not the same as the geocentric SSH as sensed by the altimeter. Corrections are needed to allow for the effects of the solid Earth tides and ocean loading. These effects cannot be considered negligible in the context of the 40 cm tidal amplitude. COLEMAN (1981) gives a complete review of an M_2 tide model determined from altimetry using Equations 2.6 and 2.7.

2.3 INTERMEDIATE PHENOMENA

Eddies are mesoscale circulatory patterns. They usually develop when western boundary currents form meanders which then break off and separate from the main stream (PARKER,1971). Eddies have interested scientists for some 40 years and have become of major interest to the oceanographic community. This is because a large proportion of the total energy in the ocean seems to be associated with eddies. Due to a lack of suitable long-term tracking techniques, little is known about their life history. What is known is that eddies have a period 20 - 400 days, spatial wavelengths 50 - 300 km magnitudes 20 - 100 cm and move at rates from 2 to 10 km per day.

The surface expression of eddies manifest either as hills or depressions in the sea surface. They can be readily identified using altimetry range data. One method for detecting eddies using this data is presented in MATHER et AL (1978a; 1979; 1980) and in COLEMAN (1979; 1981). They compared their results with remotely sensed circulation patterns in the Gulf Stream region, provided by the U.S. National Weather Service (NOAA,1978). Altimetry data can provide useful information in combination with the other remotely sensed data for analysing eddies. Recent work is usually associated with investigations of the Gulf stream (CHENEY & MARSH,1981; DOUGLAS & CHENEY, 1981; KAO & CHENEY,1982).

2.4 LONG PERIOD and QUASI-STATIONARY EFFECTS

Sea Surface Height (SSH) is defined as the height of the ocean surface above a reference surface. If this reference surface is the geoid, the height is called Dynamic Sea Surface Topography (Dynamic SST; or ζ_s) (MATHER et AL,1979; COLEMAN,1981). The free ocean surface does not lie along any equipotential surface of the Earth's gravity field (STURGES,1967). Quasi-stationary phenomena like the distribution of water density and the pattern of major surface currents cause the mean sea level (MSL) to deviate from a level surface. This dynamic sea surface topography is the dominant driving force of the geostrophic circulation (REID,1961; WYRTKI,1975, LISITZIN,1974). Altimetry ranges in combination with an accurate geoid model and satellite orbit are sensitive to the dynamic SST. Therefore they can be used to determine ocean currents on a global scale. An analysis of the underlying principles and the use of altimetry measurements for studying the dynamic SST is given by MATHER (1976), RIZOS (1980a) and COLEMAN(1981).

If the tides are excluded, the dynamics of the surface layer of the oceans can be defined by the differential equations (MATHER,1978b):

$$\ddot{x}_1 - f\dot{x}_2 = -g\,\frac{\partial \zeta_s}{\partial x_1} - \frac{1}{\rho_w}\,\frac{\partial P_A}{\partial x_1} + F_1 + O(fx_1)$$

$$\ddot{x}_2 + f\dot{x}_1 = -g\,\frac{\partial \zeta_s}{\partial x_2} - \frac{1}{\rho_w}\,\frac{\partial P_A}{\partial x_2} + F_2 + O(fx_2) \qquad (2.11)$$

where the Coriolis parameter f is given by $f=2w \sin \phi$,

x_1 and x_2 are local Cartesian coordinates in the local horizon system with x_1 oriented east and x_2 oriented north,

w is the Earth rotation rate,

F_1 and F_2 are the local horizontal stresses on the surface layer,

P_A is atmospheric pressure,

$\ddot{x}_1, \ddot{x}_2$ are accelerations,

$\dot{x}_1, \dot{x}_2$ are velocities,

The predominant component is ζ_s (MATHER et AL,1979). Information on ζ_s can be obtained from GEOS-3 and SEASAT altimetry data in combination with the most recent gravity models and precise tracking. The sensitivity of the altimetry data to the global stationary dynamic SST was investigated by MATHER et AL (1978b). The low degree harmonic features compared favourably with conventional oceanographic estimates. Altimetry can therefore be used to determine the velocity field of the

ocean surface (MATHER et AL,1979). Unfortunately there are problems in estimating ζ_s on a global or regional basis due to inadequate geoid models (MATHER et AL,1979).

One major research need in physical oceanography is the understanding of general circulation movement. This especially includes the strong western boundary currents, such as the Gulf Stream. The problem is complicated by highly variable mesoscale flow fields, which obscure the mean flow field. This necessitates long periods of continuous measurement to quantify circulation movement.

Western boundary currents transfer water from equatorial regions to high latitudes. They have large velocities and therefore large dynamic SST. For example the Gulf stream has a velocity greater than 100 cm/sec, maintained by a dynamic SST slope of 80 cm/100 Km orthogonal to the flow (NEUMANN,1966). These slopes can be observed in altimetry data. A lot of research has been done on this topic (HUANG et AL,1978; DOUGLAS & GABORSKI,1979; LEITAO et AL,1977;1978;1979a;1979b; MATHER et AL,1979;1980; GORDON & BAKER,1980; CHENEY & MARSH,1980; COLEMAN,1981; WUNSCH & GAPOSCHKIN,1980; CHENEY & MARSH,1981; DOUGLAS & CHENEY, 1981; KAO & CHENEY,1982).

2.5 COMMENTS

Altimetry data give useful information on the SSH spectrum. The application of satellite data to physical oceanography is however limited due to many error sources. Problems for oceanographic and geodetic applications of altimetry data are mainly attributed to orbital errors. On the other hand, the altimetry has been shown to be accurate to design specifications (Chapter 4). In order to obtain the best geodynamics results from altimetry data, information from both satellite geodesy and ocean dynamics should be included in any investigations. For the most accurate results, the ocean SSH spectrum must be taken into account in geoid calculations which include altimetry data. Orbital dynamics can be used to minimise errors for both geoid and oceanographic applications. That is, the general interaction of all geodynamic phenomena must be kept in mind.

For oceanographic applications ζ_s and the geoid height are needed to a high degree of accuracy. MATHER (1978d) and RIZOS (1980a) describe the geoid requirements for oceanographic applications. The accuracy required for ephemerides and the geoid depends on the part of the

spectrum being analysed. For example ephemeris errors can be easily separated from temporal features like eddies, whereas they cannot be easily separated from the tides. Geoid errors on the other hand limit the determination of the global dynamic SST to a few low degree harmonics.

Information from both satellite geodesy and ocean dynamics has been used in Chapter 6 to minimise orbital errors in altimetry derived SSH data. Special consideration is given to the determination of ocean tides. However, the reduction of systematic errors from altimetry derived SSH data has benefits for all applications of altimetry data to ocean dynamics.

C H A P T E R 3

SOLID-EARTH DYNAMICS

3.1 INTRODUCTION

Solid-Earth dynamics is the study of the motions and distortions of the solid-Earth. These motions are responsible for earthquakes, tidal waves, volcanic eruptions, mineral differentiation, mountain building and the like.

The purpose of this chapter is to describe the Earth dynamic phenomena which can be investigated using high-accuracy satellite geodesy. Australia's participation in NASA's Crustal Dynamics Program is summarised. The investigations described in Chapters 7, 8 and 9 are also relevant.

Figure 3.1 (from BARANZANGI & DORMAN,1969) shows the location of worldwide earthquake epicentres. The epicentres delineate the boundaries between tectonic plates (NASA,1972, p2.3). Most earthquakes occur in the lithosphere and this implies that they are associated with plate tectonics. The goals of any earthquake hazard reduction program are therefore associated with understanding the structure and motion of the lithosphere. Apart from distortions of the lithosphere, geodynamics also involves research into many aspects of geology, geophysics and geochemistry.

The surface of the Earth is always in motion. Both classical and space geodetic techniques are ideally suited to measure this motion. One assumption is that the displacement fields associated with earthquakes are the instantaneous expressions of plate tectonics and mantle convection. Seismicity studies in general, confirm global tectonic motions if averaged over periods longer than 50 to 100 years (LAMBECK,1981a). Geodetic measurements also give instantaneous observations of motion of the Earth's surface. This information is important for developing models to explain the structure of the Earth. However, the measurements may or may not confirm tectonic motions on a global scale. Obviously for short time periods regional displacement fields must also be accounted for if geodetic methods are to be used to determine major tectonic displacements.

The **plate tectonics** hypothesis describes the Earth's crust as consisting of more than a dozen thin crustal sheets or plates moving

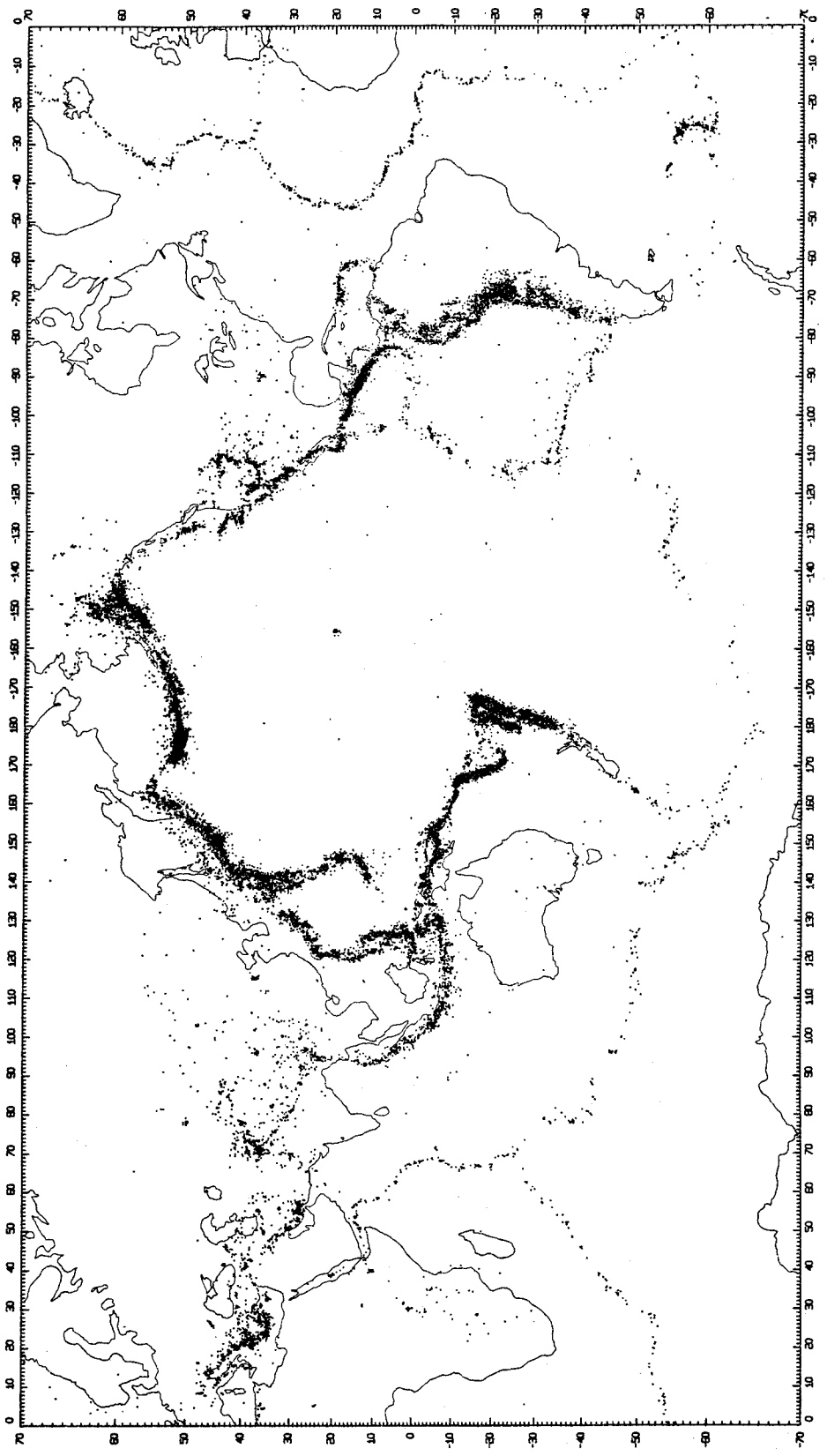
SEISMICITY OF THE EARTH, 1961-1967, ESSA, CGS EPICENTERS
DEPTHS 000-700 KM.

Figure 3.1

relative to one another. The plates spread apart along the worldwide ocean ridge systems and rift zones. Elsewhere the plates converge, with one plate being subducted with respect to the other. Large amounts of literature have been published on various aspects of the plate tectonics theory (eg. see bibliography in BIRD & ISACKS,1972; BIRD,1980). The driving mechanisms, and plate movements over geodetic time scales have not yet been verified. Indeed not everyone accepts the plate tectonics hypothesis as a valid explanation of Earth dynamics (CAREY,1976; BELOUSSOV,1979).

Many plate models now exist (MORGAN,1972; LE PICHON,1968; MINSTER et AL,1974; MINSTER & JORDAN,1978; SOLOMON & SLEEP,1974; LE PICHON et AL,1973). Essentially similar, these models depict the plate boundaries and motion. The plate velocities have been obtained from sea floor spreading rates determined from magnetic anomalies, transform fault azimuths and earthquake slip-vectors (MINSTER & JORDAN,1978; LAMBECK,1981a). They therefore represent averages over millions of years.

The internal stability of tectonic plates is important because the average plate motions determined by geological and geophysical methods are dependent on assumptions about the internal rigidity of the plates. If the viscosity of the asthenosphere is in most places similar to the value determined from post-glacial rebound data, then it is very difficult to imagine how the present rates could differ from the average rates away from the plate boundaries. However, it should be remembered that the viscosities derived from post-glacial rebound data have been obtained only on continental plates, and that the values could be considerably lower elsewhere, particularly under substantial parts of the fast moving ocean plates. As the assumed viscosity is decreased, changes in the stresses on the faults at the front and sides of plates could have a stronger effect on the overall motions and could cause them to be episodic. Simple calculations moreover, show that the plates could be quite compressible. For example, if the viscosity of the asthenosphere is ignored altogether, a 5000Km square plate which was fixed at the front and had no shear stress on the sides, could be compressed by about 20 m before the average stress on the front becomes sufficient to overcome the frictional forces along the fixed edge (STOLZ & LAMBECK,1983). This is roughly equivalent to the amount of energy released in a medium sized earthquake and corresponds to about 150 years accumulated motion of the Australian plate relative to the Antarctic

plate. The seismic activity within continents suggests that plates as a whole undergo differential stresses (SYKES,1978). Hence it is important to check the basic stability of the major plates before attempting to infer present rates of relative motion from changes in position. It is also important to understand the intraplate stresses that can cause hazardous earthquakes. Thus there is a need for much denser high-precision geodetic networks than presently available. (LAMBECK,1981a).

Measurements across the San Andreas fault in the United States indicate that plate movements are occurring now (SMITH et AL,1979b; SAVAGE et AL,1981). The motions at the plate boundaries however do not necessarily reflect the motion of the plate as a whole. After determining the stability of the plates the role of extra-terrestrial positioning techniques is to verify the plate tectonics hypothesis by directly measuring the relative motions of the plates. The fundamental problem of understanding the mechanisms that cause plate motion can then be studied. Progress can be made in minimising the hazards of earthquakes if the mechanisms can be defined. Moreover since pre-seismic deformation does occur, it needs to be understood as a premonitory phenomena for earthquake hazard reduction (LAMBECK,1981a).

Tectonic plate motion is believed to be the result of one or a combination of the following (NASA,1979):

(i) Coupling of plates to convective flow in the underlying mantle;

(ii) Negative buoyancy of subducted slabs; and

(iii) Gravitational sliding down from thermally maintained highs at the ocean ridges.

The important geophysical questions which are of relevance to geodesy, which must be answered in order to fully understand the forces that drive the plates are (NASA,1979):

(i) Are the plates moving smoothly and steadily in the same direction and with the same rates as they have been doing for periods of millions of years as determined from geological and geophysical evidence?

(ii) Does an individual plate move uniformally and smoothly as a rigid body, sliding over the underlying asthenosphere, or is the movement episodic?

(iii) What is the nature of the deformation of the plates if they are not rigid?

These questions have in common the problem of measuring relative position and movement between points on the Earth's surface. Over continents for distances less than 100 Km classical ground-based geodetic surveying methods give adequate accuracy. However, for distances up to thousands of kilometres the accuracy of these measurements deteriorates to make them unsuitable for geodynamic applications. In the last decade, space technology has developed to an accuracy which can meet these needs. The two principal space techniques, which will be used to realise geodynamic research goals are VLBI and SLR (FLINN,1981).

Geodetic measurements can make contributions in regions which are relatively close to plate boundaries, leading to better understanding of earthquake mechanisms and stress propagation as well as lithosphere and mantle rheology. It should be noted that geodetic measurements cannot provide information on movements of the lithosphere with respect to the mantle (LAMBECK,1981a). This is an important limitation for interpreting the dynamics of the Earth's interior from geodetic measurements.

Investigations into Earth dynamics can be approached from a global or regional scale. Plate tectonics is part of Earth dynamics, whereas satellite tracking data is used for other geodynamics projects as well. The deployment of the available measuring instruments has been proposed to fulfill both global and regional requirements (NASA,1979).

3.2 MEASUREMENT PROGRAMS for GLOBAL GEODYNAMICS

A global network of tracking stations is required for optimum gravity field modelling and monitoring Earth rotation. Gravity field and Earth rotation models are in turn important for modelling observations for other geodynamic investigations.

Although the laser tracking station network has been designed to satisfy geodynamic requirements, some rearrangement may be needed in order to fulfill the needs of specific projects (BENDER,1981). In principle satellite tracking techniques can be used to determine crustal strain on a global scale. The TRANET Doppler system, for which data has been collected since 1962 has been used for global tectonic calculations (ANDERLE,1978; MALYEVAC & ANDERLE,1979; McLUSKEY,1979). However these determinations resulted in spurious values for a few of the plate velocities. The results suggest that there are many error sources which

are unaccounted for. The propagation of errors from refraction and gravity modelling among others need to be carefully assessed for these solutions. The large amounts of data and computer time used for these results also show that it is probably more practical to examine regional areas in greater detail and build up a global model in stages.

The following sections describe two regional geodynamics experiments. These are in progress now. One experiment is in the United States and the other is in Australia. The author has a significant role in the latter.

3.3 SAN ANDREAS FAULT EXPERIMENT (SAFE)

A plan was devised in 1972 to systematically monitor the motion of the San Andreas fault in California, U.S.A., using laser range measurements to artificial satellites. Design studies were completed in 1973 (SMITH et AL,1973). In these studies, the positions of tracking stations located at San Diego and Quincy in California were estimated for an 8 year period using range measurements to the BE-C satellite. Error sources modelled were: GM, the Earth's gravity field, range biases, solar radiation pressure, atmospheric drag and San Diego tracking station coordinates. The study showed that with 1973 estimates of error magnitudes the baseline precision (r.m.s.) would be 10cm.

It is interesting to compare the results of the simulation study with those obtained from real data. The two tracking sites were occupied in 1972, 1974 and 1976. The Bear Lake station was added as an extra site in 1976. Range measurements were made to the BE-C satellite. A dramatic improvement in tracking quality seems to have occurred between 1972 and 1974, as the r.m.s. fits to the tracking data were reduced by about half an order of magnitude during this period. The data were very carefully selected so that force model errors would be similar at each epoch. The baseline velocities should therefore be practically unaffected by gravity model error (CHRISTODOULIDIS et AL,1981). The motion across the plate boundary was estimated to be 9 ± 3 cm/year. This agrees with terrestrial measurements in the area (SMITH et AL,1979b; SAVAGE et AL,1981). Further measurements are obviously needed to unambiguously determine if the detected motion is real.

Since then range measurements to LAGEOS have been used to determine the same baselines. These have been compared with the SAFE baseline estimates, yielding results usually consistent within the formal precision for each baseline (SMITH et AL,1979a). VLBI

measurements have been made also. The results for the same baselines from various extra-terrestrial techniques have been compared (see chapter 1, p3).

Investigations are continuing in the San Andreas fault area. CHRISTODOULIDIS & SMITH (1980) and CHRISTODOULIDIS et AL (1981) have investigated the possible accuracies obtainable with the deployment of the TLRS in the San Andreas Fault region. These results are described in Chapter 6. An experiment which was designed for Australian participation in the crustal dynamic program is described in the next section.

3.4 AUSTRALIAN PLATE DEFORMATION EXPERIMENT

Figure 3.2 summarizes the tectonics of the Australian region. At the Ninetyeast Ridge, the Indian sub-continent sector of the Australian plate appears to be meeting more resistance to the plate's general north-ward motion than the Australian sector. The area around the ridge is either a zone of major deformation or an active plate boundary (STEIN & OKAL,1978). To the south, the Australian plate is separated from the Antarctic plate by the South-east Indian Ocean Ridge and the relative motion between the two plates is estimated at about 14cm/year with Australia moving northwards (Bureau of Mineral Resources, 1979). To the north, in the tectonically complex region of Indonesia and Papua-New Guinea, the Australian plate is subducting smoothly at the Java Trench, and to the east the plate is in collision with the Pacific plate. Australia proper is relatively aseismic. However, there are regions of concentrated seismic activity that indicate stress accumulation. The Adelaide geosyncline in South Australia is a good example of this (BROWN et AL,1968). Fault plane solutions of earthquakes and in-situ stress measurements suggest a near uniform stress field across the continent and it appears the plate is subject to deformation (WEISSEL et AL,1980).

NASA's crustal dynamics program (NASA,1979) includes a campaign to measure tectonic motion and plate deformation in the South-west Pacific region. A complementary program to study the crustal dynamics of the Australasian region using satellite laser ranging methods was proposed (K.LAMBECK,unpublished manuscript,1980). It was suggested that the high accuracy laser range measurements to the LAGEOS satellite could be used to measure, and periodically remeasure, the baselines between the existing tracking stations. Transportable tracking stations could also be deployed at critically selected sites throughout the region. In this way relative motions could be determined. An Australian response to

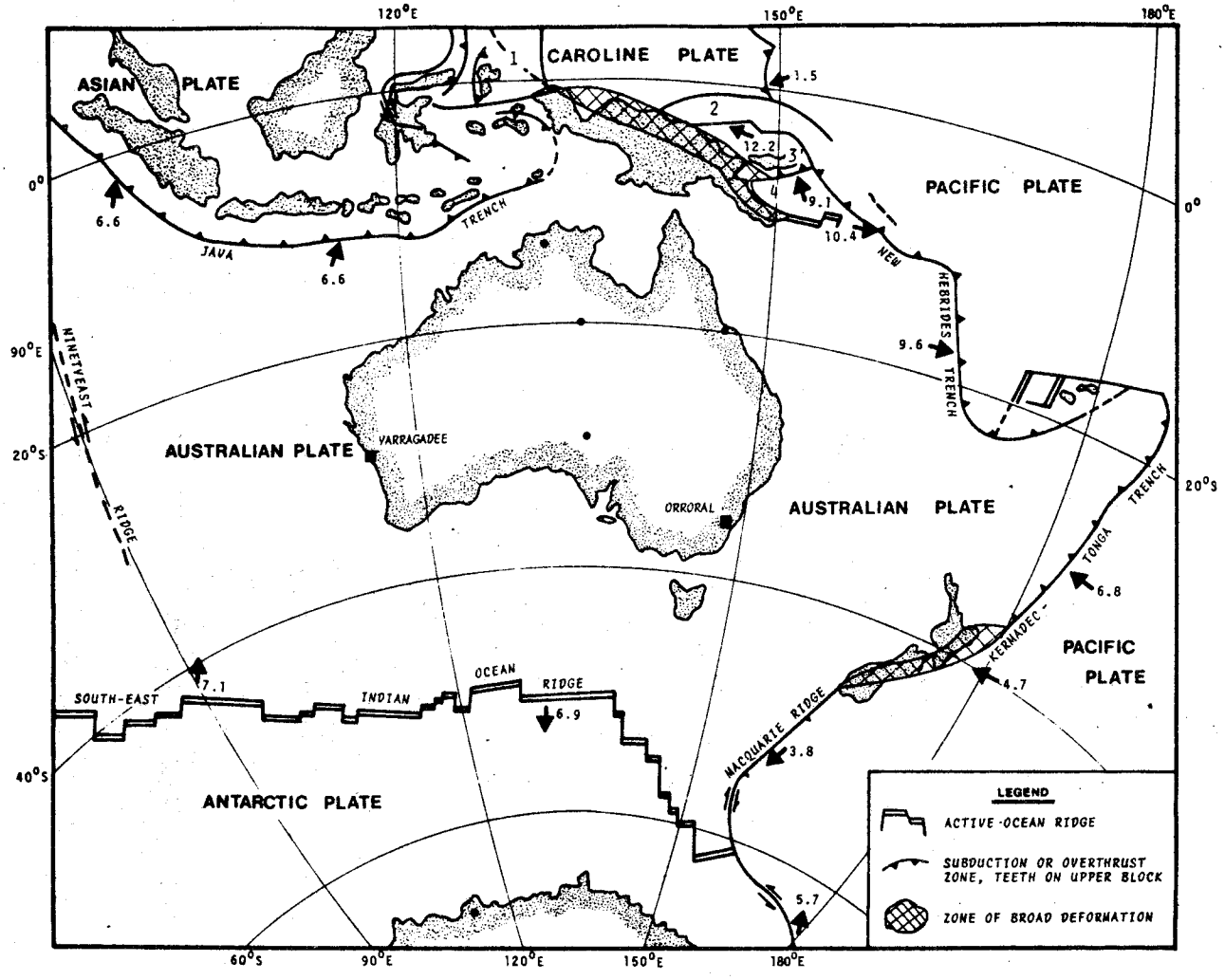

Figure 3.2

Generalised Plate Tectonics of the Australasian Region

NASA's Crustal Dynamics Program was prepared by STOLZ (1980). The main objectives of the Australian study are:-

(i) to independently test the long term reliability of the satellite laser ranging method of relative position determinations;

(ii) to determine the large scale deformation of the Australian plate; and

(iii) to measure the relative motions of the plates in the Australian region.

The project is part of the Australian response to the Lithosphere Project. Part of this dissertation involved a preliminary evaluation of the laser range processing capabilities with the computing resources available to the Department of Geodesy, University of New South Wales. These investigations are presented in chapter 7. Later investigations

are planned to evolve as follows. Initially, the relative geological stability of the Australian continent over geodetic time scales will be used to assess the accuracy of the laser data and computational processes used to determine baselines. This will be achieved by monitoring the baseline distance between Orroral Valley in the Australian Capital Territory and Yarragadee in Western Australia using the laser data to the LAGEOS satellite. Later, if the errors can be kept small enough, the range data will be used to assess the large scale east-west deformation of the Australian region. These are long term goals and their achievement is dependent on the availability of tracking data and the deployment of NASA's mobile tracking stations. The tracking station sites other than Yarragadee and Orroral have not as yet been finalised (STOLZ & MASTERS,1982). Therefore only proposal (1) can be suitably calculated at this stage. Proposals (2) and (3) can be determined only to a limited extent with existing data. This work is now well underway (Chapter 9; STOLZ & MASTERS,1982).

C H A P T E R 4

SATELLITE MISSIONS

The two satellite missions relevant to the investigations in Chapters 6 and 7 are described in this chapter. A technical description of the satellites together with the aims of the mission are presented. Important research work in the field is cited.

4.1 GEOS-3

The GEOS-3 spacecraft is shown in Figure 4.1. Orbit and satellite parameters are given in Table 4.1. The GEOS-3 project was designed to fulfill numerous aims in many interdisciplinary fields. These include improving man's knowledge of the Earth's gravity field, the size and shape of terrestrial geoid, deep ocean tides, sea state, ocean current structure, crustal structure, solid Earth dynamics and remote sensing technology (STANLEY,1979). The project was initiated in the changeover period between the National Geodetic Satellite Program and the Earth and Ocean Dynamics Application Program.

Relevant mission objectives were (GEOS-C,1974):

(i) To perform an in orbit satellite altimeter experiment in order to determine the feasibility and utility of a spaceborne radar altimeter to map the topography of the ocean surface with an absolute accuracy of ± 5 m and a relative accuracy of 1-2 m. The feasibility of measuring the deflection of the vertical at sea would also be determined. Information contributing to the technology leading to a future operational altimeter system with a 10 cm measurement capability would also be obtained.

(ii) To support the comparison of new and established geodetic and geophysical measuring systems including; radar altimeter, satellite to satellite tracking, C-band, S-band, laser and Doppler tracking systems.

(iii) To investigate solid earth dynamic phenomena such as polar motion, fault motion, Earth tides and so forth.

(iv) To refine orbit determination techniques.

The radar altimeter proved to be extremely reliable. It was designed to operate for only 1500 hours and was still working after 1900 hours of operation (STANLEY,1979). The altimetry data were systematically collected, so that the coverage is nearly global. SSH

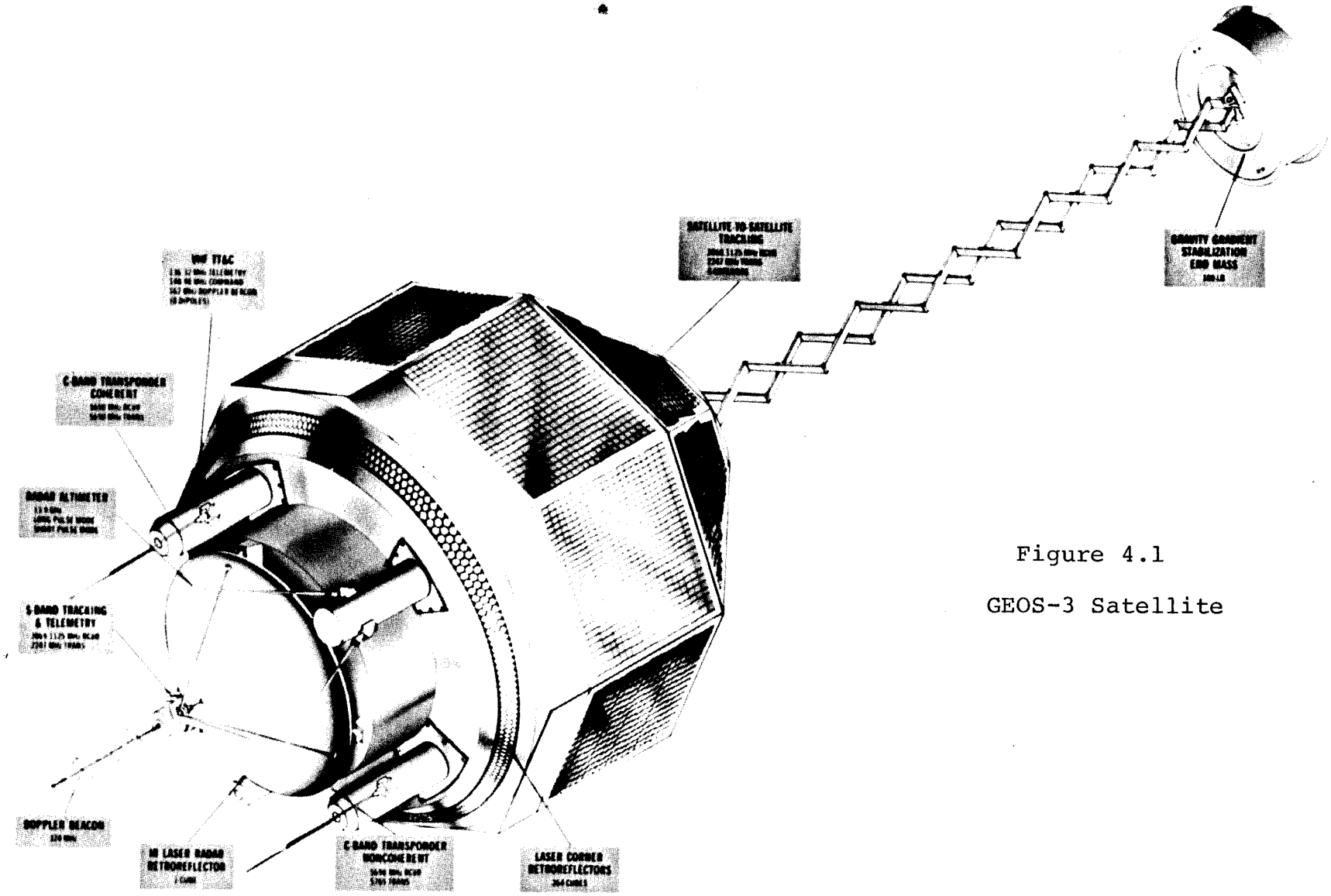

Figure 4.1

GEOS-3 Satellite

data is available between latitudes 65°N and 65°S at a minimum spacing of 0.5°. Approximately half the data is illustrated in Figure 6.2 (Chapter 6).

The mission was regarded as a success in each of the objectives for which it was designed. The one exception was the ocean tides (STANLEY,1979). Problems with tidal estimation are investigated in Chapter 6.

TABLE 4.1

GEOS-3 SPECIFICATIONS

Launch	9th April 1975
Mass	345.9 Kg
Number of Retro-reflectors	264
a	7217 Km
e	0.001
i	115°
Perigee Height	846 Km
Apogee Height	865 Km
Average Height	843Km
Period	101.7 min
$\dot{\Omega}$	2.°7 / day
$\dot{\omega}$	-0.°3 / day

The GEOS-3 altimetry data have been most successfully used for studies related to the Earth's gravity field (see Jour. Geophys. Res. Vol 84 No B8,1979). Several oceanographic studies were also undertaken. These mainly involved the Gulf Stream off the east coast of the United States. The altimeter is capable of distinguishing phenomena with amplitudes greater than 20 to 30 cm and spatial wavelengths greater than 50 Km (BRAMMER,1979). The altimetry also contain information on eddies and tides (COLEMAN,1981).

The mission clearly demonstrated potential for achieving real time results pertaining to physical oceanography (MATHER et AL,1979). However altimetry data suffers from limitations for the successful determination of many phenomena. The main limitations are associated with orbital and geoidal which errors cannot often be separated from

geodynamic features. The ocean tidal spectrum, in particular, has so far eluded all altimetry investigations although encouraging results have been obtained from refined data sets (MASTERS et AL,1979;1980; COLEMAN,1981).

It is appropriate to compare the mission achievements with its aims. By far the most common application of GEOS-3 altimetry data has been to improve models of the Earth's gravity field, especially in ocean areas. Over ocean areas the altimetry derived SSH data provided an important new source of high frequency information on the geoid. Large amounts of GEOS-3 tracking and altimetry data have been incorporated into the latest Goddard Earth Models (LERCH et AL,1977, 1978a). Literature exists on other uses such as the departures of the sea surface from the geoid. This information can be used for ocean dynamics studies as was outlined in Chapter 2. The work of MATHER et AL at the University of New South Wales was progressing towards the use of satellite data to synoptically monitor ocean currents (MATHER,1974a, 1974b, 1974c, 1975a, 1975b, 1976, 1977, 1978a, 1978b, 1978c, 1978d, 1978e; MATHER & COLEMAN,1977; MATHER & RIZOS,1979; MATHER et AL,1976a, 1976b, 1977a, 1978a, 1978b, 1979; COLEMAN,1979, 1981; RIZOS,1980a, 1980b). This work is not of specific relevance here. Hence only the publications are cited. Other publications in the same field are (LEITAO et AL,1977, 1978, 1979a 1979b; DOUGLAS & GABORSKI,1979; HUANG et AL,1978; CHENEY & MARSH,1980; GORDON & BAKER,1980; WUNSCH & GAPOSCHKIN,1980).

Other mission achievements include:

GEOS-3 orbital perturbations have been used to improve the determination the Earth's gravity field (LERCH et AL,1977) and improve knowledge of Earth tides (FELSENTREGER et AL,1979).

The tracking data has been used to determine tracking station positions (DUNN et AL,1979).

Satellite to satellite tracking data is being examined as a potential source of additional information on the gravity field (MARSH et AL,1977; KAHN et AL,1981).

The GEOS-3 altimetry data are analysed in this dissertation for orbit perturbations and ocean tides. The reduction of orbital errors is important for ocean dynamics applications of altimetry data. The investigations are presented in Chapter 6.

4.2 LAGEOS

The LAGEOS satellite is illustrated in Figure 4.2. It was launched specifically for geodynamics research and is NASA's first satellite designed solely for laser ranging experiments. The mission has been operated in two phases since the launch on May 4,1976. Phase 1 was devoted to the development of a precise ephemeris for the satellite and of laser tracking systems. Phase 2 involves the acquisition and analysis of precision satellite laser ranging data to yield information on the dynamic behaviour of the Earth. One of the principal goals of the LAGEOS mission is to provide data for NASA's Geodynamics Program as outlined in chapter 1 and Section 3.1. LAGEOS plays a dominant role in NASA's Crustal Dynamics Program, which aims to investigate plate movement and crustal deformation using space techniques.

The satellite provides a precise and essentially permanent target in space for laser ranging and investigation of :-

(i) relative movement and deformation of the Earth's tectonic plates;

(ii) variations in the motion of the Earth's polar axis and the Earth's rotation;

(iii) improved geodetic reference systems;

(iv) solid Earth and ocean tides; and

(v) satellite orbital perturbations.

LAGEOS was launched into a nearly circular orbit with a 5900 Km altitude (NASA,1978), so that only 100 spherical harmonic coefficients in the Earth's gravity field give orbit perturbations, which are 1 cm or more in amplitude (LERCH et AL,1980; CHRISTODOULIDIS et AL,1981). Except for a few resonance terms these coefficients are mostly below degree ten. The satellite is covered with 426 corner cube reflectors. 422 of these are fused silica and operate through the visible and near infra-red portions of the spectrum. The remaining four are Germanium, which is effective in the middle infra-red region (NASA,1978). The satellite is spherically symmetric, of aluminium, with a brass core and is therefore of a high density. Consequently atmospheric drag and solar radiation perturbations are both minimal and almost constant in time.

The LAGEOS satellite and orbit specifications are given in Table 4.2. A typical groundtrack pattern over the Australian region is depicted in Figure 7.1 (Chapter 7). As many as seven passes per day can be observed from one geographical location.

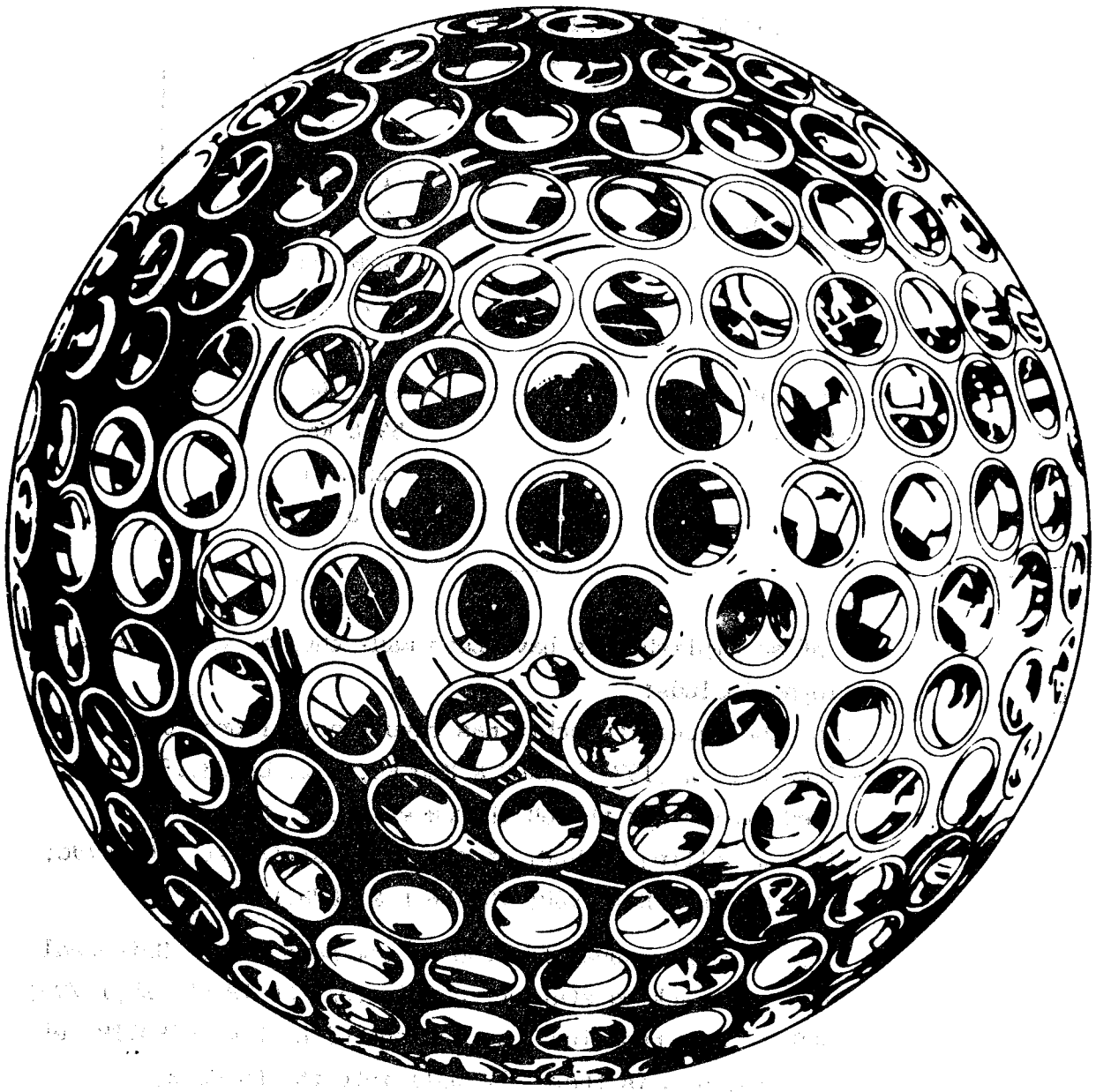

Figure 4.2

LAGEOS Satellite

TABLE 4.2

LAGEOS SPECIFICATIONS

Launch Date	May 4, 1976
Diameter	60 cm
Mass	411 Kg
Number of Reflectors	426
a	12265 Km
i	109°
e	0.004
Perigee Height	5858 Km
Apogee Height	5958 Km
Period	225 min
$\dot{\Omega}$	0.°3 / day

A number of accomplishments have been made through the analysis of LAGEOS data. These include:

- Analysis of the satellite orbit has resulted in improved gravity modelling (LERCH et AL,1977; LERCH & KLOSKO,1981; LERCH,1982).
- an improved value for the GM (LERCH et AL,1978b).
- ocean tide modelling (TAPLEY et AL,1979; SMITH et AL,1979c; CHRISTODOULIDIS & SEIFFERT,1980; TORRENCE & DUNN,1980).

The data has also been used for the determination of Universal time, pole position, tracking station coordinates (SMITH et AL,1979a; TAPLEY et AL,1980), and baselines variations with time (SMITH et AL,1982). The LAGEOS mission is therefore well into the Phase 2.

The use of range data to LAGEOS from the Australasian region for determining crustal movement is described in Section 3.4 and investigated further in Chapters 7 and 8.

CHAPTER 5

SATELLITE GEODESY

5.1 INTRODUCTION

An overview of satellite geodesy theory is presented in this Chapter. The aim is to present a summary of the information which forms the basis for GEODYN usage and later investigations. Topics include estimates of error sources in dynamic models. These errors are referred to in later chapters.

The principles of using satellite observations to determine geodetic and geodynamic parameters can be categorised as follows; satellite dynamics, Earth rotation, estimation theory and observation processing. The first three categories involve definitions of reference systems.

Satellite dynamics involves the determination of satellite position by integration of the equations of motion. The equations of motion are expressed in terms of contributions from many phenomena, like the geopotential, luni-solar potential, planetary potential, radiation pressure, earth tide potential and atmospheric drag. The modelling of each force for a near-Earth satellite is a complicated problem. The geopotential is particularly important for orbit determination and geophysics. Specific descriptions of dynamic models are beyond the scope of this chapter. The reader is referred to KAULA (1966), LERCH et AL (1974) and MARTIN et AL (1976). Spherical harmonic representation of the gravity field is described in Appendix B. Dynamic theory, which is the basis for later investigations, is described in Section 5.2. Error sources in force models are also described in more detail in Chapter 7.

Earth rotation models are fundamental for reducing any extra-terrestrial measurement. In this dissertation Earth rotation refers to the complete spectrum of Earth rotation, that is precession, nutation, polar motion and length-of-day. Models are described in Section 5.3.

Statistical estimation theory is needed to combine thousands of observations to determine particular parameters and to assign precisions and accuracies to those parameters. Procedures have an important bearing on geodynamic applications of satellite geodesy. The implications are discussed in Chapter 8. Least squares techniques are also fundamental

for all data analysis. Standard procedures are described in Section 5.4.

Observation processing involves the conversion of signals detected by tracking instruments to observations, which can be analysed for scientific results. For example, photon returns detected at a laser tracking station must be converted to time delays or range measurements for geodetic analysis. These conversions were considered to be outside the scope of this dissertation. Range measurements and UTC times are usually received as basic observation types at the University of New South Wales. The only corrections and conversions necessary are for refraction and timing biases.

Reference systems are implicitly defined in any dynamic theory. They are needed to model observations between satellites and the Earth. Hence in satellite geodesy the transformation between the inertial reference system for satellite motion and the terrestrial reference system, which is "fixed" to the Earth's surface is required. For near-Earth satellites the transformation is usually made to include only Earth rotation. This is achieved by adopting the geocentre as the origin of the inertial system.

The reference systems used in satellite geodesy are similar to astronomical reference systems and similar terminology has been adopted. In practice, the actual definitions are not necessarily the same. Care is needed to make the different reference systems compatible. A few of these problems mentioned in Chapters 7 and 8. NAGEL (1976) describes the reference systems in detail and also investigates a few associated problems. Much scientific debate has been expended on reference system definitions and their associated problems (GAPOSCHKIN,1981; GAPOSCHKIN & KOLACEK,1981).

The definition of time is also important since it enters as the independent parameter in dynamic theory. Transformations are needed to convert between the various systems of atomic time, universal time and ephemeris time, that is time systems are used to model Earth rotation and satellite motion.

All these topics, which are in themselves highly specialised research areas are all needed for dynamic satellite geodesy. Geodynamic phenomena of interest can be investigated with satellite geodesy by using the best models for all these phenomena to represent range data. The problem yet to be solved is to separate geodynamic phenomena like plate tectonic motion from the modelling effects of dynamic forces on

the satellite and Earth rotation.

The following flow diagrams (Figure 5.1) show the information needed to reduce and model range and time measurements in order to estimate geodetic coordinates. All input information is a potential error source to be minimised or remodelled.

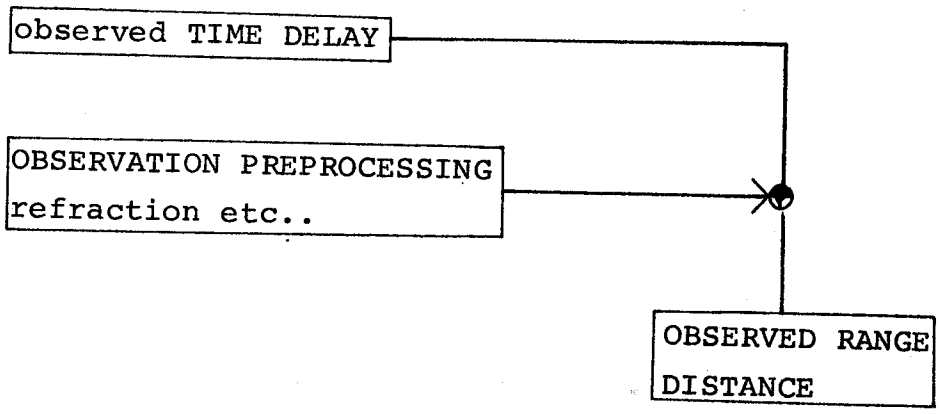

Figure 5.1a

Modelling a range and time observation

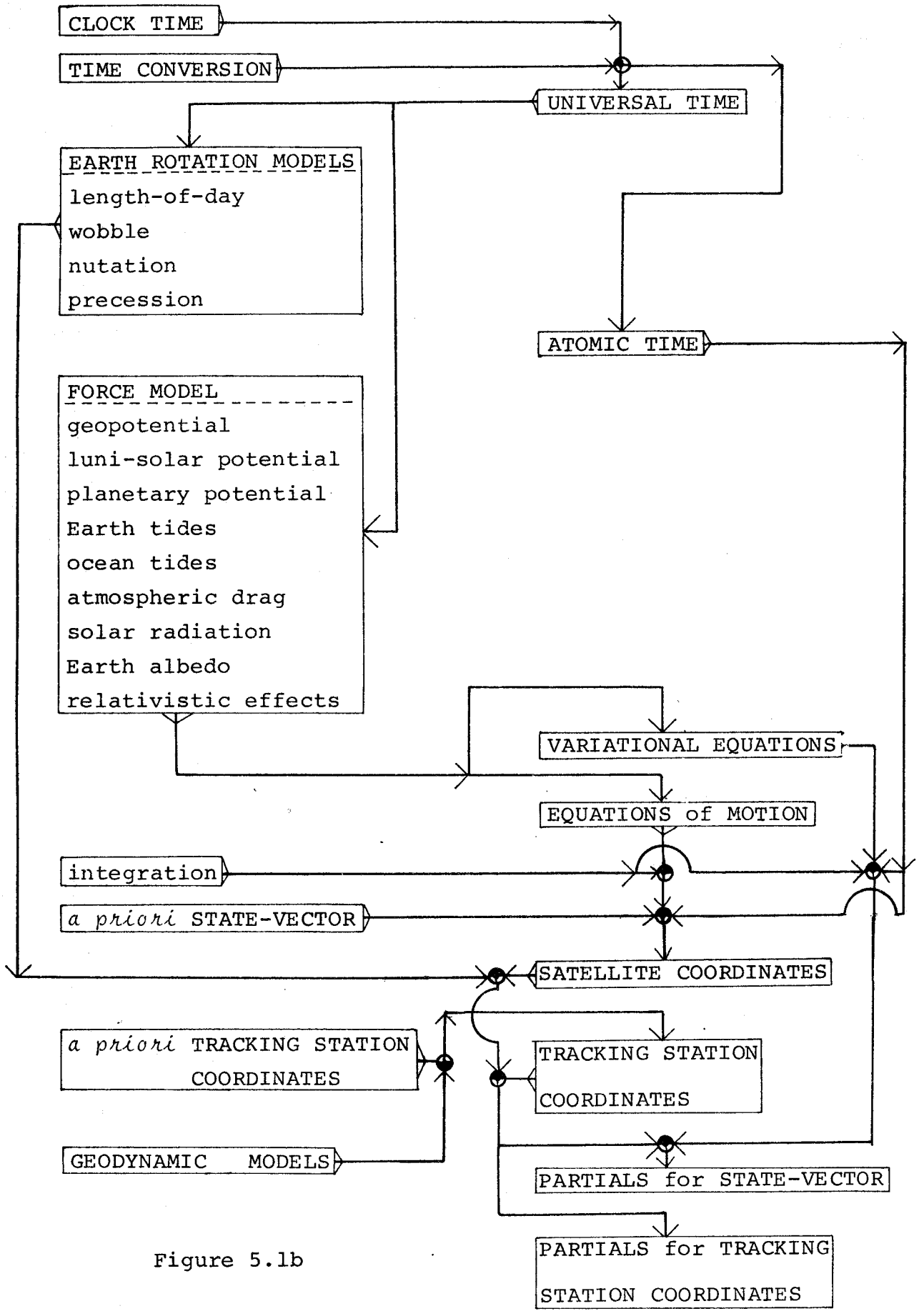
CLOCK TIME
TIME CONVERSION
UNIVERSAL TIME
EARTH ROTATION MODELS
length-of-day
wobble
nutation
precession
ATOMIC TIME
FORCE MODEL
geopotential
luni-solar potential
planetary potential
Earth tides
ocean tides
atmospheric drag
solar radiation
Earth albedo
relativistic effects
VARIATIONAL EQUATIONS
EQUATIONS of MOTION
integration
a priori STATE-VECTOR
SATELLITE COORDINATES
a priori TRACKING STATION COORDINATES
TRACKING STATION COORDINATES
GEODYNAMIC MODELS
PARTIALS for STATE-VECTOR
PARTIALS for TRACKING STATION COORDINATES

Figure 5.1b

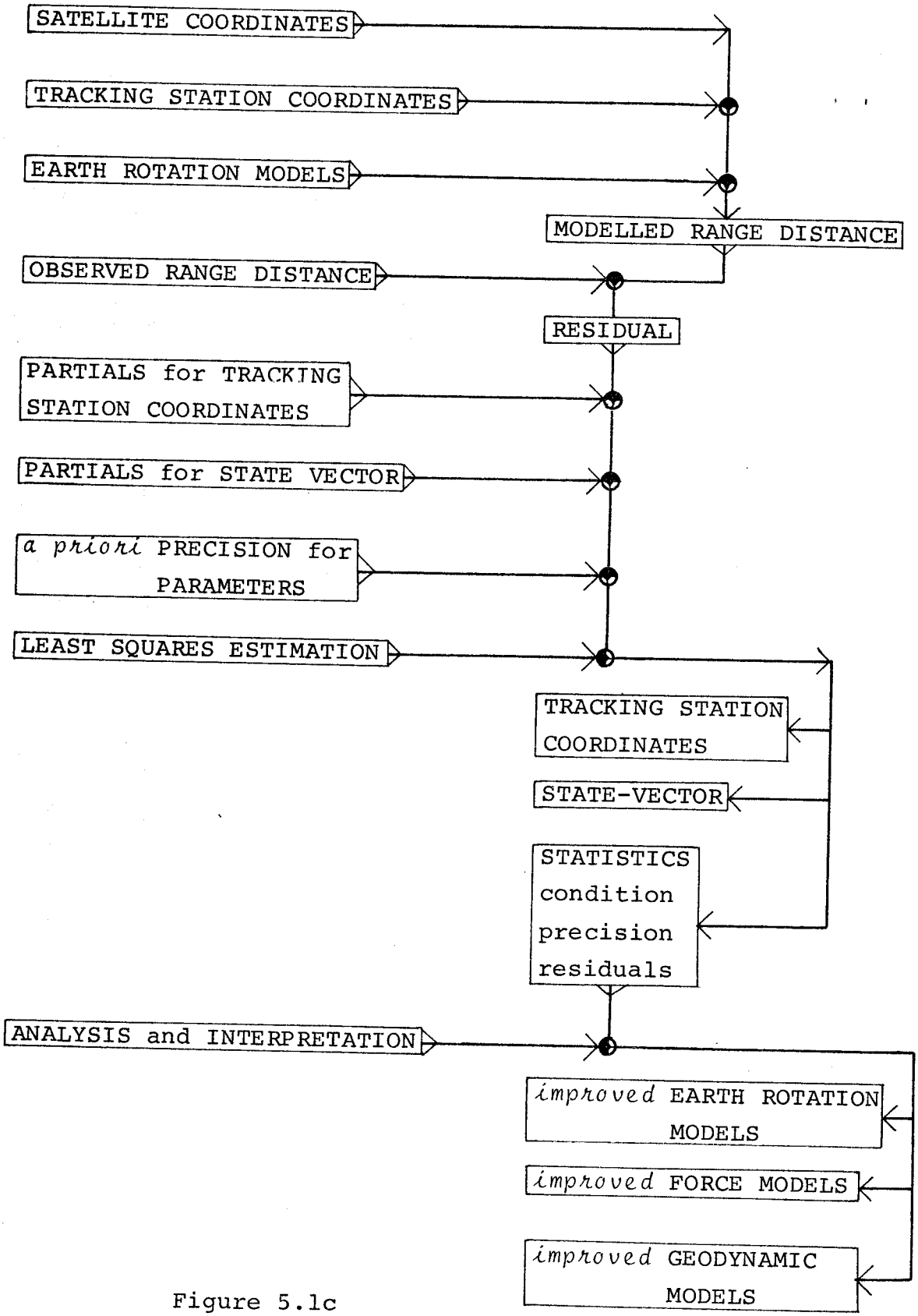
SATELLITE COORDINATES
TRACKING STATION COORDINATES
EARTH ROTATION MODELS
MODELLED RANGE DISTANCE
OBSERVED RANGE DISTANCE
RESIDUAL
PARTIALS for TRACKING STATION COORDINATES
PARTIALS for STATE VECTOR
a priori PRECISION for PARAMETERS
LEAST SQUARES ESTIMATION
TRACKING STATION COORDINATES
STATE-VECTOR
STATISTICS
condition
precision
residuals
ANALYSIS and INTERPRETATION
improved EARTH ROTATION MODELS
improved FORCE MODELS
improved GEODYNAMIC MODELS

Figure 5.1c

5.2 SATELLITE MOTION and DYNAMIC MODELS

The derivation of the equations of motion for a satellite is dealt with in standard celestial mechanics texts (for example see BROUWER & CLEMENCE,1961; MOULTON,1970; BATE et AL,1971; HAGIHARA,1972). KAULA (1966) treats the problem analytically. He derives the equations of motion for a central force model and a perturbed gravitational field using the Lagrangian treatment. This involves relating orbital parameters to anomalies in the Earth's gravity field, commonly termed the disturbing potential. His development is useful for understanding simple orbital motion and the nature of orbital errors.

The satellite position can be obtained by integrating the equations of motion. These may be written as (MARTIN et AL,1976):-

$$\ddot{\mathbf{r}} = \text{grad } U + \mathbf{A} \qquad (5.1)$$

where U is the geopotential, which is conventionally expressed in terms of spherical coordinates (Appendix B) and,

A accounts for other forces due to atmospheric drag, Earth tides, Ocean tides, solar radiation pressure and luni-solar potentials.

A reference system is defined by the spherical coordinate system adopted for the spherical harmonic expansion of U. In order to study the perturbations of near Earth satellites these spherical coordinates are conveniently transformed to Keplerian elements. The potential can be expressed as (KAULA,1966):-

$$V = \sum_n \sum_m \sum_p \sum_q V_{nmpq} \qquad (5.2)$$

where

$$V_{nmpq} = \frac{GM\, a_e^n}{a^{n+1}} F_{nmp}(i)\, G_{npq}(e)\, S_{nmpq}(\omega, M, \Omega, \theta)$$

$$2 \leq n \leq \infty \quad , \quad 0 \leq p \leq n \quad , \quad -\infty \leq q \leq \infty$$

$$S_{nmpq} = \begin{bmatrix} C_{nm} \\ S_{nm} \end{bmatrix}_{n-m\ \text{odd}}^{n-m\ \text{even}} \cos\psi_{nmpq} + \begin{bmatrix} -S_{nm} \\ C_{nm} \end{bmatrix}_{n-m\ \text{odd}}^{n-m\ \text{even}} \sin\psi_{nmpq}$$

$$\psi_{nmpq} = (n-2p)\omega + (n-2p+q)M + m(\Omega - \theta)$$

and a e i ω Ω M are Keplerian elements, respectively semi-major axis, eccentricity, inclination, argument of perigee, right ascension of the node and mean anomaly respectively.

θ is the rotational position of the Earth (sidereal time),

a_e is the semi-major axis of the Earth,

F are the inclination functions and,

G are eccentricity functions.

G(e) is proportional to $e^{|q|}$ and, as the eccentricities of most orbits are small, the summation over the index q needs to be carried out only over a small number of terms; that is $-2 \leq q \leq 2$ (KAULA,1966; LAMBECK,1980).

The acceleration of the satellite due to perturbing forces is required. This is obtained from the Lagrangian form of the equations of motion (BROUWER & CLEMENCE,1961; KAULA,1966), that is.

$$\frac{da}{dt} = \frac{2}{n\,a}\frac{\partial V}{\partial M}$$

$$\frac{de}{dt} = \frac{(1-e^2)}{n\,a^2\,e}\frac{\partial V}{\partial M} - \frac{(1-e^2)^{1/2}}{n\,a^2\,e}\frac{\partial V}{\partial \omega}$$

$$\frac{d\omega}{dt} = \frac{-\cos i}{na^2(1-e^2)^{1/2}\sin i}\frac{\partial V}{\partial i} + \frac{(1-e)^{1/2}}{na^2 e}\frac{\partial V}{\partial e}$$

$$\frac{di}{dt} = \frac{\cos i}{na^2(1-e^2)^{1/2}\sin i}\frac{\partial V}{\partial \omega} - \frac{1}{na^2(1-e^2)^{1/2}\sin i}\frac{\partial V}{\partial \Omega}$$

$$\frac{d\Omega}{dt} = \frac{1}{na^2(1-e)^{1/2}\sin i}\frac{\partial V}{\partial i}$$

$$\frac{dM}{dt} = n - \frac{1-e^2}{na^2 e}\frac{\partial V}{\partial e} - \frac{2}{n\,a}\frac{\partial V}{\partial a} \qquad (5.3)$$

The perturbations due to specific gravity field harmonics can be obtained from Equations 5.2 and 5.3 (KAULA,1966; LAMBECK,1980). Equation 5.3 can be integrated either by numerical methods or analytically to obtain variations in the Keplerian elements with time. KAULA (1966,p40) and LAMBECK (1980,p134) give theoretical solutions for the integrated perturbations of the orbital elements. These are useful for estimating orbital errors and tidal perturbations (KOZAI,1968; LAMBECK et AL,1974; BRETREGER,1978; LAMBECK,1980).

The frequency of gravitational perturbations is governed by $\dot{\psi}_{nmpq}$ (WAGNER & KLOSKO,1977), that is, gravity model perturbations are periodic with respect to ω, M, Ω θ. As the perturbations are proportional to $1/\dot{\psi}$ large effects occur when $\dot{\psi}$ is small. Deep resonance occurs when (WAGNER & KLOSKO,1977)

$$\dot{\psi} = 0 \qquad (5.4)$$

This happens when there is exact commensurability between the satellite motion and the Earth's rotation. In this case, longitudinal terms of the

gravity field yield excessively large orbit perturbations. Generally other forces are acting on the satellite, so that the orbit simply passes through this condition. It is then referred to as shallow resonance (WAGNER & KLOSKO,1977; KLOSKO & WAGNER,1979).

The harmonics for n-2p+q=0 give rise to m-daily perturbations. These are independent of the mean anomaly and are a dominant source of low degree and order gravity field information (CHRISTODOULIDIS et AL,1981).

WAGNER & KLOSKO (1977) classify the perturbations according to frequency by rewriting $\dot{\psi}$ as follows:-

$$\dot{\psi}_{mqk} = -q\dot{\omega} + \dot{\psi}_{m0k} \qquad (5.5)$$

where $k = n-2p+q$ and,

$$\dot{\psi}_{m0k} = k(\dot{M} + \dot{\omega}) + m(\dot{\Omega} - \dot{\theta}) \qquad (5.6)$$

These equations indicate that terms in resonance, with m-daily and short period variations will have $\dot{\psi}_{m0k}$ as a dominant fast frequency and $-q\dot{\omega}$ as a secondary slow frequency. A fast period is less than five days whereas a typical slow period is 180 days. These frequencies, which depend on m, define the longitude dependent gravitational harmonics for the majority of geodetic satellites (WAGNER & KLOSKO,1977). Sparse tracking data does not sample the short-period perturbations very well. Hence the coefficients of gravity field models which mainly cause short-period perturbations are poorly determined as compared to those which cause long period and secular effects. Tesseral harmonics are generally poorly determined compared to zonal harmonics. We could expect these poorly determined harmonics to produce short-period orbital errors in ephemerides, which are used for other data types. These errors should be estimable in more continuous data types like GEOS-3 altimetry (WAGNER,1979).

Much information is available in tracking data for estimating tesseral harmonics of the gravity field. Knowledge of the frequencies (Equations 5.5 and 5.6) can be used to constrain gravity field models if adequate tracking data are available (KLOSKO & WAGNER,1979; BALMINO & REIGBER,1974; REIGBER & BALMINO,1976). It is also feasible to determine periods and amplitudes of dominant orbital errors for a specific satellite by determining the perturbations from poorly determined coefficients of the geopotential. In this way gravity field models can be tailored to the orbits of specific satellites by estimating the

coefficients which are sensitive to both the orbit and the tracking data (KLOSKO,private communication,1980). A tailored model has been developed for the LAGEOS orbit (LERCH & KLOSKO,1981; LERCH,1982). CHRISTODOULIDIS et AL 1981) list a few perturbations for LAGEOS. Noticeably, resonance effects are usually orders of magnitude larger than other short period and m-daily perturbations.

Analytical theory was employed when optical observations to satellites were common (ANDERLE & TANENBAUM,1974). GAPOSCHKIN (1973) used analytical integration for the Smithsonian Standard Earth Models. Numerical integration techniques however, are now preferred for solving the equations of motion and variational equations. Techniques are described by LERCH et AL (1974), MARTIN et AL (1976) and CAPPELLARI et AL (1976) and others. Cowell numerical integration techniques are employed in GEODYN to integrate the equations of motion and variational equations. The technique is well documented (BROUWER & CLEMENCE,1961; CAPPELLARI et AL,1976; MARTIN et AL,1976). Numerical methods are much more versatile and allow complicated force models to be incorporated into the dynamic theory. This means that they are much more applicable to reducing observations to near Earth satellites than analytical techniques. The latter do not adequately model satellite orbital perturbations for current tracking quality and quantity (ANDERLE & TANENBAUM,1974). However, analytical techniques are still very important and are used in combination with numerical methods (GAPOSCHKIN,1978). Numerical methods for solving the equations of motion and variational equations are also used by NSWC (ANDERLE,1974), University of Texas at Austin (SCHUTZ et AL,1979) and Massachussets Institute of Technology (ASH,1972).

SMITH (1978) summarises the dynamic models and their limitations. Especially mentioned are the models for the gravity field, atmospheric drag, solar radiation pressure and tides. Suggestions for possible improvements are made. GAPOSCHKIN (1978) gives a similar summary, and refers especially to the progress in analytical theory. PUTNEY (1980;1981) describes the improvements to GEODYN which were implemented by 1980 and also the revisions of the models for atmospheric density and albedo radiation pressure which are proposed for introduction to current software. These probably represent the current trends in dynamic modelling procedures and are typical of the models in most dynamic satellite software.

The accuracy of the dynamic modelling can be gauged from recent LAGEOS results (SMITH & DUNN,1980). Laser range data were fitted to the LAGEOS orbit with an r.m.s of 1 m for monthly spans of data. This result was obtained using the GEM10 gravity field model, luni-solar effects, solar radiation pressure and simple tide perturbations with the GEODYN system. Thirty two months of data were fitted to 15 m r.m.s. by including a simple along-track acceleration model. From the analysis of the long term LAGEOS orbit bounds for the errors in parts of the force model were estimated. The solar radiation pressure model is believed to be accurate to a few percent and the GEM10 odd zonal coefficients to better than 0.5 parts per thousand. The cause for the perturbation in the semi-major axis is unknown (RUBINCAM,1980).

From these analyses it is evident that the limitations in most of the force models are of little consequence for the high LAGEOS orbit. This is especially so if the orbital arc lengths are less than 30 days. Therefore the LAGEOS satellite, as intended, provides a stable target for estimating geodetic and geodynamic parameters. Nevertheless, the minimisation of residual gravitational and other force model errors is a major problem for crustal motion investigations, where centimetre accuracies are required. These problems are investigated in Chapter 7 and 8.

Similar problems occur with GEOS-3. This satellite is lower in altitude than LAGEOS and has a more complicated shape (Table 4.1, Figure 4.1). Gravitational perturbations and atmospheric drag effects are therefore significant. The radial component of the orbit can be determined to about 1.5 m r.m.s. (LERCH et AL,1978c). This is still too large for tidal analyses. Possibilities for removing orbital error in tidal investigations are investigated in Chapter 6.

5.3 EARTH ROTATION

The equations of motion for a general mass M are given by the Liouville equations

$$L_i = \dot{H}_i + \varepsilon_{ijk} w_j H_k \qquad (5.7)$$

$$H_i = I_{ij} w_j + h_i \qquad (5.8)$$

$$I_{ij} = \int_m (x_k x_k \delta_{ij} - x_i x_j)\, dm \qquad (5.9)$$

$$h_i = \int_m \varepsilon_{ijk} X_j \dot{X}_k \, dm \qquad (5.10)$$

where subscripts i = 1,2,3 refer to a set of Cartesian axes, with the origin at the geocentre and an angular velocity w_i,

L_i, H_i denote components of net external torque and angular momentum respectively,

I_{ij} is the inertia tensor,

h_i is the part of the H_i arising from the motion relative to the x_i system and,

repeated indices indicate summation.

The equations of motion can be solved by making assumptions about the Earth's rigidity. These assumptions affect the inertia tensor and angular momentum of the Earth (Equation 5.8 and 5.9). The non-rigidity of the Earth distorts and introduces new spectral features to the idealised rigid body solution of the equations of motion. To acquire centimetre accuracy in geodesy, rigid body solutions of the equations of motion are inadequate. The spectrum of Earth rotation may be divided as shown in Table 5.1 (ROCHESTER,1973). (The values in the table are not quoted as the latest estimates). The classifications and expected errors are described in more detail below:

(i) **Precession** is a long period motion of the Earth's equatorial plane with respect to its orbital plane. This motion is due to luni-solar effects and has a period of about 25 700 years. The precession matrix (P) transforms from the mean-of-date system of 1950.0 to the mean of date at reference time. The components of the matrix (z,θ,ζ) are taken from the Astronomical Ephemeris and Nautical Almanac (AENA,1961) and are also listed in MARTIN et AL (1976).

$$P = R_3(-z)\, R_2(\theta)\, R_3(-\zeta) \qquad (5.11)$$

where $R_i(S)$ is a rotation of S about the i axis.

TABLE 5.1
SPECTRUM of CHANGES in the EARTH'S ROTATION
(after ROCHESTER, 1973)

Inertial Orientation of Spin Axis	Terrestrial Orientation of Spin Axis polar motion	Instantaneous Spin Rate (w)
steady precession: amp of 23.°5; period ≅ 25 700 years	Secular motion of pole: irregular, ≅ 0."2 in 70 years	Secular acceleration: $\dot{w}/w \cong -5\times10^{-10}$ per year
Principal nutation: amp of 9."2 (obliquity); period 18.6 years	"Markowitz" wobble: amp ≅ 0."02; period 24-40 years	Irregular changes: (a) over centuries $\dot{w}/w \leq \pm5\times10^{-10}$/year (b) over 1-10 years, $\dot{w}/w \leq \pm80\times10^{-10}$/years (c) over a few weeks or months ('abrupt') $\dot{w}/w \leq \pm500\times10^{-10}$/year
Other periodic contributions to nutations in obliquity and longitude: amp 1"; periods 9.3 years, annual, semi-annual and fortnightly	Chandler Wobble: amp.(variable) ≅ 0."15: period 425-440 days: damping time 10-70 years	short period variations: (a) biennial, amp: 9msec (b) annual, amp ≅ 20-25msec (c) semi-annual, amp ≅ 9msec (d) monthly and fortnightly, amps ≅ 1msec
discrepancy in secular decrease in obliquity: 0."1 /century	Seasonal wobbles: annual, amp ≅ 0."09 semi-annual, amp ≅ 0."01	
	Monthly and fortnightly wobbles: (theoretical) amps: ≅ 0."001	
	Nearly diurnal free wobble: amp ≦ 0."02; periods within a few minutes of a sidereal day	
	Oppolzer terms: amps ≅ 0."02; periods as for nutations	

Newcomb's General Precession constant, which was determined by observations and theory could be in error by approximately 1"/century (FRICKE,1971; LAUBSCHER,1976; ASTERIADAS,1977; PEASE,1977).

(ii) **Nutations** are short period oscillations of the celestial pole about the ecliptic pole. These periods are due to the complex interplay between the orbits of the Sun and Moon. They are also identical to those causing the tides (MELCHIOR,1971). The nutation matrix (N) transforms from the mean-of-date to the true-of-date systems.

$$N = R_1(-\varepsilon_T)\, R_3(-\Delta\psi)\, R_1(\varepsilon_M) \qquad (5.12)$$

where ε_T is the true obliquity of the ecliptic,
ε_M is the mean obliquity of the ecliptic and
$\Delta\psi$ is the nutation in longitude.

The adopted value of 9".21 for the principal 18.6 year nutation term could be in error by approximately 0".01 and is inconsistent with other astronomical constants (MELCHIOR,1971). The rigid-body series for nutation in longitude and obliquity are given by WOOLARD (1953). Nutation terms due to the Earth's non-rigidity are not adequately modelled. Various authors, including KINOSHITA et AL (1979), MELCHIOR (1971) and WAHR (1981a; 1981b) have calculated modified nutation terms to account for liquid core effects. These terms especially affect the annual, semi-annual, 4month, 27 day, 13.7 day and 9.1 day nutation coefficients and should more effectively model the Earth's nutations. The nutation series is currently under review. WAHR's development is the most comprehensive and is being considered for adoption by the International Astronomical Union.

(iii) **Length of Day (LOD)** is the diurnal rotation of the Earth. The Length of Day (rotation) matrix (S) transforms from the true of date system to a pseudo body-fixed system.

$$S = R_3(-\theta) \qquad (5.13)$$

where θ is the Greenwich Apparent Sidereal Time (GAST).

(iv) **Wobble** is derived from the solution of the Liouville equation without any external torques (MUNK & MACDONALD,1960; LAMBECK,1980). The Wobble transformation (W) transforms from the pseudo body-fixed system to a terrestrial system "fixed" to the body of the Earth.

$$W = R_2(-x)\, R_1(-y) \qquad (5.14)$$

The Bureau International de l'Heure (BIH) publishes 5-day pole

coordinates (x,y) with respect to the BIH mean observatory reference system. Other agencies which publish pole positions are the International Polar Motion Service (IPMS) and Defence Mapping Agency (DMA). The latter is often referred to as the Dahlgren Polar Motion Service (DPMS). If BIH pole coordinates are used there are incompletely modelled diurnal Oppolzer terms, due to the motion of the figure axis with respect to the instantaneous axis of rotation (ATKINSON,1973; STOLZ,1979). These terms are either neglected or modelled using McCLURE's (1973) analytically derived values. Although the effect has been observed in astronomical observations, these values however have not been adequately confirmed by observation, (ATKINSON,1973; MA,1978).

BIH maintains Universal and Sidereal time systems. The estimated errors for BIH are 0.5m for pole position. and 1ms for LOD (BIH,1979; LAMBECK,1980). Anomalies in Chandlerian polar motion and Length of Day (LOD) are observed, because of their unpredictable nature at some periods. One example is shown by the 10msec jump in LOD over a period of 10 days as reported by GUINOT(1970). If not accounted for these types of changes could possibly cause anomalous results for geodetic solutions. The MERIT campaign will hopefully reduce these errors by an order of magnitude. MERIT is a campaign to utilise all observation techniques to monitor and improve knowledge on the rotation of the Earth (WILKINS,1980).

MUELLER & LEICK(1979) and LARDEN (1981) summarize some of the more recent developments in Earth rotation theory. LAMBECK (1980) gives a current description for Earth rotation, especially for polar motion and LOD.

Earth rotation models are used to transform coordinates between terrestrial reference systems and inertial reference systems. It is obvious that these reference systems are not adequately defined for geodynamic applications. Errors in the Earth rotation models can have both dynamic and kinematic effects. These are described in Chapter 7. They are therefore important for any extra-terrestrial observation type. The inertial reference system in GEODYN is defined as True-of-Date at a user defined reference epoch. The inertial-terrestrial transformation in GEODYN is therefore given by:-

$$W S N P P^{-1} N^{-1}_{e e r r} \qquad (5.15)$$

where r denotes the reference epoch and

e the measurement epoch.

5.4 BAYESIAN INFERENCE and LEAST SQUARES

The underlying principle of Bayesian inference, is that there is always some a priori knowledge about parameters, which can be used for estimating parameters. The following diagram, which is taken from BOSSLER (1972) gives the flow of the Bayesian estimation scheme.

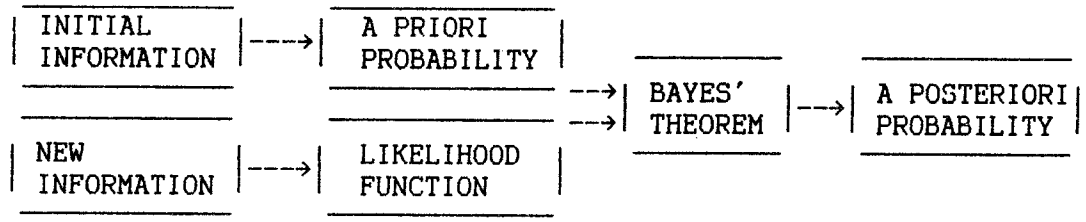

Conventional geodetic least squares adjustment procedures are a special case of the general Bayesian estimation techniques. A procedure is needed to estimate m parameters (**x**), using n observations (**l**), from the observation equation

$$\mathbf{l} + \mathbf{v} = f(\mathbf{x}) \qquad (5.16)$$

where **v** is the observation noise and

f is a functional form relating the observations to the parameters

Bayes' theorem states (BOSSLER,1972)

$$P(x|l) = \frac{P(x)}{P(l)} P(l|x) \qquad (5.17)$$

where $P(x|l)$ is the joint conditional probability density function for x given l.

$P(x)$ is the joint probability density function for x

$P(l)$ is the joint probability density function for l

$P(l|x)$ is the joint conditional probability density function for l given x.

Using Bayes' theorem, the best estimate for the parameters $\mathbf{x}_a$, can be obtained by determining the a posteriori conditional density function. This is achieved by assuming that the noise on l is normally distributed with a mean of zero and that the best estimate of **x**, is the vector, which maximises the a posteriori probability density function. The best estimate $\mathbf{x}_a$, corresponds to the maximum likelihood estimate for **x**. Due to the assumptions made for the observational noise, the variance-covariance matrix Σ_l is diagonal. Therefore $\mathbf{x}_a$ corresponds to

the mean and median (BOSSLER,1972).

If the a priori probability density function $p(x_a)$ is assumed to be normally distributed, then the a posteriori probability density function is maximised by maximising the product $P(x_a)P(l|x_a)$. This product is obtained by minimising the quadratic form (MARTIN ET AL,1976)

$$(x_a - x_a)^T \Sigma_a (x_a - x_a) + v^T \Sigma_l v \qquad (5.18)$$

where x_a is the a priori estimate of x

Σ_a is the a priori variance-covariance matrix associated with x_a.

The following development is for a general least squares solution MIKHAIL(1976,p343). For any functional model $F(l_t)$

where l_t comprises l, l_c, x, l_{ta}, v, v_c, v_x, Δ_l, Δ_c, Δ and

l is a $n \times 1$ vector of conventionally designated observations with a priori cofactor matrix Q

l_c is a $t \times 1$ vector of observations arising from the constraints with a priori cofactor matrix Q_{cc}

x is a $u \times 1$ vector of variables or parameters with a priori cofactor matrix Q_{xx}

l_{ta} denotes the vector of approximations,

v v_c v_x denote vectors of residuals and,

Δ_l Δ_c Δ represent vectors of corrections to the approximate values.

We may write

$$F_t(l_t) = 0 \qquad (5.19)$$

which can be linearised by Taylor's theorem. Second order and higher terms are neglected. Let

$A = \partial F/\partial l$ $\quad c \times n$ matrix

$B = \partial F/\partial x$ $\quad c \times u$ matrix

$A_c = \partial F_c/\partial l_c$ $\quad s \times t$ matrix

$C = \partial F_c/\partial x$ $\quad s \times u$ matrix

where F_t is partitioned into F_c and F.

The linear equations, which relate observations, parameters and constraints are therefore

$$Av + B\Delta = f_a \qquad (5.20)$$

$$A_c v_c + C\Delta = f_{ca} \qquad (5.21)$$

where

$$f_a = -\{F(l_a, x_a) - A(l_a - l)\} \qquad (5.22)$$

$$f_{ca} = -\{F_c(l_{ca}, x_a) - A_c(l_{ca} - l_c)\} \quad (5.23)$$

$$f_x = x_a - x$$

Accordingly

$$\begin{bmatrix} A & 0 & 0 \\ 0 & A_c & 0 \\ 0 & 0 & I \end{bmatrix} \begin{bmatrix} v \\ v_c \\ v_x \end{bmatrix} + \begin{bmatrix} B \\ C \\ -I \end{bmatrix} \Delta = \begin{bmatrix} f_a \\ f_{ca} \\ f_x \end{bmatrix} \quad (5.24)$$

Imposing the least squares condition gives

$$\begin{bmatrix} B^T C^T & -I \end{bmatrix} \begin{bmatrix} W_a & 0 & 0 \\ 0 & W_{ac} & 0 \\ 0 & 0 & W_{xx} \end{bmatrix} \begin{bmatrix} B \\ C \\ -I \end{bmatrix} \Delta$$

$$= \begin{bmatrix} B^T C^T & -I \end{bmatrix} \begin{bmatrix} W_a & 0 & 0 \\ 0 & W_{ac} & 0 \\ 0 & 0 & W_{xx} \end{bmatrix} \begin{bmatrix} f_a \\ f_{ca} \\ f_x \end{bmatrix} \quad (5.25)$$

where $W_a = (AQA^T)^{-1}$ (5.26)

$W_{ac} = (A_c Q_{cc} A_a^T)^{-1}$ (5.27)

$W_{xx} = Q_{xx}^{-1}$ (5.28)

By assuming Equations 5.26, 5.27, 5.28 are non singular and by introducing new auxiliaries

$$N = B^T W_a B \quad (5.29)$$

$$t = B^T W_a f \quad (5.30)$$

$$N_c = C^T W_{ac} C \quad (5.31)$$

$$t_c = C^T W_{ac} f_{ca} \quad (5.32)$$

Equation 5.25 takes the more familiar form

$$\{N + N_c + W_{xx}\}\Delta = \{t + t_c - W_{xx} f_x\} \quad (5.33)$$

or

$$\Delta = \{N + N_c + W_{xx}\}^{-1} \{t + t_c - W_{xx} f_x\} \quad (5.34)$$

When all variables have known <u>a priori</u> values and known cofactor matrices, Equation 5.34 may be used to derive least squares estimates for corrections to the approximate values assigned to the parameters. The terms N, t denote the contribution to the normal equation matrix and associated right hand side from the observations. N_c, t_c denote the contribution from the constraints and W_{xx}, $W_{xx}f_x$ denote the contribution from the <u>a priori</u> parameters. The familiar parametric least squares formula is recognisable if there are no constraints and no <u>a priori</u> variances. The use of <u>a priori</u> variances must be carefully considered for geodynamic applications as they affect the relative geometry of the estimated parameters. These estimated parameters will be referred to the fixed parameters. Bayesian least squares procedures are used in GEODYN. It is therefore easy to use subjective information to constrain geodetic solutions with this program. This complaint about Bayesian least squares has often been expressed by analysts

(BOSSLER,1972) and the effect of these procedures on geodynamic applications are investigated in Chapter 8.

Pseudo Inverse solutions minimise the trace and norm of the a posteriori variance covariance matrix for the estimated parameters, that is, they minimise

$$\mathbf{v}^T \mathbf{W} \mathbf{v} + \mathbf{x}^T \mathbf{x} \qquad (5.35)$$

Pseudo-inverses are therefore a special case of the more general Bayesian estimation. They have important properties for geodetic adjustments. These include defining the orientation and origin for "free" adjustments. These are investigated by BLAHA (1971a) and BJERHAMMAR (1973) and others. Pseudo-inverse solutions obviously have important characteristics which could be used for dynamic satellite solutions for geodetic coordinates especially if the coordinates are to be used for geodynamic applications. These properties are examined in Chapter 8. Numerical methods for determining pseudo-inverses are described in Appendix C.

Estimates of precision for parameters can be obtained from Gaussian error propagation theory. Let

$$\mathbf{dy} = \mathbf{J}\mathbf{dx} \qquad (5.36)$$

where elements of the Jacobian J are given by

$$J_{ij} = \partial y_i / \partial x_j$$

The variance-covariance matrix for the derived parameters y is

$$\Sigma_{yy} = J \Sigma_{xx} J^T \qquad (5.37)$$

and the cofactor matrices are therefore

$$Q_{yy} = J Q_{xx} J^T \qquad (5.38)$$

where $Q = \Sigma / \sigma_0^2$ and (5.39)

σ_0^2 is the variance factor.

Using the principle of propagation of variances (Equation 5.37) with Equations 5.34 we can show that

$$Q_{\Delta\Delta} = \{N + N_c + W_{xx}\}^{-1} \qquad (5.40)$$

The corresponding quadratic form can be obtained from

$$\Phi = \mathbf{v}^T \mathbf{W} \mathbf{v} + \mathbf{v}_c^T \mathbf{W}_{cc} \mathbf{v}_{cc} + \mathbf{v}_x^T \mathbf{W}_{xx} \mathbf{v}_x \qquad (5.41)$$

The estimation of the degrees of freedom for cases, which include constraints and parameters as observations is a complicated problem. BOSSLER (1972) deals with these cases. Problems are generally avoided by assuming the a priori cofactor matrices are variance-covariance matrices. This leads to the a posteriori cofactor matrix being equivalent to the variance-covariance matrix for the parameters.

Equation 5.40 can therefore be used for simulation studies where the sensitivity of the estimated parameters to the observations is desired.

Assuming that there are no constraints, then

$$Q_{\Delta\Delta} = (N + W_{xx})^{-1} \qquad (5.42)$$

The contribution of W_{xx} to $Q_{\Delta\Delta}$ is often needed. For the cases where N and Q_{xx} are non singular, we can show (MIKHAIL,1976 appendix A68) that

$$Q_{\Delta\Delta} = N^{-1} - N^{-1}(I + W_{xx} N^{-1})^{-1} W_{xx} N^{-1} \qquad (5.43)$$

The first term on the right hand side of Equation 5.38 is seen to be the cofactor matrix for the estimated parameters when only observations are used. This equation shows that the a priori matrix W_{xx} will decrease the size of the diagonal elements in $Q_{\Delta\Delta}$ relative to the case where only observations are used. This is because both N and W_{xx} are positive semi-definite. Equation 5.43 was also obtained by VAN GELDER (1978). It is an important result to take into account in sensitivity studies particularly if parameters are estimated by means of subjective a priori information. If Bayesian techniques are employed, the a posteriori parameter variances will be optimistic relative to the solution, which uses only the observations. Obviously, the effect of a priori parameter variances must be carefully considered if Bayesian techniques are used for sensitivity studies.

For sensitivity studies, where all elements of the functional form (Equation 5.19) are not usually estimated, the contribution of errors in the functional form to the solution parameters are often needed. HATCH et AL (1973) and MA (1978) give an expression for the variance-covariance matrix of the solution parameters by subdividing the parameters of the observation equation (equation 5.20) into estimated (x) and non-estimated (y) parameters. The resulting observation equation is

$$l + v = Bx + Cy \qquad (5.44)$$

where B and C are coefficient matrices of partial derivatives.

The least squares solution is obtained from

$$x = (B^T W B)^{-1} B^T W (l+v-Cy) \qquad (5.45)$$

From Equation 5.38 we have

$$Q_{xx} = (B^T W B)^{-1} B^T W Q_{l+v-Cy} \{(B^T W B)^{-1} B^T W\}^T \qquad (5.46)$$

Assuming the observations to be independent

$$Q_{l+v+Cy} = Q_v - Q_{Cy} \qquad (5.47)$$

$$Q_l = 0 \qquad (5.48)$$

$$Q_v = W^{-1} \tag{5.49}$$

$$Q_{\hat{v}} = C\,Q_{yy}\,C^T \tag{5.50}$$

The variance-covariance matrix for the parameters is

$$Q_{xx} = N^{-1} + N^{-1}B^T WCQ_{yy}C^T WBN^{-1} \tag{5.51}$$

This result is obtained after substituting Equations 5.47, 5.48, 5.49, 5.50 into equation 5.46.

The first part of the right hand side is recognisable as the Normal equation matrix for only the observations. Equation 5.51 is a convenient formula to employ with simulation studies involving satellite orbit dynamics. The contribution of errors in the dynamic models to the accuracy of the estimated parameters can be obtained from the second part of the equation.

The ORAN program (HATCH et AL,1973) (which has been used for many satellite missions) is based on this formula. Several simulations for the sensitivity of geodetic parameters to modelling procedures, have been undertaken using this program (BENDER & GOAD,1979; CHRISTODOULIDIS & SMITH,1980; CHRISTODOULIDIS et AL,1981). ORAN is designed on the same dynamic theory as in GEODYN and is used in Chapter 7 to verify and augment the results obtained from GEODYN.

CHAPTER 6

TIDES AND GEOS-3 ORBIT ERROR

6.1 INTRODUCTION

The investigation described in this chapter was aimed at finding a method of filtering the effects of orbital noise from GEOS-3 altimetry derived sea surface height (SSH) data. The principle of the method was to analyse the sea surface heights for significant orbit derived features. The results are presented in Sections 6.5, 6.6 and 6.7. A data base with less systematic noise than the original SSH data was produced by reducing the altimetry measurements to SSH using GEOS-3 ephemerides as determined by LERCH et AL (1978c). Attempts were also made to determine the M2 tide signal using crossover residuals in the Sargasso Sea area. The results are presented in Sections 6.8.2 and 6.8.3. The remaining constituents of the tidal spectrum were not studied because their amplitudes are small when compared to the dominant M2 signal. Moreover the presence of orbital and altimeter noise makes their detection nearly impossible. Similar work carried out by other authors is summarised in this section.

The GEOS-3 altimeter data have recently been used to estimate ocean tides on a regional basis. Satellite data, when compared to the discrete measurements made at tide gauge or with conventional oceanographic equipment have the advantage of sampling on a wide scale. The attempts at tidal measurement with altimeter data have proved unsuccessful to date. MAUL & YANAWAY (1978), BRETREGER (1979) and WON & MILLER (1979) estimated the tidal signal in the GEOS-3 calibration area (Sargasso Sea), while KU (1978) used an area in the Gulf of Alaska. Recent work is reported by BROWN & HUTCHINSON (1980), PARKE (1980) and DIAMANTE & NEE (1980).

MAUL & YANAWAY (1978) analysed data collected over an 18 month period in a 5°x 5° area and found that the signal to noise ratio is 1 : 10. This implies that GEOS-3 altimetry data cannot be used to resolve ocean tide information. In their analysis, altimeter observations of SSH taken from one pass of the satellite were averaged. Apart from the expected altimeter and orbital errors the average value contains an error signal due to variations from the ocean tides, geoid slope and Earth tide over the region.

BRETREGER (1979) analysed the data by modelling the regional sea surface using the technique described by MATHER et AL (1977a). With this method corrections were applied to passes of altimetry data for biases and tilts. In order to do this, passes were subdivided into smaller segments. The following formula was then used to correct the data.

$$\zeta = \zeta_{iJ} + b_i + c_i (t_{iJ} - t_{i1}) \qquad (6.1)$$

where ζ_{iJ} is the estimate of the sea surface height from the J-th element of the i-th pass,

b_i is the bias for the i-th pass,

t_{iJ}, t_{i1} are the times of the J-th and 1st segments in the i-th pass, and

c_i is the tilt for the i-th pass.

This **Bias and Tilt** analysis technique is fully described by COLEMAN (1981). It has been successfully used for many oceanographic and geoid investigations. These include determining temporal variations in the dynamic SST and geoid heights in ocean areas (MATHER et AL,1980; LERCH et AL,1978c).

By using Equation 6.1 it was assumed that the difference between two sea surface height values at a crossover point contains the tidal information. A crossover is defined as the point of intersection of two passes. The actual crossover point is defined by data in something like a 0.°2 x 0.°2 area. Any observations falling within this area are averaged to define a point observation of ζ at the centre of the area. Geoid variations within the small area should be negligible and therefore should not introduce significant errors. For later calculations in this chapter crossover has a more specific definition (Section 6.2.2).

BRETREGER (1979) used 282 passes of altimeter data in a 12° x12° area defined by latitude 31°N and longitude 288°E at the centre of the area. The results of his study differed significantly from the tide in the region. This is probably due to the high levels of systematic noise. Another possible explanation is geometrical instability introduced by the lack of very long passes of continuous data used to model the regional sea surface. A pass greater than 5000 Km is considered long. MATHER et AL (1978a) showed that some of the tidal signal is diminished if Equation 6.1 is applied to the altimetry data. This was confirmed by DOUGLAS & GOAD (1978) and DOUGLAS (1979) who showed that it is

impossible to obtain ocean tide models if tilt corrections are applied. The bias and tilt technique of filtering orbital errors from SSH data is therefore not suitable for resolving the tidal spectrum. A more sensitive filtering model must be developed.

Only a small number of Fourier coefficients are needed to successfully reproduce the empirical Mofjeld tide model in the Sargasso area (BRETREGER,1979). This tide model is fully described in Chapter 2. If the noise were random, BRETREGER's (1979) technique could have accommodated a signal to noise ratio of 1 : 10, but only 4 : 10 if the noise showed a systematic pattern over a pass length. He obtained this result by modelling the M2 tide in the Sargasso region and simulating random bias and tilts for each pass of the actual GEOS-3 altimetry distribution in the region. Had these simulations reflected reality then the M2 tide signal could be estimated in the presence of about 1 m r.m.s. systematic noise. This value has been adopted later as the maximum allowable noise level for successful tidal analyses.

WON & MILLER (1979) analysed altimeter data for the tidal signal using two narrow strips of data in the Sargasso Sea. Each strip contained over 25 passes of altimeter data. Profiles of four ocean tide constituents (M_2, O_1, S_2, K_1) were derived for the two strips. Anomolous results were attributed to GEOS-3 orbital errors. Not surprisingly the derived amplitudes and phases were in poor agreement with the MODE deep sea tide gauge data in the region (ZETLER et AL,1975).

Poor tide measurement with altimeter data are attributed to correlation of orbital errors with the tidal signal. For other parts of the spectrum (eg. temporal variability) the separation of orbital errors is not so critical as they can be removed with the bias and tilt method. Nevertheless, success with the removal of systematic orbital noise from altimetry derived sea surface heights would enhance any oceanographic investigation. Hence the aim of this chapter has wider applications than tidal analysis alone. In order to minimise orbital errors, information on the satellite orbit must be included in the reduction and interpretation of data. These problems are examined in the remainder of this chapter.

6.2 DATA BASES

Two data bases are described in the following sections. These were prepared here to study the problem of orbital error and ocean tide model recovery. The data have also been used elsewhere to determine the equatorial radius of the Earth, global dynamic SST and for analysis of the Gulf Stream and analysis of eddies (RIZOS,1980a; COLEMAN,1981).

6.2.1 GEOS-3 Altimetry Data Base - "LAS79"

The altimetry-SSH data set LAS79 was prepared by upgrading the 1977 GEOS-3 altimetry data. The latter data set was described in MATHER et AL (1978b) and will subsequently be referred to here as the **WALLOPS** data set. The distribution of these data is governed by the satellite orbit and hardware restrictions. A substantial gap exists in the data from Dec 31, 1975 (MJD 42777) to Feb 22, 1976 (MJD 42830). Moreover, hardware restrictions already mentioned in Chapter 2 caused the altimeter data to be collected in regions until a global data set was obtained.

The orbits, which are required to reduce altimetry measurements to sea surface heights were computed using the GEODYN program (MARTIN et AL,1976). The GEM10 gravity field model (LERCH et AL, 1977) was employed to integrate the orbits. Earth tides, luni-solar perturbations and atmospheric drag were also modelled. Five-day arcs of laser data were used to estimate state vectors from which the GEOS-3 ephemeris was determined. Small amounts of S-Band radar tracking data was added to a few arcs to augment sparse laser data (LERCH et AL,1978c). The orbits are referred to the tracking station network (see Figure 6.1) and the dynamic models adopted in GEODYN.

The LAS79 data base was produced as an interim data set as it did not contain all the observed altimetry data. Nevertheless, the noise signals, as shown later, are smaller than those in the WALLOPS data. The LAS79 data should therefore be more useful for oceanographic studies. However, much better results can now be obtained from the complete GEOS-3 data sets (R.COLEMAN,private communication,1981).

The WALLOPS and LAS79 data comprise observations times, latitudes, longitudes, sea surface heights, altimetry measurements and theoretical values for geoid and tide height. The sea surface heights were calculated allowing only for the effect of refraction and bias. They should contain both the signal of the sea surface spectrum and unmodelled orbital perturbations. It is therefore necessary to separate

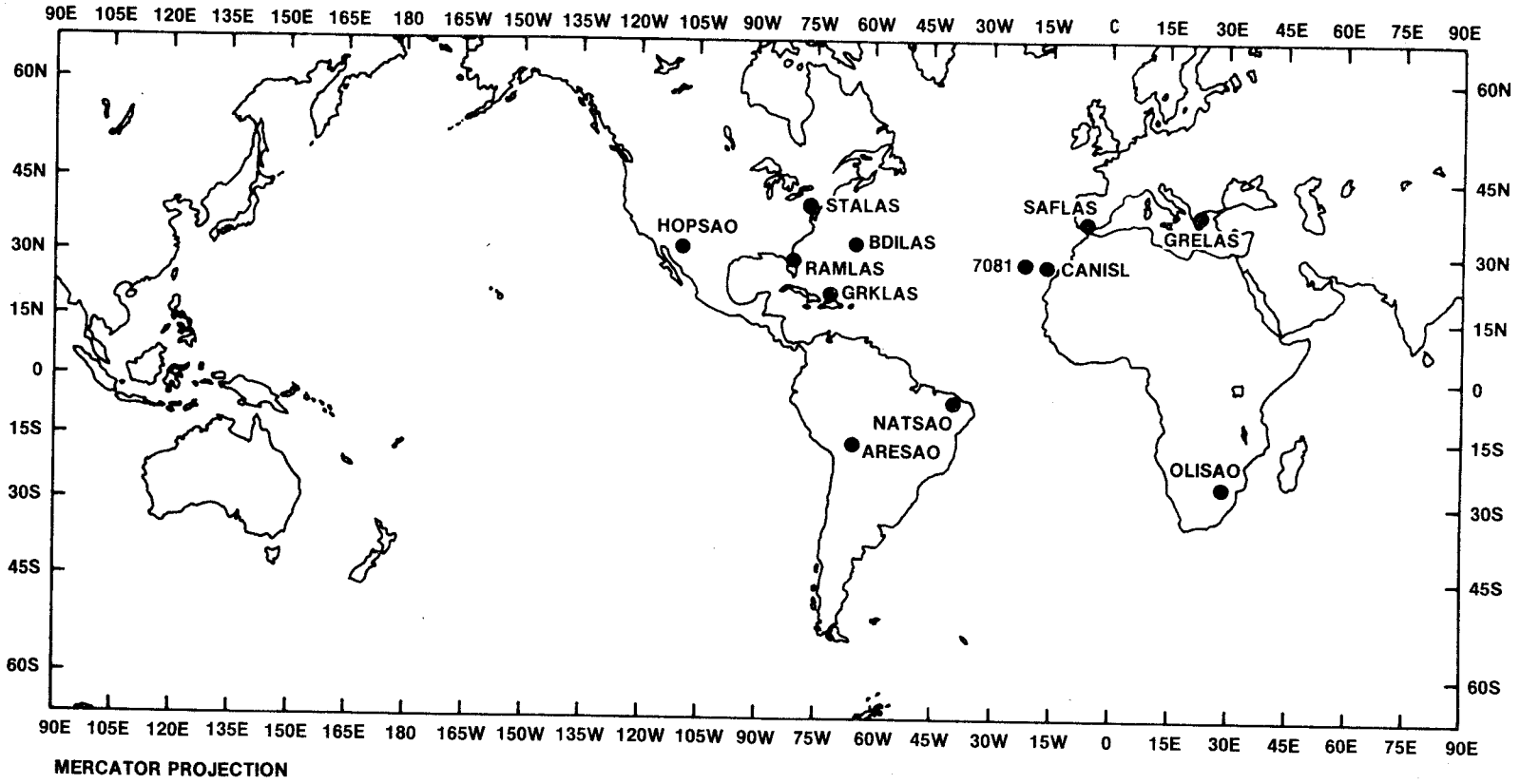

Figure 6.1

Laser Tracking Station Network used for Determining the GEOS-3 Ephemeris.

orbital errors from oceanographic phenomena.

The LAS79 data were reduced in a consistent way. The effect of systematic errors on the determination of oceanographic phenomena should therefore be predictable. The WALLOPS data on the other hand, were produced using a variety of models and the orbits were computed at one of three research centres,

- Wallops Flight Center (WFC) using the GEM7 gravity field model (WAGNER et AL,1976),
- the Naval Surface Weapons Center (NSWC), using from 16 to 60 doppler tracking stations and a gravity field model specially tailored to the GEOS-3 satellite (MATHER et AL,1978b) or,
- Goddard Space Flight Center.

The principle of tailored gravity field models was described in Section 5.2. The WALLOPS SSH data could be expected to exhibit different systematic noise patterns at different epochs. This is because of the varied reference force models and possibly also the different algorithms for determining satellite orbits. Since a more accurate gravity field model and laser tracking data of higher accuracy have been used to calculate the orbits for the LAS79 data, the orbits should in turn be better than the WALLOPS data. However, this advantage could be negated by the sparseness of the laser tracking data (see Figure 6.1) when compared to the NSWC Doppler data. The latter being an all weather tracking system uniformly distributed over the globe.

The residual precisions obtained from the LAS79 sea surface heights as shown in Section 6.2.2 are better by a factor of two compared to the WALLOPS data. This is not as much of an improvement as would be preferred. A similar data set to LAS79 produced by LERCH et AL (1978c) shows slightly better residuals for the crossovers. This is probably due to the fact that they were reduced using more stringent filtering criteria.

6.2.2 "CROSSOVER" - data set

The difference between two separate estimates of SSH from a crossover contain the signal of orbital errors and time varying oceanographic features (eg. tides and eddies). The technique used to create the CROSSOVER data base initially involved locating the intersection points of all north-south (descending) and south-north

(ascending) passes in the GEOS-3 SSH data. Data only rarely occurs at the exact crossover point. The precise time, latitude, longitude and two values of SSH for the crossover point were obtained by interpolating the data from 0.2° on either side of the crossover point. The SSH values were also identified as coming from ascending or descending passes. This proved to be useful as shown in Section 6.4.2.

An estimate of the precision for the derived crossover sea surface heights can be obtained from error propagation theory and the estimated precision of the individual data. If the internal precision for the altimeter is around the 30 cm level (MATHER et Al,1978a; STANLEY,1979) and the five or six measurements in a 0.4 degree region are considered, the estimated precision for each crossover SSH is about 15cm. This is a precision estimate and does not include systematic orbital errors.

Crossover data sets were produced from both the WALLOPS and LAS79 data sets. The 52333 global crossover points in the WALLOPS CROSSOVER data set are plotted in Figure 6.2. A crossover residual is the difference between the two observed SSH values at a crossover. The r.m.s. of the crossover residuals are tabulated below (Table 6.1). Histograms for the crossover residuals for both global and regional data sets are shown in Figures 6.3 and 6.4.

That the LAS79 data are better than the WALLOPS data can be gleaned from Figures 6.3 and 6.4. For both global and regional data sets the width of the central peak of the histogram is much narrower for the LAS79 data than the WALLOPS data. From an examination of the histograms a 10 m crossover residual was used to filter the data in most calculations. As the altimeter and tracking performance is generally good and reduction calculations are sound, residuals greater than 10 m are probably caused by incorrect time tags on the data and the like.

TABLE 6.1

CROSSOVER DATA PRECISIONS

CUTOFF DISCREPANCY (m)	WALLOPS		LAS79	
	Number of Observations	rms (m)	Number of Observations	rms (m)
∞	52333	43.0	21747	3.6
30	50323	5.6	21744	3.1
20	49772	4.9	21721	3.0
10	46727	3.8	21460	2.6
5	37530	2.4		

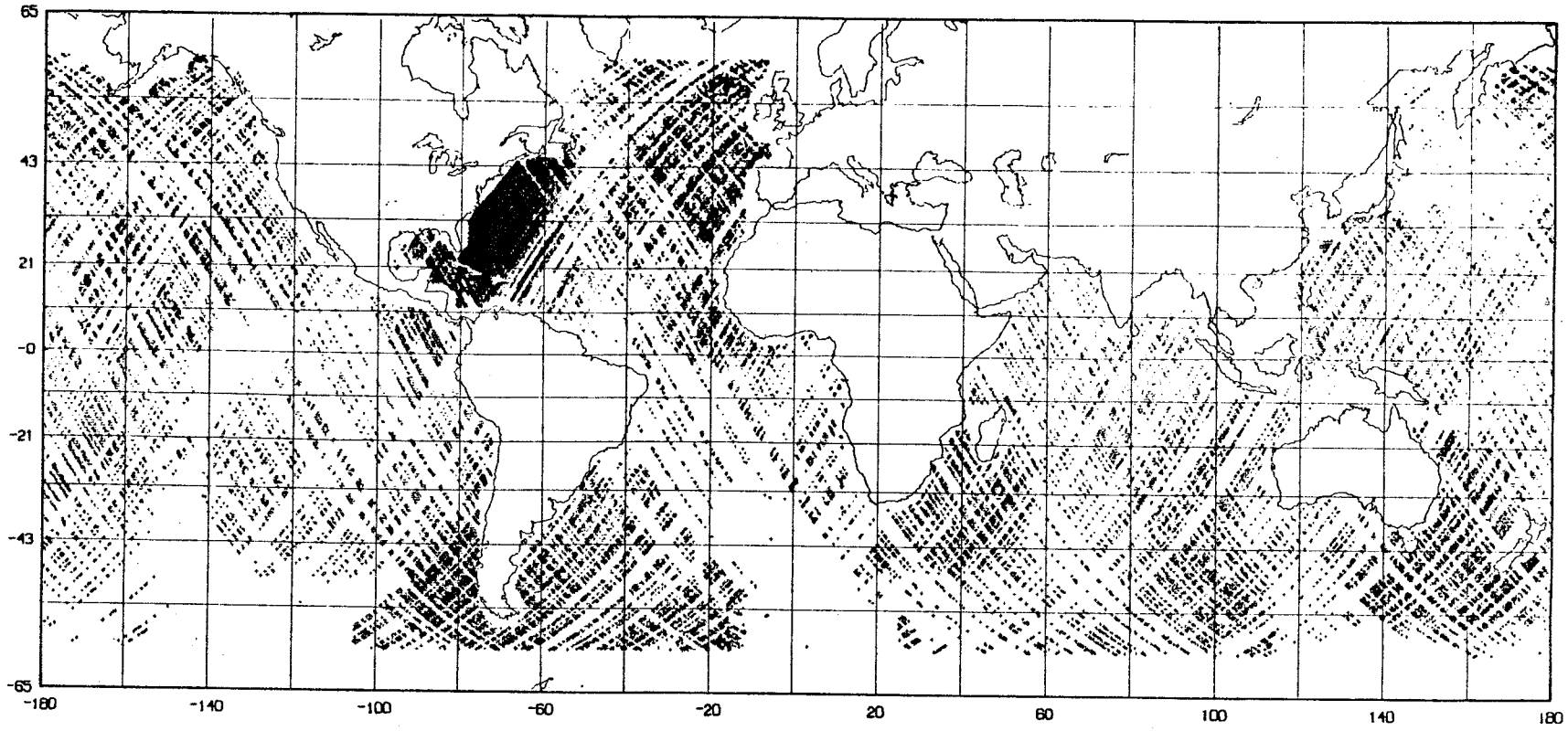

Figure 6.2

WALLOPS Global Crossover Data Set

(1975-1976)

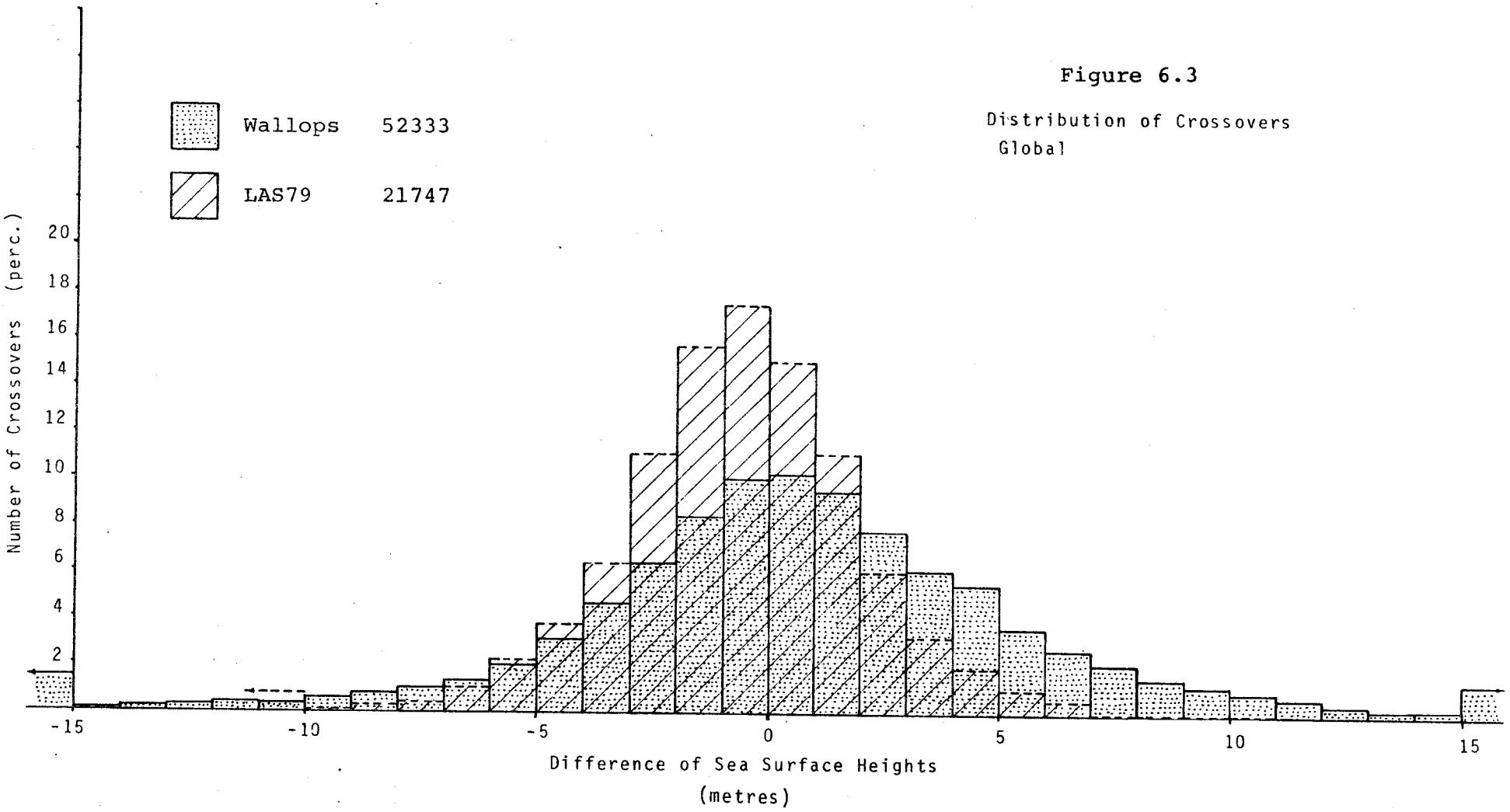

Figure 6.3

Distribution of Crossovers
Global

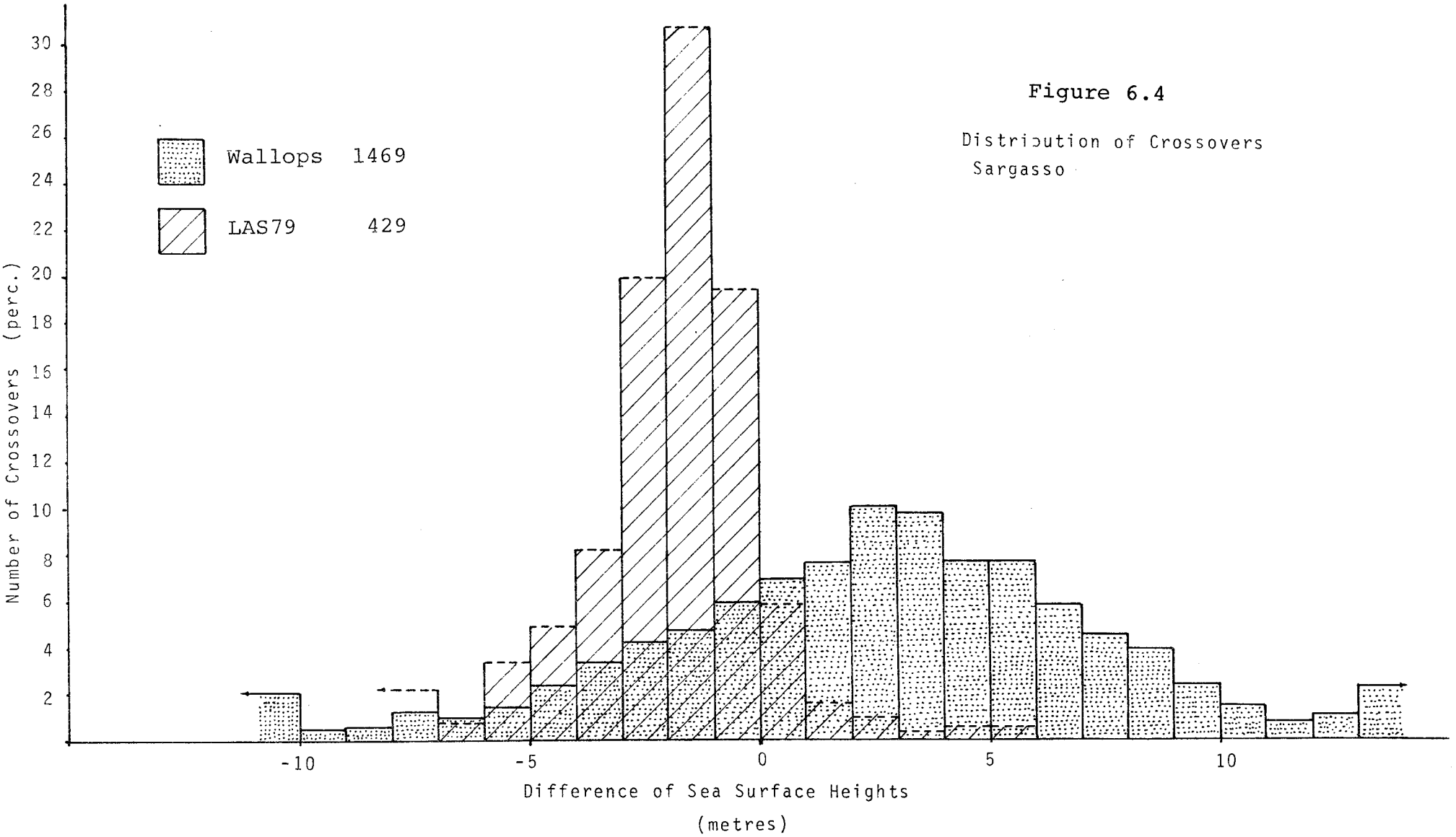

Figure 6.4

Distribution of Crossovers
Sargasso

Several passes are contaminated by substantial timing biases (LERCH et AL,1978c). Timing is critical when the altimeter measurements are correlated with the orbital ephemeris to produce SSH data. Timing biases significantly distort the signal obtained and must therefore be eliminated. The radial velocity for GEOS-3 can be as large as 20 m/sec, which means that a constant timing bias of "n" msec will result in a "2n" cm error in the reduced sea surface height. The error, if constant over long periods of time, will be equal and opposite in sign for ascending and descending passes (MATHER,1978b).

6.3 METHOD

6.3.1 Introduction

Crossovers are now commonly used to independently estimate the accuracy of satellite ephemerides (eg. LERCH et AL,1977). The technique is adapted here to estimate and model orbital errors.

In Section 6.4 a few characteristics of the GEOS-3 orbit are examined with a view to separating some of the orbital errors from oceanographic phenomena. The bias and tilt technique (Equation 6.1) has proven to be quite satisfactory for some analyses. However, the method is somewhat empirical in that it does not take into account the real nature of orbital errors as outlined below and in Chapter 5. For oceanographic analyses where the method is inappropriate, understanding the models used to create the satellite ephemeris and knowing the data sampling, can assist in finding a better method of filtering orbital errors from the data.

The underlying assumption of the bias and tilt technique is that each satellite pass independently samples the SSH in a region. The SSH data is created from altimetry and a continuous ephemeris. For the LAS79 data, each 5-day arc can be considered to represent a continuous segment of the complete GEOS-3 ephemeris. The quality of the orbit determination can be partially assessed by examining the residuals for each span of laser tracking. For 5-day arcs these have an approximate r.m.s. of 0.8 m (LERCH et AL,1978c). However, these residuals only reflect the accuracy of the orbit during the limited tracking period and not necessarily the whole arc. The largest amount of tracking data in any 5-day arc is approximately 7000 range measurements (LERCH et AL,1978c). This represents roughly two hours of tracking over five days. Clearly a large proportion of a 5-day arc of reduced sea surface heights contains noise mainly derived from the integration of gravity and other force model

errors. These errors are continuous, with periods depending on the interaction between components of the various force models (KAULA,1966; WAGNER & KLOSKO,1977; Chapter 5). Perturbations of 5 days or longer should be absorbed by the estimated state vectors. This characteristic has often been exploited to compare empirically "true" against "theoretical" orbits (SMITH & DUNN,1980). Short-period orbital errors can arise from both zonal and tesseral harmonics. Many of these coefficients are not well determined. The orbital error spectrum less than five days should therefore be rich. These periods should be observable in the altimetry derived SSH data. Errors however, are also introduced by other factors like imprecisely known tracking station positions. Hence, we should always have a preference for SSH data in regions with good tracking capabilities. The Sargasso test area is one region where good tracking has been consistently available.

The problem of removing orbital errors from the SSH data is conceptually one of spectral analysis. Significant signals at varying frequencies must be identified from data sparsely sampled in time and position. In principle, this is a less formidable task than if the errors are assumed to be random with every pass of data. One primary limitation on what can be achieved is the sampling interval. This is dictated by the altimeter rate and satellite orbital characteristics and is discussed further in Section 6.4.3

6.3.2 Spectral Analysis

The determination of the spectrum of a time series is a fairly straight forward matter if the data are equispaced. Conventional Fourier transform techniques may be used under these circumstances. The separation of the peaks in the estimated spectrum depends mainly on the length of the data set (JENKINS & WATTS,1968). For non-equispaced data however, the procedure is not so clear.

A least squares technique is used here for spectral analysis. The method is identical to the Fourier transform under certain conditions (VANICEK,1971). Details of the method and minor changes used to speed up the algorithms are presented in Appendix A. The significance of the estimated spectrum can be statistically tested with standard procedures.

One problem encountered with non equi-spaced data, in this context, is that the concept of Nyquist frequency does not have meaning. Periods shorter than the sampling interval will generally alias longer

periods in the estimated spectrum. For analyses of irregularly spaced altimetry data the problem of aliasing and correlation between frequencies is not clearly defined. The implications of the sampling distribution of GEOS-3 altimetry data for tidal analyses have therefore been investigated in Section 6.4.3.

The sampling pattern of GEOS-3 is complicated. It is difficult to perform a realistic error analysis for the altimetry data without actually using the real data. BRETREGER's (1979) study should give the most reliable estimate of the sensitivity of the SSH data to the tide spectrum. Hence BRETREGER's signal to noise ratios for successful tide recovery have been adopted. Tidal investigations are also made easier because the frequencies are well known from astronomical observations. Tides and other features with periods shorter than the minimum sampling time can therefore be estimated if the period of the irregular data is long enough to adequately sample their signals. The success of this procedure can be gauged from the a posteriori variance-covariance matrix. Least squares spectral analysis should therefore make possible the identification of features in the sea surface at varying periods. The determination of significant harmonics in the sporadic time series of SSH data or CROSSOVER data, will depend on the distribution of data in time and space. Difficulties will arise from the correlation between any orbital errors and the sea surface spectrum as sensed by the altimeter.

Other possibilities exist for analysing the data sets. The CROSSOVER data sets can be analysed by treating the two observations of SSH and time for each crossover as a time series. In order to improve this procedure the SSH values can be reduced to pseudo dynamic SSH (ζ_s) by referring them to a higher reference model. This can be achieved by subtracting the corresponding modelled geoid height from each SSH value (MATHER,1978b). If a recent Goddard Earth Model is used for the higher reference model ζ_s should lie between ±10 m. This is an order of magnitude smaller than the original SSH. These data can then be analysed for the spectrum of the SSH, using the least squares spectral analysis technique described in Appendix A. In this case, estimated frequencies higher than 1 cycle per 100 minutes (frequency of one GEOS-3 orbital revolution) could result from either geoid model error, orbital error or sea surface features. For lower frequencies the spectrum should result from orbital error. However this may not be the case if aliasing from high frequency sea surface features and geoid errors has occurred. It

must be said at this stage that the interpretation of the estimated SSH spectrum is a dubious procedure, even under ideal conditions. Nevertheless, if the significant peaks in the estimated spectrum are not highly correlated with the tides, they can be removed from the data. Spectral analysis can therefore provide a potential method for filtering orbital errors from the SSH data.

Orbital errors can be found through the entire range of time and space (Chapter 5). The dominant periods can be estimated analytically. However as shown later, empirical estimation is more viable. One possible filtering method therefore involves the determination of significant periodic orbital errors using all the data and then removing these periods from the data before using it for global or regional studies. An alternative and equally suitable method is to include these errors as additional parameters in the oceanographic analyses. Both these techniques have been adopted for this dissertation (Section 6.5 and 6.6).

6.3.3 Functional Analysis

The propagation of radial orbit error into SSH data as a function of time can also be studied using equations of the form

$$\Delta\zeta_{LM} + \sum_{i=1}^{n} \{C_i (F_i(\phi_2, \lambda_2, t_2) - F_i(\phi_1, \lambda_1, t_1))\} = v \qquad (6.2)$$

where $\Delta\zeta_{LM}$ is the difference in SSH between the L-th and M-th pass,

C_i are the parameters of the problem and,

F_i are the functional models.

Equation 6.1 is a special case of Equation 6.2. The advantage in using Equation 6.2 is that any position dependent, time independent contributions to the SSH (like those due to geoid heights) will not affect the determination of the coefficients C_i. In the analyses presented here simple functional models were adopted for F_i for both global and regional CROSSOVER data sets. These are described in Section 6.5. Coefficients were also defined to describe the tide signal in these analyses (Section 6.6)

6.4 GEOS-3 ORBIT

6.4.1 Orbital Noise in the SSH Data

Simulation studies show that the total noise signal needs to be below 1 m r.m.s if the dominant tidal signals are to be distinguished from the noise (Section 6.1). We could expect a few oceanographic features to be highly correlated with orbital noise. For these cases the noise must be modelled if the features are to be successfully determined.

It is plausible to assume that the variance of the real SSH is less than 1 m^2 (Chapter 2). Therefore any estimated features which are larger than this must come from other sources. The variance of the LAS79 CROSSOVER residuals is 6.8 m^2 (see Table 6.1), therefore the variance of the systematic noise signal is at least 5.8 m^2. This is significantly larger than the magnitude of the noise signal which will not alias the results for tidal parameters. One aim of the analysis in this chapter is to reduce this noise variance in the SSH data to an acceptable level so that the tides can be estimated. Assumedly, this level is about 1 m^2.

6.4.2 Unmodelled Radial Orbit Perturbations

One can easily show that orbital errors are not random and independent per pass as assumed for the "bias and tilt" filtering technique (Chapter 5). The predominant error source in most satellite data analyses arises from incomplete or erroneous force modelling for the equations of motion. The effect of these gravity model errors on ephemerides can be estimated by various techniques. Equations relating specific harmonic coefficients of the spherical harmonic expansion of the Earth's gravity field to orbital perturbations are given by KAULA (1966). These expressions facilitate the estimation of the frequencies and magnitudes of many perturbations, including those from Earth tides and the geopotential.

Orbital errors will vary in magnitude for all parts of the spectrum. Since sparse range data are generally not sensitive to tesseral harmonics in the gravity field, even the most recent gravity field models have limited accuracy. These harmonics should cause a wide band of unmodelled orbital perturbations with frequencies less than a few days. Moreover, since the LAS79 data set were reduced using 5-day arcs these perturbations should also be present in the SSH data.

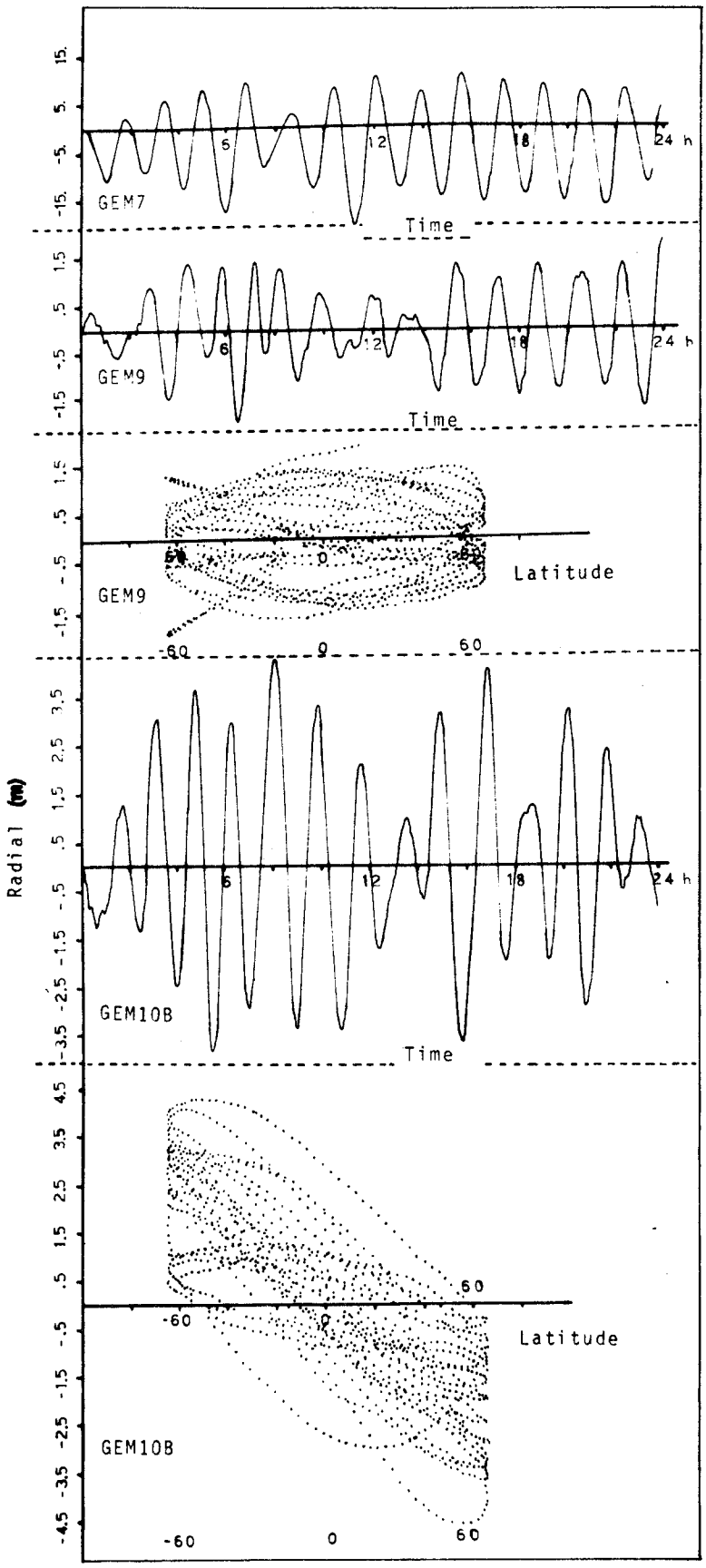

Figure 6.5

Radial Ephemeris Differences from a reference GEM10 Ephemeris due to Geopotential model.

An alternative method of estimating orbital errors is to use numerical error propagation techniques to estimate the effect of "known" dynamic modelling errors on the solution parameters. This procedure has been adopted for sensitivity studies of LAGEOS range data (Chapter 7). However, for realistic sensitivity studies of altimetry data an analytical method is preferred. This is because it is difficult to simulate realistic amounts of data.

The suggested orbital errors modelled by MATHER et AL (1978b) accounted for time dependent radial perturbations with one half, one and fourteen orbital revolutions and a resonance effect at 4.7 days. The effects of possible gravity model errors on the radial position of the satellite are illustrated in Figure 6.5. As only the radial term is of interest for altimetry measurements, the corresponding along-track and cross-track differences have not been shown. These plots were generated by determining the GEOS-3 ephemeris using GEODYN with various gravity field models. These were then plotted as radial perturbations relative to the ephemeris determined using GEM10 (LERCH et AL,1977). The other models are: GEM7 (WAGNER et AL,1976); GEM9 (LERCH et AL,1977); and GEM10B (LERCH et AL,1978a). The comparisons are interesting because the GEM9 & 10 series of gravity models were derived using common data, as shown below (LERCH et AL,1978b;1978d):

GEM9 satellite tracking
GEM10 satellite tracking + gravity
GEM10B satellite tracking + gravity + altimetry(1)
GEM10C satellite tracking + gravity + altimetry(2)

altimetry(1)- 700 globally distributed passes.
altimetry(2)- 28000 1°x1° block means.

A few coefficients will significantly differ from one gravity model to another. This is because of the differing sensitivity of data used in each model to these coefficients. These same coefficients, because they are not well determined, may produce significant perturbations in the true satellite orbit. These perturbations in turn will be observable in the independent altimetry data, which is not as sparse as the laser data. In Figure 6.5 a peak with a period of 102 minutes stands out from the rest. This happens to be one revolution of the GEOS-3 satellite orbit. There are other periods which are not as significant. These produce the noticeable beat pattern in the GEM10B plot.

The radial differences were also plotted against latitude (Figure 6.5). These indicate that on a regional basis, SSH data from

ascending passes could be radially higher or lower than those from descending passes. On the other hand the mean error is near zero, if the differences are averaged over the globe. This phenomenon is evident in the real data (PARRA et AL,1980). The frequency histogram for the data in the Sargasso region is centred about -1.5 m (Figure 6.4). As the SSH values from ascending and descending passes were sorted in the crossover data sets (Section 6.2.2), this figure indicates that SSH data from descending passes of data are consistently higher than those from ascending passes. For the global LAS79 crossovers the histogram is centred about -0.5 m (Figure 6.3), which indicates that the phenomenon averages out around the globe. Similar anomalies are present in the WALLOPS data. A possible alternative explanation from gravity modelling errors to explain this phenomenon is the presence of timing biases (Section 6.2.2).

Closer inspection of the crossover residuals revealed that the solutions for tides using only ascending passes have larger a posteriori variance factors than the corresponding solutions using only descending passes (MASTERS et AL,1979). This cannot be explained at this stage, but possibilities include variable tracking station and gravity model errors in different parts of the globe. Results from crossovers are analysed further in Sections 6.5 and 6.6.

Other orbital perturbations can be expected from incomplete force modelling. Atmospheric drag produces an along-track perturbation, which is proportional to the velocity of the satellite. This perturbation should not contribute much to the radial position over short periods of time. In any case the effect on the orbit should be negligible because drag was included as a parameter in the LAS79 orbit solutions (LERCH et AL,1978c). Earth tides produce another large perturbation. The predominant ones occur in the inclination and longitude of the ascending node of the satellite orbit with periods greater than 13 days (BRETREGER,1978). The perturbations are therefore mostly absorbed by the estimated state vectors for the 5-day arcs. Perturbations from Earth tides do exist with periods less than 100 minutes. These affect the radial position of the satellite orbit by less than 10 cm (BRETREGER,1978). They should therefore have an insignificant effect on the altimetry derived SSH, at least for the level of accuracy sought here. Nevertheless these effects as well as those of other incompletely modelled parameters mentioned earlier, need to be carefully investigated if oceanographic features with amplitudes less than 10 cm and periods less than 100 minutes are to be analysed.

6.4.3 GEOS-3 Data Distribution

GEOS-3 traces out an n° x n° grid every 25/n days. Figure 6.6 shows the ground trace for a 2 day arc. The minimum time interval between crossovers is mainly latitude dependent. This can be determined from the diagram. Also, this time interval depends on the direction of the satellite motion. The time interval between crossovers can be deduced from the following formula (MATHER,1971)

$$\sin(\lambda+\theta-\Omega) = \tan\phi \cot i \qquad (6.3)$$

where ϕ is geocentric latitude

λ is longitude

θ is Greenwich Sidereal Time

Ω is longitude of the ascending node, and

i is inclination

The predominant time varying elements give adequate accuracy here. Hence,

$$\sin\{(\lambda+\theta_0-\Omega_0) + (\dot{\theta}-\dot{\Omega})t\} = \tan\phi \cot i \qquad (6.4)$$

where $\dot{\theta}$ and $\dot{\Omega}$ are the rates of change of θ and Ω and,

θ_0, Ω_0 are initial values at time t=0.

Figure 6.7 shows a solution of Equation 6.4 for crossover time as a function of latitude. Values for θ and Ω from KLOSKO and BELOTT (1977) were used. The sampling rate of GEOS-3 for various regions can be estimated from this figure.

Assuming that the orbital perturbations are secular, Equation 6.4 will give reliable results for short time periods. The formula is unstable at high latitudes or low inclinations because of the $\tan\phi \cot i$ term. The plotted solution (see Figure 6.7) results in an error below 0.1 days for the minimum crossover time. This was considered reasonable for preliminary crossover estimates. The figure shows that the smallest time differences between crossovers occur at high latitudes. However, the subsequent crossover time is much larger. At the equator the sampling is almost equispaced at about 0.5 days. Closer study of a GEOS-3 orbit reveals that four altimeter readings can be taken within a 10°x10° degree region within 48 hours. For the Sargasso area, the best possible times of observation that can occur, assuming time = 0 for the first observation are: 0, 0.4, 0.99 and 1.39 days. Time dependent features are thus sampled at approximately half day intervals during a 48 hour period. Since the satellite groundtrack drifts in

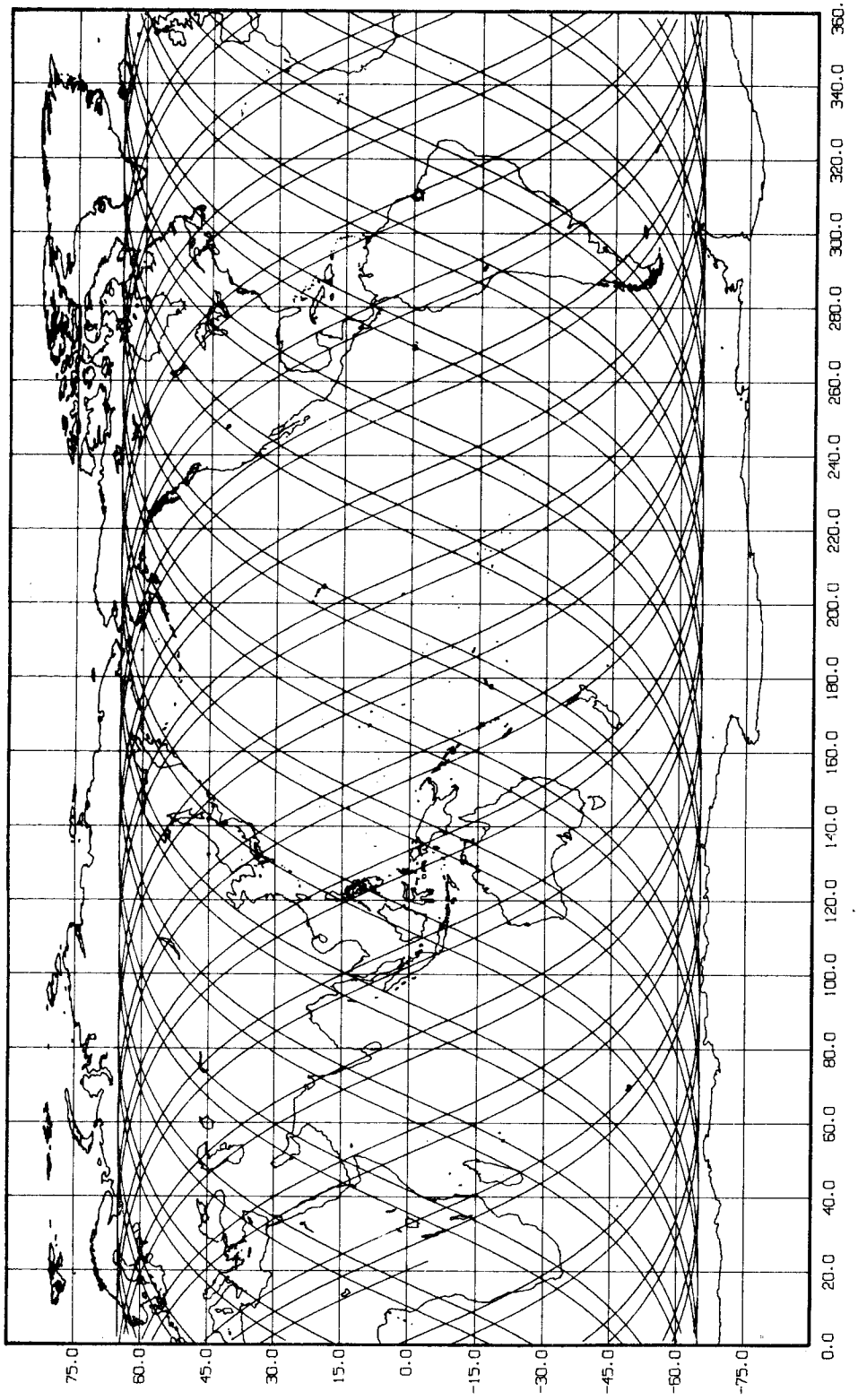

Figure 6.6

GEOS-3 2-day Groundtrack

Figure 6.7

Minimum Time for Crossover with respect to latitude.

SN-NS ... ascending to descending passes

NS-SN ... descending to ascending passes

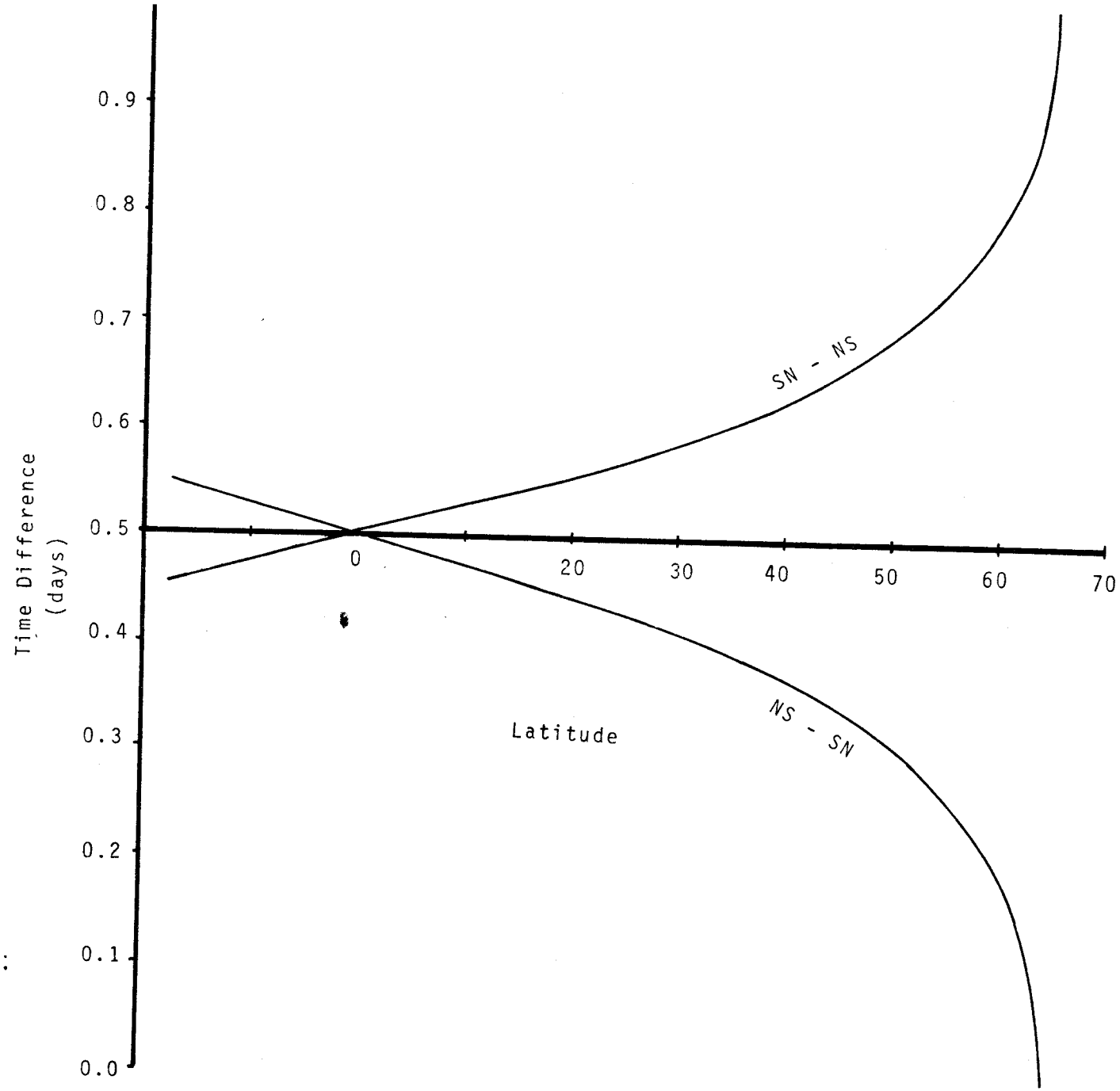

longitude this pattern is not repeated until about 5 days later. The pattern is significantly different to that adopted for a few sensitivity studies (ZETLER & MAUL,1971; BRETREGER,1978). In reality this sampling pattern is not reproduced. However, of all the regions for which data is available it closest to being optimal for the Sargasso region.

The GEOS-3 data sets used for this dissertation contain SSH data for a total period of 393 days (Section 6.2). Any features with wavelengths between the length of 1 pass (20 minutes) and the orbital groundtrack sampling rate (approximately 0.5 days) will not be sampled in a suitable fashion for optimal estimation. This suggests that long periods of altimetry data collection are needed to resolve the semi-diurnal tides and probably also the diurnal tides. The same problem arises with the SEASAT altimetry. Even though it is of higher accuracy, the sampling of the ocean surface is probably not adequate to resolve the tides because of the short duration of the mission. Combination of the two data sets may produce reasonable results. Despite these sampling problems, the large amount of data collected should make possible the recovery of the tide signal, especially when all the GEOS-3 data is available. This has been shown by many simulation experiments (ZETLER & MAUL,1971; MAUL & YANAWAY,1978; WON et AL,1978; BRETREGER,1979).

6.5 DATA ANALYSIS

6.5.1 Orbital Errors

MATHER et AL (1978b) investigated crossover discrepancies. Equation 6.2 was used in their study to constrain the satellite ephemeris and reduce the signal to noise ratio. The modelled orbital features had periods of one half, one and fourteen revolutions, and a 4.7 day resonance effect due to almost overlapping groundtracks as well as linear drifts with time. A similar study of the LAS79 CROSSOVERS was done by the author. The results are summarised in table 6.2. The above periods accounted for only 10% of the total variance of the crossover residuals. This is much less than the 85% which is required to reduce the noise level to the 1 m^2 required for tidal analysis (BRETREGER,1979). One possible explanation is in Section 6.5.2.

TABLE 6.2

ANALYSIS OF LAS79 CROSSOVERS

PERIOD (days)	[orbital revolutions]	AMPLITUDE (m) *
0.00	bias	0.5
0.035	1/2	0.145
0.071	1	0.069
0.141	2	0.091
0.494	7	0.108
0.989	14	0.044
4.680	66	0.355

A priori Variance 6.76 m^2, A posteriori Variance 6.10 m^2

* using Equation 6.2

6.5.2 Spectral Analysis

The data were spectrally analysed to identify other significant peaks in the SSH spectrum, which should be abundant with orbital perturbations (Section 6.3.1). A faster version of VANICEK's (1971) method was used (Appendix A). The LAS79 SSH were converted to quasi-dynamic SSH using the method described in Section 6.3.2. The GEM10B harmonic coefficients (LERCH et AL,1978a) were adopted to generate geoid heights. An inspection of these sea surface heights revealed no unusually "large" periodic features. This was substantiated by the spectral analysis. The spectrum was determined between periods of 0.067 and 400 days. Shorter period errors can be removed using the bias and tilt technique. In any case short period errors are difficult to separate from oceanographic features of similar period.

It is difficult to estimate the significance level for peaks in the estimated spectrum for this large data set. At the 95 % confidence level any peaks larger than 0.07 percent of the total variance are significant if a Fisher Test is used (NOWROOZI,1967). The significant peaks are greater than 0.2 percent if a CHI-SQUARE test is used (KREYSZIG,1970). The significance levels are all very small, because of the large amounts of data and assumptions about their probability distribution. For convenience only peaks larger than 1% are listed in Table 6.3. 1% of the total variance of the pseudo-dynamic SST data (approximately 100m^2) is large in comparison to the SSH spectrum. Significant peaks happen to occur at periods equivalent to one orbital revolution, two revolutions and 4.7 days. The other features have not yet been identified with any known effects, however the half day peak is close to the semi-diurnal tide spectrum.

The bandwidth of the 102 minute peak is less than 0.008 cycles per day. This corresponds to a period of about 4 sec in this part of the spectrum and indicates that it is not easy to estimate the period of orbital errors in the high frequency part of the spectrum as attempted previously. The peaks are seemingly impossible to detect without resorting to spectral analysis and this is the reason why the initial estimates as given in table 6.2 do not reveal the features obtained by spectral analysis. One exception is the 4.7 day resonance term.

The simultaneous least squares estimate of the amplitudes from the pseudo-dynamic SSH are given in column 3 of table 6.3. These correspond to the percentage variances from the spectral analysis in column 2. The a posteriori variance factor for this calculation is 6.6 m^2 and constitutes geoid model error, oceanographic and residual orbital noise. By assuming that the ocean surface contributes 1 m^2 the orbital and

TABLE 6.3

SIGNIFICANT PEAKS in the SPECTRUM
of the GLOBAL SSH DATA

PERIOD (days)	PERCENTAGE VARIANCE	ESTIMATED AMPLITUDES (m)	
			*
0.06796	1.7	0.35	0.37
0.07068 +	5.1	0.59	0.73
0.07603	3.6	0.47	0.23
0.09000	1.1	0.21	0.14
0.14352 ++	1.2	0.36	0.38
0.16024	1.1	0.31	0.15
0.50312	2.3	0.42	0.20
1.3	1.0	0.38	0.19
1.803	1.1	0.38	0.25
4.70588 +++	1.3	0.49	0.35
14.81481	1.0	0.11	0.10
19.04762	1.0	0.26	0.16
28.57143	2.2	0.30	0.25
30.76923	1.7	0.26	0.21
57.14286	1.6	0.30	0.33
80.	1.1	0.42	0.32
200.	4.5	0.63	0.19
400.	2.2	0.42	0.59
total	37.7	2.75	1.91

\+ 1 revolution
++ 2 revolution
+++ resonance
* estimated using Equation 6.2

geoid model noise account for 5.7 m^2. Furthermore by assuming the GEM10B geoid model contributes about 1 m^2 (LERCH et AL,1978d) then orbital noise contributes 4 m^2 to the variance.

A second analysis of the crossovers using Equation 6.2 and the periods derived from the spectral analysis resulted in the amplitude estimates shown in column 4 of Table 6.3. The a posteriori variance factor from this solution is 4.97 m^2. These harmonics therefore account for 27 percent of the crossover variance leaving approximately 4 m^2 of orbital noise in the data. Accordingly, the previous estimate for the orbital noise variance of 4 m^2 represents a reasonable if not pessimistic value. Unfortunately this is still 300% too large for tidal investigations. Nevertheless, it is an improvement on the previous figure obtained in Section 6.5.1.

Estimates of the tides were made concurrently with these spectral results. The results presented by MASTERS et AL (1979; 1980) and COLEMAN (1981) did not allow for any prefiltering of orbital errors. It is therefore not clear whether the removal of the orbital errors as determined in this section would have enhanced those calculations. The systematic noise is probably still too high. These studies have been discontinued, principally because improved and more complete data sets will eventually become available for both the GEOS-3 and the SEASAT missions. The techniques developed here could be used to minimise systematic noise in any future analyses. Indeed GOAD et AL (1980) have already used a similar procedure for the SEASAT data.

At this stage it is evident that the noise signal, after removal of periodic orbital errors, is still too large for tidal analyses. Either the assumptions about the nature of the errors is incorrect or noise of higher frequency than 1 cycle/100minutes is present. At this point it appears that not much can be done, in either case, to filter the errors from the tide signal.

6.5.3 Positional Dependence

The crossover data were examined in the previous section assuming that errors are only time dependent. Tests were performed to check for position dependence in the crossover residuals. For this study, in order to simplify calculations, the crossover residuals were averaged for 1° areas. Inspection of these residuals revealed that no obvious long wavelength trends exist. Contrary to previous conclusions this indicates that ascending passes are not biased with respect to descending passes

on a positional basis. A spherical harmonic analysis of the residuals also verified this. The estimated coefficients are given in Table 6.4. Furthermore, the variance of the 1° block means was large at 2.9 m^2. This figure also indicates no positional dependence, except for very small specific regions, like the Sargasso Sea. The analysis was therefore not pursued any further.

TABLE 6.4

SPHERICAL HARMONIC SOLUTION *
for the CROSSOVER RESIDUALS

degree n	order m	C_{nm}	S_{nm}
0	0	0.296	-
1	0	0.378	-
1	1	-0.158	0.074
2	0	0.124	-
2	1	-0.061	-0.203
2	2	-0.136	-0.351
3	0	-0.149	-
3	1	-0.053	-0.063
3	2	0.068	0.137
3	3	-0.048	-0.059
4	0	-0.010	-
4	1	-0.043	0.011
4	2	0.052	0.137
4	3	-0.035	-0.166
4	4	-0.006	-0.109
5	0	0.039	-
5	1	-0.013	0.033
5	2	-0.005	-0.005
5	3	0.020	0.009
5	4	-0.068	0.017
5	5	0.088	0.082

*....(fully normalised in metres)

6.6 TIDAL ESTIMATION

The formulations for estimation of the tides given in Chapter 2 can easily be modified to include terms with the frequencies of orbital errors. Alternatively, the data can be prefiltered. If the region is carefully chosen, most of the position dependent terms in the Fourier formulation are not necessary and the equation becomes a one dimensional time series. This is the case for the 5 degree area chosen by MAUL & YANAWAY (1978), which has a fairly smooth geoidal slope and uniform tide. Therefore, it is possible to model the tide with a small number of coefficients.

In order to estimate the sensitivity of the filtered data to the

tides, the mean amplitude and phase of the M2 tide in the Sargasso region were estimated and compared to the expected tide in the region. These results are given in the following sections.

6.6.1 Preliminary Estimates for the M_2 tide using CROSSOVERS in the Sargasso Sea

A preliminary regional analysis was done by the author using Crossover data in a 5°x5° area bounded by latitudes 27°N and 32°N and longitudes 287°E and 292°E. This area corresponds to that studied by MAUL & YANAWAY (1978). Solutions were obtained for coefficients representing the average M_2 tide signal, biases, linear trends and some periodic orbital errors as previously defined. The solutions display a large variation, depending on the selected parameters. This indicates that the data are insensitive to the tidal spectrum. The results are given in Table 6.5. The r.m.s. value for the residuals (σ_0) is never less than than 1.3 m. This indicates that there is a large noise signal in the data.

TABLE 6.5

ESTIMATE FOR THE M_2 TIDE
for a 5°x5° AREA in the SARGASSO SEA
model amplitude 0.4 m, phase 356°

SOLUTION TYPE **	σ_0 (m)	AMPLITUDE (m)	PHASE *
T,O,B	1.5	0.42	293
T,O,B,LT	1.3	0.25	289
T,B,LT	1.5	0.21	289
T,B	1.6	0.40	280
M2	2.4	0.59	290
M2,B	1.8	0.23	279
M2,B,LT	1.7	0.08	266
M2,B,LT,4.68	1.6	0.1	180

* PHASE in degrees with respect to Greenwich

** Parameters estimated for each solution
T ... tides M_2, K_1, O_1, P_1, S_2, N_2
O ... orbit 4.7 days, 0.5 rev, 1 rev, 2 rev, 7 rev, 14 rev
M2 ... M_2 signal only
B ... bias ascending-descending passes
LT ... linear trend
4.68 ... resonance term

Solutions were also obtained using the WALLOPS data. These were similar to the anomalous results of other investigators (see MAUL & YANAWAY,1978). The LAS79 data give results which are closer to the correct magnitude. However the phases are consistently lower than the known tide values for the region. COLEMAN (1981) obtained more reasonable results using the full Fourier formulation described in Chapter 2.

TABLE 6.6

ESTIMATE for the M_2 TIDE
for a 12°x12° AREA in the SARGASSO SEA
model amplitude 0.4 m, phase 356°

FILTER	PARAMETERS	AMPLITUDE (m)	PHASE *	σ_a (m) a priori
None	M2	0.39	308	2.18
	M2,B	0.21	321	
	M2,B,LT	0.12	352	
T1	M2	0.22	13	1.78
	M2,B	0.22	23	
	M2,B,LT	0.21	22	
T2	M2	0.24	13	1.82
	M2,B	0.24	27	
	M2,B,LT	0.24	29	
T3	M2	0.24	356	1.96
	M2,B	0.22	12	
	M2,B,LT	0.22	22	
T4	M2	0.22	346	1.93
	M2,B	0.18	6	
	M2,B,LT	0.18	2	

* PHASE with respect to Greenwich in degrees

T1 ... All periods shown in table 6.3
T2 ... T1 without the 0.50312 day term
T3 ... Periods of 0.07068 days, 0.07603 days, 4.70588 days, 28.57143 days, 200 days and 400 days.
T4 ... T3 without the 0.50312 and 400 day terms

SOLUTION PARAMETERS
M2 ...M_2 signal only
B ... bias ascending-descending
LT ...linear trend

Problems could be expected when trying to estimate the average tide for a 5° x 5° degree region. The sampling is probably ideal for a

larger 10°x10° area, as was discussed in Section 6.6.1. Hence, for a 5° x 5° area, the distribution of data with respect to time may be too sparse for optimal estimation of the tides.

6.6.2 Filtered Estimate for the M_2 tide using CROSSOVERS in the Sargasso Sea

The same technique as described in Section 6.6.1 was employed to analyse a 12°x12° degree block in the Sargasso region as shown by Figure 6.8. The larger area was selected to further improve the sampling with respect to time. The procedure was modified to remove the features previously determined by spectral analysis of the global data set before estimating the tide. This was possible because of the fairly uniform tide over the region (Figure 2.3).

Four models were used to filter the orbital errors from the data. These are summarised in Table 6.6. The table lists the results of the solutions obtained from Equation 6.2 and solving for the M_2 tide with biases and tilts. The a priori r.m.s. for the data (σ_a) show that the filtering procedures have reduced the noise in the data by approximately 30% compared to the unfiltered case (row 1). The peaks from Table 6.3 however, do not necessarily improve the regional data. This is shown by the fact that the filtering model T3 results in a larger variance than T4, even though less terms are included in the latter. Unfortunately, all the variance factors indicate that the signal to noise ratio is to small to recover the M_2 tidal signal (BRETREGER,1979).

For the regional data distribution shown in Figure 6.8 and the functional modelling of Equation 6.2, the M_2 tide turns out to be not highly correlated with the features shown in table 6.3. The highest correlation (0.3) exists between the M_2 coefficients and those for the 0.16024 day period. However, the differences between the various solutions indicate there is enough aliasing between the parameters and the noise to make tidal estimation impossible at this stage. Low correlations indicate however that long-period orbital errors can in general be removed from the data without affecting the tidal signal. The method used is therefore potentially superior to the bias and tilt technique.

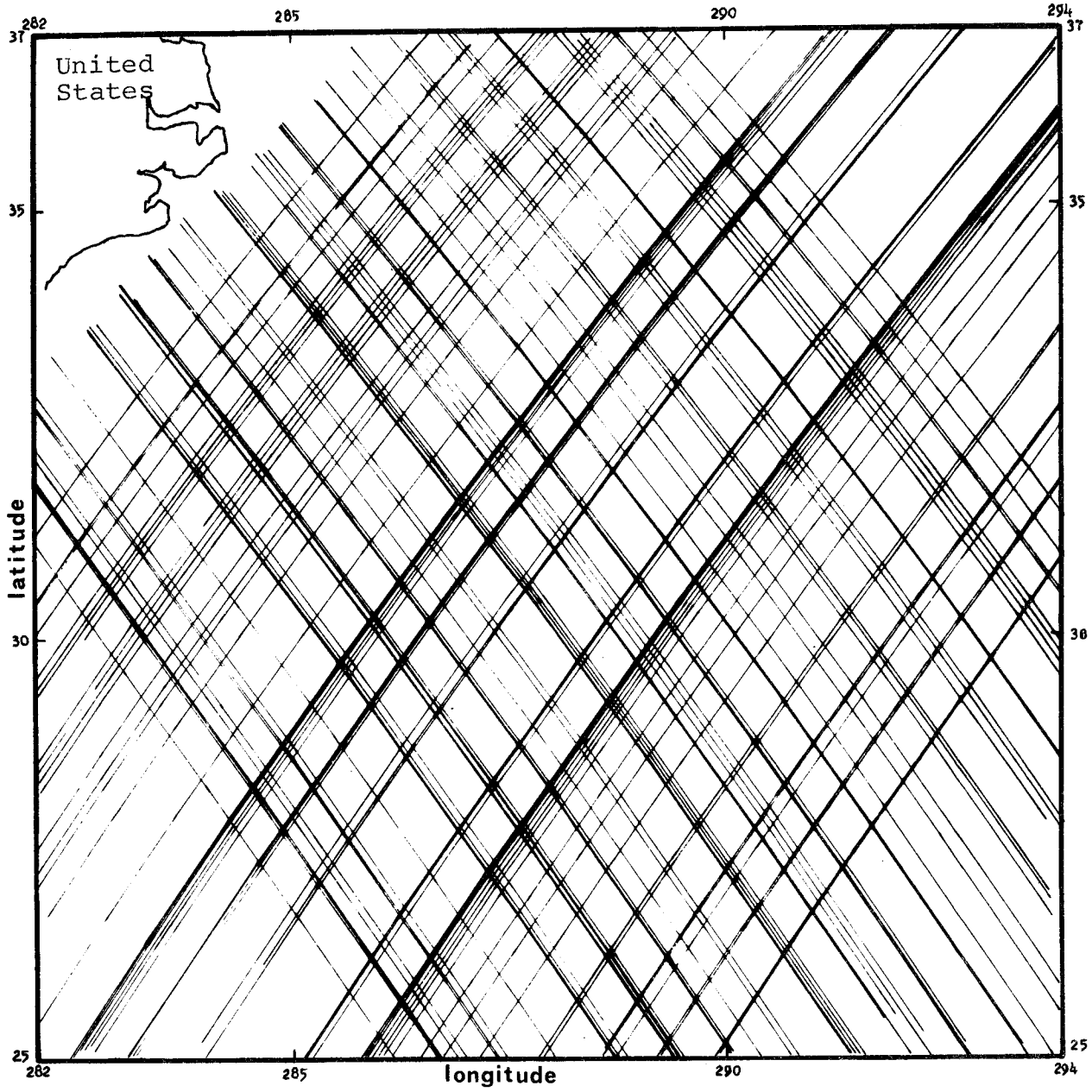

Figure 6.8

Altimetry passes in the Sargasso Sea (1975-1976)

6.7 SUMMARY

An analysis of crossover residuals revealed time dependent features in the global data sets. After these errors are removed approximately 2.2 m r.m.s of residual noise remains unaccounted for. The cause of the noise is unknown at this stage. It may not be orbital error, but can be accounted for as high frequency noise, and removed on a pass by pass basis using the bias and tilt technique. Unfortunately, this procedure also removes the tidal signal. One objective of this investigation was not achieved. That is, the signal to noise ratio for tidal estimation is still too large. However the method will be useful for future analyses of altimetry derived SSH data.

Preliminary results for the M_2 tide in the Sargasso Sea using the Crossovers are given in Section 6.6. These results were calculated concurrently with those given by COLEMAN (1981). Reliable estimates of the M_2 tide are not possible at this stage, due to the amount of noise remaining in the LAS79 data. The situation should improve when the full GEOS-3 and SEASAT data sets are available and the filtering procedures are further refined. Moreover, the noise levels are much lower in these later data sets, which along with the longer time span will produce better results.

Spectral analysis of the pseudo-dynamic sea surface heights is a useful way of estimating periodic orbital errors. Two alternatives are then possible to remove the errors, either to prefilter or to include coefficients for the simultaneous estimation of oceanographic features and orbital error. However, for larger data sets careful consideration needs to be given to making computational algorithms faster. Study of the methods used to determine satellite ephemerides and to reduce altimetry measurements to sea surface heights can result in more effective filtering procedures than presently used. The spectral analysis method should be better suited to the continuous SEASAT data. Analytical theory could possibly be used more effectively to estimate significant perturbations in the orbit. However the effectiveness of this procedure may be limited as shown in Section 6.5.2.

It is apparent from the results presented here that useful information about error sources is available if the theory and techniques used to reduce the altimetry data are known. It is obviously beneficial to include all available information in these applications of altimetry data.

C H A P T E R 7

The LARGE-SCALE CRUSTAL MOTION OF AUSTRALASIA DETERMINED by LASER RANGING : A FEASIBILITY STUDY

7.1 INTRODUCTION

The experiments undertaken by the author to determine the feasibility of processing LAGEOS laser range data at the University of New South Wales are presented in this chapter. Special attention is given to devising a suitable method of analysis for crustal motion using the LAGEOS data acquired at several sites in the Australasian region. Determinations are made of the effects of systematic errors in the range prediction models as well as the amount of random noise on the accuracy obtainable.

The geophysical questions that can be answered with position determinations of high accuracy were described in Chapter 3. The tectonic features in the Australasian region and an Australian proposal to determine crustal motion in the Australasian region were also described. The aim of high accuracy position determinations in this context is to determine the motion of terrestrial positions with respect to time.

Fixed laser ranging stations in Australia are located at Orroral valley, south west of Canberra, Australian Capital Territory, and at Yarragadee near Geraldton, Western Australia. The Orroral station belongs to the Smithsonian Astrophysical Observatory while Yarragadee belongs to NASA (Due to funding cuts within NASA the Orroral SAO laser was shut down in February 1982). Neither site is ideal from the viewpoint of local tectonics. They do however provide a baseline, with respect to which crustal motion may be measured both inside and outside Australia. By providing additional southern hemisphere tracking support, these stations are important for global geodynamics programs because they strengthen the orbit determination capability of the global laser tracking network.

The Australian National Mapping Division has commenced modifying its lunar laser ranging equipment at Orroral to track satellites as well as the Moon (GREENE,private communication,1981). The aim is to modify the telescope and to install a high technology laser and detector

capable of ranging to better than 3 cm. When this has been completed (September 1983 is the current estimate) and sufficient time has been allowed to calibrate the modified system against the Smithsonian station, the latter could be used as a quasi-transportable station at selected sites throughout Australasia. A site in Antarctica and one at Charters Towers in Queensland are now favoured (STOLZ,1981).

The accuracy with which the relative motion between two points can be determined depends primarily on the accuracy of the baseline measurement, and the period between the first and last measurements (NASA,1979). Clearly the highest feasible measurement accuracy is required in order to obtain the desired information on tectonic motion and plate distortion in the shortest possible time. Equation 7.1 gives the accuracy of relative velocity determination between two points, with baseline observations made at time intervals Δt for a total period T (NASA,1979).

$$\sigma_v = \frac{\sigma_r}{T} \left[\frac{(12T/\Delta T)}{(1+T/\Delta T)(2+T/\Delta T)} \right]^{1/2} \qquad (7.1)$$

where σ_v is the velocity accuracy between two points, and
σ_r is the baseline accuracy

For σ_r = 5cm and Δt = 5years, σ_v = 1.4cm/year after 5 years, 0.7 cm/year after 10 years and 0.3cm/year after 20 years. For σ_r = 10cm and Δt = 1 month, σ_v = 9cm/year after 1 year, 3.3cm/year after two years and 0.9cm/year after 5 years. Therefore, relative velocities greater than 10 cm/year should be observable after 2 years of observation, if at least one baseline determination, accurate to 10 cm can be made every month.

The accuracies of the laser ranging solutions for relative station positions are difficult to assess. The formal precisions give little information on the true accuracy of position determinations. Orbit modelling errors in particular degrade the results obtainable. For short orbital arcs of a few revolutions, the largest source of error in the orbital computations is usually the gravity field, but as the arc length increases to days, weeks and months atmospheric drag, solar radiation pressure, tidally induced and numerical integration errors usually begin to dominate (SMITH,1978). There are few external standards against which satellite ranging can be tested. However, since the Australian continent appears to be relatively stable (see Chapter 3), one can be fairly sure that the method is at fault if larger than expected motions are

detected. In this way, knowledge of the geodynamics of the Australian region is useful for the maintaining and ascertaining the precision of the SLR system. Error magnitudes have been systematically reduced so that estimated baselines are now consistent to better than 10 cm over a twelve month period (KOLENKIEWICZ,1981; SMITH et AL,1982).

7.2 METHOD

The orbit and geodetic parameter estimation program GEODYN (MARTIN et AL,1976) was used to construct a model for the topocentric range to the LAGEOS satellite. In GEODYN, use is made of a multitude of dynamic models. The hypothetical ranges are therefore sensitive to these models. The sensitivity of estimated tracking station positions within the Australian region to induced systematic perturbations in the dynamic models, and also to random noise in the range measurements was studied. The implications for geodynamic calculations of using dynamic satellite theory and Bayesian estimation techniques are examined in Chapter 8. The effects of model perturbations and random noise on tracking station position were determined by examining the a posteriori variance-covariance matrix and the corrections to the initial values for position and baseline length. These results are given in Section 7.4.

The simulations were based on five days of simulated tracking data, consisting of one range observed every eight seconds at Orroral and one every second at Yarragadee. All possible passes were included. The ranges for which the zenith distance exceeded 80 degrees were excluded. Furthermore, the longitude of one station Yarragadee was held fixed during the computations. The effects of these assumptions are dealt with later. A 5-day arc was chosen as a basis for the study for the following reasons:

(1) the radiation pressure and other short term orbital perturbations for LAGEOS can be modelled to a high accuracy over this period (BENDER & GOAD,1979; SMITH,1978);

(2) assuming that all possible data is collected, the baseline precisions do not improve significantly after five days of data collection and;

(3) the amount of data is of manageable size.

We were also influenced by the fact that analysts at Goddard Space Flight Center have generally adopted 5-day arcs (SMITH et AL,1979a; CHRISTODOULIDIS & SEIFFERT,1980).

7.2.1 "Range Data".

Simulated topocentric ranges were obtained at the required time interval by:

- generating an hypothetical LAGEOS ephemeris with GEODYN. The groundrack is depicted in Figure 7.1;

- transforming the ephemeris to the same reference system as the tracking station coordinates;

- calculating the range observations for periods, when the satellite was above the horizon for a given tracking station and;

- reprocessing so as to create a data base, which exactly fits the GEODYN dynamic models.

The ephemeris from GEODYN is obtained by numerically integrating the equations of motion for the satellite. The main perturbing force is the Earth's gravity field. Other perturbations modelled were atmospheric drag, solar radiation pressure, and the effect of Earth tides. The GEM9 gravity field model (LERCH et AL, 1977) was adopted as the reference gravity model.

The ephemeris produced by GEODYN refers to a True-of-Date coordinate system. Thus it was necessary to model length-of-day, polar motion and nutation in right ascension, in order to transform the ephemeris to the terrestrial reference system. The transformation used was:-

$$T = WS$$

$$T = \begin{bmatrix} \cos\theta & -\sin\theta & -x\cos\theta - y\sin\theta \\ \sin\theta & \cos\theta & -x\sin\theta + y\cos\theta \\ x & -y & 1 \end{bmatrix} \qquad (7.2)$$

where x,y are are components of pole position and

θ is the Greenwich Apparent Sidereal Time.

In this transformation terms less than $O(10^{-12})$ were neglected.

The tracking stations at which the satellite was in view at any time were determined by calculating when the elevation angles to the satellite were positive. The simulated range observations at the desired tracking time interval were obtained by interpolating the ephemeris and calculating the range distance from

$$\rho = s - r$$

where ρ is the range measurement vector,

s is the position vector of the satellite and,

r is the tracking station position vector.

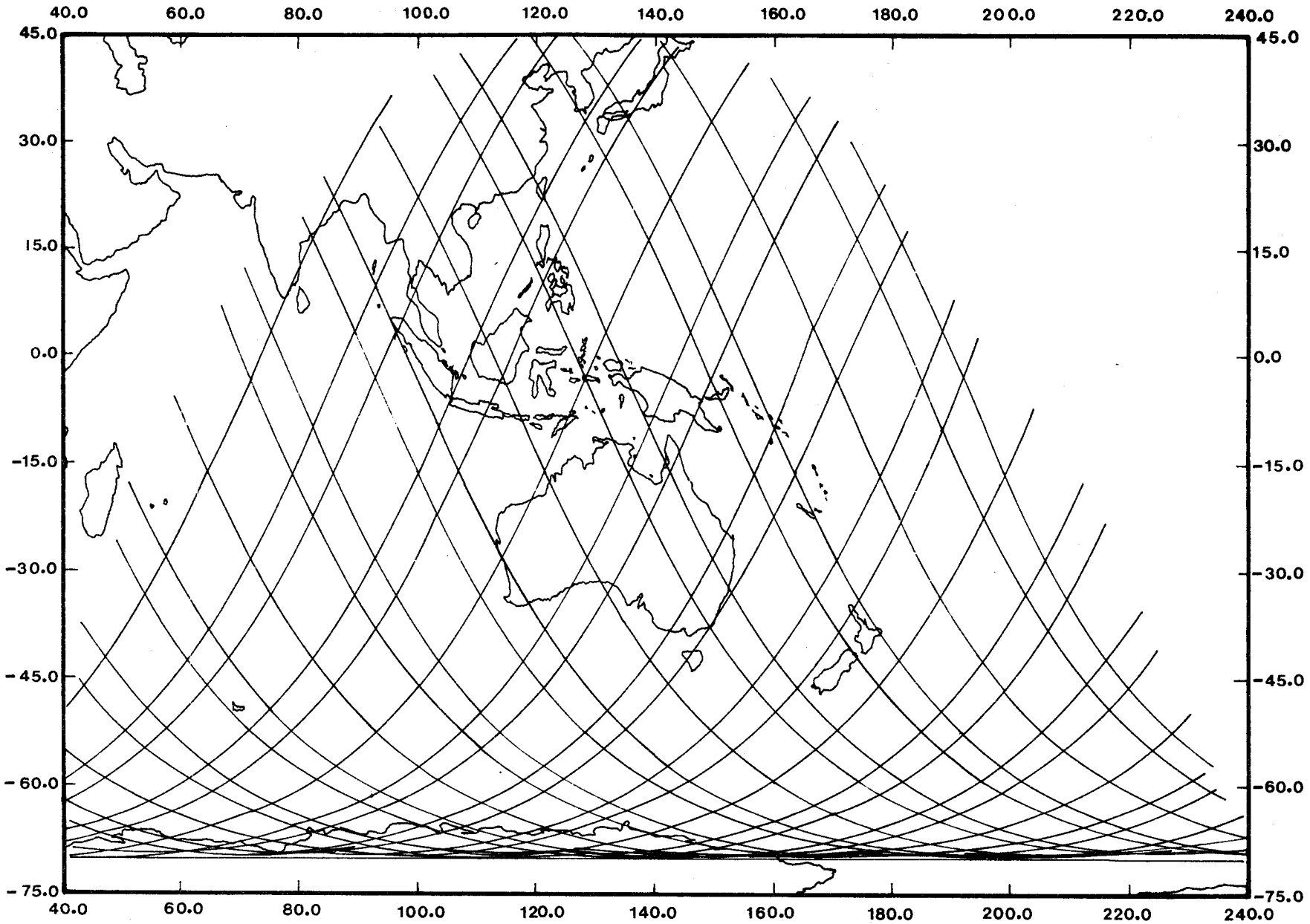

Figure 7.1

2-day
LAGEOS
GROUNDTRACK

At the time that these investigations were made, GEODYN had an option to generate simulated data if the observation times of the range measurements were available. Later versions of the program can simulate data without initial data. The method for generating simulated range data, as described in this section, is therefore now redundant.

7.3 SYSTEMATIC PERTURBATIONS

Estimated tracking station positions are affected by many sources of error. These errors result from:

- the force model, which is used to determine the orbit,
- the transformation model, which relates terrestrial positions to the reference system in which the equations of motion are integrated,
- the numerical limitations of the computer and
- observational errors.

The dominant error source in dynamic solutions for tracking station position arise from gravity model errors. The LAGEOS orbit and physical characteristics (see Chapter 4) were specifically designed to minimise errors. Atmospheric drag and solar radiation pressure perturbations are small because of the spherical shape and high density of the satellite. Indeed the atmospheric drag model used in GEODYN produces zero acceleration at the altitude of LAGEOS. Moreover, only a small number of coefficients representing the Earth's gravity field significantly perturb the orbit. These are mostly below degree 10 except for a few zonals and resonance coefficients (LERCH et AL,1980).

SMITH and DUNN (1980) conclude that the presently available dynamic models are inadequate to describe the LAGEOS orbit over many months. For short arcs of a few revolutions the dominant error sources are not as easy to identify. Except for resonance perturbations the effects of tesseral harmonics are short term and periodically cancel out (KAULA,1966). These perturbations are therefore hard to detect in sparse tracking data (WAGNER & KLOSKO,1977).

CHRISTODOULIDIS et AL (1981) and LERCH et AL (1980) identify the predominant gravity model perturbations. Frequencies and magnitudes are given as well as the possible parameters which could absorb them in a solution system.

7.3.1 Force Model Errors

SMITH (1978) concludes that the limitations imposed on short arc orbital calculations are derived from gravity modelling. One aim of this dissertation was to ascertain computational procedures for minimising gravity model error in determinations of tracking station position and especially in baselines.

The most common technique used to solve for tracking station positions with laser range data is to simultaneously estimate tracking station positions and epoch state vectors for multiple passes of the satellite. This is referred to as the **long-arc method.**

CHRISTODOULIDIS & SMITH (1980) and CHRISTODOULIDIS et AL (1981) have done an error analysis for the prospective use of the TLRS in the San Andreas Fault region of the United States. This investigation is of interest here, because there are many similarities to the work in this chapter. Errors due to range biases, refraction, GM and gravity field coefficients less than degree 10 were included in the study. The variance-covariance matrix for the GEM9 gravity field model (LERCH et AL,1977) was chosen as a plausible error model for the gravity field. CHRISTODOULIDIS et AL (1981) found that the harmonics, which significantly affected baseline measurements were :- S_{76} , S_{77} , S_{22} , C_{76} , S_{32} , S_{66}, C_{32} , S_{31} , S_{97} , C_{33} , C_{44} , C_{22}. These coefficients are in general those which are expected to significantly perturb the LAGEOS orbit (CHRISTODOULIDIS et AL,1981). They also found that an error of one part in 10^7 in GM contributes 1.8 cm to the total baseline error of 3.1 cm. This is significant. The remaining gravity model errors contributed 0.4 cm to the total error in the baseline measurements. GM can therefore be a dominant error source if it is not treated correctly in any solution.

The dominant resonance effect, with a period of about three days, is due to the order six gravity coefficients. These effects should be mainly absorbed by the state vector if the arc lengths are kept to a few days. M-daily and other short-period perturbations could be problem error sources if the data do not adequately sample the perturbations, that is, the errors cannot be estimated or averaged out. The other effects due to the low-order tesseral harmonics may only be removed from geodetic solutions if the arcs are long enough, so that the errors cancel out (CHRISTODOULIDIS et Al,1981). The periods of these errors must be kept in mind when selecting the optimimum arc length for orbital

or geodetic position calculations. Short period terms may be eliminated, if single-pass solutions are used. However, it is not clear if single-pass multi-arc solutions will remove all short-period perturbations to the centimetre accuracy level required for geodynamics. It is obviously a difficult task to determine the optimum technique for minimising the total error from gravity modelling.

The changes in positions and baseline for Orroral and Yarragadee, due to induced changes in certain coefficients of the gravity field model, are described below. The GEODYN program was used for the solutions. It was assumed that the actual errors in the gravity model were known. This is essentially the same procedure as adopted by CHRISTODOULIDIS & SMITH (1980) and CHRISTODOULIDIS et AL (1981). However, these authors used the ORAN program, which was not available in Australia at that stage.

The ORAN program was specifically designed for this type of error analysis. A multitude of error sources can be modelled and the effects of these errors on derived parameters can be estimated (HATCH et AL,1973). One ORAN run is equivalent to many GEODYN runs. The results obtained with GEODYN can therefore be obtained more efficiently with ORAN. For example, the individual contributions of all gravity field coefficients can be obtained in one run of ORAN compared to one run per coefficient with GEODYN. The principles of ORAN are described in Chapter 5.

GEM9 was used as the reference gravity model. An error model was adopted for the gravity field by perturbing the GEM9 coefficients with the values given in Table 7.1. These perturbations of the coefficients represent changes in the gravity field due to specific changes in the Earth's shape (MATHER et AL,1977b). The model does not represent real errors in the gravity field models. Nevertheless, it should give an idea of the effect of errors in the low degree coefficients (less than degree 5) on estimated tracking station positions. Several of the coefficients, which CHRISTODOULIDIS & SMITH et AL (1980) found to be significant were included. The coefficients with especially large perturbations were C_{20}, C_{21}, C_{22}, S_{21}, S_{22}. The changes to the other coefficients were very small. The effect of most low degree tesseral harmonics may not be evident in these analyses.

A third model contained the low-degree coefficients of GEM9 and the high degree coefficients (greater than degree 5) of GEM10B (LERCH et

AL,1978a). This model should show the effect of perturbations in higher degree coefficients on position determinations.

TABLE 7.1

Spherical Harmonic Coefficients for Gravity Model Changes

C	S	ERROR MODEL	Gravity Model coefficient
2 0		-1.043e-08	-0.10826375e-02
3 0		3.823e-11	0.25359250e-05
4 0		-1.940e-11	0.16245986e-05
5 0		-2.025e-12	0.22698397e-06
2 1		1.128e-10	-0.16351803e-09
3 1		1.130e-11	0.21907807e-05
4 1		7.683e-14	-0.50552741e-06
5 1		-1.261e-12	-0.42051426e-07
2 2		4.536e-09	0.15756781e-05
4 2		1.329e-12	0.78843844e-07
	2 1	-5.910e-10	-0.58267056e-08
	3 1	1.130e-11	0.27268204e-06
	4 1	-4.027e-13	-0.44125055e-06
	5 1	-1.261e-12	-0.79002974e-07
	2 2	-2.576e-09	-0.90488902e-06
	4 2	-7.548e-13	0.14818883e-06

Other force model errors are discussed by BENDER & GOAD (1979) and CHRISTODOULIDIS et AL (1981). Errors due to Earth albedo radiation pressure and upper atmosphere radiation pressure result in along-track ephemeris errors of 2 to 3 cm and orbital plane errors of 5cm/month. Tidal effects are more serious, but in general they are long-period and will be absorbed by the state vectors. This feature has been exploited for studying tide perturbations on satellite orbits (SMITH & DUNN,1980; SMITH et AL,1979c). Atmospheric drag is almost non-existant at the altitude of the LAGEOS orbit, although, RUBINCAM (1980) attributes the observed along track perturbation of about 1.1mm/day to an unmodelled drag effect. Except for the tides, these perturbations are all very small in magnitude. They are also long-period effects and should not affect tracking positions estimated from short arcs of a few days. CHRISTODOULIDIS et AL (1981) substantiated these findings. Their results show that errors in solar radiation pressure only becomes significant for 70 day arcs, but that tides and ocean loading effects are negligible.

For satellite solutions of tracking station position scaling problems need to be carefully considered. Scale is partly associated with the force model and can be introduced from both GM and the speed of

light. The LAGEOS orbit is especially sensitive to GM (CHRISTODOULIDIS et AL,1981). This implies that the speed of light and the value of GM must be consistent. If this is not so solutions for geodetic position will be aliased by the two "scaling" parameters. An alternative is to estimate GM simultaneously along with the geodetic parameters. This procedure was used for GEM9 (LERCH et AL,1977) and has also been adopted by STOLZ et AL (1981). The effects of possible GM errors are investigated later (Section 7.4.1).

7.3.2 Inertial-to-Terrestrial Transformation Errors

The transformation model is used to calculate the orientation of the Earth with respect to inertial space. It is conventionally divided into precession, nutation, length-of-day and polar motion (Chapter 5). One requirement for the transformation is to convert terrestrial dependent gravity forces to inertial space for solution of the equations of motion. Any errors in the transformation will therefore propagate into the calculated position of the satellite as pseudo-force model errors. These are referred to as dynamic effects. Perturbations in the calculated orbit can therefore be due to erroneous precession, nutation, sidereal time, and polar motion models (LAMBECK,1973; REIGBER,1981).

The geophysical significance of the low degree harmonics is described in Appendix B. The position of the geocentre is defined as the origin by defining $C_{10} = C_{11} = S_{11} = 0$. The degree two coefficients define the orientaton of the principal inertia tensor with respect to the terrestrial reference system. Specifically, C_{21} and S_{21} define the orientation of the "figure axis", which is important for geodetic reference systems. These quantities have conventionally been held fixed for orbital calculations. Yet, they differ significantly between various gravity models (see LERCH et AL,1974,1977,1978a; BALMINO et AL,1976). This means that the reference systems for these gravity models are different.

The Eulerian equations of motion define the angular momentum of a rotating body through its inertia tensor and angular velocity. C_{21} and S_{21} are therefore directly tied to the dynamics of Earth rotation because of their relationship to the inertia tensor. Bounds can be placed on their magnitudes because the rotation of the Earth has been monitored regularly since the beginning of the 20th century.

The logic of this procedure is as follows. The locations of gravity measurements are defined with respect to a terrestrial reference

system. Satellite orbital perturbations are defined with respect to a terrestrial reference system, through the previously mentioned inertial-to-terrestrial transformation (Chapter 5). If we assume that the transformation models are correct and consistent then the low-degree harmonics of a combination gravity field, as derived from these observations, will define the orientation of the inertia tensors with respect to our terrestrial coordinate system.

Observations of the Earth's polar motion define the orientation of the instantaneous axis of rotation with respect to the observatory positions. In the case of the BIH these positions define the terrestrial reference system (GUINOT & FEISSEL,1968; BIH,1979). Thus we have the orientation of the rotation axis with respect to our terrestrial coordinate system, which is hopefully the same as that used for the gravity model. Theoretically the instantaneous axis of rotation for a rigid non-excited body undergoes circular motion around the principal axis of inertia (figure axis) (MUNK & MACDONALD,1960). It is well known from observations that for the Earth the average period of the motion is approximately 14 months. It is therefore possible to determine the position of the "figure axis" with respect to the rotation axis, which is in turn defined relative to our terrestrial coordinate system. This can be done by determining the average position of the axis of rotation and means that it is possible to define C_{21} and S_{21} from polar motion data. If rotational and tidal deformation are included, the path of the figure axis can still be easily determined (REIGBER,1981).

Summarising the argument so far, C_{21} and S_{21} are defined by the gravity models. These coefficients are also defined by the orientation of the figure axis with respect to the terrestrial reference system. This orientation can be determined in an average sense from the orientation of the instantaneous rotation axis, which is in turn monitored by organisations like BIH. It is therefore possible to determine C_{21} and S_{21} from polar motion observations. NAGEL (1976) and REIGBER (1981) have both performed these types of calculations.

The values determined from polar motion observations can be compared with the gravity model values, assuming that they both refer to the same reference system. The comparisons of C_{21} and S_{21} determined by gravity and polar motion data do not agree. There is an inconsistent set of parameters being used for most dynamic satellite calculations. The problem is complicated further by the non-rigidity of the Earth.

Theoretical calculations show that for a non-rigid Earth undergoing rotational and tidal deformation, the figure axis has a diurnal, sixty-metre oscillation with respect to the Earth's surface (McCLURE,1973). This means that the diurnal variation of C_{21} and S_{21} is as large as their average magnitude. These variations can be significant for orbital calculations (REIGBER,1981). Reference systems defined by C_{21} and S_{21} are obviously unsuitable for geodynamical applications. It is hard to imagine that they would not affect geodetic position calculations if they are not accounted for. This is especially the case if the sensitivity of baselines to C_{21} and S_{21} is considered (CHRISTODOULIDIS,1981). These coefficients will result in diurnal m-daily orbital perturbations. The tide model used in GEODYN should however minimise the diurnal effects. A few investigators do correct the C_{21} S_{21} coefficients to the published polar motion values (SCHUTZ et AL,1979;1980). Range data to LAGEOS should be sensitive to orbital perturbations caused by inconsistency between parameters which define reference systems. Evidence of residual tidal frequencies does exist (CHRISTODOULIDIS & SEIFFERT,1980). REIGBER (1981) has investigated several of these problems for the GEOS-2, DlD and BEC satellites.

Transformation model errors will propagate into the modelled ranges because of the incorrect conversions of satellite and tracking station positions to the same reference system. These errors in the transformation models are referred to as kinematical effects and will be absorbed by the solution parameters. Estimated tracking station coordinates should therefore change from epoch to epoch with periods of the transformation errors. For example, latitudes should change with dominant fourteen month and annual periods if polar motion is not modelled. Nevertheless, if simultaneous observations are used, inter-tracking station baselines should be unaffected because the transformations, by definition, preserve scale. Care should however be exercised with non-simultaneous data as often used in long-arc solutions, because the errors from each tracking station may not propagate equally into baselines. It is not clear under these conditions that estimated baselines can be expected to be invariant with time.

The spectrum of Earth rotation is summarised in Chapter 5. Knowledge of errors is obviously important to the interpretation of geodetic positions, which have been determined using dynamic techniques. Care must be exercised with pole coordinates given by the different authorities, because their reference parameters are different and also

periodically updated. For example, the BIH system changed substantially in 1979 (BIH,1979). Any data analysed before and after that date, without accounting for the reference system change will be affected. The same care will need to be used when a new nutation series is adopted by IAU (Chapter 5). The comparison of geodetic coordinates from different organisations is complicated by these problems.

The problem of defining a unique, invariant reference system for geodetic position is very complicated and has not been solved at present to the required accuracy for geodynamic calculations. Therefore, crustal motion at this stage can only be determined from inter-tracking station baselines. If all the possible Earth rotation error sources are considered, it is reasonable that dynamically determined tracking station coordinates could change by up to 50cm from epoch to epoch. The criterion for determining the optimum epoch length is to determine that epoch length for which short period errors cancel out and long period errors are adequately modelled. Nevertheless, even with this optimum procedure, geodetic positions will change significantly with time. Results for tracking station positions have improved dramatically in recent years (SMITH et AL,1982). Various alternatives can be used to minimise errors:

(i) Use arc lengths which are much longer than the periods of the expected errors, so that the errors average out.

(ii) Use short arc lengths and eliminate the errors through combination of parameters, such as derived baselines.

(iii) Simultaneously estimate the erroneous models.

There are inherent problems with each of these methods.

7.4 RESULTS

7.4.1 Gravity Model Errors

Figures 7.2 to 7.4 give the variations in tracking station position as a result of the simulated gravity model errors alone. The modelled errors were described in Section 7.3.1. Tracking station positions (ϕ,λ,h) of Orroral and Yarragadee and a satellite state vector (XYZ,$\dot{X}\dot{Y}\dot{Z}$) representing arc lengths from one to five days were solved for. The longitude of Yarragadee was held fixed. The reason for this is given in Chapter 8.

Table 7.2 gives the mean and r.m.s. for the range residuals from the previously described solutions. The gravity models described in

Section 7.3 were used in these solutions. The GRIM2 gravity field model (BALMINO et AL,1976) was added to show the effect of a completely independent model. The r.m.s. of the GEM9 solution was zero (row 1). This showed that the data fits the a priori dynamic models perfectly. Note that the two perturbed gravity models resulted in smaller r.m.s. values than the GRIM2 model.

In Figures 7.2 to 7.4 a dependence of the results on arc length is immediately apparent. The latitudes of the tracking stations show similar variations over the 5 days (Figure 7.2). The longitudes of Orroral are grouped around +0."02 (Figure 7.3). This is the error in the Yarragadee longitude, which was fixed. The change in height of the two tracking stations are noticeably less correlated (Figure 7.4). These similar variations between the estimated latitudes and longitudes indicate that gravity model errors will propagate "equally" into coordinates. Relative positions between tracking stations (ie. baselines) will be affected less by these perturbations. This is shown below.

TABLE 7.2

RANGE RESIDUAL RMS and MEAN for
PERTURBED GRAVITY MODELS

GRAVITY MODEL	TS *	R.M.S (m)	MEAN
GEM9	1	0.000	0.000
	2	0.000	0.000
GEM9 + low degree terms	1	0.140	0.016
	2	0.075	0.013
GEM9 + high degree terms	1	0.062	-0.001
	2	0.035	0.007
GRIM2	1	1.106	-0.001
	2	0.723	-0.048

* ...Tracking Stations (1) Orroral
(2) Yarragadee

As would be expected, the higher degree spherical harmonic coefficients have a smaller effect on positions than the low degree harmonics. However, in both cases the errors are larger than one standard deviation for each position determination, which are represented by error bars in the Figures. Gravity model errors could be more of a problem than observation noise for these arc lengths.

The optimum arc length, that is, one for which gravity modelling errors are minimised, is not clearly evident from these Figures. Solutions using the same data, but processed as individual one day arcs show better consistency than the equivalent cumulative longer arc solution. This is again as expected, because the effect of erroneous gravity modelling should become smaller as the arc length is made smaller and less dependent on orbital dynamics. This may not be the case if short-period gravity model errors are more dominant in reality. The short-period errors may not show up in these analyses, because as previously stated, the modelled errors in the tesseral harmonics were small (Section 7.3.1). The dependence of the results on arc lengths longer than 5-days was not investigated for the reasons given in Section 7.2.

The baseline solutions, which were derived from the position values shown in Figures 7.2 to 7.4, are shown in Figure 7.5. The above remarks apply to these solutions as well. Since the nature of real gravity model errors is unknown, it is not possible to select the best arc length for which gravity model errors propagating into estimated baselines are minimised.

The single-pass short-arc case was investigated by using nearly-simultaneous observations from the first 1.5 days of data. Three tracking station positions and a state vector for each of 5 passes over the region were estimated. The Yarragadee longitude was again held fixed. This technique is called **single-pass multi-arc (SPMA)**. The gravity model errors for the baseline (Figure 7.6) are significantly reduced. However, it was necessary to introduce the third tracking station, namely Darwin (3), in order to achieve a stable solution. The problem of numerical instability is examined in Chapter 8.

For the SPMA solution, the errors due to the force model are small, but the baseline precisions are much worse. With all possible passes observed and with the a priori range precisions used in the simulations, it would take about three weeks to achieve the same precision as a one day long-arc. Therefore the problem of minimising gravity model error is outweighed by the lack of observations and their precision.

The optimum procedure will minimise both gravity model errors and effects of observation noise. From these results arc lengths of between

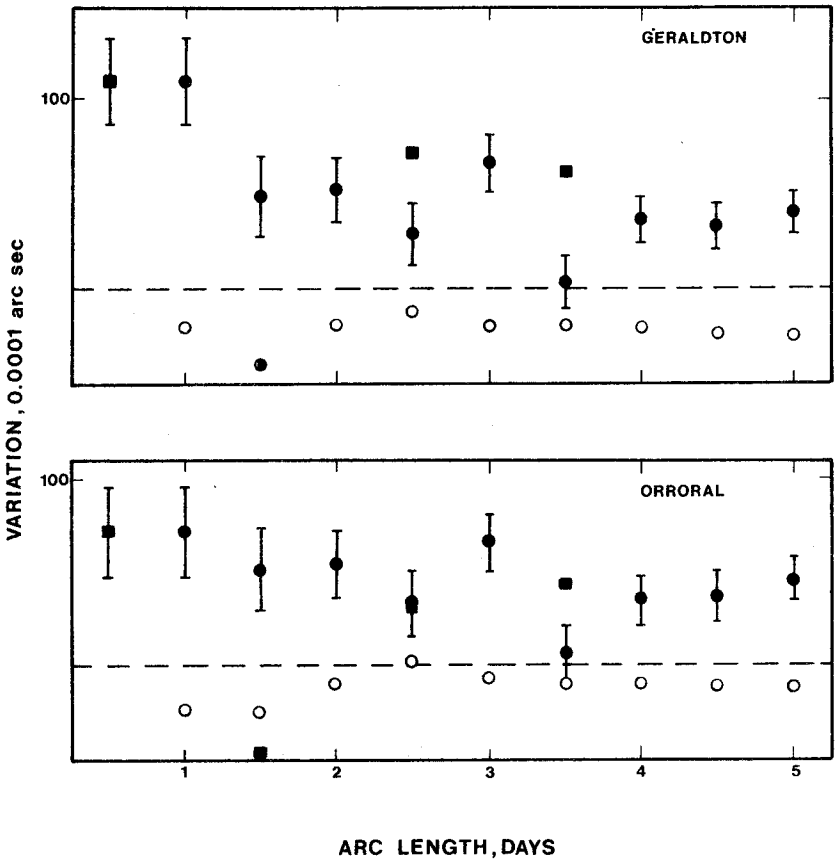

Figure 7.2

Variation of Latitude with respect to arc length due to Geopotential Error.

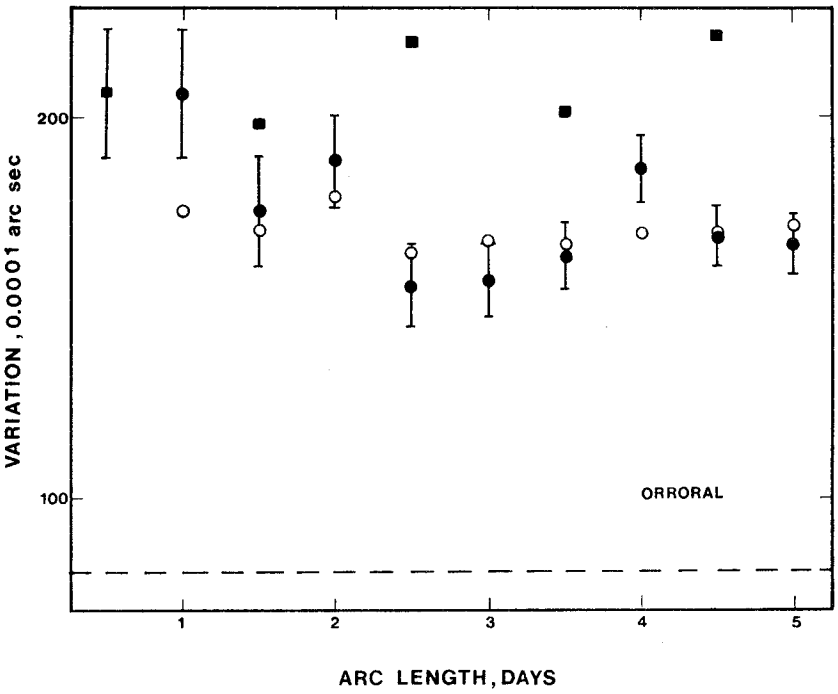

Figure 7.3

Variation of Longitude with respect to arc length due to Geopotential Error.

(see page 104 for explanation of diagram)

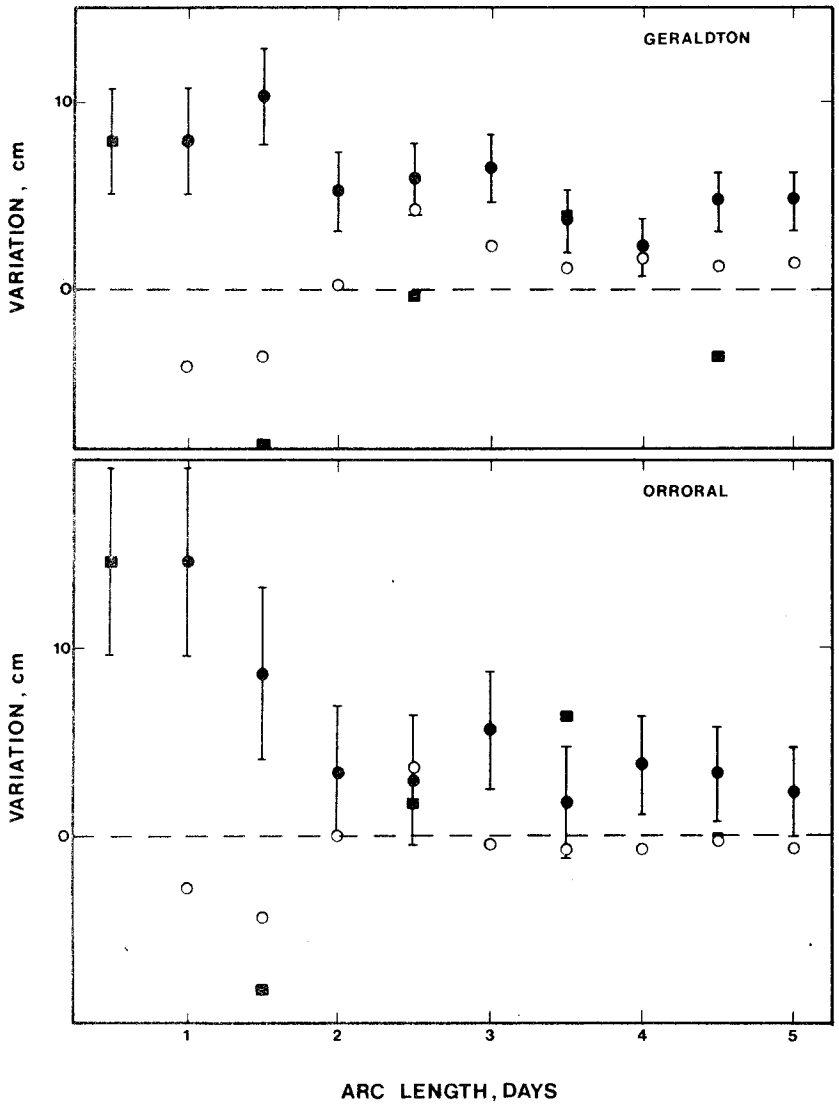

Figure 7.4

Variation of Height with respect to arc length due to Geopotential Error.

(○) high degree gravity field harmonics

(●) low degree gravity field harmonics

(■) low degree harmonics using individual one-day arcs

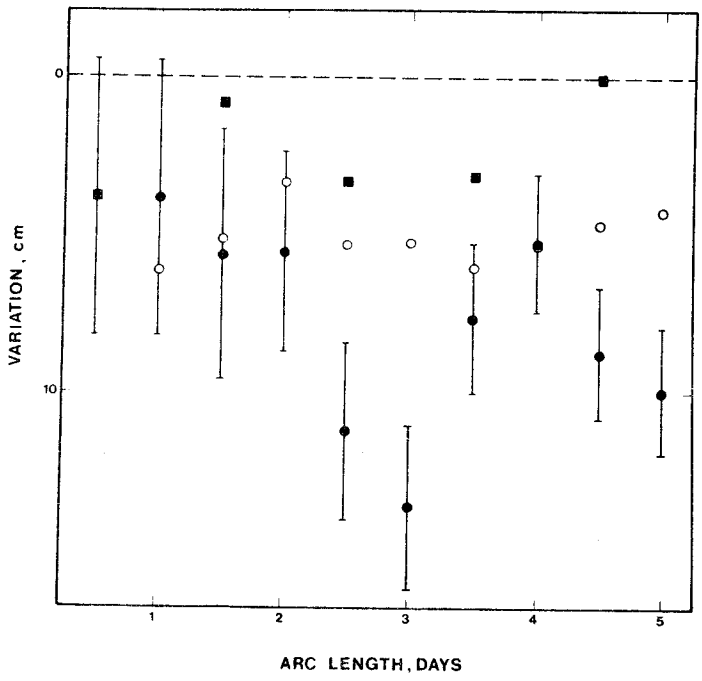

Figure 7.5

Variation of Baseline with respect to arc length due to Geopotential Error.

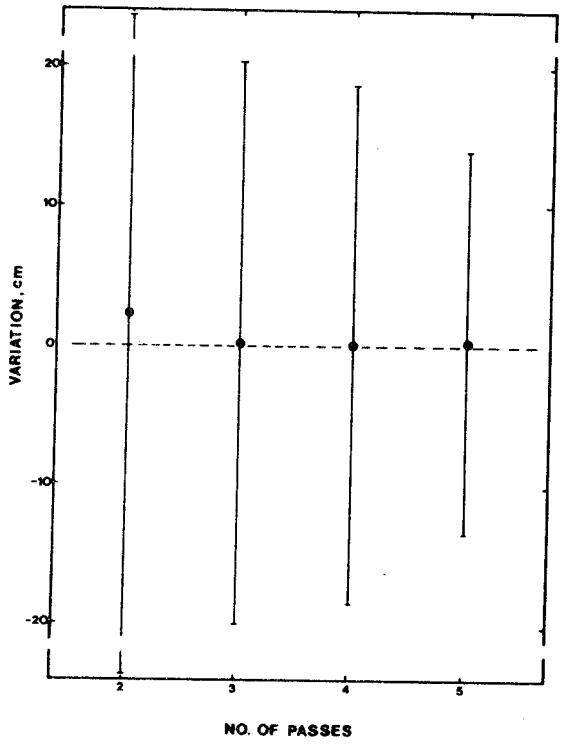

Figure 7.6

Variation of Baseline with respect to number of Passes due to Geopotential Error. (SPMA Solution)

one pass and one day would seem to be ideal.

Indications from these preliminary results however, are that errors in GM could be larger than the gravity field coefficients. In order to study the problem of an erroneous value for GM, the five days of simulated data were reduced as five separate one-day arcs. Each arc included an estimate for three tracking station positions and one state-vector. By affecting the station heights GM errors propagate into long-arc baselines as a scale error. The error in GM of 4 parts in 10^7 propagated into the baselines on average as a 3 parts in 10^7 error. This is larger than the current error estimate for GM. However it is smaller than the dispersion of GM values estimated from various methods (LERCH et AL,1978b). The r.m.s. of the baseline error was itself 1.5 parts in 10^7. This means means that GM does not propagate as a constant error for all solutions. Any estimated baseline velocities from positions estimated with an erroneous GM value will therefore be epoch dependent. It is unclear if the GM error will become constant and less data distribution dependent for longer arc lengths. Obviously this could not be investigated with the current data and computer limitations. The problem needs further study.

It is theoretically possible to estimate GM and perhaps also a few low degree coefficients in long-arc type solutions (BENDER & GOAD,1979; VAN GELDER,1978; SMITH et AL,1982)). GM has been simultaneously estimated along with tracking station positions from LAGEOS range data (LERCH et AL,1977; 1978b). For this reason STOLZ et AL (1981) solved for GM along with their baseline estimates. For SPMA solutions, GM cannot be estimated successfully, because of the unstable solutions. The previously stated advantages of SPMA are therefore nullified if GM is considered to be a dominant error source.

7.4.2 Random Tracking Noise

Figure 7.7 shows the improvement of baseline precision for arc lengths longer than one day. Table 7.3 gives the results for the same baseline for arc lengths less than one day. For arc lengths less than one day the precisions obtainable were noticeably dependent on the distribution of the data.

The standard deviations improve dramatically after three passes (Table 7.3). Improvement in precision is relatively slow after this. As would be expected the improvement in precision at 3 passes coincides with the fulfilment of more stable geometric conditions. A solution

procedure can therefore be devised which minimises both gravity model errors and random noise effects. This would be a multi-arc method in which state vectors, representing arc lengths between 0.5 and 1 day, and station positions for epochs greater than 5 days, are estimated.

For longer arc lengths the observational procedure does not have to be rigidly adhered to, because the tracking stations do not have to be observing simultaneously. All possible passes were assumed to be observed for this study. This is obviously unrealistic and longer observing periods will be required to achieve these results from the actual data. Indeed the real data must be examined before any decisions can be made about the most feasible computational procedure. This is especially the case for existing data. About 20 percent of the total possible passes were observed in 1980. This meant that it was virtually impossible to obtain enough data for baseline solutions in Australia with epochs less than three days (Chapter 9; STOLZ et AL,1981).

TABLE 7.3
BASELINE PRECISION for VARIOUS ARC LENGTHS

No. passes	hours**	precision* (m)
1	2	-
2	5.5	2.962
3	10.5	0.879
4	14.5	0.059
5	18	0.053
6	21	0.047
7	25	0.044

* standard deviation
** nearest half hour

7.4.3 Polar Motion

In Section 7.3 it was concluded that the transformation errors, between the inertial and terrestrial reference systems, can affect dynamically determined positions. Baselines should however remain largely unaffected.

The effect of wobble errors on positions and baselines are examined in this section. Zero values were substituted into the calculations for the previously used BIH values. Polar motion was therefore assumed to be non existant, introducing into the calculations a kinematic error of about 4m with a dominant period of about 14 months. For the epochs of solution used up to 5 days, this error is therefore

essentially a bias. It should be noted that this error has not been propagated into the orbit.

The following formula can be used to calculate the corresponding change in latitude for the pole coordinates (GUINOT & FEISSEL,1968).

$$\Delta\phi = x \cos\lambda - y \sin\lambda \qquad (7.3)$$

The BIH pole coordinates, used to create the data were

$$x = 0.''130 \quad \text{and} \quad y = 0.''255.$$

These values substituted in Equation 7.3 give

$$\Delta\phi_{\text{ORRORAL}} = -0.''243 \text{ and,}$$

$$\Delta\phi_{\text{YARRAGADEE}} = -0.''282.$$

From the one day long-arc solution

$$\Delta\phi_{\text{ORRORAL}} = -0.''241 \text{ and,}$$

$$\Delta\phi_{\text{YARRAGADEE}} = -0.''282$$

The erroneous pole positions therefore mainly affected the derived latitudes, as expected. However, most importantly,the baseline between the two tracking stations remained unaffected. Similar results were obtained for a five-day arc and SPMA.

7.4.4 Diurnal Polar Motion

The diurnal polar motion subroutine in GEODYN is based on McCLURE'S (1973) development. The amplitude of the motion is of the order of 60cm and also has a predominant 14-day beat period (NAGEL,1976). The omission of this effect results in the following errors for a one-day long arc:

$$\Delta\phi_1 = 0.''0001, \quad \Delta\lambda_1 = 0.''0201,$$

$$\Delta h_1 = -0.001m,$$

$$\Delta\phi_2 = 0.''0001, \quad \Delta\lambda_2 = 0.''0200,$$

$$\Delta h_2 = -0.009m$$

The effect on tracking station position is small, possibly because the diurnal signal has been sampled effectively through a full wavelength. The baseline discrepancy was -0.001m. This is negligible for geodynamics calculations.

The results from a five-day arc are:

$$\Delta\phi_1 = -0.''001, \quad \Delta\lambda_1 = 0.''0201$$

$$\Delta h_1 = 0.004m$$

$$\Delta\phi_2 = -0.''001, \quad \Delta\lambda_2 = 0.''0200$$

$$\Delta h_2 = -0.007m$$

These results are of similar magnitude to the one-day arc, although the changes in latitude are slightly larger. The effect of non-

simultaneous passes, as discussed previously, is a possibility (see Section 7.3.2). Since the effect on baselines was negligible, the study of this effect was not continued at this stage. SPMA solutions similarly resulted in unaffected baselines.

7.4.5 Common Timing Bias

In order to study the effect of timing biases the same timing bias was introduced to both tracking stations. One second was added to the observations at both Orroral and Yarragadee. The longitude of Yarragadee was held fixed. The most significant changes occurred for Mean Anomaly, Argument of Perigee and Right Ascension of the Node. The Right Ascension of the Node changed by 0."004, which is equivalent to 1.0 sec. The timing bias therefore, propagated into the estimated satellite position. However, the estimated baseline remained unaffected.

The realistic situation of independent timing biases hopefully does not exist as it is difficult to remove during the solution process. Time should be maintained at tracking stations to better than 10^{-6}sec (B.GREENE,private communication,1981). Timing errors are hopefully not a problem.

7.4.6 Data Quality, Quantity and Distribution

In this section, the effect on the station baseline precision of data quality, quantity and distribution is studied. In Figure 7.7 the precisions, which are obtainable from long arcs are shown. Various combinations of plausible range accuracies were used. The precision improves rapidly with the number of observed passes. Beyond five days, there is little improvement in accuracy. The precision obtainable, should however be much improved when the second Orroral laser commences operation.

Results obtained were determined by assuming that one range is observed every eight seconds at Orroral and every one second at Yarragadee. Ranges were only used when the elevation angle of the satellite is greater than 10 degrees. The elevation restriction is unrealistic. In Australia the lasers may not be fired below 20° elevation because of the danger to the aircraft (MORGAN,personal communication,1980). This is not a disadvantage however, because refraction errors increase significantly on the amount of data observable and also baseline precision are shown in Table 7.4. The precisions given in Figure 7.7 deteriorate by factor of two if a 20° elevation restriction was imposed. Baseline precisions should be at the

2-4 cm level after two days of tracking if the long-arc method is used to estimate positions and the NATMAP laser is operating. The dominant problem therefore is to minimise systematic error from gravity modelling.

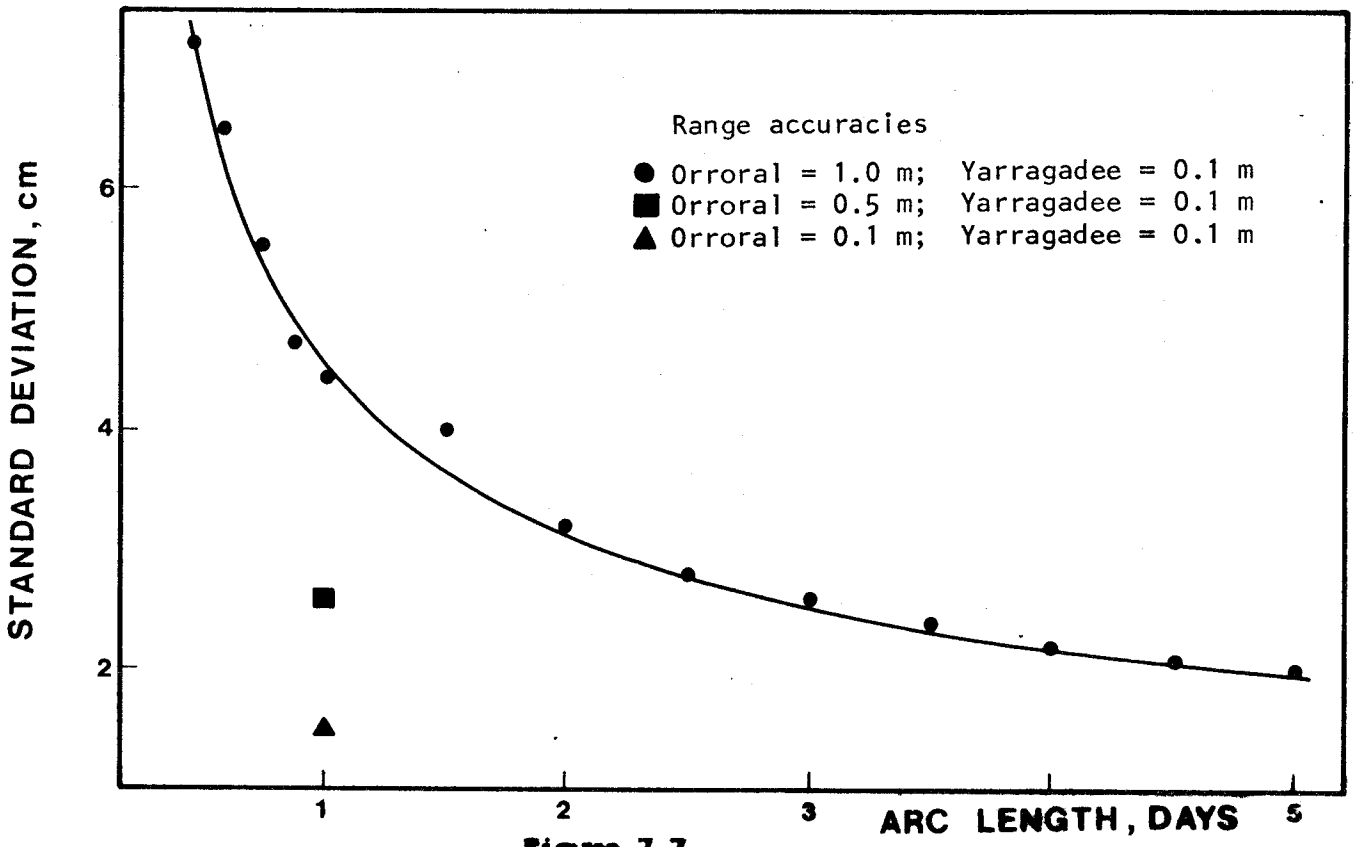

Figure 7.7
Precision of Baseline with respect to arc length

TABLE 7.4
DATA LOST AND BASELINE PRECISION for VARIOUS ELEVATION CUTOFF

Elevation Cutoff (°)	Data lost (%)	precision loss (%)
0	0	0
10	22	16
15	34	34
20	47	84

In Table 7.5 the computing time on a FACOM M160S and precision for the Orroral-Yarragadee baseline are given with respect to the amount of data, data rate and a priori range precision. Using normal points to represent up to 5 minutes of data has little effect on the precision of baselines. Furthermore, the amount of computer time required to process a 1 day arc of 100 second duration normal points is smaller by about an

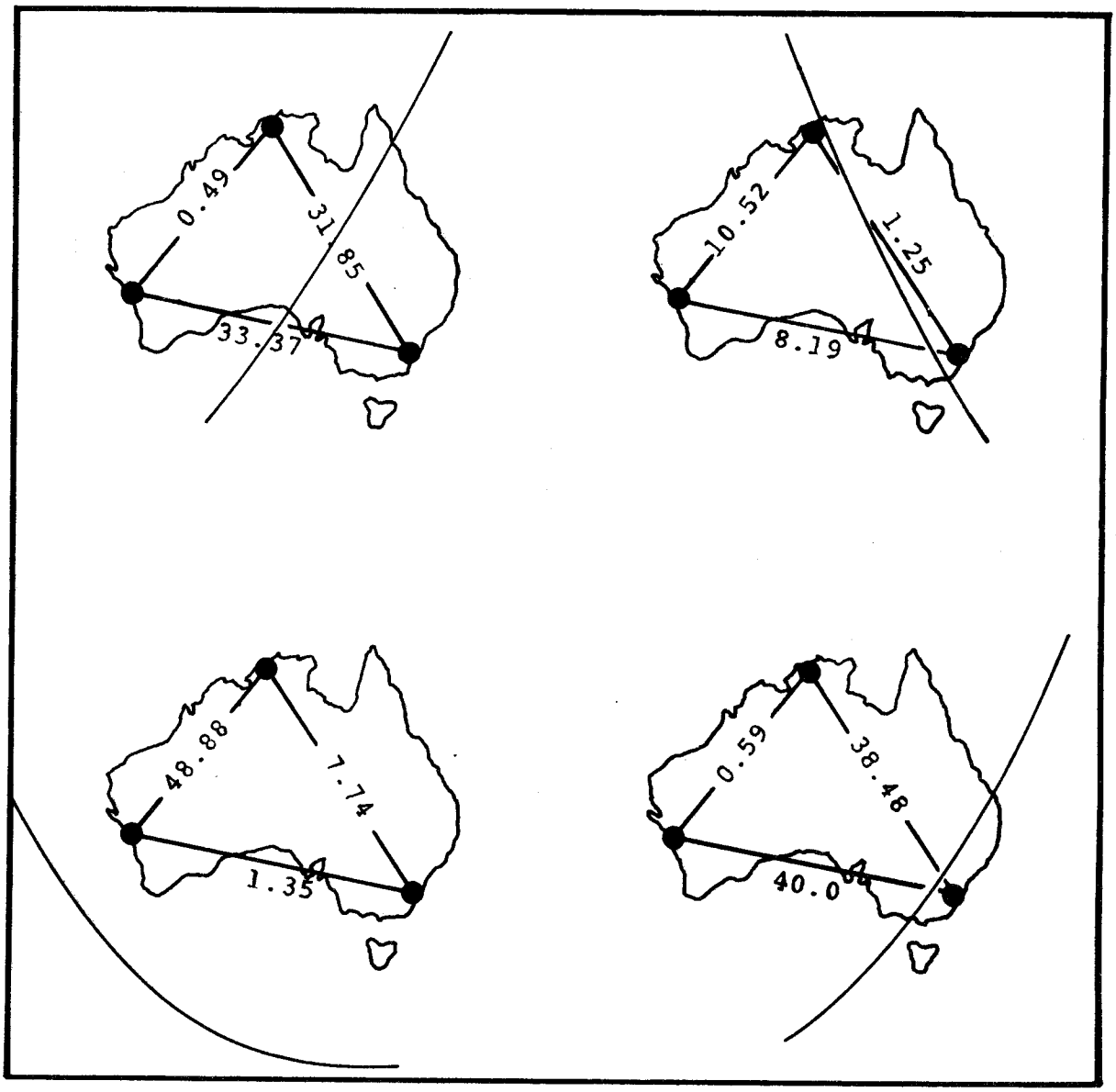

Figure 7.8

The Dependence of Baseline Precisions on the Azimuth of the Satellite Groundtrack.

(Baseline Precision in metres)

order of magnitude, compared to that required to process the full amount of data. There are advantages in compressing the range observations to normal points before analysis. This has been substantiated (Chapter 9; MASTERS et AL (1982).

The effect of network geometry on the results obtainable is shown in Figure 7.8. These solutions were obtained from single passes of data. The precisions show that along-track baselines are more accurately determined than across-track baselines. DUNN et AL (1979) and CHRISTODOULIDIS et AL (1981) arrived at a similar conclusion. East-west baselines will not be as well determined as north-south baselines, unless the data are well distributed in the East-west direction.

TABLE 7.5
BASELINE PRECISION and CPU TIMES for
VARIOUS AMOUNTS of DATA and a priori PRECISION

No. Obs.	(1) **	(2) *	CPU Time min	CPU Time sec	σ_B (m)
17985	8 1.0	1 0.1	40	00	0.041
2241	8 1.0	100 0.1	7	42	0.044
2241	8 0.1	100 0.1	7	42	0.015
333	100 0.1	100 0.1	4	05	0.021
167	200 0.1	200 0.1	3	41	0.030
110	300 0.1	300 0.1	3	32	0.037
2241	8 0.5	100 0.1			0.026
2241	8 0.5	100 0.05			0.022
2241	8 0.5	100 0.02			0.021
2241	8 0.5	100 0.01			0.021
2241	8 0.1	100 0.1			0.015

σ_B .... Precision of baseline

* Tracking Stations:- (1) Orroral
(2) Yarragadee

** For each solution:-
The top row gives the data rate (eg. one range every eight seconds).

The bottom row gives the a priori standard deviation of the data in metres (eg. 1 m at Orroral, 0.1 m at Yarragadee).

7.5 ORAN RESULTS

The ORAN program (HATCH et AL,1973) was made available by NASA. The analyses in the previous sections were checked and augmented using this program. Some changes in procedure were adopted. In particular the variances of the GEM9 gravity field (LERCH et AL,1977) were used for the gravity error model. This is a more realistic assessment of gravity modelling errors. The effects on baselines of range biases, timing biases, refraction, Earth tide orbital perturbations and solid tidal uplift were estimated.

Error sources, other than those due to incorrect gravity modelling, were found to have significant effects on position determinations. Table 7.6 shows the effect of the various error sources on the Orroral-Yarragadee baseline determination. The same data distribution as previously used was adopted. Only error sources greater than one centimetre are shown. Timing biases were ignored since they are not expected to be a problem in practice. The results further emphasise the previously mentioned problem with GM.

TABLE 7.6

CONTRIBUTION of MAIN ERROR SOURCES* to the ORRORAL-YARRAGADEE BASELINE

ERROR SOURCE	1 DAY	2 DAY	3 DAY	5 DAY	SINGLE PASS M.A.
biases	7	4	4	4	5
gravity	22	16	20	18	10
refraction	4	2	2	2	12
tidal uplift	3	4	4	4	6
GM	35	22	23	21	4
TOTAL	42	28	31	28	18
w/o GM	24	17	21	19	17

M.A. multi-arc

* ERROR SOURCE CONTRIBUTIONS (contributions in centimetres)

biases	0.1m
GM	1×10^{-7}
Gravity Model	3 * GEM9 Variances
Refraction	1%
Earth Tides	0.01 in k_2 Love number
Solar radiation	10% of reflectivity coefficient
Pole position	0."01
Tidal uplift	50% of degree 2 effect

For the SPMA solutions short-period gravity modelling errors are at the 10cm level. Surprisingly, the refraction errors are also large. If GM can be estimated successfully in the longer arc solutions there is little benefit in using single pass multi-arc solutions. This is especially the case if the baseline precisions (see Figures 7.6 & 7.7) are included in the error estimate for the baseline. There is little basis for differentiating between the error budgets for arc lengths between one and five days. The longer arc length is therefore more feasible as the precisions will be better.

7.6 CONCLUSION

One method of analysis for crustal motion is to reduce simultaneously observed satellite passes over the region using a single-pass multi-arc method. Systematic baseline errors due to gravity modelling should be small in this case. These short arc lengths however are not as strong statistically as longer arcs. On the other hand, the disadvantage with longer arcs is that it is difficult to completely remove systematic sources of error like that from gravity modelling. The "best" procedure is somewhere between these two extremes.

The results are dependent on the adopted error models. It is evident from the investigation with GEODYN, that if only gravity model errors and tracking noise are considered, the optimum arc length is around 0.5 days and should contain at least four passes. The deviation of one-day long-arc results (Figure 7.5) is about 5 cm. The combined error budget could therefore be minimised by using a multi-arc technique with 0.5 to 1 day arcs. Sub-decimetre baselines could be obtained in less than five days. In practice, high accuracy baselines will take much longer to obtain, mainly because of weather restrictions and other observational limitations.

The ORAN study showed that the results obtained with GEODYN were probably optimistic. There is little benefit in selecting arc lengths between one and five days in order to minimise systematic errors. This means that longer arc lengths are better as the precision of the baselines will be better. It was evident that systematic errors and not tracking noise provide the accuracy bounds for long-arc solutions. Unless gravity model errors decrease significantly with arcs longer than five days, the optimum epoch for solutions is about five days. From these investigations there is also little benefit in using the SPMA procedure. Short-period gravity model errors are still significant, the

solutions are not stable and the baseline precisions are not very good. The precisions obtained for the SPMA solutions indicate that completely geometric configurations would result in poor baselines over the epochs considered here.

It must be understood that there is no unique way of processing data in order to minimise the total error budget. The brief ORAN study and the results of CHRISTODOULIDIS et AL(1981) show that systematic error can be kept at an acceptable level if the arc lengths are increased to 30 days. This allows the orbital dynamics to constrain the solution and most errors tend to average out. For longer arc lengths, there is also the possibility of simultaneously estimating GM and other specific gravity field coefficients, which significantly perturb the orbit. The optimum arc length for 100% tracking efficiency is about five days. However, SMITH et AL (1982) obtained baselines consistent to better than 5 cm for monthly solutions. These results suggest that current error estimates are reasonable.

Care should be taken with kinematic and dynamic Earth rotation errors. These problems require further study, especially if non-simultaneous observations are used.

30-day long-arcs cannot be processed on University of New South Wales computers at present, because the CPU time is not available. Thirty days of data could however be processed using a multi-arc technique, so that the long computer runs are split up over many days. Alternatively, they could be deferred until normal point algorithms are perfected. The possibility of using arcs longer than 5-days should be investigated. These results must be reviewed for the gravity model tailored to LAGEOS. The tailored model should reduce the gravity model error by two or three times (LERCH & KLOSKO,1981; LERCH,1982).

If the data are compressed into normal points substantial reductions in computer time are possible without much loss in precision. This is an important problem, particularly if the data aquisition rates of new generation lasers considered. Various research groups are now investigating possible procedures. Some developmental work has been done in Chapter 9.

In order to analyse the sensitivity of tracking data to geodynamic phenomena all the possible error sources need to be included. Hence it is important to include the latest information on Earth rotation and

force model accuracies in any sensitivity analysis. These analyses have provided the basis for the subsequent research program at the University of New South Wales, which is now well underway (STOLZ & MASTERS,1982).

C H A P T E R 8

ESTIMABILITY of DYNAMIC SATELLITE GEODESY

8.1 INTRODUCTION

Estimability refers to the parameters which can be independently determined from a given observation type. Estimability of laser ranges arose in connection with the feasibility study described in Chapter 7. A description of the problems and relevant background material are given below. In Sections 8.2 and 8.3 the principles of dynamic solutions for geodetic position using range measurements are described. Numerical results for the ranks and conditions of simple dynamic solutions are presented in Section 8.4. The implications of these results are described in Sections 8.4 and 8.5.

The problems studied are:

(i) What is reference coordinate system for coordinates which have been determined with dynamic satellite geodesy?

(ii) What parameters can be estimated with dynamic satellite geodesy?

(iii) How many independent constraint equations are needed to invert the observation equations, that is, how many parameters must be fixed?

These important questions need to be answered if dynamic satellite geodesy is to be applied to Earth dynamics. The change in shape of geodetic networks is of importance for the determination of strain. Coordinates and their associated variance-covariance matrix are needed at different epochs (BRUNNER,1979). The reference systems in dynamic satellite geodetic theory are defined by the theory and solution procedures. These definitions must be carefully considered, otherwise any estimated coordinates will be difficult to interpret. The reference systems become especially important for the comparison of results from different measuring techniques.

By examining past dynamic determinations of tracking station coordinates one notices that the problem of what to constrain has been avoided (LERCH et AL,1974; SMITH et AL,1979a,1979b; DUNN et AL,1979). Recent practice is to hold fixed the longitude of one tracking station (SMITH et AL,1979a; CHRISTODOULIDIS & SEIFFERT,1980; TAPLEY et AL,1980). The lack of concern on the problem was recognised by GRAFAREND & LIVIERATOS (1978) and also VAN GELDER (1978) who states "questions of

estimability.... up to recently were ignored, not explicitly stated or tacitly assumed to be known". VAN GELDER's investigations centred on analysing the estimability of range measurements for a few simple dynamic satellite orbits. The results should apply to more complicated cases. The imprecisely defined rank defects in dynamic satellite networks clearly show a need for a careful examination of dynamic estimation procedures.

It is well known that if only the geometry of a range observation is used to estimate coordinates, the design matrix is rank deficient by the number of free transformation parameters in the network. For a 3-dimensional network the free parameters are three translations and three rotations (BLAHA,1971a; BRUNNER,1979). This means that a minimum of six independent constraint equations are necessary to determine coordinates from the system of range observation equations. This "minimal set of constraints" uniquely define the reference system for the estimated coordinates. They also make the design matrix rank full (BLAHA,1971a). The determination of rank is important because the estimated parameters and their variance-covariance matrix will be affected by the constraints used to eliminate rank defects enabling the equations to be solved. The determination of the rank of the design matrix defines the rank of the minimal set of constraints. If more constraint equations than the "minimal set of constraints" are applied, the system will be overconstrained and the estimated parameters will be distorted. Strain resulting from solution procedures is obviously undesirable for geodynamic applications.

The matter is not so straightforward for dynamic satellite solutions. Several people have examined rank defects of geodetic satellite networks over the last decade. Among these are TSIMIS (1973), ARUR (1977), GRAFAREND & HEINZ (1978), VAN GELDER (1978), GRAFAREND et AL (1979).

ARUR (1977) studied the rank defects present in the solutions obtained from the SAGA Doppler tracking reduction program. ARUR analytically determined the linear dependence between the design matrix coefficients. His results showed the rank defect to be six, the same as for the geometric case.

The simultaneous estimation of tracking station positions, satellite orbital motion and the coefficients of a spherical harmonic series representing the Earth's gravity field was given special

attention by GRAFAREND & HEINZ (1978). A first-order analytical theory was used in their study. The rank defect was

$$N(N+2) + 3S + 16 - n$$

where N is the degree of the spherical harmonic series representing the gravity field,

S is the number of tracking stations and,

n is the number of observations.

This implies that the rank defect depends on the number of observations. VAN GELDER (1978) studied the parameters estimatable from range observations for a few simple secular dynamic satellite models. He expanded the range equation in such a way that the linear dependence between parameters could be determined. The conclusions are limited because the analyses were restricted to secular orbit perturbations and a simple Earth rotation model. These models do not allow the constraining effect of the neglected terms to be fully appreciated. However, they do show where weakness or extreme ill-conditioning could be expected if a more complete dynamic procedure is analysed. High correlation exists between the longitude, right ascension of the ascending node for the orbit and the reference Greenwich Apparent Sidereal Time (GAST).

On the surface these results are all seemingly different. A remark by GRAFAREND & LIVIERATOS (1978) emphasises the disparity between the various fields of thought on these matters and also the need for our own study to clear up what method should be used to define the coordinate system. They point out "many textbooks state that the advantage of dynamic satellite geodesy with respect to its geometrical counterpart is with respect to the supply of absolute coordinates to geodesists. .....from the analysis of terrestrial networks, one has learnt that there is no observation to inform about the translation degrees of the network, that is the datum for origin". However, the reference coordinate system in dynamic satellite geodesy is not directly comparable with that of terrestrial networks. Dynamic theory as shown later falls between two extremes. "Absolute" means that no constraints are used to define the reference system for the reference system invariant range observations. The quotation shows the misunderstanding that can occur if classical geodetic concepts are applied to dynamic satellite geodesy without carefully considering the implications. It should be noted that dynamic reference system is not necessarily fixed.

In the dynamic formulation range observations can be considered as a time series sample of the distance between two moving points. Estimating parameters from this time series can be thought of as spectral analysis. This means that the data sampling will have a large effect on the estimatable parameters. Clearly, only relative velocity between the two points will affect the range measurement with respect to time. The similarity to range rate observations is therefore obvious. Nevertheless, even the relative velocity between the two points is governed by the "laws of motion". Any dynamic theory by definition has a reference system. A series of ranges over a period of time between two points will contain information on the reference system. If this information is estimatable, constraints are not necessary for estimating coordinates. Hence, one can conclude that dynamic satellite geodesy can produce "absolute" coordinates. The proviso to this conclusion is that the type of motion for the two points has a significant effect on the estimability of the observations.

8.2 RANGE EQUATIONS

8.2.1 Analytically Derived Estimability of Range Observations

It is well known that estimability can be gauged by examining the linear dependence between the coefficients of parameters of the range equation or range observation equations. This can be done analytically or numerically. Of course only simple cases can be studied analytically. A few of these are given below. Numerical methods are used in Section 8.4 to study complicated cases.

The range ρ is measured between two moving points A(r) and B(x) (Fig. 8.1). The range equation is:

$$\rho^2 = r^2 + x^2 - 2\mathbf{r}^T \mathbf{x} \qquad (8.1)$$

$$= r^2 + x^2 - 2\, r\, x \cos\alpha \qquad (8.2)$$

where $\alpha = \theta_0 + \Delta\theta - \omega_0 - \Delta\omega$ (8.3)

$\mathbf{r}$ is the tracking station station position vector and,

$\mathbf{x}$ is the satellite position vector,

θ is the polar angle of r,

ω is the polar angle of x,

the subscripts (0) denote initial conditions

The parametric range observation equation is obtained by differentiation (Chapter 5):

$$\rho_0 + v = \rho_c + d\rho \qquad (8.4)$$

where ρ_o is the observed range

ρ_c is the modelled (calculated) range

v is the noise

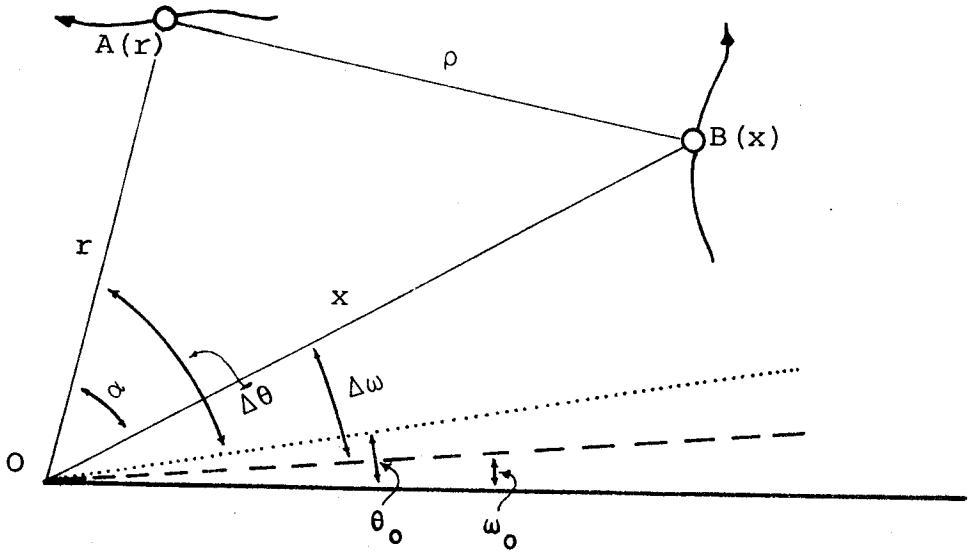

Figure 8.1

Range Observations

Furthermore, the range observation equation at any time t may expanded to:

$$\rho_o + v = \rho_c + \partial\rho/\partial x\, dx + \partial\rho/\partial r\, dr \qquad (8.5)$$

where $\partial\rho/\partial r$ are the partials of range with respect to station coordinates,

$\partial\rho/\partial x$ are the partials of range with respect to the satellite coordinates,

For a dynamic system, both r and x vary with respect to time. In 3-dimensional Cartesian coordinates the corresponding partials for the tracking station and satellite coordinate at time t are equal but of opposite sign, that is

$$\partial\rho/dr = -\partial\rho/dx \qquad (8.6)$$

Coefficients derived from Equation 8.6 are used for the design matrix in the geometric formulation. The position of the satellite and the tracking station positons are estimated at each observation time from strictly simultaneous observations. In this way the observation equations are independent of orbital dynamics. It is clear that the coefficients for tracking station and satellite coordinates are linearly dependent. A minimal set of constraints is therefore necessary to obtain

a solution for these equations. At least six observations from each of four tracking stations are needed (BLAHA,1971b; TSIMIS,1973).

The motions of the two points A and B can be defined by laws of motion. These laws can be in either classical or relativistic reference frames. For satellite geodesy the laws would be the Euler-Liouville equations for the dynamics of Earth rotation and the laws of gravitation for satellite motion. The determination of position from these laws requires integration of the force model starting with initial conditions for position and velocity. The integrated position of A and B at any time is governed by the starting position, the time and the force model. Thus

$$R = f(\mathbf{r}_0, \dot{\mathbf{r}}_0, t) \tag{8.7}$$

$$S = h(\mathbf{s}_0, \dot{\mathbf{s}}_0, t) \tag{8.8}$$

where f and h are functional forms.

R and S are tracking station and satellite positions in an inertial reference system.

Conventionally f is only time dependent. Therefore

$$R = T\,\mathbf{r} \tag{8.9}$$

where T is the transformation matrix between terrestrial and inertial reference systems including contributions from precession, nutation, wobble and rotation (Chapter 5).

h is also well-defined by the adopted force model.

In GEODYN, the force model includes the Earth's gravity field, luni-solar and planetary gravity fields, atmospheric drag, solar radiation pressure and Earth tide effects (Chapter 5). The range vector is

$$\rho = S - R \tag{8.10}$$

We are interested in the parameters that can be estimated from ρ. ρ is a function of $\mathbf{s}_0$, $\mathbf{r}_0$ and t. These parameters can be estimated if their functional relationship is defined and estimatable. The partials for the range observation with respect to satellite position can be transformed to estimate s_0 as follows.

$$\frac{\partial \rho}{\partial s} \rightarrow \frac{\partial \rho}{\partial s}\frac{\partial s}{\partial s_0}\, ds_0 \tag{8.11}$$

$\partial\rho/\partial s$ and $\partial\rho/dr$ can be determined directly from the <u>a priori</u> tracking station and satellite positions at each observation time. The

$\partial s/\partial s_0$ values are determined by solving the variational equations, that is

$$\frac{\partial \ddot{s}}{\partial s_0} = \frac{\partial \ddot{s}}{\partial s}\frac{\partial s}{\partial s_0} + \frac{\partial \ddot{s}}{\partial \dot{s}}\frac{\partial \dot{s}}{\partial s_0} + \frac{\partial \ddot{s}}{\partial p} \qquad (8.12)$$

where p are explicit forcing parameters such as gravity field harmonic coefficients.

If simplified force models are used Equation 8.16 has an exact solution. Analytical expressions for the partials can be developed from dynamic theory (BROUWER,1959; LYDDANE,1963). KAULA (1966) gives the partial derivatives for satellite position. He uses simplified two-body force models for the derivations. On the other hand the numerical integration procedures incorporated in the GEODYN program can manage more complicated force models without the analytical derivation of the solution to the equations of motion and the variational equations. Indeed, for the force models now used, the equations of motion can only be solved using numerical methods. In these cases, linear dependence between the partial derivatives can only be determined by numerical methods.

The degrees of freedom for these types of solutions will depend on the epoch length (ie. arc length) and will be much higher than the geometric case. Precisions for the dynamically estimated parameters will be much better than for the equivalent geometric solution. However the accuracy of dynamic solutions must be determined by analysing the formal precision for the baselines and also the error propagation from the non-estimated force and rotation models. This was carried out in Chapter 7. The following examples demonstrate the principles of the dynamic formulation.

8.2.1.1 General Range Equation

The transformation between polar and Cartesian coordinates is:

$$\mathbf{x} = x \begin{bmatrix} \cos(\omega_0 + \Delta\omega) \\ \sin(\omega_0 + \Delta\omega) \end{bmatrix} \qquad (8.13)$$

$$\mathbf{r} = r \begin{bmatrix} \cos(\theta_0 + \Delta\theta) \\ \sin(\theta_0 + \Delta\theta) \end{bmatrix} \qquad (8.14)$$

and $$d\rho = ((r - x\cos\alpha)dr + (x - r\cos\alpha)dx + r\,x\,\sin\alpha\;\partial\alpha/\partial\omega_0\;\; d\omega_0 + r\,x\,\sin\alpha\;\partial\alpha/\partial\Delta\omega\;\; d\Delta\omega + r\,x\,\sin\alpha\;\partial\alpha/\theta_0\;\; d\theta_0 + r\,x\,\sin\alpha\;\partial\alpha/\partial\Delta\theta\;\; d\Delta\theta)/\rho \qquad (8.15)$$

The coefficients for the parameters $d\omega_0$, $d\theta_0$, $d\Delta\omega$, $d\Delta\theta$ differ only by the terms $\partial\alpha/\omega_0$, $\partial\alpha/\partial\theta_0$, $\partial\alpha/\partial\Delta\omega$, $\partial\alpha/\partial\Delta\theta$. At this stage, where no assumptions have been made about the motion of A or B, the parameters within the range equation or the coefficients in the observation equations for an epoch of measurements will in general be linearly independent. For a dynamic formulation it is also feasible for $\Delta\omega$ to be a function of ω_0 because the gravitational force is position dependent. It is therefore possible for the initial conditions to be estimatable due to the definition of the laws of motion. This means that the reference system is defined by the dynamical theory used to model the motion of A and B.

The estimability of the initial conditions will depend on their analytical formulation. It is clear from Equation 8.15 that the partials will be similar if the motion of the two points is similar. In practice this will affect the conditioning of the matrix rather than causing rank defects. However, there is little difference between an extremely ill-conditioned and a rank defective matrix (Appendix C).

8.2.1.2 Time Dependent Dynamics

The dynamics can be simplified by expressing the terms for $\Delta\omega$ and $\Delta\theta$ as functions of time $\omega(t)$ and $\theta(t)$, then

$$\partial\alpha/\partial\omega_0 \cong -1$$
$$\partial\alpha/\partial\theta_0 \cong 1$$

and

$$\partial\alpha/\Delta\omega \cong \partial\omega(t)/\partial\omega_i$$
$$\partial\alpha/\Delta\theta \cong \partial\theta(t)/\partial\theta_i \qquad (8.16)$$

where the subscripts refer to the components of the functional form. Upon substitution of the functional relationships for the parameters Equation 8.15 reduces to

$$
\begin{aligned}
d\rho = \{&(r - x\cos\alpha) && dr \\
&+(x - r\cos\alpha) && dx \\
&- r\,x\sin\alpha && d\omega_0 \\
&- r\,x\sin\alpha\ \partial\omega(t)/\partial\omega_i && d\omega_i \\
&+ r\,x\sin\alpha && d\theta_0 \\
&+ r\,x\sin\alpha\ \partial\theta(t)/\partial\theta_i && d\theta_i\ \}/\rho
\end{aligned}
\qquad (8.17)
$$

Corrections to the zero degree terms ω_0 and θ_0 clearly cannot be estimated independently. However, $d\omega_i$ and $d\theta_i$ can be estimated if their analytical representations are linearly independent. This will often be the case for the non-linear models of satellite motion, which apply over long time periods. However as the epoch of observations becomes shorter the equations for satellite motion and Earth rotation will become analytically similar and closer to being linearly dependent. This change from linear independence to dependence with the shortened epoch will cause the design matrix to change from well-conditioned to ill-conditioned and in the limit, to rank deficient. This explains why ARUR (1977) obtained a rank defect of six for his method of analysis of the short-arc observation equations.

8.2.1.3 Simplified Dynamics

VAN GELDER's (1978) clock analogy stems from Equation 8.17 by defining the motion of A as

$$\Delta\theta = \dot{\theta}t, \qquad (8.18)$$

B as

$$\Delta\omega = \dot{\omega}t \qquad (8.19)$$

and assuming r and s to be constant (circular motion). Equation 8.17 then reduces to:

$$
\begin{aligned}
d\rho = \{&(r - x\cos\alpha) && dr \\
&+(x - r\cos\alpha) && dx \\
&- r\,x\sin\alpha && d\omega_0 \\
&+ r\,x\sin\alpha && d\theta_0 \\
&- r\,x\sin\alpha\ t && d\dot{\omega} \\
&+ r\,x\sin\alpha\ t && d\dot{\theta}\ \}/\rho
\end{aligned}
\qquad (8.20)
$$

Noting that the motions for $\Delta\omega$ and $\Delta\theta$ are identical, this equation indicates that only r, x, $(d\theta_0 - d\omega_0)$ and $(d\dot{\theta} - d\dot{\omega})$ are estimatable. This result is the same as was obtained by VAN GELDER (1978), that is, for the circular model of motion adopted, range observations cannot be used to estimate the starting vectors $d\theta_0$ and $d\omega_0$ or the velocities

$d\theta$ and $d\omega$ of the two points.

If the motion is more complicated, the estimatable parameters change and may become observation dependent. An hypothetical example can be derived from Equation 8.17 by defining

$\Delta\theta = \sin at$

$\Delta\omega = \dot{\omega}t$

The estimatable parameters are r, x $(d\theta_0 - d\omega_0)$, da, $d\dot{\omega}$. However, in this case the estimability depends on the sampling of the data. If the observations sample every $t=\Pi/a$ then da and $d\omega_0$ cannot be estimated independently.

Three dimensional cases and more complete dynamic systems were analysed in this way by VAN GELDER (1978). Sample observation equations from GEODYN are analysed with numerical methods in Section 8.4. The dynamic observation equation was developed previously without the constraining effect of Earth rotation being made obvious. VAN GELDER (1978) did not study the constraining effect of Earth rotation in detail. He examined the effect of polar motion on the estimability of parameters from the range equation and found that polar motion was estimatable. GRAFAREND & LIVIERATOS (1978) reached this same conclusion. Both conclude that the observation equations would be extremely ill-conditioned but that polar motion is estimatable. All of VAN GELDER's (1978) expansions of the range equation show that the GAST cannot be separated from the right ascension of the ascending node for the satellite and the longitude of the tracking station. Nevertheless, the finer structure of the Earth rotation should be estimatable. SCHUTZ et AL (1979), SMITH et AL (1979b) and CHRISTODOULIDIS & SEIFFERT (1980) have analysed LAGEOS range data for the fine structure of Earth rotation. LLR data has been used in a similar manner (MULHOLLAND,1980).

It is apparent that the rank defect of the equations depends on the dynamic theory. Results for analytical rank analyses cannot be extrapolated from simple to complicated dynamic formulations.

8.2.2 Summary

Range observations are <u>not</u> sensitive to parameters which exhibit similar motion. From VAN GELDER's investigations it is apparent that GEODYN design matrices for state vectors and tracking station position should have a rank defect of one. This will be due to the high correlation between the longitude reference and right ascension of the

node. If one of these parameters is fixed the matrix will have full rank.

For the current dynamic models the optimum precision for both computations and measurements must be chosen. With regard to rank deficiency, VAN GELDER (1978,p90) states ".... it depends on how erroneous the initial set of parameters is". Roundoff error and extreme ill-conditioning may still occur. The condition and error sources for a dynamic satellite solution should therefore be carefully ascertained before inferring anything from the estimated parameters. Statistics about the solution are as important as the parameters themselves. The noise in the system of observation equations will consist of tracking and modelling noise. This noise will in general bias any estimated parameters, making it difficult to separate geodynamic phenomena from inadequate modelling procedures. Many geophysical phenomena are of the magnitude of the errors in the tracking data (Chapters 1, 2 and 3) and therefore have not been modelled accurately. Estimating one geodynamic phenomenon therefore involves separating many other geophysical effects from the data. Of course this is the problem to be overcome with dynamic satellite geodesy. Hence, it is important to gauge the effect of systematic modelling errors and noise on solutions.

Apart from trivial cases, such as insufficient parameters, there is an important category of range adjustment problems for which a unique solution is impossible (BLAHA,1971a). Linear dependence between parameters of the range equation or observation equation coefficients from a range equation does not necessarily reveal all the rank defects of a network of equations. Critical data distributions may occur similar to those examined by BLAHA (1971b) and TSIMIS (1973). Potentially singular network configurations for the range observations have not been investigated here. They will be apparent when the precision of the parameters are examined. Rank deficiency can also occur due to the formulation of the parameters. For example, if the eccentricity is small the argument of perigee and the true anomaly are highly correlated. These problems are somewhat artificial and can be circumvented using different coordinates (KAULA,1966). At this point the solution procedures are critical to the inferred meaning of the estimated coordinates. These are examined in the next section.

8.2.3 The Effect of Solution Techniques

In GEODYN the set of observation equations are solved using a Bayesian estimation scheme (Chapter 5), in which the quantity

$$v^T P v + x^T Q x \qquad (8.21)$$

is minimised. Note that

$P = \Sigma_v^{-1}$ and,

$Q = \Sigma_x^{-1}$,

where Σ_v is the a priori variance-covariance matrix for the noise v and, Σ_x is the a priori variance-covariance matrix of the parameters x.

The solution and variance-covariance matrix for the parameters is obtained by inversion of

$$A^T P A + Q \qquad (8.22)$$

The parameters and variance-covariance matrix are biased by Q, the a priori variance-covariance matrix for the parameters (Chapter 5). The normal equation matrix N is obtained from

$$N = A^T P A. \qquad (8.23)$$

If N is singular, then the solution procedure must eliminate any rank defects before the inverse can be estimated. The a priori variance-covariance matrix for the parameters can be designed to achieve this (Chapter 5). There are many alternatives for inverting N.

For strain calculations the tracking station positions in the adjustment should not be overconstrained. A set of constraining equations with a higher rank than the minimal set of constraints should not be applied. Otherwise the strain results will be influenced by the solution procedure as well as the observations. For a conventional geodetic network, the reference system is defined by the constraints or fixed parameters. If a pseudo-inverse is used, the reference system is defined by the centroid and mean orientation of all coordinates. These are conventionally referred to as "inner coordinates" for which baselines are undistorted (BLAHA,1971a). If constraints are arbitrarily assigned they must eliminate rank defects, so that the other parameters will be referred to the constrained parameters and will be positioned correctly relative to each other (BLAHA,1971a). If more parameters than necessary are held fixed, the solution will be overconstrained and baselines will be distorted. A familiar example of the problem occurs when more than two coordinates and one orientation are held fixed in a classical dimensional geodetic network adjustment.

Only a few specific a priori variance-covariance matrices will

give a pseudo-inverse solution (Chapter 5). Equation 8.22 can always be inverted if the off-diagonal elements of the constraint matrix are zero and the diagonal terms are small. This procedure gives a pseudo-inverse solution referred to here as infinitesimal bordering (Appendix C). The Bayesian least squares estimation scheme in GEODYN, will always give a solution if non-zero a priori variances are used. However, the confidence levels of the estimated parameters and the effect of the a priori variance-covariance matrix should be carefully assessed for this type of procedure before interpretting the results. Arbitrarily assigning the a priori variances in a Bayesian estimation procedure is therefore not recommended.

Another reason for exercising extreme care with Bayesian estimation is that the a posteriori precisions taken from the inverse matrix will be optimistic if a priori variances are too small for the estimated parameters (VAN GELDER,1978; Chapter 5). Unless the residuals are carefully examined the precisions for the parameters will be optimistic.

As shown in Section 8.2, it is possible to estimate the rank defects of simple dynamic observation equations. However, it is not clear what the rank of the observation equations used in GEODYN is. It is not valid to blindly adopt the same constraints as apply to geometric procedures, especially if errors of the order of a few centimetres are not acceptable. Extrapolating analytical results to more complicated dynamic formulations may not be valid. Hence, numerical methods are used in this chapter to analyse for rank defects of the GEODYN solutions in Chapter 7 (Section 8.4).

8.3 SUMMARY

The analytically derived rank defects of the design matrix for dynamic solutions are not the same as for the geometric case. Theoretical analyses of dynamic networks by various authors differ. VAN GELDER's (1978) results for the estimability of range observations may apply to the GEODYN observation equations. Numerical methods are widely used for the complicated dynamic modelling used in GEODYN. The only feasible method to analyse the solutions in Chapter 7 for rank defects and ill-conditioning is by numerical methods.

Estimated parameters depend on the constraint equations used to make the design matrix rank full. These constraints enable the design matrix to be inverted. It is better to have a reference system clearly

defined by the constraints used to eliminate known rank defects, rather than a system which is implicitly defined and unclear. The determination of the rank defects of the design matrix and the "minimal set of constraints" is important. By holding one longitude fixed, the design matrix for tracking station coordinates and satellite state-vector are assumed to have a rank defect of one. If one is the correct rank deficiency then solutions will be overconstrained and distorted if other coordinates are held fixed as well.

With Bayesian least squares it is possible to make a poor choice of the a priori variance-covariance matrix for the parameters. Solutions will always be obtained, but they will be difficult to interpret. If the a priori variances of the parameters are too small, the estimated parameters and their variance-covariance matrix will be overconstrained. This in turn will produce distorted baselines with optimistic precisions and will result in erroneous geodynamic interpretations. Alternatively, if under-constraint occurs the solution will be ill-conditioned. In this case the estimated parameters will not be accurate.

Coordinates will depend on the force model used to derive the satellite motion, the Earth rotation model used to derive the motion of the tracking station and the constraints used to remove rank defects from the design matrix. The reference systems defined in the dynamic models obviously should be consistent. Methods of separating dynamic modelling errors from geodynamic phenomena are needed. Otherwise dynamically determined coordinates will be time dependent with spectra similar to the geodynamic phenomena of interest, such as plate tectonics. This problem was examined in Chapter 7.

8.4 RESULTS USING NUMERICAL METHODS

In this section sample GEODYN solutions for tracking station position are analysed for rank deficiency and condition. The effect of overconstraint is also studied. The results were obtained using the simulated data set described in Section 7.2. One day of data consisted of approximately 2200 range observations, corresponding to seven passes over the Australian tracking stations at Orroral and Yarragadee. The numerical algorithms described in appendix C were employed.

The size of the design matrix was 2200 x 39 in one case. This was far too large for easy analysis. Calculations were simplified by analysing the normal equations instead. The largest matrix to analyse was reduced to 39 x 39. This procedure is justified because the normal

equation matrix has the same rank as the design matrix (BLAHA,1971a). The Normal Equations also have a condition defined by that of the design matrix (NOBLE,1973). Moreover, as least squares solutions are calculated from normal equations, the rank and condition of the normal equations are more relevant.

As only the design matrix is involved, solution vectors are not needed for the the determination of pseudo-rank and condition. Since the "data" exactly fit the GEODYN dynamic models (Section 7.4) the differences between estimated parameters and the a priori values used to create the data will indicate the distorting effect of the solution procedures and any numerical roundoff problems. The effects of ill-conditioning on computer arithmetic should be negligible. This is justified in that even the most ill-conditioned solutions with no constraint whatsoever gave the correct parameters. Changes in the solution parameters can therefore be used to gauge the effect of the solution procedures and models on the estimated parameters.

8.4.1 One-Day Long-Arc

The observation design matrix coefficients were calculated for the ϕ, λ and h of the two tracking stations as well as one epoch state vector. It was assumed that all possible data were observed, that is breakdowns and weather disruptions were not allowed for.

Columns 2 to 7 of Table 8.1 give the differences between the estimated tracking station positions and the a priori values.

Column 1 shows the constraints which have been applied.

Column 9 gives the pseudo-rank, after constraints were applied, as determined using a Gaussian elimination algorithm (appendix C). This indicates if the constraints eliminated the pseudo-rank defects or not. For this calculation the tolerance level for the pseudo-rank was 13 digits. This a few digits less than the computer accuracy. When the tolerance was reduced to 8 digits, (the level of accuracy for the dynamic models), the pseudo-rank dropped by 4 when compared to that for the previous calculation. This demonstrates that the calculations need to be carried out to high accuracy. In this instance, at least 13 significant figures were required, otherwise the sensitivity of the dynamic models is lost. The same results were obtained with the Singular Value Decomposition (SV) routine (Appendix C). For the SV algorithm 12 parameters were still estimated because the rank defect was removed by the pseudo-inverse constraint. Interestingly, the rank defect of one is

TABLE 8.1

DIFFERENCES BETWEEN ESTIMATED AND A PRIORI COORDINATES
for a ONE-DAY LONG-ARC SOLUTION

CONSTRAINT	PARAMETER							***
	ϕ1 (")	λ1 (")	h1 (m)	ϕ2 (")	λ2 (")	h2 (m)	N	PSEUDO RANK
NONE	0	0.0001	0	0	0.0001	0	12	11
S.V.	0	0.2092	0	0	0.2092	0	12	12
δI	0	0.2000	0	0	0.2000	0	12	11
λ2 *	0	0.0200	0	0	0.0200 f	0	11	11
$(\phi,\lambda)2$**	-0.0056	0.0160	0.076	-0.0063 f	0.0158 f	0.050	10	10
$(\phi,\lambda,H)2$*	-0.0027	0.0185	0.075	-0.0200 f	0.0200 f	-1.000 f	9	9
XYZXYZ **	-0.0046	0.0165	0.067	0.0053	0.0159	0.050	6	6

* ..... parameter fixed
** ..... parameter fixed and solution iterated
*** ..... Gaussian elimination algorithm
δI ..... infinitesimal bordering
S.V. ..... singular value decomposition (1 constraint equation applied)
f ..... fixed parameter
N ..... Number of parameters in solution

$(\phi,\lambda,h)2$ ..... position for station number 2
(1) ORRORAL
(2) YARRAGADEE

TABLE 8.2 a
MATRIX CONDITION
for a
ONE-DAY LONG-ARC SOLUTION

	CONSTRAINT											
	NONE			S,V			δI			λ2		
	e	ki	σ^2	e	ki	σ^2	e	ki	σ^2	e	ki	σ^2
X	1 E+02	5 E+09	7 E+03	1 E+02	5 E+03	5 E-03	1 E+02	2 E+08	3 E+02	1 E+02	5 E+03	6 E-03
Y	4 E-06	2 E+10	2 E+05	4 E-06	15	2 E-04	1 E-04	7 E+08	9 E+03	2 E+02	4 E+02	4 E-03
Z	1 E+03	2 E+04	2 E-03	1 E+03	9 E+03	1 E-02	1 E+03	9 E+03	1 E-03	1 E+03	9 E+03	1 E-02
$\dot{X}$	5 E+09	4 E+11	0.4	5 E+09	7 E+03	7 E-09	5 E+09	2 E+10	1 E-02	5 E+09	3 E+02	3 E-10
$\dot{Y}$	4 E+13	4 E+11	1 E-02	4 E+13	3 E+04	8 E-10	4 E+13	2 E+10	6 E-04	4 E+13	2 E+04	7 E-10
$\dot{Z}$	5 E+10	88	8 E-10	5 E+10	68	7 E-10	5 E+10	67	7 E-10	5 E+10	66	7 E-10
$\phi 1$	8 E+05	6.2	8 E-06	8 E+05	4.3	6 E-06	8 E+05	4.3	6 E-06	8 E+05	4.2	6 E-06
$\lambda 1$	5 E+04	2 E+08	5 E+02	5 E+04	5.0	1 E-05	5 E+04	9 E+06	23	3 E+05	1.1	3 E-06
h1	7 E+02	2.0	3 E-03	7 E+02	1.5	2 E-03	7 E+02	1.6	2 E-03	7 E+02	1.5	2 E-03
$\phi 2$	2 E+06	48	9 E-06	2 E+06	30	5 E-06	2 E+06	30	5 E-06	2 E+06	29	5 E-06
$\lambda 2$	7 E+05	2 E+09	5 E+02	7 E+05	4.6	1 E-05	7 E+05	1 E+08	23	NA	NA	NA
h2	5 E+03	4.4	1 E-03	5 E+03	3.4	7 E-04	5 E+03	3.5	8 E-04	5 E+03	3.5	7 E-04
K	1 E+19			NA			4 E+17			2 E+11		

TABLE 8.2 b

	CONSTRAINT								
	$(\phi,\lambda)2$			$(\phi,\lambda,h)2$			$\dot{X}\dot{Y}\dot{Z}XYZ$		
	e	ki	σ^2	e	ki	σ^2	e	ki	σ^2
X	8 E+02	1 E+03	1 E-03	9 E+02	9 E+02	1 E-03	NA	NA	NA
Y	2 E+02	3 E+02	4 E-03	2 E+02	3 E+02	4 E-03	NA	NA	NA
Z	7 E+03	2 E+03	4 E-04	6 E+03	2 E+03	4 E-04	NA	NA	NA
$\dot{X}$	5 E+09	3 E+02	3 E-10	5 E+09	3 E+02	3 E-10	NA	NA	NA
$\dot{Y}$	4 E+13	3 E+02	7 E-11	4 E+13	2 E+03	6 E-11	NA	NA	NA
$\dot{Z}$	5 E+10	66	7 E-10	5 E+10	66	7 E-10	NA	NA	NA
$\phi 1$	8 E+05	1.2	2 E-06	8 E+05	1.1	2 E-06	8 E+05	1.0	1 E-06
$\lambda 1$	2 E+05	1.1	3 E-06	5 E+04	1.1	3 E-06	5 E+04	1.0	3 E-06
h1	3 E+05	1.1	2 E-03	7 E+02	1.0	2 E-03	7 E+02	1.0	2 E-03
$\phi 2$	NA	NA	NA	NA	NA	NA	6 E+06	1.0	2 E-07
$\lambda 2$	NA	NA	NA	NA	NA	NA	4 E+06	1.0	2 E-07
h2	3 E+03	1.3	3 E-03	NA	NA	NA	4 E+03	1.0	2 E-04
K		2 E+11			2 E+11			9 E+03	

NA .... not applicable
e .... eigenvalues
ki .... condition numbers for parameters
K .... condition number for matrix

$(\phi,\lambda,h)2$ .... coordinates for station 2
(1) ORRORAL
(2) YARRAGADEE

σ^2 .... variance ϕ seconds of arc squared
λ seconds of arc squared
h m^2

the same as expected from the analytical analyses (Section 8.2).

The effect of ill-conditioning is not apparent from Table 8.1 (because the data fit the dynamic models of GEODYN perfectly). For these data the solution must be extremely ill-conditioned to give incorrect results. This can be gleaned from row one of Table 8.1, which shows that the difference between the estimated and a priori coordinates is negligible and that the relative positions are preserved. If data was contaminated with noise, these results were found to be significantly different. This result was expected as the a posteriori variances were large (Table 8.2). These are characteristics of an ill-conditioned solution.

The condition of the system of equations can be obtained from Table 8.2, which gives the eigenvalues, condition numbers and variances for the parameters. The highly correlated parameters are shown in table 8.3. The best solutions, that is the ones which resulted in the correct relative positions and good condition, were obtained using singular value decomposition or by holding one longitude fixed. The longitudes are biased towards the free network constraint of +0."2092 or the fixed longitude of +0."02 respectively. These two methods were essentially equivalent, because both of them had one independent constraint equation applied. These results confirm that the coordinates depend on the independent constraints, which are used to remove rank defects (Section 8.2).

TABLE 8.3
HIGHLY CORRELATED PARAMETERS
(>0.99)*

X	Y	$\dot{X}$	$\dot{Y}$	λ1	λ2
Y		$\dot{X}$	$\dot{Y}$	λ1	λ2
$\dot{X}$			$\dot{Y}$	λ1	λ2
$\dot{Y}$				λ1	λ2
λ1					λ2

* (no a priori constraints)
1 Orroral 2 Yarragadee

Tables 8.2 and 8.3 do not make clear all the deficiencies of the system of equations. The range of the eigenvalues (K) gives a good indication whether the numerical inversion of the matrix is feasible or not. If K is greater than the number of significant figures used on the computer arithmetic then the equations are singular for practical purposes. The

approximations (k_i) can only be interpretted in broad terms. However, they do show the number of significant digits, which are lost in the calculation of each estimated parameter. For these solutions a parameter probably loses significance when k_i is greater than 10^8. For the ill-conditioned, no constraint (column 1) and infinitesimal bordering (column 3) solutions, X, Y, $\dot{X}$, $\dot{Y}$, λ_1 and λ_2 should lose significance. Results from these solutions would be meaningless. The variance-covariance matrix gives an estimate of the precision of and correlation between parameters. It is difficult to assess rank defects unless "good" a priori precisions for the solution are available. No attempt is made to quantify good, as it is easier to calculate the pseudo-rank. The variances contain similar information to the condition numbers k_i, although they are difficult to interpret as compared to the latter (see rows four and five of column 3).

From these tables the change from pessimistic to optimistic precisions with the addition of constraints is subtle. Overconstraint would probably not be noticed under normal circumstances. This emphasises the difficulty of detecting the overconstrained situation without calculating the pseudo-rank. Unless a great deal of care is exercised Bayesian least squares procedures can easily lead to overconstrained solutions. The effect of overconstraint can be observed in rows five, six and seven of Table 8.1. Too many fixed parameters resulted in biased absolute and relative positions. Also, the precisions are optimistic, as is evident from columns six seven and eight of Table 8.2.

The difference between the biased relative positions and the a priori positions is small. However, the differences are in the 0 to 10 cm range. This is of the order of magnitude for the geodynamic phenomena, which are of interest. The differences would not be a problem for baseline velocities if the constraint propagated equally for all data. This was investigated by calculating separate one day arc solutions over the 5 days of simulated data. The results showed that the error propagation from the fixed a priori coordinates was arc dependent. This problem may be minimised by using longer arc lengths so that the data distribution is closer to optimum. Nevertheless, at this stage one must conclude that the biases from overconstraint will be epoch dependent and will distort strain calculations.

With the unconstrained solution (row one of Table 8.1, column one of Table 8.2 and Table 8.3) the poorly determined parameters were λ and

the $\dot{X}\dot{Y}XY$ components of the state vector. This indicates high correlation between tracking station longitude and the right ascension of the ascending node for the satellite orbit. The remaining parameters, as expected, were constrained by the dynamic modelling process, leaving the design matrix and hence the normal equations matrix rank deficient by one. The one constraint equation can be introduced by holding one longitude fixed. Alternatively, a pseudo-inverse technique such as singular value decomposition can be used. Either procedure will result in unbiased baseline measurements. These results confirm the claims previously made in Section 8.2. The actual estimated coordinates depend on the dynamic reference system and constraining equations. If the orientation of the coordinate system is important then the solution technique is important. In this case the problem of maintaining the reference system also becomes a problem as these "absolute" coordinates must vary with time for current dynamic models (Chapter 7).

In principle, the conclusions drawn from the one-day arc results should be applicable to any arc length, especially longer ones. Trial solutions for a five-day arc verified this. Shorter arc lengths should be much more susceptible to ill-conditioning and the effects of data distribution. This was discussed in Section 8.2. In the next section a single-pass multi-arc solution is analysed.

8.4.2 Single-Pass Multi-Arc

For the long-arc procedure, the satellite orbital dynamics makes solutions possible with only two tracking stations. This is not the case with single-passes. A third tracking station was therefore placed at Darwin to improve solution stability.

A normal equation matrix was determined from about 1.5 days of data using only simultaneous observations. Simultaneous in this context, meant that each pass of data must be observed in part by all three tracking stations. The matrix contained thirty nine coefficients for the estimation of five state vectors and three tracking station positions.

Table 8.4 shows the differences between the estimated tracking station positions and the a priori positions. Unbiased relative positions and well-conditioned matrices were only obtained when one tracking station longitude was held fixed or the SV algorithm was used with one independent constraint equation. This is an interesting result as it differs from ARUR's (1977) conclusions for the Satellite Doppler system.

TABLE 8.4

DIFFERENCES BETWEEN ESTIMATED and A PRIORI COORDINATES
for a SINGLE-PASS MULTI-ARC SOLUTION

CONSTRAINT	PARAMETER									N	PSEUDO RANK
	ϕ1 (")	λ1 (")	h1 (m)	ϕ2 (")	λ2 (")	h2 (m)	ϕ3 (")	λ3 (")	h3 (m)		
NONE	0	0.0309	0	0	0.0309	0	0	0.0309	0	39	38
S.V.	0	-0.0946	0	0	-0.0946	0	0	-0.0946	0	39	39
δI	0.0014	-0.0727	-0.003	-0.0011	-0.0722	-0.002	-0.0013	-0.0725	-0.002	39	38
λ2	0	0.0200	0	0	0.0200f	0	0	0.0200	0	38	38
(ϕ,λ)2	-0.0012	0.0292	0.007	-0.0200f	0.0200f	0.018	-0.0016	0.0132	-0.010	37	37
(ϕ,λ,H)2	-0.0043	0.0474	-1.110	-0.0200f	0.0200f	-1.000 f	0.0040	0.0210	-1.080	36	36
Q1	0.0133	-0.0409	0.016	0.0090	-0.0364	0.023	0.0114	-0.0407	0.020	39	39
Q2	0.0001	0.0000	-0.002	-0.0002	-0.0001	-0.002	-0.0001	-0.0002	-0.002	39	38

S.V. ..... Singular Value Decomposition (1 constraint equation applied)
δI ..... Infinitesimal Bordering
Q1 ..... σ position = 10 m; σ state vector = 10 m
Q2 ..... σ position = 10 m; σ state vector = 100 m
f ..... fixed parameter
N ..... number of parameters

(ϕ,λ,h)2 ..... Position for station 2
(1) ORRORAL
(2) YARRAGADEE
(3) DARWIN

TABLE 8.5 a
MATRIX CONDITION
for a
SINGLE-PASS MULTI-ARC SOLUTION

	CONSTRAINT											
	NONE			S.V.			δI			$\lambda 2$		
	e	ki	σ^2	e	ki	σ^2	e	ki	σ^2	e	ki	σ^2
$\phi 1$	1 E+06	2 E+03	2 E-03	1 E+06	2 E+03	2 E-03	1 E+06	2 E+03	2 E-03	9 E+05	2 E+03	2 E-03
$\lambda 1$	7 E+04	2 E+13	7 E+08	7 E+04	2 E+03	1 E-02	7 E+04	4 E+05	2	2 E+05	1 E+02	5 E-04
h1	5 E+02	7 E+02	0.9	5 E+02	6 E+02	0.7	5 E+02	6 E+02	0.7	5 E+02	6 E+02	0.7
$\phi 2$	2 E+05	1 E+04	2 E-03	2 E+05	5 E+03	1 E-03	2 E+05	7 E+03	1 E-03	2 E+05	5 E+03	1 E-03
$\lambda 2$	3 E+05	3 E+13	7 E+06	3 E+05	4 E+04	1 E-02	3 E+05	7 E+06	2	NA	NA	NA
h2	20	4 E+03	0.8	20	2 E+03	0.5	20	2 E+03	0.5	20	2 E+03	0.5
$\phi 3$	4 E+06	6 E+03	1 E-03	4 E+06	6 E+03	1 E-04	4 E+06	6 E+03	1 E-03	4 E+06	6 E+03	1 E-03
$\lambda 3$	2 E+06	2 E+13	7 E+06	2 E+06	2 E+04	6 E-03	2 E+06	6 E+06	2	2 E+06	3 E+03	8 E-04
h3	2 E+03	5 E+03	0.9	2 E+03	3 E+03	0.6	2 E+03	3 E+03	0.6	2 E+03	3 E+03	0.6
K		1 E+22			NA			1 E+22			4 E+13	

TABLE 8.5 b

	CONSTRAINT											
	$(\phi,\lambda)2$			$(\phi,\lambda,h)2$			Q1			Q2		
	e	ki	σ^2	e	ki	σ^2	e	ki	σ^2	e	ki	σ^2
$\phi 1$	7 E+05	2 E+03	2 E-03	9 E+05	1 E+03	2 E-03	1 E+06	1 E+03	1 E-03	1 E+06	2 E+03	2 E-03
$\lambda 1$	3 E+05	5 E+01	2 E-04	3 E+05	1 E+02	3 E-05	7 E+04	3 E+03	1 E-02	7 E+04	7 E+03	3 E-02
h1	5 E+02	6 E+02	0.7	5 E+02	4 E+01	4 E-02	5 E+02	4 E+02	0.5	5 E+02	5 E+02	0.6
$\phi 2$	NA	NA	NA	NA	NA	NA	2 E+05	5 E+03	1 E-03	2 E+05	7 E+03	1 E-03
$\lambda 2$	NA	NA	NA	NA	NA	NA	3 E+05	6 E+04	1 E-02	3 E+05	1 E+05	3 E-02
h2	20	2 E-03	0.5	NA	NA	NA	20	2 E+03	0.4	20	2 E+03	0.5
$\phi 3$	8 E+06	3 E+03	5 E-04	6 E+06	3 E+03	4 E-04	4 E+06	5 E+03	8 E-04	4 E+06	6 E+03	9 E-04
$\lambda 3$	3 E+06	2 E+03	6 E-04	3 E+06	2 E+03	6 E-04	2 E+06	4 E+04	1 E-02	2 E+06	2 E+05	3 E-02
h3	2 E+03	3 E+03	0.6	2 E+03	1 E+02	2 E-02	2 E+03	3 E+03	0.5	2 E+03	3 E+03	0.6
K		7.5 E+12			8 E+12			3 E+12			2 E+13	

(condition statistics for state vectors have not been shown)

NA .... not applicable

e .... eigenvalues

ki .... condition numbers for parameters

K .... condition number for matrix

$(\phi,\lambda,h)2$ .... coordinates for station 2
(1) ORRORAL
(2) YARRAGADEE
(3) DARWIN

σ^2 .... variance ϕ seconds of arc squared
λ seconds of arc squared
h m^2

The orbital dynamics for one pass of LAGEOS is capable of constraining the dynamic solution. Nevertheless, the eigenvalues, condition numbers and pseudo-ranks indicate that the equations are not as well conditioned as they are with the longer arc lengths. The k_i values show that the estimated parameters from the single-pass solutions lose one or two more significant figures in the solution than the one-day long-arc. Many of the estimated parameters are therefore probably meaningless, although from Table 8.5 one may conclude that the tracking station positions are correct. As the orbit was not of specific interest the condition of the five state-vectors are not shown. These were not well determined. In general, the parameter precisions are not as good as the equivalent long-arc solution, mainly because more parameters are estimated. In order to obtain equivalent precisions much longer periods of data observation are needed.

Two additional constraint models were adopted in order to show the effect of the Bayesian estimation procedure with a poorly chosen constraint matrix (Tables 8.4 and 8.5).
For Constraint Q1, a priori standard deviations of 10 m for the tracking station positions and state vectors were adopted. These are an order of magnitude larger than the simulated errors. The estimated parameters are distorted, but the matrix is well conditioned.
For Constraint Q2, a priori standard deviations of 10 m for the tracking station positions and 100 m for the state vectors were adopted. These result in almost correct coordinates. However, the matrix is ill-conditioned.

These results show the fine line between overconstraint and underconstraint. The Q1-type solution, which is overconstrained would distort strain calculations. The Q2 type solution, which is ill-conditioned would be numerically unstable. Obviously it is important to estimate the the pseudo-rank for any solutions, where the rank is not clearly defined. Great care should be exercised in selecting a priori variances of the constraint matrix if Bayesian least squares is used. This result reaffirms some researcher's reservations for the Bayesian estimation scheme (VAN GELDER,1978,p105). The implications of these results for other investigations is interesting as many analysts arbitrarily apply a priori variances in Bayesian least squares solutions (MORGAN,1981). These effects should be carefully analysed and not assumed to have minimal effect if the a priori information has no real observational basis.

8.5 CONCLUSIONS

The numerical results, presented in Section 8.3, confirm the analytically derived results of VAN GELDER (1978). The pseudo-rank defect of GEODYN observation equations for the sample solutions is higher than the dynamic result of GRAFAREND & HEINZ (1978) but less than that of the geometric formulation. Tracking station longitude and right ascension of the ascending node for the LAGEOS satellite orbit are highly correlated. When only the tracking station positions and satellite state vectors are being estimated, a satisfactory method for obtaining well conditioned solutions is to fix one longitude. This procedure was adopted for the investigations presented in Chapter 7 and also later analyses of LAGEOS range data (STOLZ et AL,1981). The matter is not so clear if single-pass solutions are used. The same results were obtained as for the long-arc case. However, the solutions were less stable. In all these cases the reference system is defined by the dynamic models and the fixed reference longitude.

Many satellite observations exist for determining position. Here only topocentric range measurements to the LAGEOS satellite were examined. These numerical analyses were made for one specific data set. The results should be applicable to other satellites and positioning systems, though care needs to be exercised. VAN GELDER (1978) found that range, range rate and range difference systems have similar estimability. This is reasonable as range and range rates are essentially the same measurement over a period of time.

In estimability studies where the rank defects of design matrices are sought, conclusions drawn from simplified cases should only be used as indicators for more complicated problems. Correct results will only be obtained if the solution procedures are carefully set up and analysed. With the complicated modelling procedures that are now commonly used, numerical methods are the only feasible ones for analysing dynamic solutions. These procedures are relatively easy to include in any solution system. Now that coordinates accurate to 10 cm are a reality (SMITH et AL,1982) careful consideration should be given to the affects of solution procedures. Great care should be exercised when interpreting parameters estimated with Bayesian procedures. It is too easy to include subjective information with these procedures without realising the effects.

C H A P T E R 9

ANALYSIS OF LAGEOS LASER RANGE DATA

9.1 INTRODUCTION

Preliminary processing and geodetic analysis of laser range data to LAGEOS are presented in this chapter. The geodynamic goals of this work are described in Sections 3.4 and 7.1. These analyses represent the start of an ongoing project to analyse LAGEOS range data (STOLZ & MASTERS,1982) and include:

1) Processing real laser range data rather than simulation studies. Experience has shown that many unforeseen problems occur during the analysis of real data. These problems need to be identified and overcome.

2) Determining the Orroral-Yarragadee baseline as a first step to fulfilling the geodynamic aims of Chapter 3. The solutions are not being presented as the optimum way of determining geodetic baselines from SLR data as results can always be improved upon. The baselines also provide a basis for examining data quality, force models, Earth rotation models and solution procedures. The baselines can be compared with simulation studies for any variation in expected accuracies, because the distance between Orroral and Yarragadee is not expected to move more than a centimetre per year (DENHAM et AL,1979; WEISSELL et AL,1980). During this process the requirements for computing efficiency can be determined with a view to analysing all available LAGEOS laser range data. These requirements will be closely allied to assessing the computational needs for any continuing Australian Crustal dynamics program.

3) Determining whether geodynamics results can be estimated from current data and how long it will take to detect crustal deformation with a continued measuring program.

The data initially received from the United States National Space Science Data Center (NSSDC) in connection with the experiment described in Chapters 3 and 7 contained laser range measurements to LAGEOS for the first six months of 1980. These data have since been updated to

February, 1982 and are currently being analysed using the experience shown in this dissertation. A few results are presented in STOLZ & LAMBECK (1983).

Examination of these data show that Yarragadee and Orroral have been observing regularly from late 1979 until early 1982, when the Orroral SAO station was closed down. In this period, Yarragadee has tracked almost an order of magnitude more passes than the other tracking stations, excluding Orroral and Arequipa. On a few occasions, Yarragadee as tracked up to 5 passes in one day. However, the average amount of tracking is in the range 10-30% of the total possible number of passes. Optimum observation distributions have thus not been maintained for the "best" determinations of the Orroral-Yarragadee baseline. However, there are 157 simultaneous passes (between Orroral and Yarragadee) in the two-year period. These occurred mostly in mid-1980.

Early analyses of these data and the results given in Chapter 7 show that it would be expedient to prefilter and compress the data to normal points. These procedures were developed and are described in Sections 9.2 and 9.3 (MASTERS et AL,1982). Baseline solutions were determined for nine arcs of less than 4 days duration between January and May, 1980. The methods and results are described in Section 9.3 (STOLZ & MASTERS,1982) and compared with Doppler positions and the terrestrial geodetic networks. The variations of these baselines are compared with the expected errors as determined in simulation studies in order to ascertain the accuracy of the data.

9.2 FILTERING AND NORMAL POINTS

9.2.1 Introduction

Preliminary geodetic analyses with LAGEOS range data revealed many random outliers within passes of usually consistent data. However, it was apparent that SAO data from Orroral contained few or no outliers. Outliers must be removed from final geodetic analyses in order to obtain the best results. Procedures for removing bad data are referred to here as filtering. Experience has shown that filtering random outliers in range data sets before geodetic analysis is necessary to optimise computational efficiency.

In Section 9.2.2 the method adopted by the author for prefiltering LAGEOS laser range data at U.N.S.W. is described. The effectiveness of

the procedure is demonstrated in Section 9.2.2.1.

Range data from the global configuration of laser tracking stations are required for optimum geodynamic calculations. Laser tracking stations are being upgraded to be more efficient, with improved precision and faster pulse repetition rates. Data compression techniques will have an increasing role to play in order to achieve geodynamic results in an expeditious manner. Compressed data are usually referred to as Normal Points. It is generally considered that the use of Normal Points will become a standard procedure for analysing SLR data (PEARLMAN,1982). Outliers need to be removed prior to compressing data. The procedures for prefiltering and forming normal points have therefore been considered here as one pre-processing procedure.

Several filtering techniques are in use (PEARLMAN,1982). By far the most common approach is to compare each observation with a modelled counterpart obtained from, amongst other things, an orbit computed using all available data (TAPLEY et AL,1982). This procedure has the advantage of detecting long period errors in the data and is therefore very useful for examining the performance of laser trackers. However, range and timing biases of small magnitude, say less than 40cm and 100microsec respectively are basically still impossible to detect (EANES et AL,1982).

The purpose of the filter described in this chapter is to remove random outliers in the range data set. This can be achieved by utilizing the fact that the range varies with time very nearly as a quadratic curve. The detection of long period range biases and timing biases is regarded as part of the later geodetic analysis problem.

Range data in compressed form have been employed by lunar laser ranging analysts for many years (MULHOLLAND,1980). The nature of the lunar laser observing process, which requires only a few observations distributed over what typically amounts to 10 minutes, makes it quite natural to consider some means of compressing the data into "normal points". ABBOT et AL(1973) operate on the difference between the observed delay and one computed from a high-precision mathematical model of the positions and velocities of both the laser and the lunar retroreflector. This residual is usually small and is represented by a very low-order time polynomial. The order of the polynomial is chosen in such a way that the information content of the raw data is retained

and so that the error in representation is much smaller than the observational uncertainty.

There are several possible approaches to the LAGEOS data compression problem. For example, one could devise a method based on range residuals, similar to the LLR procedure. This method has been adopted by several groups of analysts (e.g. EANES et AL,1982). However, the process would be time consuming since it requires a sophisticated model for the LAGEOS orbit and, if computer resource conservation is an important consideration, then little benefit would be gained. On the other hand, one could proceed like GAMBIS (1982), who represents the range over a pass by a single time polynomial which he then interpolates to yield 10-15 normal points. The procedure of using high order polynomials does introduce interpolation problems if the data in the normal point band is sparse (GAMBIS,1982). Also, normal points within a pass will be correlated, depending on the interpolating polynomial. This correlation would require more refined geodetic solution procedures. An alternative method for compressing raw measurements is presented in Section 9.2.3 (MASTERS et AL,1982). The method is, in principle, the same as that of GAMBIS (1982), whose analysis was carried out at the same time and independently of those in this chapter.

9.2.2 Filtering

Examination of LAGEOS data has shown that the variation of range with time closely resembles a quadratic curve. (The second derivative was calculated for a few passes of data and found to vary between zero and $4 m/s^2$. The second derivative with respect to time, over short periods (say 5 minutes) is fairly constant, that is

$$\ddot{\rho} \cong \text{const.} \tag{9.1}$$

Successive differences of the derivative can be easily used to detect outliers in the range data as given below

$$\Delta\ddot{\rho} = W^T \rho \tag{9.2}$$

where

$$W^T = [w_1 \;\; w_2 \;\; w_3 \;\; w_4] \tag{9.3}$$

$$\rho^T = [\rho_1 \;\; \rho_2 \;\; \rho_3 \;\; \rho_4] \tag{9.4}$$

subscripts denote four consecutive observations, and

$$w_1 = -2/\Delta t_1 (\Delta t_1 + \Delta t_2) \tag{9.5}$$

$$w_2 = 2(\Delta t_1 + \Delta t_2 + \Delta t_3)/\Delta t_1 \Delta t_2 (\Delta t_2 + \Delta t_3) \tag{9.6}$$

$$w_3 = -2(\Delta t_1 + \Delta t_2 + \Delta t_3)/\Delta t_2 \Delta t_3 (\Delta t_1 + \Delta t_2) \tag{9.7}$$

$$w_4 = 2/\Delta t_3 (\Delta t_2 + \Delta t_3) \tag{9.8}$$

Δt denotes time elapsed between consecutive observations.

In practice

$$\Delta\ddot{\rho} = \pm(a+b) \qquad (9.9)$$

where a represents the effect of random tracking error, and
b the effect of truncation error.

An error bound for $\Delta\ddot{\rho}$ may be obtained from

$$\sigma^2_{\Delta\ddot{\rho}} = \sum_{i=1}^{4} w_i \, (\sigma_a^2 + \sigma_b^2) \qquad (9.10)$$

where

σ_a^2 is the variance of the range measurement, and
σ_b^2 is the variance of the truncation error due to using an incorrect polynomial representation.

σ_a is generally known, whereas σ_b must be estimated.

As previously stated, $\Delta\ddot{\rho}$ should be almost zero within the error bounds, due to random tracking errors. In the presence of outliers, $\Delta\ddot{\rho}$ will behave erratically. This fact can be used to identify and remove outliers. From Equations (9.5-9.8) it is apparent that the main contribution to $\Delta\ddot{\rho}$ is from the 2nd and 3rd observations of the four observations contributing to the 2nd derivative. It is a simple task to devise an iterative scheme to determine, pass by pass, which observations are bad. The method (which readily lends itself to automation on a computer) is similar to that adopted by astronomers to detect errors in ephemeris tables (BROUWER AND CLEMENCE, 1961).

It is also possible to estimate the precision of the tracking data from a sample of $\Delta\ddot{\rho}$ values. Error bounds for the filtering procedure can therefore be derived from the precision of the data rather than an a priori estimate. Assuming constant range precision and zero truncation error in Equation 9.10, we obtain

$$\sigma_a^2 = \sigma^2_{\Delta\ddot{\rho}} \; / \; \Sigma w_i^2 \qquad (9.11)$$

and

$$\sigma^2_{\Delta\ddot{\rho}} = 1/n \sum_{n} \Delta\ddot{\rho}^2 \qquad (9.12)$$

If the data is filtered pass by pass, the error bound can be easily iterated to the estimated precision of the tracking data.

The effect of truncation error was determined by estimating the

r.m.s. difference between "perfect" range data and the corresponding ranges modelled by an order 2 polynomial. "Perfect" refers to the data having no random tracking errors. These data were determined using the orbital theory described by MARTIN et AL (1976), with the best available models for the forces perturbing the LAGEOS motion. The r.m.s. difference is plotted in Figure 9.1 for time spans of 0-300 secs. This difference was found to be consistent with the variations of real passes of data.

Figure 9.1 shows that the filter based on variation in $\Delta\ddot{\rho}$ should: perform well up to 30 sec.; be marginally effective between 30 sec. and 100 sec., and fail beyond 100 secs. Large gaps in the data will thus reduce the efficiency of the filter. Also, it will only be marginally effective with SAO data due to the lower repetition rate. However, this lack of effectiveness will not be a problem as experience has shown that SAO data needs little or no filtering. The relative contributions of each ρ_i to $\Delta\ddot{\rho}$ will also mean that the filter is only marginally sensitive to errors in the first and last points in a pass.

9.2.2.1 Filtering Results

The filter was tested on real data. Figures 9.2 and 9.3 show the residuals for two typical LAGEOS passes over the Yarragadee site. The data and outliers are uniformly distributed over the pass shown in Figure 9.2, whereas in Figure 9.3 a portion of the outliers occurs at the beginning of the pass where the data are sparse. The passes, before filtering, are shown in Figure 9.2a and 9.3a. The same passes after filtering are shown in Figures 9.2b and 9.3b. The filter determines its own value for the range precision and the rejection level is set accordingly. As expected, the filter behaves well except when large data gaps occur within a pass. Obviously long period trends must also be present in the filtered data. The filter was used on about six months of laser range tracking data to LAGEOS. About 2% of data were rejected on this filtering basis. The average range precision for Yarragadee and Orroral was approximately 8 cm and 40 cm respectively. However, the precision of Orroral varied between 20 cm and 100 cm. The problem with data gaps is the main limitation with this method. It can be overcome by including more data for the detection of each outlier or by including further filtering with the accompanying normal point procedure. The latter procedure was adopted as it was easy to implement.

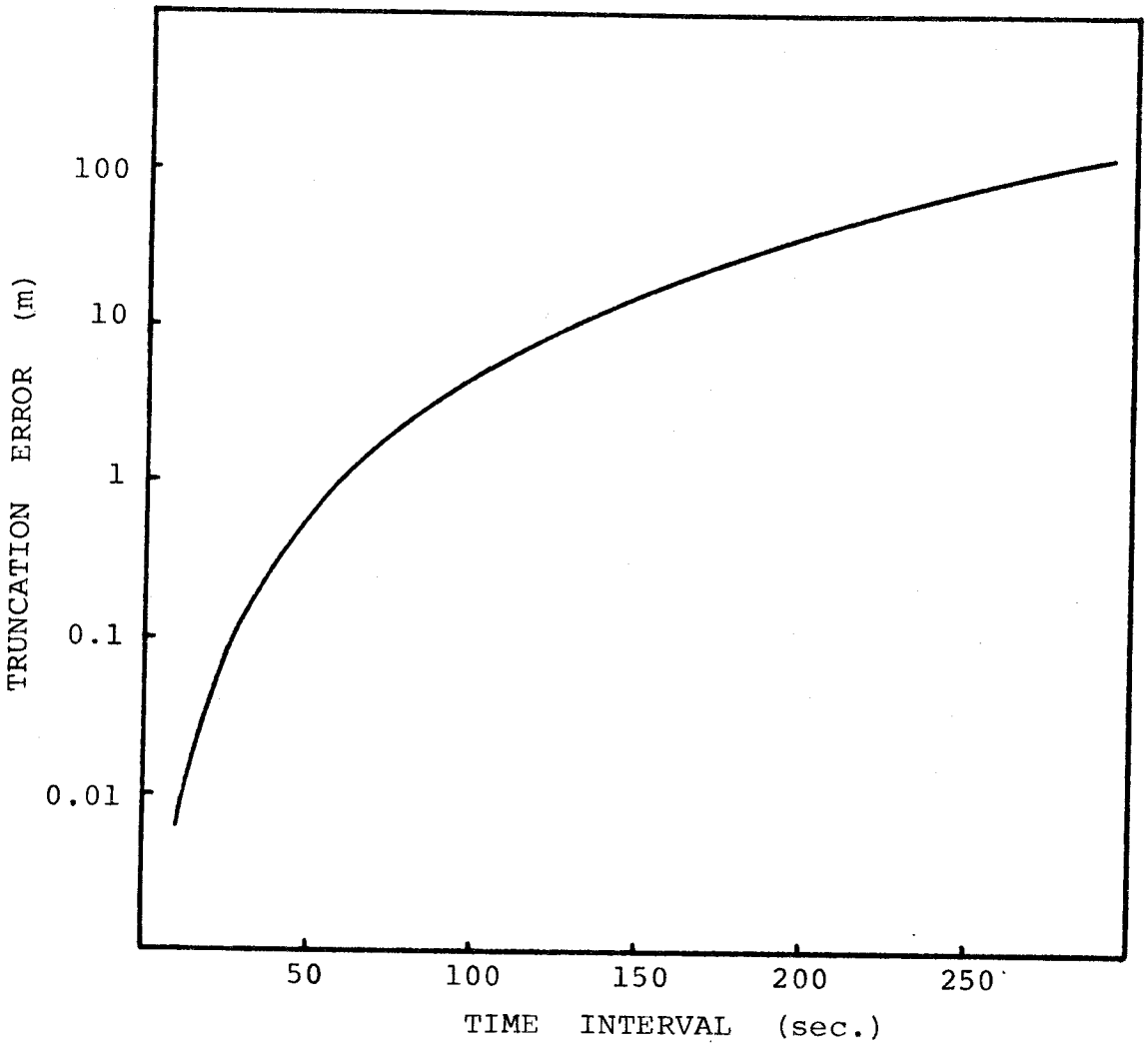

FIGURE 9.1

Truncation error with time span for laser range data to LAGEOS .

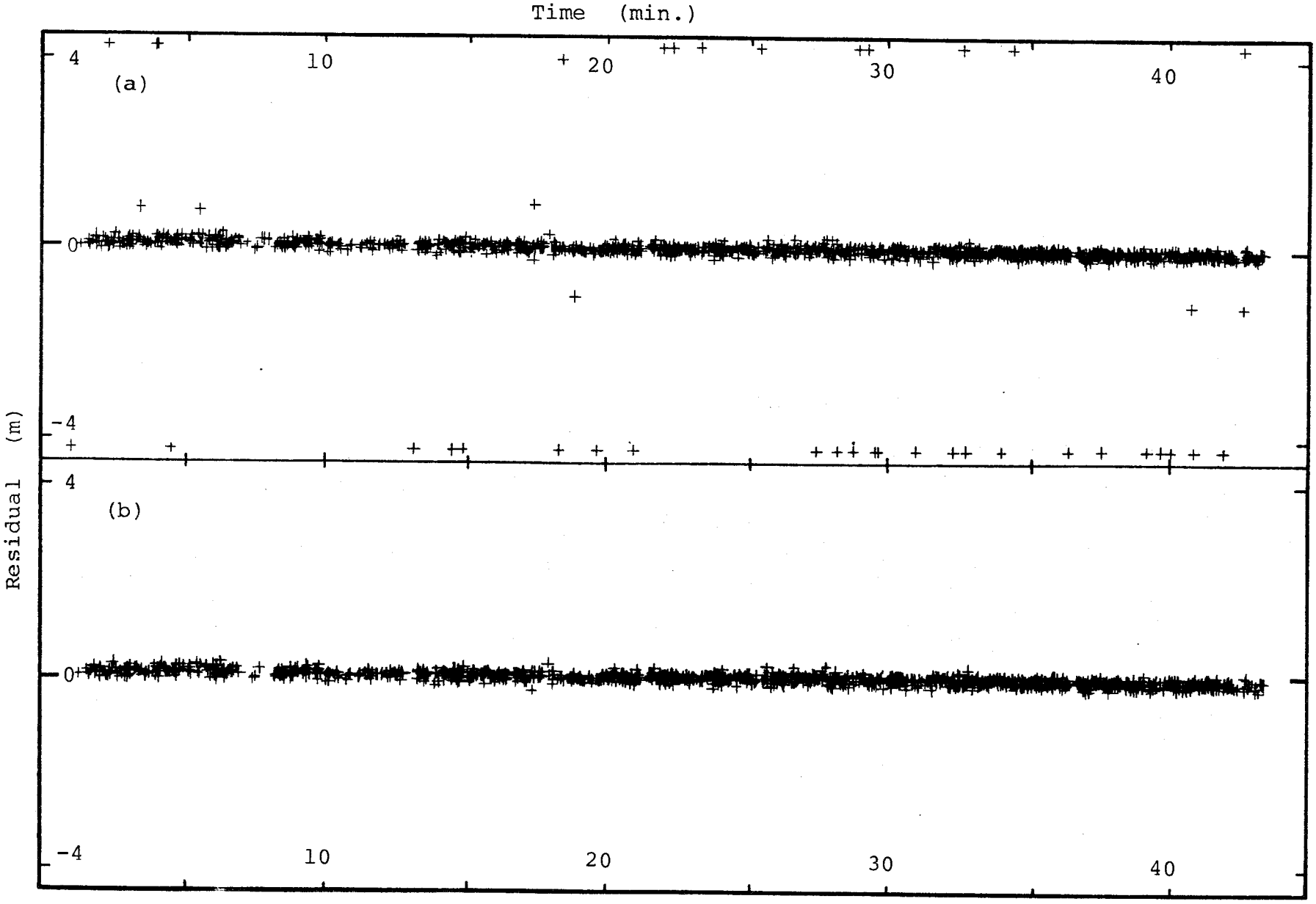

FIGURE 9.2 (a) Laser range residuals without filtering
(b) same as (a) with filtering

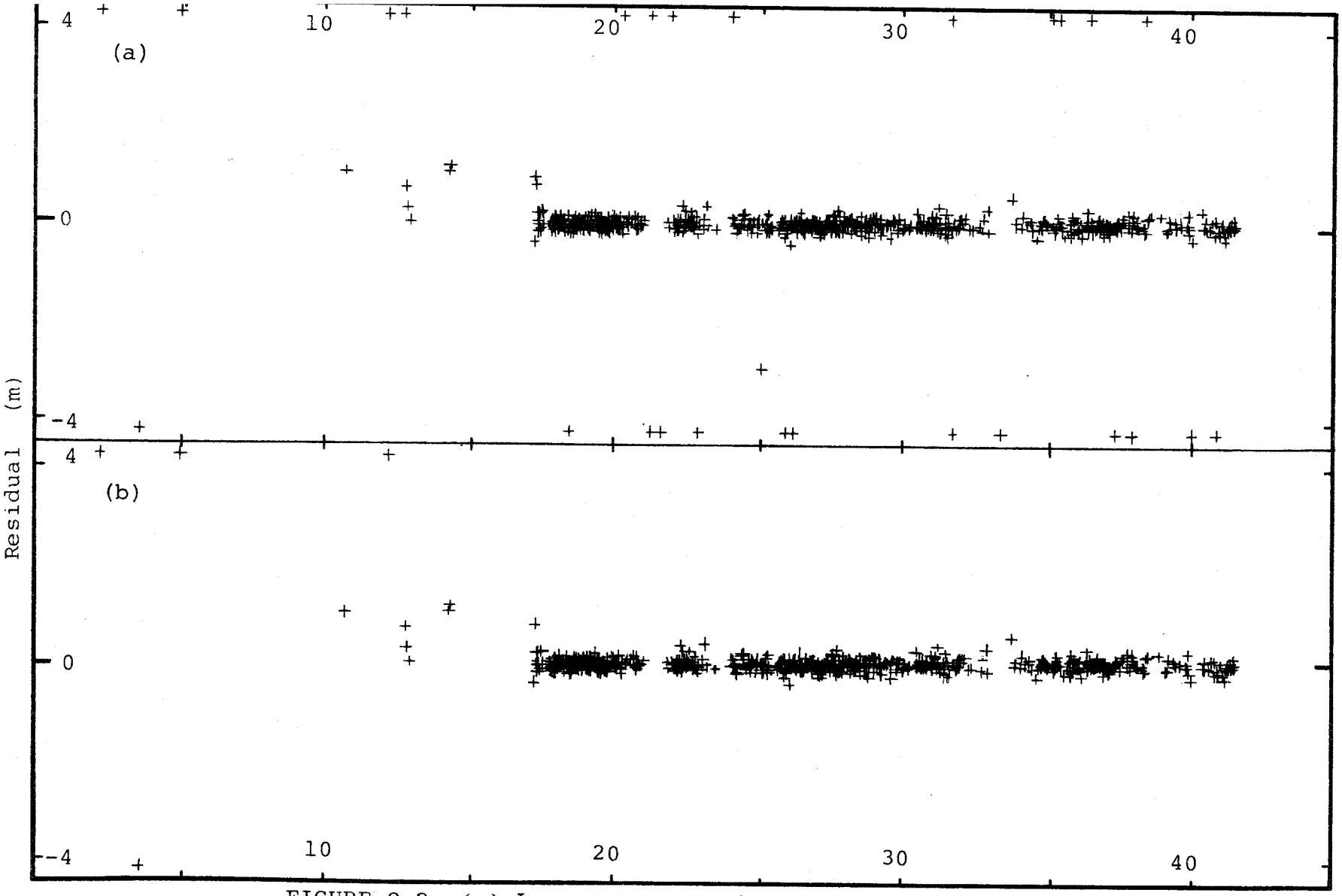

FIGURE 9.3 (a) Laser range residuals without filtering
(b) same as (a) with filtering

9.2.3 Normal Points

The issues to be considered for normal point procedures are:

1) To select the time-interval over which the raw data are to be compressed.

2) To decide on the type of polynomial to be fitted to the raw data over this interval, and to determine the appropriate order of the polynomial.

3) To choose the point on the curve which best represents the normal point, and

4) To estimate the accuracy of the normal point.

Chebyshev polynomials were chosen because they are simple to program and commonly used for interpolation of ephemerides. Standard least squares procedures were used to carry out a piecewise-fit of these polynomials to the range data and to determine the precision of the normal points (see Chapter 5). The Chebyshev polynomial representation is given by:

$$\rho(x) = \sum_{i=0}^{n} d_i \, C_n(x) \qquad (9.13)$$

where n is the order of the polynomial, and

$$C_n(x) = \cos n \cos^{-1} x \qquad (9.14)$$

Stable solutions are obtained for the coefficients d_i if the argument x is normalised so that

$$-1 \leq x \leq 1$$

Simple recursives can be used to calculate $C_n(x)$

$$C_n(x) = 2x \, C_{n-1}(x) - C_{n-2}(x) \qquad (9.15)$$

Experience has shown that one should be wary of interpolating with high-order polynomials, especially if the data are sparse. GAMBIS (1982) found this problem when compressing data by fitting high-order polynomials to complete passes of data. Interpolation problems were avoided here by estimating the time period for which the polynomial order could be kept low (say $n < 5$) and fitting the polynomials piecewise to passes of data. This procedure also avoids correlation problems between the calculated normal points. The time-interval over which the data are to be compressed and the order of the polynomial to be fitted to the data both need to be determined empirically. The time-interval should be long enough to significantly reduce the amount of

data yet not so long as to remove important signals or make the dynamic solutions ill-conditioned.

In Figure 9.4 the mean square departure of "perfect" MOBLAS range measurements from Chebyshev polynomials of order 3-9 are plotted as solid circles. The polynomials have been fitted piecewise to 1 day of data at intervals of 100 sec. The formal error of the normal point for **a priori** range precisions of 5 and 10 cm (MOBLAS) is shown by broken lines. The combined effect of truncation error (solid circles) and range measurement error (broken lines) is considered to be an estimate of the precision of the normal point, and is smallest for the polynomial of order 4. These calculations were repeated with real data and for time intervals of 100, 150, 200 and 250 seconds. The results are summarized in Table 9.1. On the basis of these calculations, a compression interval of 150 sec. represented by a polynomial of order 4 is recommended.

TABLE 9.1

R.M.S. CURVE FITS to RANGE DATA

Polynomial Order	Data Span, sec.			
	100	150	200	250
3	0.1	0.2		
4	0.08	0.08	0.09	
5	0.08	0.08	0.08	0.08
6	0.08	0.08	0.08	

There are several possibilities for the time of interpolation for the normal point:

1) The mean time over which the data are compressed.

2) The time of the observation closest to mean time, or

3) A time in the region where the data are densest.

There is little to choose between options (1) and (2). Option (2) has the advantage that the data is not actually being interpolated. Any errors due to sparse data should therefore be minimised. Option (3) has the disadvantage of being complicated to program.

Finally, the data forming each normal point can be further filtered by analysing the residuals of the least squares curve fits. This is a standard least squares analysis procedure.

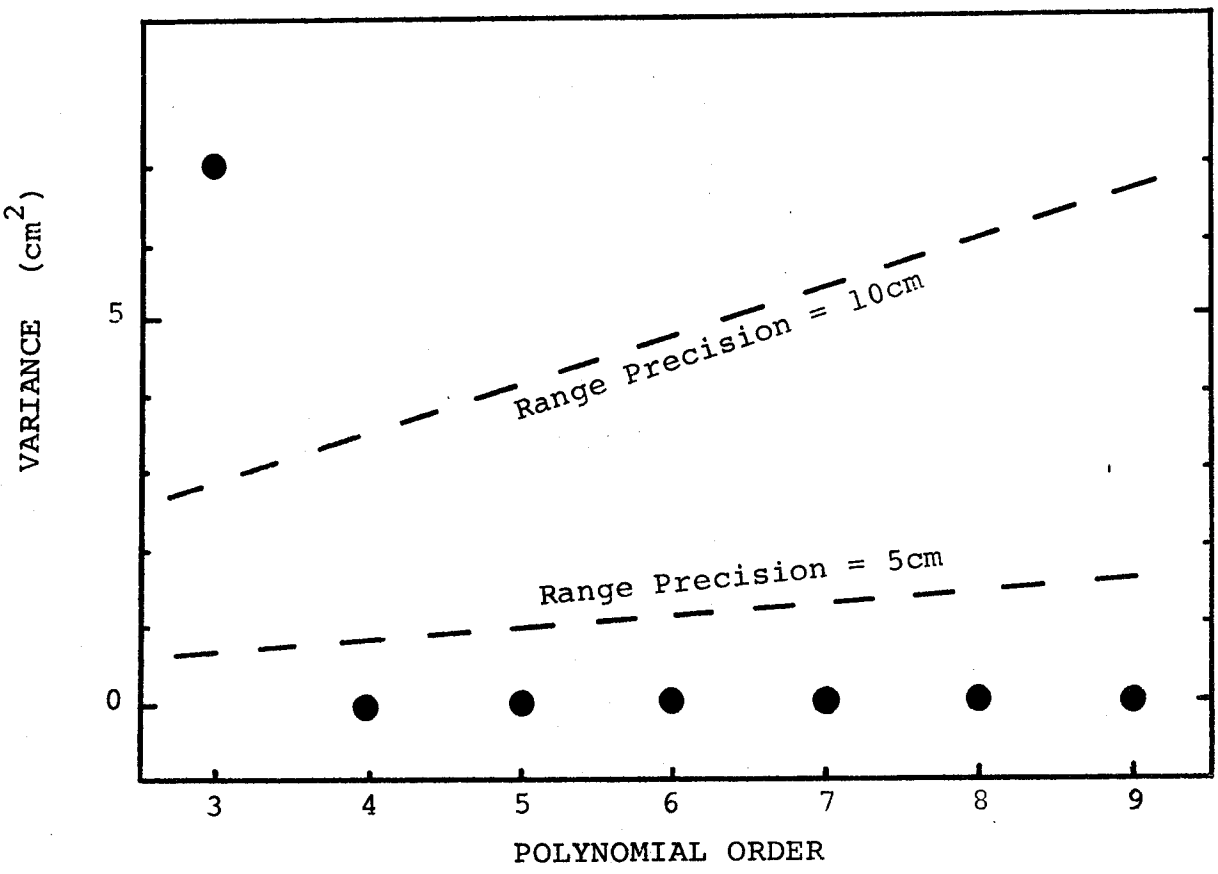

FIGURE 9.4

Truncation error for varying orders of polynomial
(solid circles)

Variance of normal point for <u>apriori</u> range precisions of 5 and 10 cm
(broken lines)

9.2.3.1 Normal Point Results

A typical 150 sec., order 4 polynomial, normal point residual pattern for a good pass of LAGEOS data is shown in Figure 9.5. Signals with periods longer than 300 sec. are not removed. The normal points were determined at the mean times.

In order to determine whether the Orroral-Yarragadee baseline measurements are degraded by data compression, several orbital arcs tracked from Orroral, Yarragadee, Greenbelt (STALAS), American Samoa, Owens Valley and Goldstone were selected. The latter tracking stations are MOBLAS sites. This configuration ensured that a strong Orroral-Yarragadee baseline measurement was obtained. The details are presented in Section 9.3. The Orroral-Yarragadee baseline was solved for using the full data rate and from the same data compressed into 150 sec. normal points. The number of raw ranges which made up each normal point varied widely and, therefore, the precision of each normal point was different. The precision was usually of the order (2 cm) for a priori range precision of 10 cm. The Orroral SAO data have a lower precision and slower pulse repetition rate than the NASA tracking stations. As little would be achieved in CPU savings these data were not compressed to normal points. Five degrees of freedom are lost in the determination of the normal points. The relative weight between the normal points and raw data can therefore change slightly, that is the relative weighting between the SAO and MOBLAS/STALAS data can change. In the solutions, the MOBLAS/STALAS data were weighted to be four times more precise than the Orroral data. The data set was compressed to about 4% of the original size. This compression resulted in a 10-20 times reduction in CPU time per arc.

In Figure 9.6 the differences between the baseline measurements obtained from full data rate and from compressed data are given. Each set differs by less than the baseline measurement precision (error bars). However, the data for both sets of baselines are meant to be the same and should therefore give exactly the same answers. Table 9.2 gives the estimated standard deviations for the baselines taken from the least squares solution. The differences between the standard deviations indicate that some information is lost in the compression to normal points. In order to check that the baseline differences shown in Figure 9.6 were due to solution instability, or biased normal points, baseline solutions were recalculated with the orbit fixed to the values determined with the full rate data. These solutions are well-

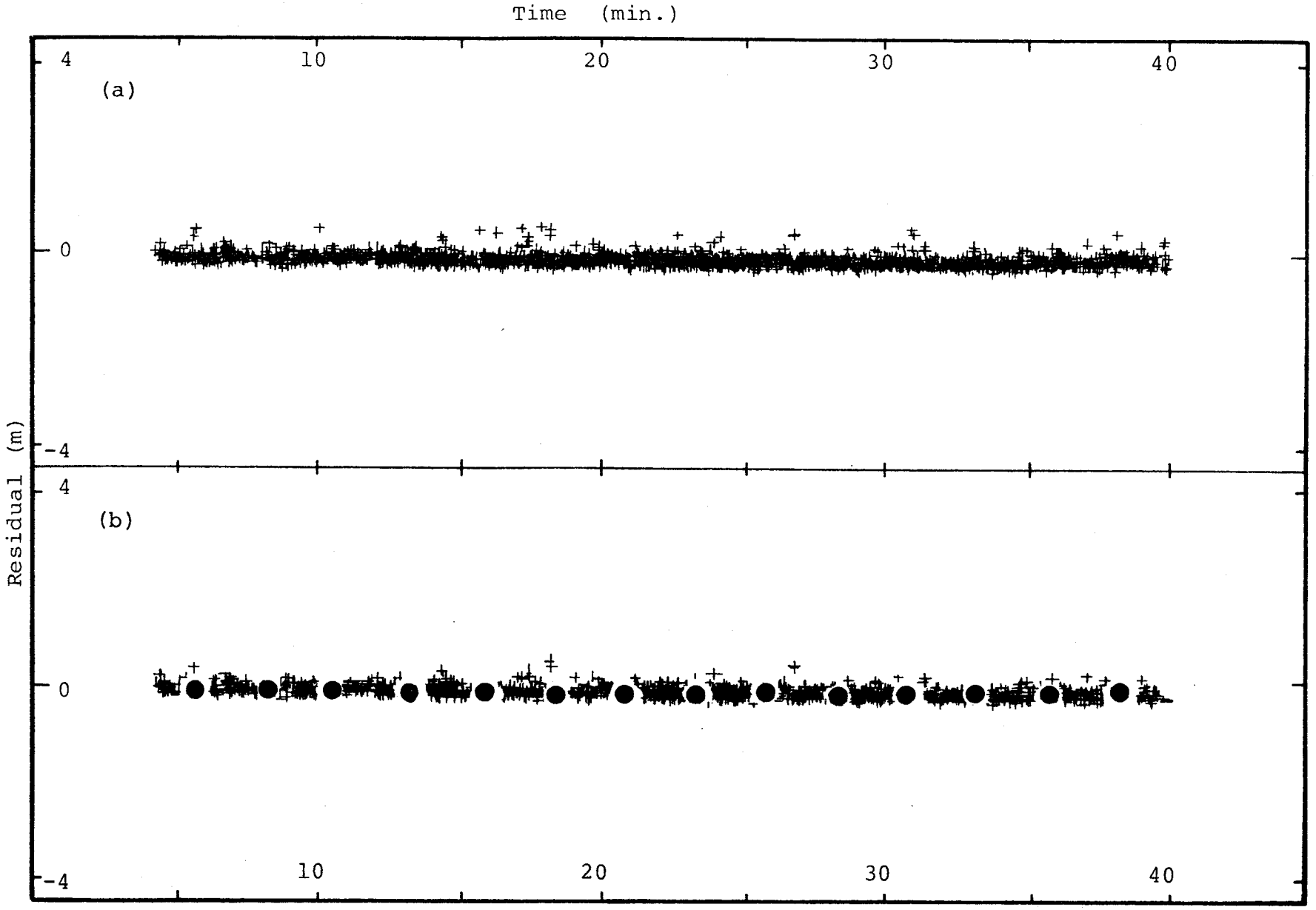

FIGURE 9.5 (a)Raw range measurements over one pass
(b)The same pass with normal points and filtering

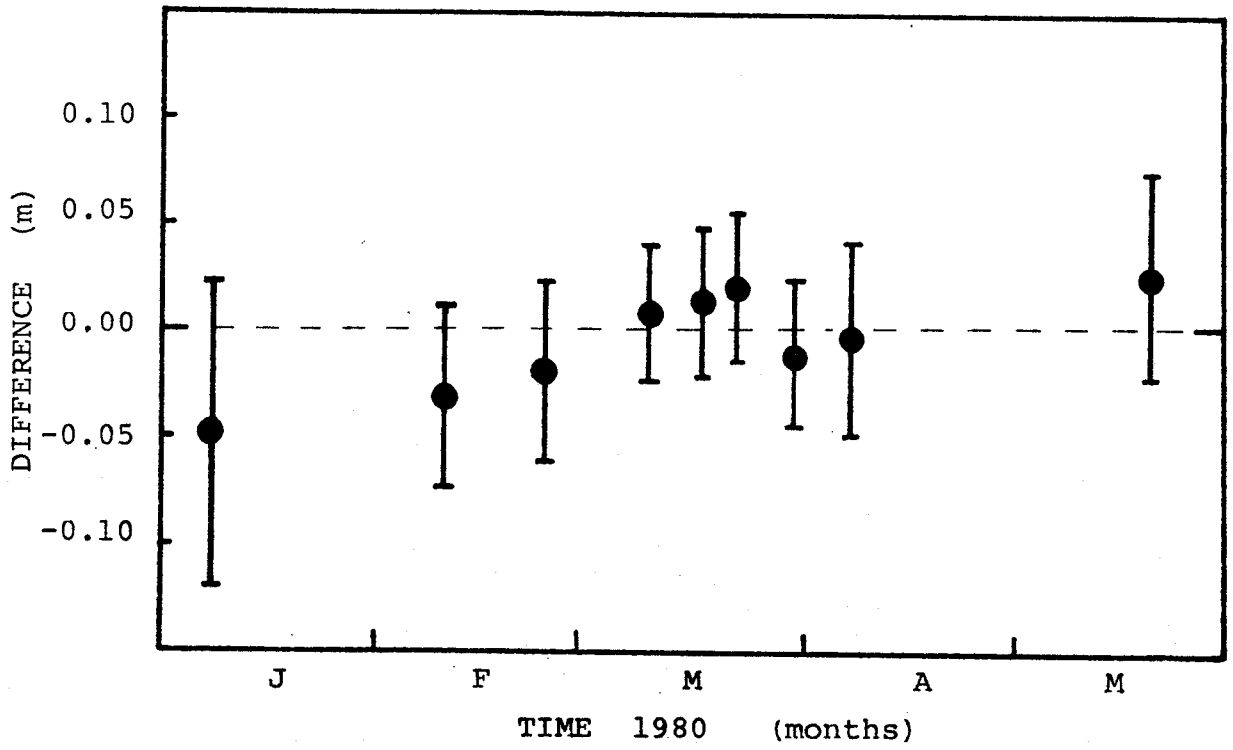

FIGURE 9.6

Difference between Orroral-Yarragadee baseline measurements obtained from full data rate and the same data compressed to 150 sec. normal points

conditioned (Chapter 8) and if differences still occur they must be due to the normal point calculations. Conversely, if the differences are negligible, the discrepancies must be the result of ill-conditioning due to data distribution and pass geometry. With the orbit fixed, the baseline measurement agreed at the millimetre level. This shows that the normal point method is sound, but care should be exercised with the geodetic solutions, especially if longer time bands are used for the normal point compression interval.

TABLE 9.2

BASELINE PRECISION FOR SHORT ARCS

Arc no.	raw data σ (cm)	normal points σ (cm)
1	3.4	3.5
2	5.7	7.2
3	4.2	4.3
4	3.5	4.1
5	3.1	3.2
6	3.2	3.5
7	3.6	3.8
8	4.7	4.7
9	5.0	5.1

9.3 THE BASELINE BETWEEN ORRORAL AND YARRAGADEE

9.3.1 Introduction and Method

Nine arcs of four days' duration or less were chosen over a period of 130 days, with at last three passes of data from both Orroral and Yarragadee. These requirements also made easy comparisons with simulation studies. When available, simultaneous observations between Orroral and Yarragadee were included. Data was also included for American Samoa and mainland U.S. stations STALAS, Goldstone and Owens Valley. The tracking station network is shown in Figure 9.7. The arc length, data distribution and station configuration were chosen to ensure that a strong baseline solution between Orroral and Yarragadee was obtained and that the amount of data was of a manageable size. These were the first baseline solutions attempted in Australia (STOLZ et AL,1981).

The U.S. tracking stations are not essential for the solutions

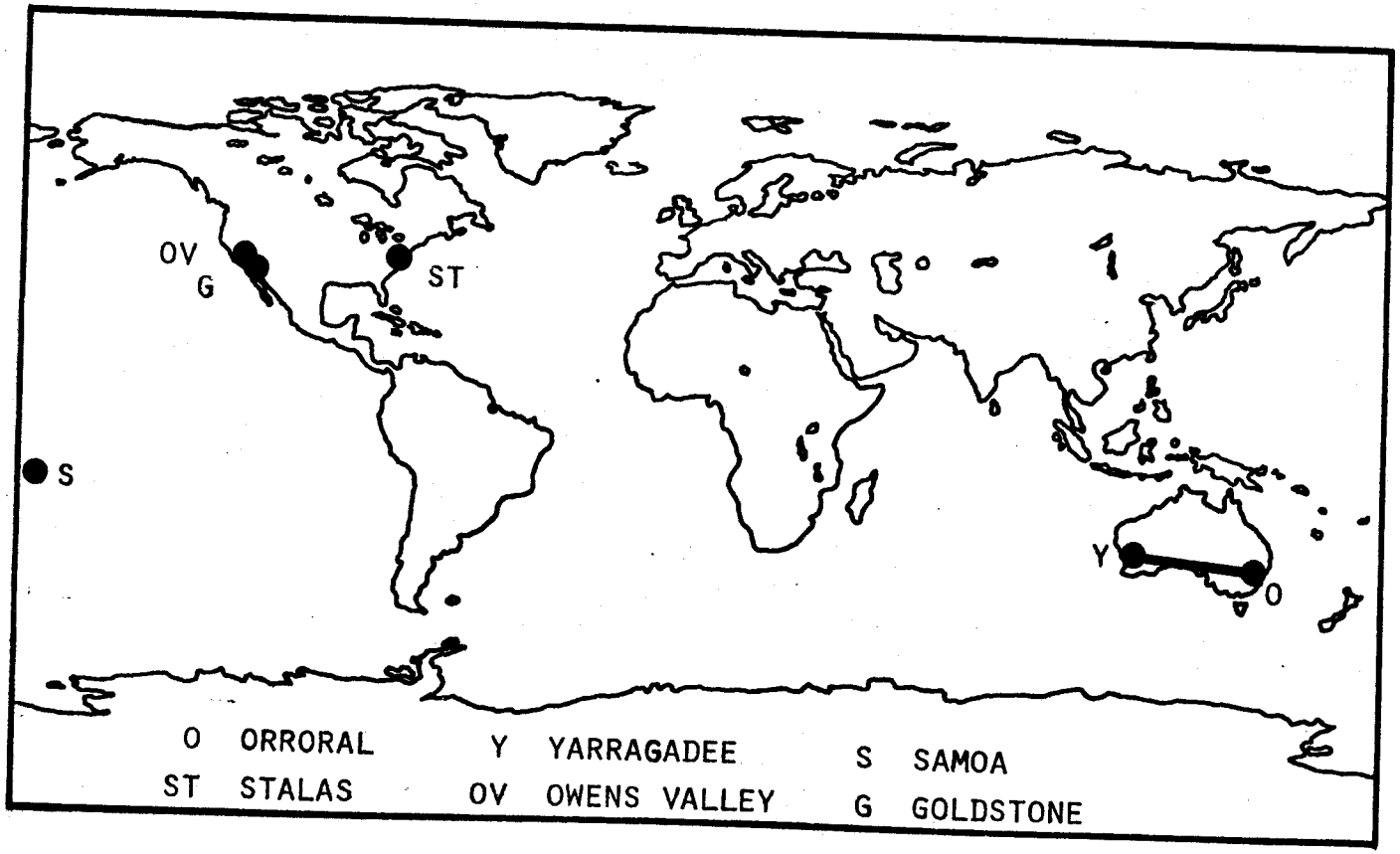

FIGURE 9.7
Laser Tracking Network

(see Chapters 7 and 8). However, experience has shown that the orbit solutions converge faster with a global tracking network. Geodetic solutions were obtained using the GEODYN program (MARTIN et AL.,1976) (see Chapter 5). To scale the solutions the speed of light was adopted as 299792458 m/s. The GEM10 gravity field model was used for orbital integration. Other force models included luni-solar potentials, solid Earth tides and solar radiation pressure. BIH pole and time values were used to model the Earth's wobble. Rigid-Earth Precession and Nutation series were used.

Solution parameters included tracking station positions, one orbit epoch state vector and a value for GM. The scale of the solutions will be dominated by the speed of light because GM is estimated. As discussed in Chapters 7 and 8, the Orroral longitude was held fixed (see Chapter 8). The models were later changed in order to improve the baseline results. Specifically, the PGSL1 and GEML2 gravity models were used for orbit integration.

The arc length for the solutions (3-4 days) is much shorter than the period of most non-gravitational force model effects. Dominant errors could be expected from residual short-period gravity model perturbations. The ORAN program was used to ascertain the effects of errors on baseline measurements. Plausible errors were adopted for fixed tracking station positions, solar radiation pressure, refraction, range biases, pole position and gravity field coefficients. Three times the variances of the GEM9 gravity field were adopted for the gravity field errors. These errors are summarised in Table 9.3.

Table 9.3 indicates that baseline variations between independent solutions should be principally due to the effects of gravity modelling errors and to a lesser extent errors in the models for atmospheric refraction, measurement biases and solid tidal uplift. No attempt was made to duplicate actual data distributions. It is reasonable to assume that these simulation results are optimistic. Note that the Orroral-Yarragadee baseline is supposed to be stable for the duration of these measurements (see Chapter 3).

9.3.2 Results

The Orroral-Yarragadee baseline measurements are plotted in Fig 9.8a. The values refer to the distance between the optical axes of the telescope at the two tracking stations. The mean value is 3196328.86m. Individual measurements deviate by up to 0.86m from the

mean. Without the January solution, the deviation is 0.31m. This variation is consistent with the error analysis (Table 9.3) and also the feasibility study in Chapter 7.

TABLE 9.3

PROPAGATION OF ERRORS INTO BASELINE

ERROR SOURCE	error	BASELINE ERROR (cm)
Gravity Field	GEM 9	27
Refraction	1% of refractive index	5
Biases	10cm	8
Tidal Uplift	10% of effect	2
Fixed Station Positions	1cm	4
Random Errors	10cm	2

Improved gravity field models have become available since the computation of these first results. The new models are estimated to have improved by 2 to 3 times over GEM10 (LERCH et AL,1982). The baselines shown in Figure 9.8a were recomputed with the PGSL1 (Figure 9.8b) and GEML2 (Figure 9.8c) gravity field models. Except that the contribution from gravity field errors can be reduced by about a factor of 3 the error budget in Table 9.3 still applies. The total for the errors is therefore reduced to a r.m.s. of 10 cm. Unless long periods between measurements are adopted this error budget is still too large for geodynamic analyses. Also, the error budget is no longer dominated by gravity modelling. Range biases, if present, could become a significant problem at the subdecimetre level.

The recomputed baselines are shown in Figure 9.8b and 9.8c. For PGSL1 (Figure 9.8b), individual baseline measurements deviate by up to 0.68m from the mean of 3 196 328.75m. For GEML2 (Figure 9.8c), the measurements deviate by up to 0.63m and the mean is 3 196 328.73m. The deviation of January solution from the mean has not improved with changes in gravity model. This result is inconsistent with the other solutions. Apart from the January solution, the r.m.s. of the baseline variations has improved from 0.26m for GEM10 to 0.17m for PGSL1 to 0.10m for GEML2. Also the r.m.s of the range residuals improved by 20%. The major discrepancy and also experience with the January solution shows that the data is not modelled correctly for the arc. The problem needs

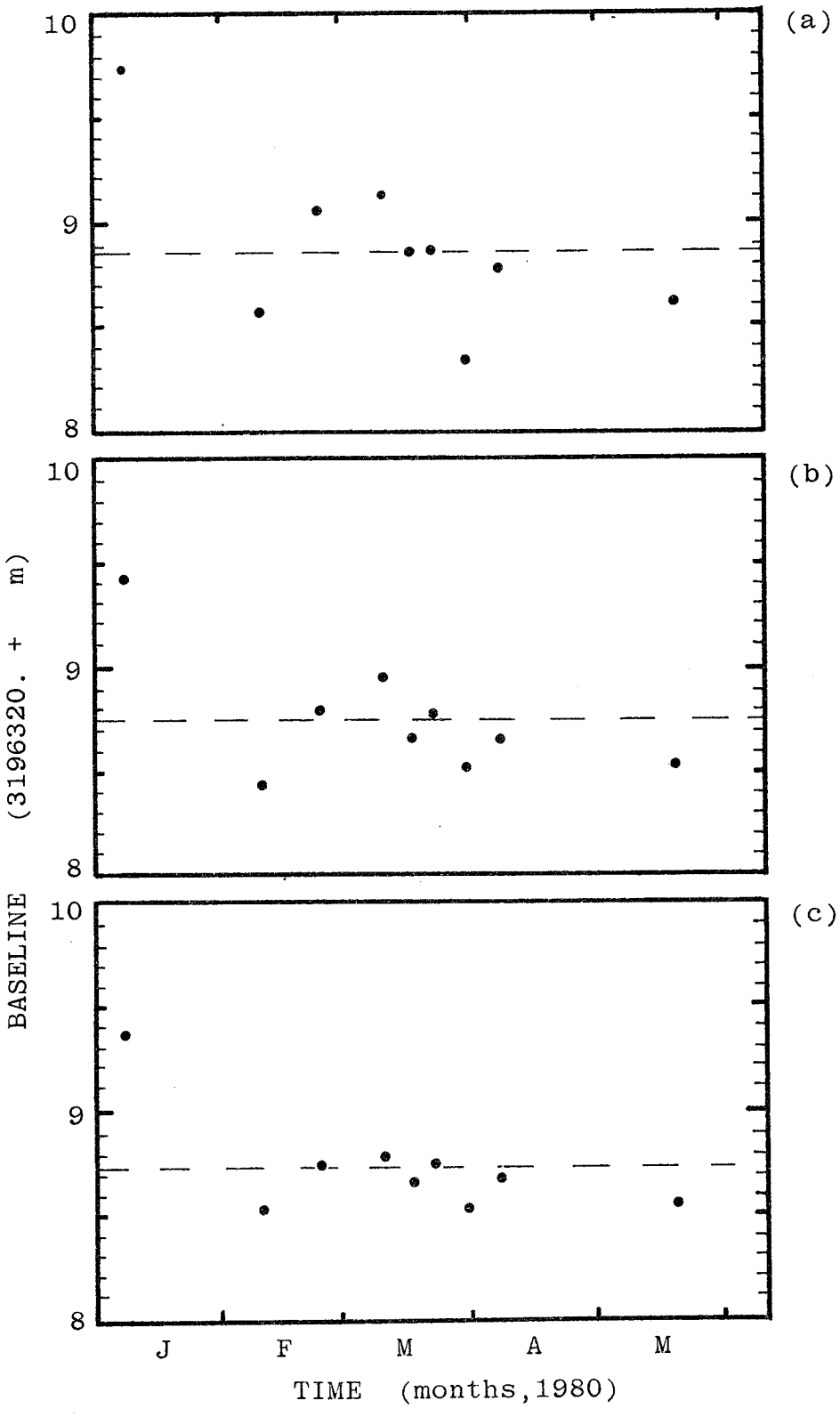

FIGURE 9.8

Baseline Solutions

(a) Using GEM10 gravity field model

(b) Using PGSL1 gravity field model

(c) Using GEML2 gravity field model

to be examined further. The other solutions are consistent with the error analyses and the expected improvement in gravity field modelling.

The precision for each baseline as determined from the solutions is typically of O(5cm). Systematic errors are therefore the major source of inconsistency between baseline measurements. The residuals of the normal points for Yarragadee have a typical r.m.s. of 3-6 cm, which further verifies the accuracy of the normal point procedure.

Analyses of longer 30-day arcs have been performed separately (STOLZ & LAMBECK,1983). These long arc solutions included estimates of the pole position. When these laser derived pole values were used in the four-day arc solutions instead of BIH values, the poor January solution improved dramatically to within 20 cm of the mean. However, great care should be exercised in interpretting this result, as the improvement may not necessarily be due to improved pole positions. Firstly, none of the other solutions changed more than 1 or 2 cm with the change of the pole. Secondly, the simulations in Chapter 7 and Section 9.3 indicated that the baselines should be largely unaffected by erroneous pole values. A reasonable alternative explanation to that of erroneous pole values is that there is an unmodelled effect in the January solution which, due to data distribution is correlated with the tracking station position. This effect has been absorbed into the pole solutions for the 30-day arcs, where the station positions are constrained over 30 days of data. However, it is surprising that the change in pole position could have such a dramatic effect on only one solution. These problems are currently under investigation. The data distribution in the January solution must play a much more important role than previously expected for the pole to have the large effect. This discrepancy points to a deficiency in the previous simulation experiments, but emphasises the discussion in Section 7.3.2. on the effect of the pole with non-simultaneous and poorly distributed data sets.

Laser derived pole values from most analysts (BIH,1980) do indicate a jump in the x pole path at this time period against the smooth BIH pole path. Therefore the change in pole is not unique to the 30-day arcs from the University of New South Wales.

9.3.3 Discussion

The baseline measurements are in good agreement with those determined by other investigators as well as with solutions obtained

from classical techniques and Doppler satellite observations. The comparisons are described in the following sections.

The comparison with other LAGEOS investigators is straightforward. The only proviso is that the scaling parameters GM and the speed of light are consistent for the compared solutions. Values for the Orroral-Yarragadee baseline have been determined at Goddard Space Flight Center, the University of Texas and Deutsches Geodätisches Forschungsinstitut (CHRISTODOULIDIS & SMITH,1982; TAPLEY et AL,1980; REIGBER et AL;1982).

The NAVSAT Doppler position system has been used to augment the Australian Geodetic Survey (LEPPERT,1977). The Doppler coordinates were calculated as point positions on the DMA's NWL9D precise ephemeris. The Division of National Mapping has made available the connections between the Orroral and Yarragadee tracking stations and the Australian Geodetic Datum (STEED, 1980,private communication). A comparison between Doppler positions and AGD was therefore possible.

The Doppler connection between Orroral and Yarragadee must be considered as poor for the following reasons. Firstly, Orroral was observed in late 1975 and Yarragadee in August, 1979. Secondly, only 20 passes were observed at Orroral. A further complication in comparing Doppler to laser ranging is the inherent scale difference between the systems. The precise ephemeris has usually been found to be scaled larger than the scale of other space and terrestrial techniques due to the use of different values for GM and the centre of mass for the NNSS satellites. HOTHEM (1979) compared NWL9D positions with SLR and VLBI in the U.S. He found the Doppler positions to be scaled too large by 0.4ppm, which agreed with values determined by other analysts. However, the value he used for GM with the SLR data in these analyses was 398 600.5 km^3/sec^2, whereas the commonly accepted value for SLR to LAGEOS is now 398 600.44km^3/sec^2. The different values for GM should result in about another .3 ppm scale difference between laser baseline solutions and Doppler values.

The problem is complicated further if terrestrial measurements are compared with Doppler. These comparisons generally indicate a scale difference of 1 ppm. An Australian comparison, with a value of 1.1 ppm confirmed this value (ALLMAN & STEED,1980). The scaling problem could be avoided if consistent models were used to analyse all space techniques. Needless to say, any comparison which agrees to within 0.5

ppm with Doppler can be considered acceptable. In this chapter, the Doppler value for the Orroral-Yarragadee baseline was determined by calculating the chord distance between the two Doppler positions and applying the scale factor of 1.1ppm derived by ALLMAN & STEED (1980).

Finally, the Orroral-Yarragadee baseline determined by SLR can be compared with the Australian Geodetic Datum AGD (BOMFORD, 1967) and also a recent geodetic adjustment (ALLMAN & STEED, 1980). An agreement to no better than 1 ppm could be expected with the AGD due to basic models used in calculating the survey. These models include a non-simultaneous adjustment of the observations, poor estimates of systematic error in coastal tellurometer traverses and no corrections for deflection of the vertical, skew normals and geoid spheroid separation. These assumptions have been corrected in more recent adjustments (ALLMAN AND STEED, 1980). Agreement to 1 ppm could be expected for the latter adjustment.

The coordinates in a conventional geodetic datum are latitude and longitude. The distance between two points on the Earth's surface calculated from latitude and longitude is scaled by the ellipsoidal height. The best values for orthometric height and geoid height are therefore needed in order to obtain reasonable baseline comparisons between terrestrial and space techniques. In Australia, there are many complications introduced into this seemingly simple calculation through legal definitions of the AGD and also the history of the observations used to determine the datum (see BOMFORD,1967; FRYER,1971; ROELSE et AL,1971). For example, the Australian Height Datum was determined after the AGD (ROELSE, 1971). The GMA80 Datum (ALLMAN & STEED,1980) is consistent within itself. The problem of ascertaining the best geoid heights arises. FRYER's (1971) geoid values are at present the best in the Australian region. However, these values need to be corrected for a datum shift of 10.9 m (at the Johnston Origin) before being used with the GMA80 latitude and longitudes. (Note, the geoid heights are correct for the AGD66). The datum change at the origin is equivalent to a geocentric shift of the ellipsoid of:

$dx = -6.71$ m

$dy = 7.15$ m

$dz = 4.77$ m

The change in geoid height at a point (ϕ, λ) can be calculated from

$$dN = \cos\phi \cos\lambda dx + \cos\phi \sin\lambda dy + \sin\phi dz \qquad (9.16)$$

with these values:

$dN_{ORRORAL}$ = 10.45

$dN_{YARRAGADEE}$ = 10.47

The spheroid height is obtained by combining these corrections with Fryer's geoid heights and AHD orthometric heights. The axis to axis Orroral-Yarragadee baseline was determined to be 319 6327.01m using GMA80 coordinates and 319 6324.63m using AGD66 coordinates. Further scaling errors could be introduced into these calculations due to the fact that the AHD heights were constrained to Mean Sea Level and not the geoid (ROELSE et AL,1971) and also the difference in the speed of light used for EDM and laser ranging. These errors should be at the 0.1 ppm level for baseline calculations. Fryer's geoid should be accurate to, say, 2m. GMA80 should agree with the laser measurement to approximately 0.5 ppm. The values from various investigations are summarised in Table 9.4. TAPLEY et AL(1980) used about three years of global data for their SLR solution. However, there are only about six months of Yarragadee data in their baseline estimate. KOLENKIEWICZ's (1981,private communication) value is the average of 11 separate measurements obtained from 30-day orbital arcs acquired in 1980. More recent values for the baseline determined at GSFC agree to within about 10cm of this value (CHRISTODOULIDIS & SMITH,1982). REIGBER et AL (1982) also have presented an average value from January, 1980 to June, 1981. The value is only a few centimetres different to the GSFC and UNSW values.

TABLE 9.4

BASELINE SOLUTIONS

Solution	Baseline (m) 3 196 300 +	Difference from UNSW (m)	(ppm)
AGD66	24.63	-4.10	-1.3
GMA80	27.01	-1.72	-0.5
Doppler	28.52	-0.21	-0.07
Tapley et al.	28.47	-0.26	-0.08
Kolenkiewicz	28.95	0.22	0.07
Reigber et al.	29.06	0.33	0.10
UNSW	28.73	--	--

The Doppler value is well within 1 ppm of the laser ranging values. The GMA80 estimate is .5 ppm different to the UNSW laser value.

This discrepancy is well within the expected tolerance for the terrestrial survey, geoid heights and levelling surveys. The discrepancy with the AGD66 is 1.2ppm, which is reasonable for the early geodetic datum.

The different measuring techniques are in agreement. One remaining problem is to reduce the differences between individual analyses of the same LAGEOS data. REIGBER et AL (1982) obtained 33 cm r.m.s. for the variation between individual monthly solutions. CHRISTODOULIDIS & SMITH (1982) obtained 6cm. REIGBER et Al (1982) obtained a large mean value. However, he used a larger value for GM than other analysts. His baseline value should be shortened to be consistent with the other estimates.

9.4 CONCLUSION

Laser range data to LAGEOS were analysed for the baseline distance between the Orroral and Yarragadee tracking stations in Australia. Initial problems involved data management and removing random outliers in the NSSDC range data. An efficient filter routine was developed which, except for a few special cases, removed the random outliers. These special cases could be handled easily in the routine which was developed to compress the raw ranges to normal points (Section 9.2.3). The optimum polynomial order and normal point compression interval was chosen as 4th order for 150 sec. bands of data. This criterion made efficient handling of the raw data possible and also significantly reduced the amount of data used in any subsequent analysis without removing important signals. Precision of tracking data determined using these routines was typically 10 cm for Yarragadee, 40 cm for Orroral and 3 cm for Yarragadee normal points.

The savings in CPU time resulting from the use of these routines are significant and will make any future geodetic analyses more efficient, especially when the complete LAGEOS data set is being analysed. Up to 90 days of data can be analysed in one computer run, compared to five days previously.

The filter routine does not remove systematic range biases and epoch timing biases. Neither can these biases be determined accurately with post analysis techniques. An important problem which needs to be overcome with SLR for geodynamic calculations is the determination and elimination of range biases and timing biases with effects on baselines less than 10cm.

The loss of baseline precision when normal points are used indicates that ill-conditioning must be carefully assessed with short arc lengths.

The actual baseline distance is not essential for geodynamics, as movements are of interest. However, the mean value for the baseline agrees with the terrestrial geodetic network and Doppler positions to within expected tolerances. SLR can be combined with terrestrial data in order to strengthen terrestrial geodetic networks.

The preliminary estimates of the Orroral-Yarragadee baseline, except for one case, had a variation over the 130 day period in 1980 which agreed with the estimated error magnitudes. It is impossible to include every possible error source in a simulation experiment. The reason for the one poor solution is therefore unknown at this stage and is currently under examination. The accuracy of the data, force models, Earth rotation models and effect of data distribution need to be carefully assessed from the real solutions. Apart from the one poor solution, the small variation of the baseline over the 130 days suggests that the data can be expected to be accurate to 10 cm.

For optimum geodynamic analyses, methods for reducing systematic errors to subdecimetre level need to be developed. This development will probably involve using longer arc lengths. With say, monthly solutions accurate to 10 cm, baseline distortions of 1 cm/year can be detected after five years in the Australian region (see Chapter 7). The detection of intra-plate deformation on the geologically stable Australian continent will need a long period of consistent measurement. However, the stability of the baseline has proved useful for verifying the accuracy of the SLR technique.

The determination of intra-plate deformation is important for understanding the rheology of the Earth and the nature of the forces that drive the tectonic plates (STOLZ AND LAMBECK, 1983). The introduction in late 1983 of the NATMAP laser, which has higher accuracy and a faster pulse repetition rate than the existing SAO system, is vital for the continued monitoring of the Orroral-Yarragadee baseline distance to enable the detection of crustal motion. However, the analysis of the existing two years of data can be refined to yield more consistent results.

Deformation of the one baseline distance across the Australian

continent will, however, yield little useful geodynamic information. The propagation of this deformation throughout the tectonic plate is needed. A combination of many geodetic techniques will therefore have an important role to play in solving geodetic problems. The use of many measuring techniques will make correct comparisons between all techniques an important problem to investigate. The comparisons in Section 9.3 only touch on the problems involved.

With much help from NASA, the University of N.S.W. now has the capability of analysing SLR data. In order to have a useful, ongoing Australian geodynamic program, this facility must be used in close association other terrestrial techniques and other space techniques like LLR, GPS, VLBI and NNSS Doppler. Terrestrial methods and Doppler are fairly well developed and used in Australia. For example, the Markham Valley Deformation surveys in Papua New Guinea (COOK & MURPHY,1974; SLOAN & STEED,1976) and the New Britain Doppler survey (MORGAN,1981). Geodetic VLBI is currently being investigated (STOLZ et AL,1983) and the development of GPS techniques is anticipated. The SLR analyses in this chapter are therefore an important start to an ongoing geodetic program for geodynamics in Australia.

CHAPTER 10

CONCLUSIONS

Several extra-terrestrial measuring techniques can make significant contributions to geodynamics. These techniques include Satellite Laser Ranging, Lunar Laser Ranging, Very Long Baseline Interferometry, Satellite Doppler, Global Positioning System and Radar Altimetry. Applications of Radar Altimetry and Satellite Laser Ranging were investigated in this thesis.

The GEODYN program was used as the basic computational tool for most of the calculations. The ORAN program was also used. Detailed knowledge of satellite geodesy was used to determine the utility of GEODYN and to ascertain the accuracy of results estimated with it. The capability of applying GEODYN to specific geodynamic research has therefore been developed.

Altimetry measurements are sensitive to the Sea Surface Height spectrum. GEOS-3 altimetry measurements and ephemerides determined by laser ranging were used to estimate the M_2 ocean tide in the Sargasso Sea. Systematic errors in the LAS79 Sea Surface Height data were too large for tidal estimation. This is a negative result in that the tides were not successfully estimated. However, no-one to my knowledge has succeeded as yet in estimating ocean tides with altimetry data. A few periodic errors were determined by spectrally analysing the data. After removing these estimated periods, the variance of the noise signal was reduced by about 30%. However, assuming that BRETREGER's (1979) estimate of 1 m for the minimum amount of systematic noise is correct, the final crossover residual variance of 4.9 m^2 was still too large for estimating the M_2 tide.

The spectral analysis procedure adopted could be further improved to estimate orbital errors. However, the large crossover residuals in the data cannot be attributed to long period orbital error. The "bias and tilt" filtering technique successfully reduces systematic errors. The different results between the bias and tilt and spectral analysis techniques indicate that systematic errors have shorter periods than one revolution of the GEOS-3 orbit, but longer periods than one pass (approximately 20 min.). Little can be done therefore to separate

systematic noise from the diurnal and semi-diurnal ocean tidal signals, without recomputing the ephemerides with more accurate gravity models. The sampling of the GEOS-3 orbit also precludes optimum tidal estimation, as regional areas are sampled at most every half day. Procedures need to be developed to reduce systematic noise from altimetry data before the ocean tides can be determined successfully. More use can be made of orbit theory for analysing altimetry derived SSH data.

Satellite laser range data can be used to determine accurate tracking station coordinates and satellite orbits. Laser range data were used by LERCH et AL (1978c) to determine the ephemerides, which were used to reduce the GEOS-3 altimetry data to Sea Surface Height data.

Deformation of the lithosphere can be obtained from accurate geodetic positions of tracking stations. It is feasible to undertake crustal dynamic research at the University of New South Wales with the existing computing facilities. Error analyses show that sub-decimetre precisions can be obtained from long-arc solutions for baselines using only a few days of observations. Range tracking precision does not provide the limit for the accuracy of the tracking station coordinates and baselines. The accuracy of baselines is limited by the accuracy of the dynamic models. The dominant error sources are biases and geopotential model. There is little difference between the systematic errors propagated into arc lengths of one to five days. Longer arc lengths will produce the best results if significant parameters like GM can be simultaneously estimated with the state vectors and tracking station coordinates. In this case there is no benefit in Single-Pass Multi-Arc solutions.

Other conclusions from the feasibility study are:

- Computer times are mainly dependent on the amount of data. In these cases if large amounts of data are collected such as is the case with new systems like the TLRS, or if longer arc lengths are desired, compressing range data to normal points may be necessary;
- East-west baselines will not be as well determined as north-south baselines due to the almost north-south LAGEOS orbit;
- Baseline precisions will improve when the National Mapping laser becomes operational at Orroral Valley.

Further investigations are necessary. These are in progress and include:

- error analysis of arc lengths longer than five days.
- error analysis of dynamic models not previously investigated.
- error analysis of solutions with strictly simultaneous data.

The estimability of dynamic satellite geodesy was investigated. The results confirm those of VAN GELDER (1978). For long-arc solutions only one tracking station longitude needs to be fixed to obtain undistorted geodetic coordinates. The other parameters are constrained by the satellite dynamics and Earth rotation. This means that the reference system for geodetic coordinates is defined by the dynamic models and the fixed reference longitude.

Analytical determinations of the estimability of range observations are useful. However, results cannot always be extrapolated from simple to dynamic cases. The dynamic theory must be carefully formulated to obtain reliable results, otherwise the problem may be oversimplified. For this reason concepts of estimability for conventional geodesy cannot be applied directly to dynamic satellite geodesy.

For geodynamic applications where centimetre accuracy is required the effects of solution procedures on results must be carefully ascertained. Bayesian least squares procedures have inherent dangers of introducing subjective a priori information into solutions. With these procedures decimetre errors for geodetic coordinates can also be introduced because solutions are easily overconstrained or left ill-conditioned. Information on pseudo-rank and condition of least squares solutions is important for reliable interpretation of any results.

Laser range data to LAGEOS have been analysed for the baseline between Orroral and Yarragadee. Software has been developed to filter the data and compress it to normal points. Baselines calculated with 3-day arcs are consistent to 10cm if the data distribution is good. These results are consistent with error analyses and compare well with doppler positions and the Australian Geodetic Network.

It is important for us to improve baseline solutions to sub-decimetre consistency before any meaningful geodynamic results can be obtained over short time periods. In Australia combinations of various space and terrestrial techniques will also be important for deriving geodynamic information. Further work needs to be done on:

- improving dynamic models
- using longer arc lengths

- minimising range and timing biases
- analysing all the available data in the Australian region
- combination of space and terrestrial techniques

Comprehensive knowledge of satellite geodesy and geodynamics makes optimum investigation of specific geodynamic phenomena, such as ocean tides and crustal strain, possible. One aim of this dissertation, to develop an expertise in satellite geodesy which can be applied to geodynamics, has been achieved. This expertise is now being used to investigate the large-scale crustal deformation of Australasia by laser ranging to LAGEOS (STOLZ & MASTERS,1982; STOLZ & LAMBECK,1983).

REFERENCES

ABBOT R.I, SHELUS,P.J., MULLHOLLAND J.D., SILVERBERG E.C., 1973. "Laser Observations to the Moon - Identification and Construction of Normal Points for 1969-1971", Astron.J.,78,pp784-793.

AENA,1961, "Explanatory Supplement to the Astronomical Ephemeris and Nautical Almanac". Her Majesty's Stationary Office, London, 533pp.

ALLMAN J.S, & STEED J.B., 1980, "Geodetic Model of Australia 1980". NATMAP Tech. Report No. 29, Canberra, Australia, 90pp.

ANDERLE R., 1974, "Transformation of Terrestrial Survey Data to Doppler Satellite Datum". Journal of Geophys. Res. Vol. 79(35), December, 5319-5330.

ANDERLE R., 1978, "Determination of Plate Tectonic Motion from Doppler Observations of Navy Navigation Satellites". NSWC/DC TR-3884, Dahlgren, Virginia, August, 10pp+app.

ANDERLE R. & TANENBAUM M.C., 1974. "Practical Realisation of a Reference System for Earth Dynamics by Satellite Methods". In proc. of IAU Coll. no. 26 On Reference Coordinate Systems for Earth Dynamics, Torun, Poland 26-31 August, 341-380.

ARUR MANOHAR G., 1977. "Experiments for Improving Positioning by Means of Integrated Doppler Satellite Observations and NNSS Broadcast Ephemeris". The Ohio State University report No. 258, October, 129pp.

ASH M. E. 1972. "Determination of Earth Satellite Orbits". Massachussets Institute of Technology, Lincoln Laboratory, Technical Note 1972-5, April, 257pp.

ASTERIADAS G., 1977. "Determination of Precession and Galactic Rotation from Proper Motions of the AGK3". Astron. Astrophys. 56, 25-38.

ATKINSON R. d'E., 1973. "On The Dynamical Variations of latitude and time". The Astronomical Journal, Vol 78 No. 1 February, 147-151.

BALMINO G. REIGBER C.H. 1974. "Equations of Condition for 13th Order Harmonics in the Geopotential". Groupe de Recherches de Geodesie Spatiale, Bull. No. 14, 85pp.

BALMINO G., REIGBER C., MOYNOT C., 1976. "The GRIM 2 Earth Gravity Model". Deutsche Geodatische Kommission, Reihe A, Heft Nr. 86, München, 34pp.

BARAZANGI M., DORMAN J., 1969, "World Seismicity Maps". ESSA, C & GS 1961-1971, Bull. Seismol. Soc. Amer., vol 59.

BATE R.R., MUELLER D.D., WHITE J.F., 1971. "Fundamentals of Astrodynamics". Dover, 455pp.

BELOUSSOV V.V., 1979. "Why Do I Not Accept Plate Tectonics". EOS Trans. Am. Geophys. Union Vol. 60 no. 17, April, p207.

BENDER P.L. 1978. "Some U.S. Views on Scientific Opportunities in Ocean and Earth Dynamics". Proc. ESA Workshop on Space Oceanography Navigation and Geodynamics. Schloss Elmau Germany Jan 16-21, 19-23.

BENDER P.L. 1981. "Determination of Worldwide Tectonic Plate Motions and Large Scale Intra-Plate Distortions". Proposal to NASA April, 12pp.

BENDER P.L., GOAD C. 1979. "Probable Lageos Contributions to a Worldwide Geodynamics Control Network". Proc. of 2nd Int. Symp. on the Use of Artificial Satellites for Geodesy & Geodynamics". Vol 2 National Technical University, Athens, Greece, 145-161.

B.I.H., 1979. Bureau International de l'Heure, Annual Report for 1979, 188pp.

BIRD J.M., ISACKS B., (ed.), 1972. "Plate Tectonics". Selected papers from J.Geophys.Res, American Geophysical Union, Edition 1, 951pp.

BIRD J.M. (ed.) 1980. "Plate Tectonics". Selected papers from publications of the American Geophysical Union, edition 2, 986pp.

BJERHAMMAR A, 1973. "Theory of Errors and Generalised Matrix Inverses". Elsevier Scientific Pub. Co. Amsterdam, 420pp.

BLAHA G., 1971a. "Inner Adjustment constraints with Emphasis on Range

Observations". The Ohio State University Report No. 148, January, 85pp.

BLAHA G., 1971b. "Investigations of Critical Configurations for Fundamental Range Networks". The Ohio State University Report No. 150, March, 274pp.

B.M.R. see: Bureau of Mineral Resources

BOMFORD G., 1962. "Geodesy" Oxford University Press. 561pp.

BOMFORD A.G. ,1967. "The Geodetic Adjustment of Australia 1963-1966". Survey Review, Vol XIX, No. 144, April.

BOSSLER J.D., 1972. "Bayesian Inference in Geodesy". Ph.D dissertation, Department of Geodetic Science, The Ohio State University. 79pp.

BOSSLER J.D., GOAD C.C., BENDER P.L., 1980. "Using the Global Positioning System (GPS) for Geodetic Positioning". Bull. Geod. 54(1980), 553-563.

BRAMMER R.F., 1979. "Estimation of the Ocean Geoid Near the Blake Escarpment using GEOS-3 Satellite Altimetry Data". Journal of Geophys. Res. Vol 84(B8) July, 3843-3851.

BRETREGER K., 1978. "Earth Tide Effects on Geodetic Observations". Unisurv S-16, School of Surveying, University of New South Wales, Sydney, Australia, 160pp.

BRETREGER K., 1979. "Ocean Tide Models from GEOS 3 Altimetry in the Sargasso Sea". Aust. Jour. Geod. Phot. Surv. No. 30, June. 1-14.

BROUWER D., 1959. "Solution of the Problem of Artificial Satellite Theory without Drag". The Astronomical Journal 64(1274), October, 378-397.

BROUWER D. & CLEMENCE G.M., 1961. "Methods of Celestial Mechanics". Academic Press, London. 598pp.

BROWN D.A., CAMPBELL K. S. W., CROOK K. A. W., 1968. "The Geological Evolution of the Australian Continent". Pergamon Press, Sydney.

BROWN R.D. & HUTCHINSON M.K., 1980. "Ocean Tide Determination from Satellite Altimetry". COSPAR/SCOR/IUCRM Symposium: Oceanography from Space, Venice, Italy, May 26-30.

BRUNNER F., 1979. "On the Analysis of Geodetic Networks for the Determinaton of the Incremental Strain Tensor". Survey Review No. 192 VolXXV, 56-67.

Bureau of Mineral Resources., 1979. "Earth Science Atlas of Australia". Canberra, Australia. 8pp.

CAPPELLARI J.O., VELEZ C.E., FUCHS A.J., 1976. "Mathematical Theory of the Goddard Trajectory Determination System". Goddard Space Flight Center X-582-76-77, 600pp.

CAREY S.W., 1976. "The Expanding Earth". Elsevier, Amsterdam, 470pp.

CARTWRIGHT D.E., EDDEN A.C., SPENCER R., VASSIE J.M., 1980. "The Tides of the Northeast Atlantic Ocean". Phil.Trans.R.Soc.Lond., A1436, 87-139.

CHENEY R.E. & MARSH J.G., 1980. "SEASAT Altimeter Observations of Dynamic Topography in the Gulf Stream Region". J. Geophys. Res., 86(C1), 473-483.

CHENEY R.E. & MARSH J.G., 1981. "Oceanic Eddy Variability measured by GEOS-3 Altimetry Crossover differences". EOS, Transactions of the American Geophysical Union, Vol 62, No. 45, November 10, 743-752.

CHRISTODOULIDIS D.C. & SEIFFERT E., 1980. "Earth Rotation and Tidal Effects on the LAGEOS Satellite". EOS Trans. Am. Geophys. Union (Abstract), 61, May, p212.

CHRISTODOULIDIS D.C. & SMITH D.E., 1980. "Geodetic Precisions expected from LAGEOS". EOS Trans. Am. Geophys. Union (Abstract), 61, No. 46, November 11, p936.

CHRISTODOULIDIS D.C & SMITH D.E., 1982. "SL5 Geodetic Solution". Laser System Performance and Data Quality presented at the 3rd Crustal Dynamics Working Group Meeting, Oct28-29.

CHRISTODOULIDIS D.C., SMITH D.E., KLOSKO S., 1981. "Prospects for TLRS Baseline Accuracies in the Western U.S.A." (Draft only), February.

COLEMAN R., 1979. "On the Recovery of Ocean Dynamic Information from Satellite Altimetry". Interdisciplinary Abstract 19/13, XVIIth General Assembly of the International Union of Geodesy and Geophysics. p598. (Now in Marine Geodesy 1980 4(4) 351-386).

COLEMAN R., 1981. "A Geodetic Basis for Recovering Ocean Dynamic Information from Satellite Altimetry". Unisurv S19, School of Surveying, University of New South Wales, Australia, October, 331pp.

COLOMBO O., 1979. "Algorithms for Spherical Harmonic Analysis". EOS Trans. Am. Geophys. Union Vol 60 no. 46 p809. 4pp.

COLOMBO O. & RIZOS C. 1979. Documentation for Harmonic Analysis Program. (unpublished) School of Surveying, University of New South Wales, Sydney, Australia. 23pp.

COOK, D.P.,MURPHY B., 1974. "Crustal Movement Survey": Markham Valley, Papua New Guinea, 1973". NATMAP Report No. 18.

CSC see: Computer Sciences Corporation.

Computer Sciences Corporation. 1976. "SOLVE II Program Description and User's Guide" May. 446pp.

DENHAM D., ALEXANDER L.G., WOROTNICKI G, 1979. "Stresses in the Australian Crust; Evidence from Earthquakes and in situ stress measurements". BMR.J.Aust.Geol.Geophys.,4,289-95.

DIAMANTE. J. M. & NEE T., 1980. "Application of Satellite Radar Altimeter Data to the Determination of Regional Tidal Constituents and the Mean Sea Surface". COSPAR/SCOR/IUCRM symposium: Oceanography from Space, Venice, Italy, May 26-30.

DOUGLAS B.C., 1979. Comment on "Mapping Ocean Tides with Satellites: A Computer Simulation" by I.J. WON, J.T. KUO, R.C. JACHENS. Journal of Geophys. Res. Vol 84(B12), 6909-6910.

DOUGLAS B.C. & GOAD C.C., 1978. "The role of Orbit Determination in Satellite Altimeter Data Analysis". Boundary Layer Meteorology, 13, 245-251.

DOUGLAS B.C. & GABORSKI P.D. 1979. "Observation of Sea Surface Topography with GEOS-3 Data". Journal of Geophys. Res. Vol 84(B8), 3893-3896.

DOUGLAS B.C & CHENEY R.E., 1981. "Ocean Mesoscale Variability from Repeat Tracks of GEOS-3 Altimeter Data". Journal of Geophys. Res. Vol 86(C11) November 20, 10931-10937.

DRAGERT H., LAMBERT A. LIARD J., 1981. "Repeated Precise Gravity

Measurements on Vancouver Island, British Columbia". Journal of Geophys. Res. Vol 86(b7), July 10, 6077-6105.

DUNN P.J., TORRENCE M., SMITH D.E., KOLENKIEWICZ R., 1979. "Base Line Estimation using Single Passes of Laser Data". Journal of Geophys. Res. Vol 84 (B8), July 30, 3917-3920.

EANES R.J., SCHUTZ B.E., TAPLEY B.D., 1982. Laser System Performance and Data Quality presented at the 3rd Crustal Dynamics Working Group Meeting, Oct28-29.

FELSENTREGER T., MARSH J., WILLIAMSON R., LAMBECK K., 1979. "Ocean Tide Parameters and the Acceleration of the Moon's Mean Longitude from Satellite Orbit Data". Interdisciplinary Abstract 20/03, XVIIth General Assembly of the International Union of Geodesy and Geophysics. p611.

FLINN E. A., 1981. "Application of Space Technology to Geodynamics". Science, Vol. 213, July, 89-96.

FORSYTHE G. & MOLER C., 1967. "Computer Solution of Linear Algebraic Systems". Prentice-Hall series in Automatic computation,148pp.

FREY H., 1980. "Crustal Dynamics Project Observing Plan for Highly Mobile Systems 1981-1986" NASA Tech.Mem. 82029, October, 39pp.

FRICKE W., 1971. "A rediscussion of Newcomb's Determination of Precession". Astron. Astrophys. 13, 298-303.

FRYER J.G., 1971. "The Geoid in Australia". NATMAP Technical Report No. 13, Canberra, Australia, May.

GAMBIS D., 1982. "Satellite Laser Tracking: Construction of Normal Points". in Proc. Fourth Int. Workshop on Laser Ranging Instrumentation, P.Wilson (ed), Geod. Inst. Univ. Bonn, West Germany,pp80-93.

GAPOSCHKIN E.M., 1973. "Smithsonian Standard Earth III". Smithsonian Astronomical Observatory Report 353, 388pp.

GAPOSCHKIN E.M., 1978. "Recent Advances in Analytical Satellite Theory", Applications of Satellite Geodesy to Geodynamics, I.I. Mueller (ed.), The Ohio State University, Report No. 280,

197-206.

GAPOSCHKIN E.M., 1981. "56th Colloquium of the International Astronomical Union". EOS Trans. Am. Geophys. Union Vol 62 no. 39, 685-686.

GAPOSCHKIN E.M. & KOLACZEK B. (ed.), 1981. "Reference Coordinate Systems for Earth Dynamics". Vol 86 proc. of 56th Coll. of IAU, Warsaw, Poland, 396pp.

GEOS-C, 1974. "GEOS-C Mission Plan". Wallops Flight Center, National Aeronautics and Space Administration, Virginia, U.S.A. December.

GOAD C.C, DOUGLAS, B.C. AGREEN R.W., 1980. "On the Use of Satellite Altimeter Data for Radial Ephemeris Improvement". The Journal of the Astronautical Sciences, Vol. XXVII No. 4 October-December, 419-428.

GORDON A.L. BAKER T.N., 1980. "Ocean Transients as Observed by GEOS-3 Coincident Orbits". Journal of Geophys. Res. Vol 85(C1), 502-506.

GRAFAREND E. & HEINZ K., 1978. "A Rank Defect Analysis of Satellite Geodetic Networks II - Dynamic Mode". Manuscripta Geodaetica 3, 135-136.

GRAFAREND E. & LIVIERATOS E., 1978. "A rank Defect Analysis of Satellite and Geodetic Networks I - Geometric Mode and Semi-Dynamic Mode". Manuscripta Geodaetica 3, 107-134.

GRAFAREND E., KLEUSBERG A., RICHTER B., 1979. "Free Doppler Network Adjustment". Proc. 2nd Int. Symp. on Satellite Doppler Postioning, Vol 2, Austin, Texas, U.S.A. January 22-26. 1053-1069.

GUINOT B., 1970. "Short Period Terms in Universal Time". Astron. Astrophys., 8, 26-28.

GUINOT B. & FEISSEL M., 1968. "BIH Annual Report for 1968". International Council for Scientific Unions, 109pp.

HAGIHARA Y., 1972. "Celestial Mechanics". Massachussets Institute of Technology Press, 919pp.

HATCH W., GOAD C., MARTIN C.F., 1973. "Mathematical Description of the ORAN Error Analysis Program". Planetary Sciences Rep. No. 009-73, WOLF Research & Development Corp, 111pp.

HEISKANEN W.A. & MORITZ H., 1967. "Physical Geodesy". W.H. Freeman and Co., 364pp.

HENDERSHOTT M.C., 1972. "The Effects of Solid Earth Deformation on Global Ocean Tides". Geophys.J.Roy.Astron. Soc. 209, 389-402.

HOBSON E.W., 1965. "Spherical and Ellipsoidal Harmonics". Chelsea Publishing Co. 1965, 500pp.

HOTHEM L.D. 1979, "Determination of Accuracy, Orientation and Scale of Satellite Doppler Point Positioning Coordinates". Proc. 2nd Int. Symp. on Satellite Doppler Positioning, Austin, Texas, U.S.A., January 22-26, 609-630.

HUANG N.E., LEITAO C.D., PARRA C.G., 1978. "Large-Scale Gulf Stream Frontal Study using GEOS-3 Radar Altimeter Data". Journal of Geophys. Res. Vol 83(C9), 4673-4682.

IBM, 1966. "IBM Application Program". System/360 Scientific Subroutine Package, 454 pp.

ICL, 1980. Inter-Union Commission on the Lithosphere Program Constitution, Initial Recommendations. An Inter-Disciplinary Project of IUGG and IUGS. August, 42pp.

ICL, 1981. "Dynamics and Evolution of the Lithosphere. The framework for Earth Resources and the Reduction of Hazards". Inter-Union Commission on the Lithosphere Report No. 1. April, 62pp.

JENKINS G.M. & WATTS D.G., 1968. "SPECTRAL ANALYSIS and its applications". Holden-Day, San Francisco, California, 525pp.

KAHN W.D., KLOSKO S.M., WELLS W.T., 1981. "Mean Gravity Anomalies from a Combination of Apollo/ATS-6 and GEOS-3/ATS-6 SST Tracking Campaigns". NASA Tech.Mem. 82120, April, 46pp.

KANASEWICH E.R., 1975. "Time Sequence Analysis in Geophysics". The University of Alberta Press, 364pp.

KAO T.W. & CHENEY R.E., 1982. "The Gulf Stream Front: A Comparison between SEASAT Altimeter observations and Theory". Journal of Geophys. Res. Vol 87(C1), January 20, 539-545.

KAULA W. M., 1966. "Theory of Satellite Geodesy". Blaisdell Pub. Co., 120pp.

KAULA W.M., 1969. The Terrestrial Environment Solid-Earth and Ocean Physics Application of Space and Astronomic Techniques. Williamstown Report, August.

KINOSHITA H., NAKAJIMA K., KUBO Y., NAKAGAWA I., SASAO T., YOKOYAMA K., 1979. "Note on Nutation in Ephemerides". International Latitude Observatory of Mizusawa, VOL. XII No. 2, 71-108.

KLOSKO S.M. & BELLOT R.P., 1977. "EQUIX: The GEOS-3 Equator Crossing Program". EG&G Washington Analytical Services Center Inc., Wolf Research Development Group.

KLOSKO S. & WAGNER C.A., 1979. "Spherical Harmonic Representation of the Gravity Field from Dynamic Satellite Data". presented at XVIIth General Assembly of the International Union of Geodesy and Geophysics, Canberra, Australia, December 2-15, 48pp.

KOLENKIEWICZ R., 1981. "Preliminary Lageos and VLBI Baseline Intercomparison". Lageos Technical Bulletin 1(4), 2.

KOLENKIEWICZ R. & RYAN J., 1981. "Laser Range and VLBI Intercomparisons". (Abstract) Third Annual NASA Geodynamics Program Review, Crustal Dynamics Project, Geodynamics Research, Goddard Space Flight Center, Greenbelt, Maryland, January 26-29, p17.

KOZAI Y., 1968. "Love's Number of the Earth Derived from Satellite Observations". Publ. Astron. Soc. Japan, 29, 24-26.

KREYSZIG E., 1962. "Advanced Engineering Mathematics". Wiley, 866pp.

KREYSZIG E., 1970. Introductory Mathematical Statistics". J. Wiley & Sons Inc, 470pp.

KU L., 1978. "The Computation of Tides, Satellite and Geoidal Heights from Altimeter Data". (Abstract) EOS Trans. Am. Geophys. Union Vol 59 no. 4, p261.

LAMBECK K., 1973. "Precession, Nutation and the Choice of Reference System for Close Earth Orbits". Celestial Mechanics 7, 139-155.

LAMBECK K., 1980. "The Earth's Variable Rotation". Cambridge University Press, 449pp.

LAMBECK K., 1981a. "Some Geodetic Aspects of the Plate Tectonics Hypothesis". Reference Coordinate Systems for Earth Dynamics. Vol. 86 proceedings, Reidel Pub. Co. 1981, 87-102.

LAMBECK K., 1981b. "Flexure of the Ocean Lithosphere from Island Uplift, Bathymetry and Geoid Height Observations: The Society Islands". Geophys. J. Roy. Astron. Soc. 67, 91-114.

LAMBECK K., CAZENAVE A., BALMINO G., 1974. "Solid Earth and Ocean Tides Estimated from Satellite Orbit Analyses". Rev. Geophys. Space Phys., 12, 421-434.

LAPLACE P.S., 1775. "Recherches sur quelques points de systeme du monde". Mem.Acad.Roy.Soc. 88 177.

LARDEN D., 1981. "Monitoring the Earth's Rotation by Lunar Laser Ranging". Ph.D. Thesis, School of Surveying, University of New South Wales, Sydney, Australia, 280pp.

LARDEN D.R. & BENDER P.L., 1980. "Expected Accuracy of Geodetic Baseline Determination using the GPS Reconstructed Carrier Phase Method. (Draft only), 31pp.

LAUBSCHER R.E., 1976. "Dynamical Determinations of the General Precession in Longitude". Astron. Astrophys. 51, 9-20.

LAWSON C. & HANSON R., 1974. "Solving Least Squares Problems". Prentice Hall Series in Automatic Computation, 340pp.

LEITAO C.D., HUANG N.E., PARRA C.G., 1977. "Ocean Current Surface Measurement using Dynamic Elevations obtained by the GEOS-3 Altimeter". Proc. AIAA Symp. on Satellite Applications to Marine Tech., New Orleans, November15-17, 43-49.

LEITAO C.D., HUANG N.E., PARRA C.G., 1978. "Final Report of GEOS-3 Ocean Current Investigation Using Radar Altimeter Profiling". NASA Tech.Mem. 73280, Wallops Flight Center, Virginia, U.S.A., 31pp.

LEITAO C.D., HUANG N.E., PARRA C.G., 1979a. "The Variations of Geostrophic Kinetic Energy over the Northwestern Atlantic Ocean". Interdisciplinary Abstract 19/10, XVIIth General Assembly of the International Union of Geodesy and Geophysics, p596.

LEITAO C.D., HUANG N.E., PARRA C.G., 1979b. "A Note on the Comparison of Radar Altimetry with IR and in-situ Data for the Detection of the Gulf Stream Surface Boundaries". Journal of Geophys. Res. Vol 84(B8), 3969-3973.

LE PICHON X., 1968. "Sea Floor Spreading and Continental Drift". Journal of Geophys. Res. Vol 73, 3661-3697.

LE PICHON X., FRANCHETEAU J., BONNIN J., 1973. "Plate Tectonics". Elsevier, Amsterdam. 300pp.

LEPPERT K., 1977. "The Australian Doppler Satellite Survey. 1975-1977". NATMAP Technical Report No.21, Canberra, Australia.

LERCH F.J., 1982. "Gravity Model Improvement for LAGEOS". Abstracts 4th Annual Conference on the NASA Geodynamics Program Crustal Dynamics Project, Geodynamics Program, Goddard Space Flight Center, Greenbelt, Maryland, January 26-29, p98.

LERCH F.J. & KLOSKO S.M., 1981. "Gravity Improvement Using Laser Data: Progress Report". First Crustal Dynamics Working Group Meeting, Goddard Space Flight Center, Sept 1-3.

LERCH F.J., WAGNER C.A., RICHARDSON J.A., BROWND J.E., 1974. "Goddard Earth Models (5 and 6)". NASA X-921-74-145, Goddard Space Flight Center, Greenbelt, Maryland. December, 89pp + app.

LERCH F.J., KLOSKO S.M., LAUBSCHER R.E., WAGNER C.A., 1977. "Gravity Model Improvement using GEOS-3 (Gem 9 and 10)". NASA X-921-77-246, Goddard Space Flight Center, Greenbelt, Maryland, 121pp.

LERCH F.J., WAGNER C.A., KLOSKO S.M., BELOTT R.P., LAUBSCHER R.E., TAYLOR W.A., 1978a. "Gravity Model Improvement using GEOS-3 Altimetry (GEM10A and 10B)". presented at 1978 Spring Annual Meeting of the American Geophysical Union, Miama, Florida, April.

LERCH F.J., LAUBSCHER R.E., KLOSKO S.M., SMITH D.E., KOLENKIEWICZ R., PUTNEY B.H., MARSH J.G., BROWND J.E., 1978b. "Determination of the Geocentric Gravitational Constant from Laser Ranging on Near-Earth Satellites". Geophys. Res. Lett. 5, 1031-1034.

LERCH F.J., BELLOT R.P., KLOSKO S.M., LITKOWSKI E.M., 1978c. "Laser Reference Orbits and Altimeter Validation for GEOS-3". presented at Marine Geodesy Symposium, University of

Miami, Florida.

LERCH F.J., WAGNER C.A., KLOSKO S.M., BELOTT R.P., 1978d. "Goddard Earth Model Development for Oceanographic Applications". presented at Marine Geodesy Symposium, University of Miami, Florida.

LERCH F.J., WELLS W., KLOSKO S.M., 1980. "Gravity Model Improvement using Laser Data". Crustal Dynamics Meeting, October.

LERCH F.J., KLOSKO S.M., PATEL G.B., 1982. "A Refined Gravity Model for LAGEOS (GEM-L2)". Geophys.Res.Lett. Vol.9 No.11, November, pp 1263-1266.

LISITZIN E., 1974. "Sea Level Changes". Elsevier, Amsterdam. 286pp.

LYDDANE R.H., 1963. "Small Eccentricities or Inclinations in Brouwer Theory of the Artificial Satellites". The Astronomical Journal 68(8), October, 555-558.

McCLURE P., 1973. "Diurnal Polar Motion". NASA X-592-73-259, Goddard Space Flight Center, Greenbelt, Maryland, September, 109pp.

McLUSKEY D., 1979. "Recovery of Plate Tectonic Movement from Doppler Satellite Observations". presented at XVIIth General Assembly of the International Union of Geodesy and Geophysics, Canberra, Australia, December 2-15, 48pp.

MA C., 1978. "Very Long Baseline Interferometry Applied to Polar Motion, Relativity and Geodesy". Ph.D. dissertation, NASA Tech.Mem. 79582, Goddard Space Flight Center, Greenbelt, Maryland, May, 367 pp.

MALYEVAC C. & ANDERLE R., 1979. "Determination of Plate Tectonic Motion from Doppler Observations of Navy Navigation Satellites". proc. 2nd Int. Symp. on Satellite Doppler Positioning Vol. 1, Austin, Texas, Jan 22-26.

MARSH J.G., DOUGLAS B.D., CONRAD T.D., WELLS W.T., WILLIAMSON R.G., 1977. "Gravity Anomalies Near the East Pacific Rise with Wavelengths Shorter than 3300Km Recovered from GEOS-3/ATS-6 Satellite to Satellite Doppler Tracking Data". NASA Tech.Mem. 79553, Goddard Space Flight Center, Greenbelt, Maryland, December, 270pp.

MARTIN T.V., OH I.H., EDDY W.F., KOGURT J.A., 1976. "GEODYN Systems

Descriptions". NAS 5-22849, Task 009, Goddard Space Flight Center, Greenbelt, Maryland.

MASTERS E.G., COLEMAN R., BRETREGER K., 1979. "On Orbital Errors and the Recovery of Ocean Tide Models Using Satellite Altimetry". Aust.J.Geod.Photo.Surv., 31, December, 127-152.

MASTERS E.G., COLEMAN R., BRETREGER K., 1980. "On the Recovery of Regional Ocean Tide Models using Satellite Altimetry". Marine Geodesy 4(4), 331-349.

MASTERS E.G., STOLZ A., HIRSCH B., 1982. "On Filtering and Compressing LAGEOS Range Data" Bull. Geod. (in press).

MATHER R.S., 1971. "The Analysis of the Earth's Gravity Field". School of Surveying, University of New South Wales, January. 172pp.

MATHER R.S., 1974a. "Quasi-Stationary Sea Surface Topography and Variations of Mean Sea Level with Time". Unisurv G21, School of Surveying, University of New South Wales, Sydney, Australia, 18-72.

MATHER R.S., 1974b. "On the Solution of the Geodetic Boundary Value Problem for the Definition of Sea Surface Topography". Geophys. J. Roy. Astron. Soc. 39, 87-109.

MATHER R.S., 1974c. "Geoid Definitions for the Study of Sea Surface Topography from Satellite Altimetry". proc. Applications of Marine Geodesy, Marine Technology Society, Washington D.C. 179-290.

MATHER R.S., 1975a, "On the Evaluation of Stationary Sea Surface Topography using Geodetic Techniques". Bull.Geod., 115, 65-82.

MATHER R.S. 1975b. "Mean Sea Level and the Definition of the Geoid". Unisurv G23, School of Surveying, University of New South Wales, Sydney, Australia, 68-79.

MATHER R.S., 1976. "Some Possibilities for Recovering Oceanographic Information from the SEASAT Mission". Unisurv G24, School of Surveying, University of New South Wales, Sydney, Australia, 103-122.

MATHER R.S., 1977. "The Analysis of GEOS-3 Altimeter Data in the Tasman and Coral Seas". NASA Tech.Mem. 78032, Goddard Space

Flight Center, Greenbelt, Maryland, 34pp.

MATHER R.S., 1978a. "On the Recovery of a System of Reference in Four Dimensions for Ocean Dynamics". Boundary-Layer Meteorology, 13, 231-244.

MATHER R.S., 1978b. "A Geodetic Basis for Ocean Dynamics". Bolletino di Geodesia e Scienze Affini, XXXVII(2-3), 285-308.

MATHER R.S., 1978c. "The Role of the Geoid in Four Dimensional Geodesy". Marine Geodesy 1(3), 217-252.

MATHER R.S., 1978d. "The Earth's Gravity Field and Ocean Dynamics". NASA Tech.Mem. 79540, Goddard Space Flight Center, Greenbelt, Maryland, May, 26pp + app.

MATHER R.S., 1978e. "The Influence of the Permanent Earth Tide on the Determination of Quasi-stationary Sea Surface Topography". Unisurv G28, School of Surveying, University of New South Wales, Sydney, Australia, 76-83.

MATHER R.S. & COLEMAN R., 1977. "The Role of Geodetic Techniques in Remote Sensing the Surface Dynamics of the Oceans". In: Using Space Today and Tomorrow, Napolitano, L.G. (ed). Pergamon Press, Oxford, 163pp.

MATHER R.S. & RIZOS C., 1979. "The Shape of Global Mean Sea Level from GEOS-3 Altimetry". Aust.J.Geod.Photo.Surv. No. 31, December, 153-160.

MATHER R.S., COLEMAN R., COLOMBO O.L., 1976a. "On the Recovery of Long Wavelength Sea Surface Topography from Satellite Altimetry". Unisurv G24, School of Surveying, University of New South Wales, Sydney, Australia, 21-46.

MATHER R.S., RIZOS C., HIRSCH B., BARLOW B.C., 1976b. "An Australian Gravity Data Bank for Sea Surface Topography Determinations (AUSGAD 76)". Unisurv G25, School of Surveying, University of New South Wales, Sydney, Australia, 54-84.

MATHER R.S., COLEMAN R., RIZOS C., HIRSCH B. 1977a. "A Preliminary Analysis of GEOS-3 Altimeter Data in the Tasman and Coral Sea". Unisurv G26, School of Surveying, University of New South Wales, Sydney, Australia, 27-45.

MATHER R.S., MASTERS E.G., COLEMAN R., 1977b. "The Role of Non-Tidal

Gravity variations in the Mainenance of Reference Systems for Secular Geodynamics". Unisurv G26, School of Surveying, University of New South Wales, Sydney, Australia, 1-25.

MATHER R.S., COLEMAN R., HIRSCH B. 1978a. "The Analysis of Temporal Variations in Regional Models of the Sargasso Sea from GEOS-3 Altimetry". NASA Tech.Mem. 79549, Goddard Space Flight Center, Greenbelt, Maryland, May, 52pp.

MATHER R.S., LERCH F.J., RIZOS C., MASTERS E.G., HIRSCH B., 1978b. "Determination of some Dominant Parameters of the Global Dynamic Sea Surface Topography from GEOS-3 Altimetry". NASA Tech.Mem. 79558, Goddard Space Flight Center, Greenbelt, Maryland, May, 40pp.

MATHER R.S., RIZOS C., COLEMAN R., 1979. "Remote Sensing of Ocean Circulation with Satellite Altimetry". Science, Vol 205, May, 11-17.

MATHER R.S., COLEMAN R., HIRSCH B., 1980. "Temporal Variations in Regional Models of the Sargasso Sea from GEOS-3 Altimetry". J.Phys.Oceanogr., Vol 10 No.2, 171-185.

MAUL G.A. & YANAWAY A., 1978. "Deep Sea Tides Determination from GEOS-3". NASA Contractor Report 141435, Wallops Flight Center, Virginia, 26pp.

MELCHIOR P., 1966. "The Earth Tides". Pergamon, Oxford, 458pp.

MELCHIOR P., 1971. "Precession, Nutation and Tidal Potential". Celestial Mech. 4, 190-212.

MELCHIOR P., 1978. "The Tides of the Planet Earth". Pergamon Press, Oxford, 609pp.

MIKHAIL E., 1976. "Observations and Least Squares". (with contribution by F. Ackermann), Dun-Donnelly, New York, 497pp.

MINSTER J.B., JORDAN T.H., MOLNAR P., HAINES E., 1974. "Numerical Modelling of Instantaneous Plate Tectonics". Geophys. J. Roy. Astron. Soc. 36, 541-576.

MINSTER J.B., JORDAN T.H., 1978. "Present Day Plate Motions". Journal of Geophys. Res. Vol 83(B11) November, 5331-5354.

MOFJELD H.O., 1975. "Empirical Models for the Tides in the Western North

Atlantic Ocean". NOAA Technical Report ERL 340-AOML 19, Boulder, Colorado, 27pp.

MORGAN W.J., 1972. "Plate Motions and Deep Mantle Convection". In: R.Shagan (ed.), Hess Volume, Geol-Soc.Am.Mem., 132, 7-22.

MORGAN P., 1981. "Simulation Studies for Crustal Motion Monitoring by Doppler in Papua New Guinea". Aust.J.Geod.Photo.Surv., No. 35, December, 15-62.

MOULTON F.R., 1970. "An Introduction to Celestial Mechanics". Dover, 436pp.

MUELLER I.I., LEICK A., 1979. "Defining the Celestial Pole". Manuscripta Geodaetica 4(2), September, 149-183.

MULHOLLAND J.D., 1980. "Scientific Achievements from Ten Years of Lunar Laser Ranging". Rev. Geophys. Space Phys. Vol. 18, No. 3, 549-564.

MUNK W.H. & MACDONALD G.J.F., 1960. "The Rotation of the Earth". Cambridge University Press, 323pp.

NAGEL E., 1976. "Die Bezugssysteme der Satellitengeodäsie". Dissertation Doktor Ingenieurs, Deutsche Geodätische Kommission, Reihe C, Heft Nr. 223 München, 139pp.

NAGLER R.G. & McCANDLESS S.W., 1975. "Operational Oceanographic Satellites, Potentials for Oceanography Climatology Coastal Processes and Ice". Jet Propulsion Lab., Pasadena, California, NASA, 12pp.

NASA. see: National Aeronautics and Space Administration

National Aeronautics and Space Administration, 1972. "Earth and Ocean Physics Applications Program". Vol. 2-Rationale and Program Plans, September.

National Aeronautics and Space Administration, 1978. Announcement of Opportunity, Laser Geodynamics Satellite (Lageos) A.O. No. OSTA 78-2, September, 12pp+app.

National Aeronautics and Space Administration, 1979. "Application of Space Technology to Crustal Dynamics and Earthquake Research". Tech. Paper 1464, Washington D.C., 257pp.

NEUMANN G., 1968. "Ocean Currents". Elsevier Oceanography Series, Vol. 4 352 pp.

NOAA/National Weather Service, 1978. Gulfstream 4(1-12), U.S. Govt. Printing Office, Washington D.C.

NOBLE B., 1973. "Methods for Computing the Moore-Penrose Generalised Inverse and Related Matters". in: Proc. of an Advanced Seminar sponsored by Mathematical Research Center, Zuhair Nashed M. (ed.), University of Wisconsin, Madison, October 8-10, (Academic Press, 1976, 245-301).

NOWROOZI A.A., 1967. "Table for Fisher's Test of Significance in Harmonic Analysis". Geophys. J. Roy. Astron. Soc. 12, 517-520.

PARKE M.E., 1980. "Tides on the Patagonian Shelf from the SEASAT Radar Altimeter". presented at COSPAR/SCOR/IUCRM Symposium Oceanography from Space, Venice, Italy, May 2-30, 1980.

PARKER C.E., 1971. "Gulf Stream Rings in the Sargasso Sea". Deep Sea Research, 18, 981-993.

PARRA C.G., LEITAO C.D., HUANG N.E., 1980. "Geoidal and Orbital Error Determination from Satellite Radar Altimeter". presented at COSPAR/SCOR/IUCRM Symposium Oceanography from Space, Venice, Italy, May 2-30, 1980.

PEARLMAN M.R., 1982. "Some Current Issues in Satellite Laser Ranging". in Proc. Fourth Int. Workshop on Laser Ranging Instrumentation, P.Wilson (ed), Geod. Inst. Univ. Bonn, West Germany,pp568-578.

PEASE G.E., 1977. "Estimates of Precession and Polar Motion Errors from Planetary Encounter Station Location Solutions". DSN Progress Report 42-43, Jet Propulsion Laboratory, Pasadena, California, 29-49.

PUTNEY B. 1980. "GEODYN Program Systems Development". Earth Survey Applications Division Research Report (L. Carpenter (ed.), 1979. Tech.Mem. 80642, January,p4-2.

PUTNEY B., 1981. "Progress Report for Geodynamics Program Systems". Third Annual NASA Geodynamics Geodynamics Program Review, Crustal Dynamics Project, Geodynamics Research, Goddard Space Flight Center, Greenbelt, Maryland, January 26-29 p59.

REID,Jr J.L., 1961. "On the Geostrophic Flow at the Surface of the

Pacific Ocean with respect to the 1000-Decibar Surface". Tellus 13(4), 489-502.

REIGBER C., 1981. "Representation of Orbit Element Variations and Force Function with Respect to Various Reference Systems". Bull.Geod. 55, 111-131.

REIGBER C.H. & BALMINO G., 1976. "Even and Odd Degree 13th Order Harmonics from Analysis of Stable near resonant Satellite Orbits". Groupe de Recherches de Geodesie Spatiale Bull No. 15, March, 1-46.

REIGBER,C.H., DREWES H., MÜLLER H., RIZOS C.,1982. "Capabilities of LAGEOS ranging data for Baseline Determinations". presented at 3rd Int. Symposium, The Use of Artificial Satellites for Geodesy and Geodynamics, Porto Hydra Greece, September 20-25.

RIZOS C., 1980a. "The Role of the Gravity Field in Sea Surface Topography Studies". Unisurv S17, School of Surveying, University of New South Wales, Sydney, Australia. 286pp.

RIZOS C., 1980b. "The Contribution of Sea Surface Topography Studies to the Understanding of Global Ocean Circulation". Aust.J.Geod.Photo.Surv., No. 32, December, 59-92.

ROCHESTER M.G., 1973. "The Earth's Rotation". EOS Trans. Am. Geophys. Union Vol 54 769-780.

ROELSE A., GRANGER H.W., GRAHAM J.W., 1971. "The Adjustment of the Australian Levelling Survey 1970-1971". NATMAP Technical Report No. 12, Canberra, Australia.

RUBINCAM D., 1980. "Atmospheric Drag as the Cause of the Secular Decrease in the Semi-Major Axis of LAGEOS's Orbit". Geophys.Res.Lett. Vol 7, No.6, June, 468-470.

SAVAGE J.C., PRESCOTT W.H., LISOWSKI M., KING N.E., 1981. "Strain Accumulation in Southern California 1973-1980". Journal of Geophys. Res. Vol 86(b8) August, 6691-7002.

SCHUTZ B.E., TAPLEY B.D., RIES J., EANES R., 1979. "Polar Motion Results from GEOS-3 Laser Ranging". Journal of Geophys. Res. Vol. 84(B8) July, 3951-3958.

SCHUTZ B.E., TAPLEY B.D., EANES R.J., 1980. "LAGEOS Orbital Analysis". Institute for Advanced Study in Orbital Mechanics, The

University of Texas at Austin, October.

SCHWIDERSKI E.W., 1980. "On Charting Global Ocean Tides". Rev.Geophys.Space.Phys., Vol. 18, No. 1, February, 243-268.

SILVERBERG E., 1978. "Mobile Satellite Ranging". in proc. 9th GEOP Conference, Dept. of Geodetic Science, Rep. No. 280, I.I. Mueller (ed.), The Ohio State University, Columbus, 41-46.

SILVERBERG E., 1981. "First Operational Activity with TLRS". (Abstract) Third Annual NASA Geodynamics Program Review, Crustal Dynamics Project, Geodynamics Research, Goddard Space Flight Center, Greenbelt, Maryland, January 26-29, p3.

SILVERBERG E. & BYRD D.C., 1981. "A Mobile Telescope for Measuring Continental Drift". Sky and Telescope, May, 405-408.

SLOANE B.J.& STEED J.B., 1976. "Crustal Movement Survey: Markham Valley, Papua New Guinea, 1975". NATMAP Technical Report No. 23, Canberra,Australia.

SMITH D.E., 1978. "Recent Advances in Computational Techniques". in proc. 9th GEOP Conference, Dept. of Geodetic Science, Rep. No. 280, I.I. Mueller (ed.), The Ohio State University, Columbus, 207-211.

SMITH D.E. & DUNN P.J., 1980. "Long Term Evolution of the LAGEOS Orbit". Geophys.Res. Lett (7), No.6, June, 437-440.

SMITH D.E., KOLENKIEWICZ R., AGREEN R.W., DUNN P.J., 1973. "Dynamic Techniques for Studies of Secular Variations in Position from Ranging to Satellites". proc. Symp. on Earth's Gravitational Field & Secular Variations in Position, R.S.Mather and P.V.Angus-Leppan (ed.), School of Surveying, University of New South Wales, Sydney, Australia, November 26-30, 291-314.

SMITH D.E., KOLENKIEWICZ R., DUNN P.J., TORRENCE M.H., 1979a. "Determination of Station Coordinates from LAGEOS". in proc. 2nd Int. Symp. On the Use of Artificial Satellites for Geodesy and Geodynamics VOL 2, National Technical University, Athens, Greece, 162-172.

SMITH D.E., KOLENKIEWICZ R., DUNN P.J., TORRENCE M., 1979b. "The

Measurement of Fault Motion by Satellite Laser Ranging". Tectonophysics, 52, 59-69.

SMITH D.E., CHRISTODOULIDIS D., DUNN P.J., 1979c. "Earth and Ocean Tidal Effects on the LAGEOS Satellite". Interdisciplinary Abstract 20/19, XVIIth General Assembly of the International Union of Geodesy and Geophysics, Canberra, Australia, p625.

SMITH D.E., DUNN P.J., CHRISTODOULIDIS D., TORRENCE M., 1982. "Global Baselines from Laser Ranging". Abstracts 4th Annual Conference on the NASA Geodynamics Program Crustal Dynamics Project, Geodynamics Program, Goddard Space Flight Center, Greenbelt, Maryland, January 26-29, p58.

SOLOMON S., SLEEP N., 1974. "Some Simple Physical Models for Absolute Plate Motions". Journal of Geophys. Res. Vol 79(17) June, 2557-2567.

STANLEY H.R. 1979. "The GEOS-3 Project". Journal of Geophys. Res. Vol 84(B8) July, 3779-3783.

STEIN S. & OKAL E., 1978. "Seismicity and Tectonics of the Ninety-East ridge Area: Evidence for Internal Deformation of the Indian Plate". Journal of Geophys. Res. Vol 83, 2233-2245.

STOLZ A., 1979. "Precise Modelling Aspects of Lunar Measurements and their use for the Improvement of Geodetic Parameters". Deutsche Geodätische Kommission, Reihe A, Heft Nr. 90, München, 23pp.

STOLZ A., 1980. "Geodetic Determination of the Large Scale Crustal Motion of Australia". Proposal to Australian Research Grants Committee, 11pp.

STOLZ A., 1981. "Determination of the Large Scale Crustal Motion of Australasia by Satellite Laser Ranging". Proposal to NASA in response to Announcement of Opportunity A.O. No. OSTA 80-2.

STOLZ A. & MASTERS E.G., 1982. "Studying the Tectonics of Australia by Satellite Laser Ranging". The Australian Surveyor, March, Vol 31 No. 1, 34-44.

STOLZ A. & LAMBECK K., 1983."Geodetic Monitoring of Tectonic Deformation in the Australian Region". J.Geol.Soc.Aust. (in press)

STOLZ A., MASTERS E.G., HIRSCH B., 1981. "Preliminary Baseline Values from Range Measurements to the LAGEOS Satellite". Aust.J.Geod.Photo.Surv., No.35, December, 69-77.

STOLZ et AL,1983. "Geodetic Surveying with Quasar Radio Interferometry". The Australian Surveyor, Vol. 31 No.5 March, pp305-314.

STURGES W., 1967. "Slope of Sea Level along the Pacific Coast of the United States". Journal of Geophys. Res. Vol 72(14), pp3627-3637.

SYKES L.R., 1978. "Intraplate Seismicity, Reactivation of Preexisting Zones of Weakness, Alkaline Magmatism, and other Tectonism Postdating Continental Fragmentation". Rev. Geophys. Space. Phys. 16, 621-688.

TANNER J.G., TORGE W., 1979. International Report on Geodesy, Section III - Gravimetry, Summary of Activities, 1975-1979, 11pp.

TAPLEY B.D., SCHUTZ B.E., EANES R.S., 1979. "Solid Earth Dynamics using LAGEOS Range Observations". Interdisciplinary Abstract 06/19, XVIIth General Assembly of the International Union of Geodesy and Geophysics, Canberra, Australia. p196.

TAPLEY B.D., SCHUTZ B.E., EANES R.J., 1980. "Preliminary Tracking Station Solutions based upon LAGEOS Range Observations". Institute for Advanced Study in Orbital Mechanics, The University of Texas at Austin, 6pp.

TAPLEY B., SCHUTZ B.E., EANES R.J., 1982. "A Critical Analysis of Satellite Laser Ranging Data".
in Proc. Fourth Int. Workshop on Laser Ranging Instrumentation, P.Wilson (ed), Geod. Inst. Univ. Bonn, West Germany,pp523-567.

TORRENCE M.H., DUNN P.J., 1980. "Polar Motion and Change of Length of Day from LAGEOS". (Abstract) EOS Trans. Am. Geophys. Union Vol 61, p212.

TSIMIS E., 1973. "Critical Configurations (Determinantal Loci) for Range and Range-Difference Satellite Networks". The Ohio State University Report No. 191, January, 153pp.

VAN GELDER B.H.W., 1978. "Estimability and Simple Dynamical Analyses of Range (Range Rates and Range Differences) Observations to

Artificial Satellites". The Ohio State University Report No. 284, 270pp.

VANICEK P., 1971. "Further Development and Properties of the Spectral Analysis by Least Squares". Astrophys. Space Phys. 12, 10-33

WAGNER C.A., 1979. "The Geoid Spectrum from Altimetry". Journal of Geophys. Res. Vol 84(B8), July, 3861-3871.

WAGNER C.A., LERCH F.J., BROWND J.E., RICHARDSON J.A., 1976. "Improvement in the Geopotential Derived from Satellite and Surface Data (GEM 7 and 8)". NASA Report X-921-76-20, Goddard Space Flight Center, Greenbelt, Maryland, 11pp.

WAGNER C.A., KLOSKO S.M., 1977. "Gravitational Harmonics from Shallow Resonant Orbits". Celestial Mechanics 16, 143-163.

WAHR J.M., 1981a. "Body Tides on an Elliptical Rotating Elastic and Oceanless Earth". Geophys.J.Roy.Astron. Soc. 64, 677-703.

WAHR J.M., 1981b. "The Forced Nutations of an Elliptical Rotating Elastic and Oceanless Earth". Geophys.J.Roy.Astron.Soc. 64, 705-727.

WEISSEL K., ANDERSON R.N., GELLER C.A., 1980. "Deformation of the Indo-Australian Plate". Nature Vol. 287, 284-291.

WILKINS G.A. (ed.), 1980. "Project Merit". Royal Greenwich Observatory, 77pp.

WILSON P., BOUCHER C., PAQUET P., 1978. "EDOC-2 Status Report with a summary of some Preliminary Results of Second European Doppler Observation Campaign". proc. 2nd Symp. on the Use of Artificial Satellites for Geodesy and Geodynamics, Vol II, National Technical University, Athens, Greece, pp42-62.

WON I.J., KUO J.T., JACHENS R.C., 1978. "Mapping Ocean Tides with Satellites, A computer Simulation". J.Geophys.Res Vol. 83, No. B12, 5947-5960.

WON I.J., & MILLER L.S., 1979. "Oceanic Geoid and Tides from GEOS-3 Satellite Altimetry Data in the Northwestern Atlantic Ocean". Journal of Geophys. Res. Vol 84(B8), 3833-3842.

WOOLARD E.W., 1953. "Theory of the Rotation of the Earth around its Center of Mass". Astron. Papers Am. Ephem. Naut. Almanac

15, 1, 128pp.

WUNSCH C., GAPOSCHKIN E.M., 1980. "On using Satellite Altimetry to Determine the General Circulation of the Oceans with Application to Geoid Improvement". Rev.Geophys.Space.Phys Vol. 18, No. 4, 725-745.

WYRTKI K., 1975. "Fluctuations of the Dynamic Topography in the Pacific Ocean". J.Phys.Oceanogr. 5, 450-459.

ZETLER B.D. & MAUL G.A., 1971. "Precision Requirements for a Spacecraft Tide Program". Journal of Geophys. Res. Vol 76(27), 6601-6605.

ZETLER B., MUNK W., MOFJELD H., BROWN W., DORMER F., 1975. "MODE tides". J.Phys.Oceanogr Vol. 5, 430-441.

A P P E N D I X A

A.1 SPECTRAL ANALYSIS

Non-periodic functions can be represented by periodic functions (JENKINS & WATTS,1968). In Fourier analysis, the periodic functions are sines and cosines. They have the following important properties:

(i) an approximation consisting of a given number of terms achieves the minimum square error between the signal and the approximation.

(ii) they are orthogonal so that the coefficients can be determined independently of one another (JENKINS & WATTS,1968).

The mean square average power of a signal s sampled at intervals Δ for a period T producing N sample values s_i is

$$1/N \sum_{i=-n}^{n-1} s_i = R_0^2 + R_n^2 + 2 \sum_{m=1}^{n-1} R_m^2 \qquad (A.1)$$

where R_m are amplitudes for the m-th harmonic of the time series,

R_0 is the mean,

R_n is the amplitude for fundamental frequency.

The average power can be decomposed into contributions from each harmonic.

A measure of s_i about the mean is the variance

$$\sigma^2 = \frac{1}{N} \sum_{i=-n}^{n-1} (s_i - R_0)^2 \qquad (A.2)$$

$$= R_n^2 + 2 \sum_{i=-n}^{n-1} R_m^2 \qquad (A.3)$$

For the continuous infinite case the Fourier transform of s(t) is

$$S(f) = \int_{-\infty}^{\infty} s(t)\, e^{-j2\Pi ft}\, dt \qquad (A.4)$$

where f is frequency and

$j = \sqrt{-1}$

S(f) represents the distribution of signal strength with frequency and is therefore useful for analysing time series.

Due to the orthogonal properties for equi-spaced data sets, the

calculation of R_m is straightforward:

$$R_m^2 = A_m^2 + B_m^2 \qquad (A.5)$$

where

$$A_m = \frac{1}{N} \sum_{i=-n}^{n-1} s_i \cos 2\Pi mi/N \qquad (A.6)$$

$$B_m = \frac{1}{N} \sum_{i=-n}^{n-1} s_i \sin 2\Pi mi/N \qquad (A.7)$$

Computer programs which are used to calculate Fourier transforms can be made much more efficient by taking advantage of the periodic properties of the sine and cosine functions. The Fast Fourier transform uses this property. The number of operations (N^2 for a conventional Fourier transform), is reduced by N log N (KANASEWICH,1975). Fast Fourier techniques reduce computation time by about two orders of magnitude.

A.1.1 Aliasing

As the power spectrum is obtained from discrete time series sampling of a continuous signal, there is a high frequency limit to the estimated power spectrum. All the spectral information is contained within the **principal interval**

$$0 \leq f \leq f_N$$

where f_N is the **Nyquist or folding frequency** defined by

$f_N = 1/2\Delta$.

Frequencies higher than the Nyquist frequency are not sampled by a discrete time series. It is therefore impossible to distinguish frequencies above the Nyquist frequency from those in the principal interval. If signals with higher frequencies than the Nyquist frequency are present, their power is reflected or **aliased** into the power spectrum over the principal range (KANASEWICH,1975). Figure A.1 illustrates that at least two signals fit discrete data points (*). This in principle shows the problem of distinguishing between signals above and below the Nyquist frequency after digitization.

Harmonics above the Nyquist frequency must be attenuated by a high cut filter before calculating the power in order to eliminate aliasing. Alternatively the frequencies, which are contributing to the power at a set frequency should be determined. If as occurs in many physical applications, non equi-spaced data are obtained the fundamental concepts of spectral analysis are not clearly defined. This remark applies in

particular to the Nyquist frequency.

FIGURE A.1

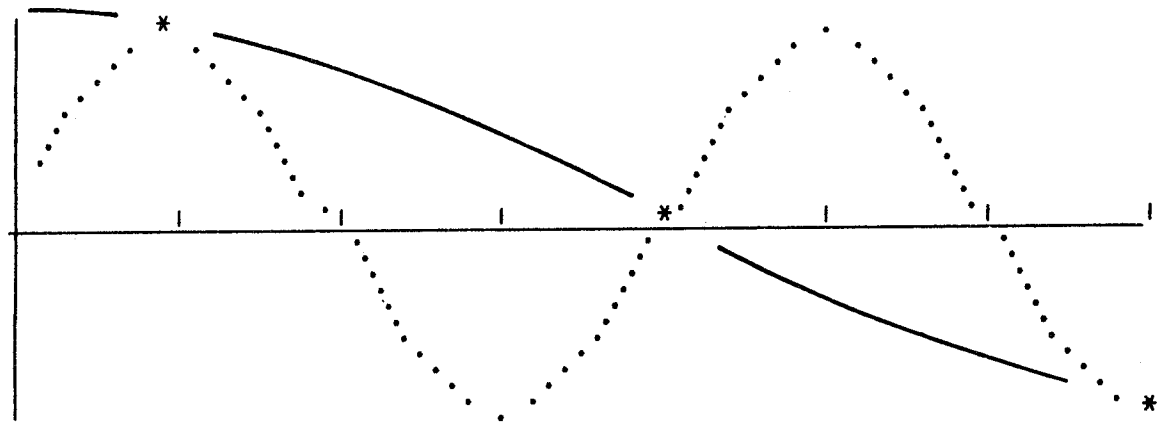

A.1.2 Confidence Limits

Confidence limits for the estimated spectrum can be obtained in several ways.

The χ^2 test is defined by

$$\frac{\nu C(f)}{\chi^2_{\nu,1-\alpha/2}} \leq \Gamma(f) \leq \frac{\nu C(f)}{\chi^2_{\nu,\alpha/2}} \qquad (A.8)$$

ν is degrees of freedom
$C(f)$ is the sample spectrum
$\Gamma(f)$ is the spectrum

Tabulated values for statistical distributions are usually not available for large amounts of data. An approximation to the χ^2 distribution is given by (KREYZIG,1970)

$$\chi^2_{\alpha,\infty} = \frac{1}{2}\{t_{2\alpha,\infty} + \sqrt{(2\nu-1)}\}^2 \qquad (A.9)$$

or

$$\chi^2_{1-\alpha,\infty} = \frac{1}{2}\{t_{2\alpha,\infty} - \sqrt{(2\nu-1)}\}^2 \qquad (A.10)$$

The F test can also be used to determine which are the significant peaks in the estimated spectrum (NOWROOZI,1967). A function f(x) can be decomposed as

$$f(x) = a_0 + \sum_{k=1}^{m} \{a_k \cos w_k x + b_k \sin w_k x\} \qquad (A.11)$$

where $w_k = 2\Pi kx/n$ and

$n = 2m+1$.

The probability that

$$\max(a^2 + b^2)/2\sigma_0^2 > g \qquad (A.12)$$

is α. This probability can be calculated from

$$\alpha \cong m\,(1-g)^{m-1} \qquad (A.13)$$

A.2 LEAST SQUARES SPECTRAL ANALYSIS

VANICEK's (1971) spectral analysis program includes estimates of the contribution of a frequency w to the overall variance of a time series F(t). Let

$$S^2(F,T) = \sum_t (F(t)-T(t))^2 \qquad (A.14)$$

and

$$T(t) = \cos wt + \sin wt$$

then the contribution of P to S from the frequency w is given by (VANICEK,1971)

$$P_w = \sum_t F(t)^2 - S^2 \qquad (A.15)$$

The calculation of the maximum contribution of w to S leads to the minimisation of S^2. This is a standard least squares problem, which can be solved using a set of normal equations. If F(t) is sampled at equidistant time intervals, P_w is the contribution of the frequency w to the n-times variance of F (JENKINS & WATTS,1968). A specific choice of frequencies to represent the harmonic constituents of the time series results in the normal equations matrix being diagonal. In this case the method is equivalent to the conventional Fourier transform (VANICEK,1971). The program was specifically designed to analyse irregularly spaced and noisy data.

The calculation speed was improved for this dissertation by introducing recursive formulae for the summation terms in the formation of the normal equations. If data is equi-spaced the Fast Fourier Transform is the most appropriate method. However, only the set of frequencies (w) is equi-spaced. Nevertheless speed can be gained over individual spectral point calculations by introducing the following well known recursives for sine and cosine terms.

$$\begin{aligned} k\cos mx &= 2k\cos x\cos(m-1)x - k\cos(m-2)x \\ k\sin mx &= 2k\cos x\sin(m-1)x - k\sin(m-2)x \end{aligned} \qquad (A.16)$$

k is a constant and m is an integer.

Any sin and cos terms can be expressed in the following matrix form

$$\begin{bmatrix}\cos\ wt\\ \sin\ wt\end{bmatrix} = \begin{bmatrix}\cos\ m\Delta wt & -\sin\ m\Delta wt\\ \sin\ m\Delta wt & \cos\ m\Delta wt\end{bmatrix}\begin{bmatrix}\cos\ w_0 t\\ \sin\ w_0 t\end{bmatrix} \qquad (A.17)$$

where $w = w_0 + m\Delta w$

$= 2\Pi/T$

and T is the period.

w_0 is the initial period.

The order of the loops in the Fourier algorithm were changed so that all spectral values were accumulated for every data point, rather than separately. This is possible because usually only a relatively small number of spectral values need to be calculated in comparison to the amount of data. These spectral values can therefore be accumulated in core for the whole calculation. The efficiency of the algorithm depends on the number of spectral values which can be accumulated in core. The recursive routine was found to be about 2.5 times faster than the non-recursive routine. This was significant for the analyses in this dissertation.

A P P E N D I X B

SPHERICAL HARMONICS and POTENTIAL

A function which is defined over a sphere can be represented by a series of spherical harmonics (HOBSON,1931), that is

$$F(\phi,\lambda) = \sum_{n=0}^{\infty} 1/R^{n+1} \sum_{m=0}^{n} P_{nm}(\mu)\{A_{nm}\cos m\lambda + B_{nm}\sin m\lambda\} \qquad (B.1)$$

where $P_{nm}(\mu)$ are the Legendre functions of degree n and order m, and

R is the radial distance to the point of evaluation.

For a continuous distribution of density the Earth's gravitational potential may be written

$$W_G = G\iiint_V \rho/r \; dv \qquad (B.2)$$

where ρ is the density of mass within the Earth,

r is the distance from the point of evaluation to the volume element dv and

G is the gravitational constant.

The force vector, F, due to the gravitational potential is given by the gradient of the potential (HEISKANEN & MORITZ,1967)

$$F_G = -\nabla W_G \qquad (B.3)$$

where $\nabla = \frac{\partial}{\partial x_i}\, i$

The Geopotential W, is the sum of the potentials due to gravitation W_G; deformation W_D, from other masses and Earth rotation W_R, that is

$$W = W_G + W_D + W_R \qquad (B.4)$$

The gravity force vector, **g**, is the gradient of potential

$$\mathbf{g} = -\nabla W \qquad (B.5)$$

The second derivative of geopotential is discontinuous at the surface of the Earth. For regions exterior to the Earth and its atmosphere the second derivative of geopotential is continuous and satisfies Laplace's equation. Hence

$$\nabla^2 W = 0 \qquad (B.6)$$

where $\nabla^2 = \frac{\partial^2}{\partial x_i^2}\, i$

Equation B.1 is a solution of Laplace's equation (HEISKANEN & MORITZ,1967). Spherical harmonics therefore represent a convenient method of describing the geopotential on a global scale. Furthermore

they provide a particularly convenient method of computing the force model required for integration of the equations of motion for satellites.

There are $(n+1)^2$ coefficients of degree n. Hence a large number of Legendre polynomial evaluations often need to be evaluated. This means that spherical harmonics are not very efficient for high degree and orders. However, calculation times can be significantly reduced by using some recursive formulae when gridded data is involved. These formulae are similar to those employed for the Fast Fourier Transform (COLOMBO,1979; COLOMBO & RIZOS,1979).

The surface harmonic series are conventionally divided into three classes.

(1) Zonals (order m=0, and the degree n) give rise to n+1 bands between n nodal parallels of latitude. Even degree harmonics are symmetrical about the equator, while those of odd degree are asymmetrical about the equator.

(2) Tesserals ($0<m<n$) give rise to n-m nodes along parallels of latitude. In addition the cos $m\lambda$ term has m zeros in the range $0<\lambda<\Pi$ which results in nodal lines coinciding with meridians spaced λ/m apart.

(3) Sectorials (m=n) give rise to m longitude dependent nodal lines in the range $0<\lambda<\Pi$.

The low degree and order coefficients have specific physical significance (HEISKANEN & MORITZ,1967). These are important for reference system definitions. The geopotential at a point P may be written in two ways, that is

$$W_P = G \iiint 1/r \, dm \qquad (B.7)$$

and

$$W_P = \sum_{n=0}^{\infty} 1/R^{n+1} \sum_{m=0}^{n} p_{nm}(\sin\phi) \{a_{nm}\cos m\lambda + b_{nm}\sin m\lambda\} \qquad (B.8)$$

The 1/r term in Equation B.7 can be expressed in terms of Legendre polynomials. If this is done and coefficients are compared one finds that for

<u>n=0</u>

$$a_{00} = GM$$

<u>n=1</u>

$$a_{10} = I_{13} = GM\bar{X}_3$$

$$a_{11} = I_{11} = GM\bar{X}_1$$

$$b_{11} = I_{12} = GMX_2$$

where $\bar{X}_i$ are the coordinates of the centre of mass and I_{ij} is the first order inertia tensor.

n=2

$$a_{20} = G\{(I_{211}+I_{222}/2)-I_{233}$$

$$a_{21} = 2GI_{213} \qquad b_{21} = 2GI_{223}$$

$$a_{22} = G\{I_{222}-I_{211}\}/2 \qquad b_{22} = GI_{212}$$

where I_{ijk} is the j-th row, k-th column of the i-th order inertia tensor.

I_{2ij} is given by

$$I_{2ij} = \iiint (\delta_{ij}R^2 - X_i X_j)\ \rho\ dV \qquad (B.9)$$

where δ_{ij} is the Kronecker delta.

I_{2ii} are the moments of inertia about the X_i axes.

If the coordinate axes are aligned with the principal axes of inertia, then the off diagonal terms of the inertia tensor are zero. Setting

$$a_{21} = b_{21} = 0$$

in the expression for the geopotential therefore aligns the polar inertia tensor with the reference system axis. Similarly, a_{22} and b_{22} define the position of the inertia tensor in the equatorial plane.

The coefficients a and b are related to the C and S by the formula (MATHER,1971)

$$C_{nm} = a_{nm}/GMa_e^n$$

where a_e is the equatorial radius of the Earth

Specifically of interest in geodesy are C_{00}, C_{10}, C_{11}, S_{11}, C_{21}, S_{21}. They define reference systems in the context of astronomy and satellite geodesy. Thus, if the reference ellipsoid is to be geocentric and the reference axes are to be aligned with the Earth's principal axis of inertia, the C_{10}, C_{11}, S_{11} and C_{21}, S_{21} will be zero.

The flattening f of the reference ellipsoid, which best fits the geoid is of relevance to geodesy and is defined by (MATHER,1971)

$$C_{20} = m/3-2f/3-3mf/7+f^2/3 + O\{f^3\}$$

and

$$C_{40} = 4f^2/5 - 4mf/7 + O\{f^3\}$$

where $m = a_e^3 w^2 /GM$ and

w is the Earth's angular velocity.

A P P E N D I X C

NUMERICAL METHODS

C.1 ILL-CONDITIONING and RANK DEFICIENCY

The solution of a set of observation equations

$$Ax + b = l + v \qquad (C.1)$$

using floating-point arithmetic is that of a perturbed set of equations (NOBLE,1973):

$$(A+E)x + b = l + v + f \qquad (C.2)$$

where E and f are small perturbations to A and l respectively. If E is non-zero the rank of A does not necessarily equal the rank of (A+E). Therefore it is possible for a theoretically singular matrix to be numerically non-singular. The conclusion can be drawn that a seemingly "good" inverse can be obtained for a theoretically singular design matrix. To infer physical meaning to the estimated parameters under these conditions would not be valid. Detecting this occurrence is one problem with practical calculations.

In computing terms, ill conditioning and rank deficiency are often synonomous (FORSYTHE & MOLER,1967). Theoretically speaking, constraints are necessary to remove rank defects, whereas condition can be improved by including higher quality and more well distributed observations and adding constraints. However the use of constraints to improve ill-conditioned matrices introduces problems of interpretation for the estimated parameters. With regard to satellite networks, where the observation quality and distribution are basically fixed, there is a problem of deciding between the effects of overconstraint and ill-conditioning. This will involve a decision about the rank of the design matrix and the effect of noise on the estimated parameters.

C.2 NUMERICAL ALGORITHMS for SOLVING EQUATIONS and DETERMINING RANK

As the outcome of numerical rank determinations is algorithm dependent and may not represent the true algebraic rank, it is referred to as **pseudo-rank** (LAWSON & HANSON,1974). Algorithms for pseudo-rank determination are essentially based on the calculation of a threshold tolerance level where extreme ill-conditioning degenerates into rank deficiency in the computer.

The logic of any pseudo-rank determination procedure is as follows. If two computer registers, a and b contain values which are

nearly identical, that is if $a = b + 10^{-n}$, then the finite calculation of a-b to n digit accuracy will be zero and not 10^{-n}. If this situation occurs for a solution algorithm the equations are pseudo-rank deficient. The number of pseudo-rank defects will show the minimum number of independent constraint equations, which are necessary to make the system of equations non-singular. The determination of pseudo-rank can therefore provide a basis for practical solution of equations without over or under-constraint.

In the **Gaussian elimination** technique, the system of equations Ax=b is solved by reducing A to upper triangular form. This is achieved by means of the algorithm

$$b_{ik} = a_{ik} - n_{jk}a_{ij}/n_{jj} \qquad (C.3)$$

where n_{jj} is the pivot element and

the i, k subscripts refer to the i-th row, k-th column in the matrix A.

For full pivoting elimination, the rows and columns are interchanged so that n_{jj} is the largest remaining element. Thus if n_{jj}/n_{j-1j-1} is less than the set tolerance or machine precision, the remaining rows and columns are considered to be linearly dependent. This is a common procedure for determining pseudo-rank (IBM,1966).

Singular Value Decomposition (SV) is one of many orthogonal decomposition pseudo-inverse techniques for solving linear equations. The technique was developed in the 1960's and is described in LAWSON & HANSON (1974). Numerical analysts regard it as being the least susceptible to ill conditioning (NOBLE,1973; LAWSON & HANSON,1974), but the method is not the most efficient.

The design matrix A (equation C.1) can be decomposed so that (LAWSON & HANSON,1974)

$$A = USV^T \qquad (C.4)$$

where S is the diagonal matrix of singular values of A

U, V correspond to the orthogonal eigenvectors of at A^TA and AA^T respectively.

Since the matrices U and V are orthogonal by definition the pseudo-inverse is

$$A^+ = VS^{-1}U^T \qquad (C.5)$$

The system flow for determining A^+ involves: decomposing A into the component matrices of singular values S and eigenvectors U, V;

deciding which singular values should be zero and setting them to zero; and calculating the pseudo-inverse (equation C.5). Since S is diagonal, it is easily inverted. The last calculation is therefore fairly trivial. If the zero singular values are correctly chosen the solution obtained from this inverse will minimise the norm of the a posteriori variance covariance matrix and hence give a pseudo inverse (LAWSON & HANSON,1974). The technique can therefore be used for determining least squares estimates of parameters.

The pseudo-rank of A is implicitly determined by the choice of zero singular values. LAWSON & HANSON (1974) give four methods of achieving this. Any of these are suitable. The technique employed in this dissertation is to compare the cumulative sum of the squares of the singular values to a preset tolerance level, which depends on the estimated roundoff error in the calculation, and also on the size of the matrix.

An alternative method of obtaining a pseudo-inverse is by appending an orthogonal border to the design matrix. This is one way of obtaining the geodetic free network or inner coordinate adjustment (BLAHA,1971a; BOSSLER,1972). The matrix of normal equations is

$$A^TA + D^TD \qquad (C.6)$$

The minimal set of constraints D, preserves the position of the centroid and the mean orientation of all coordinated points (BLAHA,1971a). The similarity of D^TD to the Bayesian constraint matrix is apparent. The free network adjustment is therefore a special case of general Bayesian estimation.

An approximate pseudo-inverse referred to as **Infinitesimal Bordering** can be obtained by using the Bayesian formula (Equation 8.22) with $W = \delta I$ where δ is a small constant and I is the identity matrix (BJERHAMMAR,1973). This method is extremely ill-conditioned and is only recommended for estimating variances (BJERHAMMAR,1973).

C.3 STATISTICS and CONDITION

Confidence levels for the estimated parameters are important for any analyses. These are usually obtained from the variance-covariance matrix. The inverse of the normal equation matrix is the matrix of weight coefficients called a co-factor matrix (MIKHAIL,1976). If the a priori estimate of the observation noise variance is correct then the co-factor matrix will be the variance-covariance matrix for the

parameters. Otherwise, the variance-covariance matrix must be derived using estimates of the variance factors with the co-factor matrix. BOSSLER (1972) gives formulae for determining the a posteriori variance-covariance matrix for Bayesian least squares estimation.

The effect of ill-conditioning is that the estimated parameters lose significance because of the accumulation of errors, that is almost any parameter value will satisfy the least squares condition. The inverse does not exist if the equations are singular. The a posteriori variance-covariance matrix therefore indicates the effect of observation noise and data distribution on parameters, but does not clearly show if the matrix is singular. An indication that all is not well is that a few parameters may have unusually large variances.

The most common procedure employed to determine the condition of a matrix is to examine the eigenvalues **e**. The **condition number K** for a matrix is given by

$$K = e_{MAX} / e_{MIN} \qquad (C.7)$$

where e_{MAX} and e_{MIN} are respectively the maximum and minimum eigenvalues

FORSYTHE & MOLER (1967), BJERHAMMAR (1973), LAWSON & HANSON (1974) and most least squares analysis texts give the derivation of this condition number.

A different approach was adopted for the SOLVE program (Computer Sciences Corporation,1976) and has now been incorporated in GEODYN (MARTIN et AL,1976). A condition number k_i is calculated for each parameter. This number is an estimate of the ratio of the expected estimated parameter value to the true value and is obtained from

$$k_i = N_i V_i \qquad (C.8)$$

where N_i, V_i are the diagonal elements of the normal matrix and it's inverse respectively.

It is assumed that V can be calculated to the same accuracy as N. Ill-conditioning results in large condition numbers. Moreover, because this condition number is an estimate of the expected relative error for a parameter, the number of significant figures lost in the calculation of the parameter is obtained from the logarithm of k_i. This condition number is compatible with the definition of ill-conditioning (NOBLE,1973), that is, small changes in the original matrix result in large changes for the inverse. The advantage of this technique is that the statistical significance of the estimated parameters is easily estimated without calculating the eigenvalues.

Publications from
THE SCHOOL OF SURVEYING, THE UNIVERSITY OF NEW SOUTH WALES
P.O. Box 1, Kensington, N.S.W. 2033
AUSTRALIA

Unisurv Reports - G Series

Price (excluding postage): $2.00

G3. R.S. Mather, "The establishment of geodetic gravity networks in South Australia", Uniciv Rep. R-17, 26 pp.

G14. A. Stolz, "The computation of three dimensional Cartesian co-ordinates of terrestrial networks by the use of local astronomic vector systems", Unisurv Rep. 18, 47 pp.

G15. R.S. Mather, "The Australian geodetic datum in earth space", Unisurv Rep. 19, 130 pp.

G16. R.S. Mather et al, "Communications from Australia to Section V, International Association of Geodesy, XV General Assembly, International Union of Geodesy and Geophysics, Moscow 1971", Unisurv Rep. 22, 72 pp.

G17. Papers by R.S. Mather, H.L. Mitchell & A. Stolz on the following topics:- Four-dimensional geodesy, Network adjustment and Sea surface topography, Unisurv G 17, 73 pp.

G18. Papers by L. Berlin, G.J.F. Holden, P.V. Angus-Leppan, H.L. Mitchell & A.H. Campbell on the following topics:- Photogrammetry co-ordinate systems for surveying integration, Geopotential networks and Linear measurement, Unisurv G 18, 80 pp.

G19. R.S. Mather, P.V. Angus-Leppan, A. Stolz & I. Lloyd, "Aspects of four-dimensional geodesy", Unisurv G 19, 100 pp.

G20. Papers by J.S. Allman, R.C. Lister, J.C. Trinder & R.S. Mather on the following topics:- Network adjustments, Photogrammetry, and 4-Dimensional geodesy, Unisurv G 20, 133 pp.

G21. Papers by E. Grafarend. R.S. Mather & P.V. Angus-Leppan on the following topics:- Mathematical geodesy, Coastal geodesy and Refraction, Unisurv G 21, 100 pp.

G22. Papers by R.S. Mather, J.R. Gilliland, F.K. Brunner, J.C. Trinder, K. Bretreger & G. Halsey on the following topics:- Gravity, Levelling, Refraction, ERTS imagery, Tidal effects on satellite orbits and Photogrammetry, Unisurv G 22, 96 pp.

G23. Papers by R.S. Mather, E.G. Anderson, C. Rizos, K. Bretreger, K. Leppert, B.V. Hamon & P.V. Angus-Leppan on the following topics:- Earth tides, Sea surface topography, Atmospheric effects in physical geodesy, Mean sea level and Systematic errors in levelling, Unisurv G 23, 96 pp.

G24. Papers by R.C. Patterson, R.S. Mather, R. Coleman, O.L. Colombo, J.C. Trinder, S.U. Nasca, T.L. Duyet & K. Bretreger on the following topics:- Adjustment theory, Sea surface topography determinations, Applications of LANDSAT imagery, Ocean loading of Earth tides, Physical geodesy, Photogrammetry and Oceanographic applications of satellites, Unisurv G 24,151pp.

G25. Papers by S.M. Nakiboglu, B. Ducarme, P. Melchior, R.S. Mather, B.C. Barlow, C. Rizos, B. Hirsch, K. Bretreger, F.K. Brunner & P.V. Angus-Leppan on the following topics:- Hydrostatic equilibrium figures of the Earth, Earth tides, Gravity anomaly data banks for Australia, Recovery of tidal signals from satellite altimetry, Meteorological parameters for modelling terrestrial refraction and Crustal motion studies in Australia, Unisurv G 25,124pp.

G26. Papers by R.S. Mather, E.G. Masters, R. Coleman, C. Rizos, B. Hirsch, C.S. Fraser, F.K. Brunner, P.V. Angus-Leppan, A.J. McCarthy & C. Wardrop on the following topics:- Four-dimensional geodesy, GEOS-3 altimetry data analysis, Analysis of meteorological measurements for microwave EDM and Meteorological data logging system for geodetic refraction research, Unisurv G 26, 113 pp.

G27. Papers by F.K. Brunner, C.S. Fraser, S.U. Nasca, J.C. Trinder, L. Berlin, R.S. Mather, O.L. Colombo & P.V. Angus-Leppan on the following topics:- Micrometeorology in geodetic refraction, LANDSAT imagery in topographic mapping, Adjustment of large systems, GEOS-3 data analysis, Kernel functions and EDM reductions over sea, Unisurv G 27, 101 pp.

G28. Papers by S.M. Nakiboglu, H.L. Mitchell, K. Bretreger, T.A. Herring, J.M. Rueger, K.R. Bullock, R.S. Mather, B.C. Forster, I.P. Williamson & T.S. Morrison on the following topics:- Variations in gravity, Oceanographic and geodetic levelling, Ocean loading effects on Earth tides, Deflections of the vertical, Frequencies of EDM instruments, Land information systems, Sea surface topography, Accuracy of Aerial Triangulation and Questionnaire to Surveyors, Unisurv G 28, 124 pp.

G29. Papers by F.L. Clarke, R.S. Mather, D.R. Larden & J.R. Gilliland on the following topics:- Three dimensional network adjustment incorporating ξ, η and N, Geoid determinations with satellite altimetry, Geodynamic information from secular gravity changes and Height and free-air anomaly correlation, Unisurv G 29, 87 pp.

From June 1979 Unisurv G's name was changed to Australian Journal of Geodesy, Photogrammetry and Surveying (Aust.J.Geod.Photo.Surv.).

Australian Journal of Geodesy, Photogrammetry and Surveying

Price (surface mail postage inclusive): Individuals $7.00
Institutions $10.00

J30. Aust.J.Geod.Photo.Surv. No. 30, (June, 1979), 127 pp.:
Bretreger, "Ocean tide models from GEOS-3 altimetry";
Trinder & Smith, "Rectification of LANDSAT data";
Nakiboglu & Lim, "Numerical test of initial value method";
Herring, "The accuracy of deflections of vertical";
Angus-Leppan, "Radiation effects on temperature of metal tape";
Covell, "Errors of short range distance meters", and
Nasca, "Contour lines in engineering".

J32. Aust.J.Geod.Photo.Surv. No. 32, (June, 1980), 121 pp.:
van Gysen, "Gravimetric deflections of the vertical",
Fraser, "Self calibration of non-metric camera",
Rizos, "Ocean circulation from SST studies",
Trinder, "Film granularity and visual performance".

J33. Aust.J.Geod.Photo.Surv. No. 33, (December, 1980), 85 pp.:
Burford, "Controlling geodetic networks";
Masters & Stolz, "Crustal motion from LAGEOS";
Fraser, "Variance analysis of adjustments", and
Brunner et al., "Incremental strain near Palmdale".

J34. Aust.J.Geod.Photo.Surv. No. 34, (June, 1981) 94, pp.:
Welsch, "Variances of geodetic observations";
Gilliland, "Outer zones effects on geoid", and
Khalid, "Models of vertical refraction".

J35. Aust.J.Geod.Photo.Surv. No. 35 (December, 1981), 106pp.:
Kahar, "Geoid in Indonesia";
Morgan, "Crustal motion in Papua New Guinea";
Masters et al, "LAGEOS range filter";
Stolz et al, "Baseline values from LAGEOS", and
Bishop, "Digital elevation models".

J36. Aust.J.Geod.Photo.Surv. No. 36 (June, 1982), 97pp.:
Nakiboglu and Torenberg, "Earth's gravity and surface loading";
Nakiboglu, "Changes in sea level and gravity";
Villanueva, "Geodetic boundary value problem";
Stolz and Harvey, "Australian geodetic VLBI experiment";
Gilliland, "Free-air geoid for South Australia";
Allman, "Geoid for S.E. Asia and S.W. Pacific", and
Angus-Leppan, "Gravity measurements in levelling".

J37. Aust.J.Geod.Photo.Surv. No. 37 (December, 1982), 113pp.:
Niemeier, Teskey, & Lyall, "Monitoring movement in open pit mines";
Banger, "Refraction in levelling";
Angus-Leppan,"GPS - prospects for geodesy", and
Zwart, "Costs of integrated surveys".

J38. Aust.J.Geod.Photo.Surv. No. 38 (June, 1983), 93pp.:
Forster, "Radiometric registration of LANDSAT images";
Fryer, "Photogrammetry through shallow water";
Harvey, Stolz, Jauncey, Niell, Morabito and Preston,
"Australian geodetic VLBI experiment";
Gilliland, "Geoid comparisons in South Australia", and
Kearsley, "30' mean gravity anomalies from altimetry".

J39. Aust.J.Geod.Photo.Surv. No. 39 (December 1983):
Coleman & Lambeck, "Crustal motion in South Eastern Australia - is there any evidence for it?";
Salih, "The shape of the geoid in The Sudan";
Rueger, "The reduction of mekometer measurements", and
Angus-Leppan, "Preliminary study for a new levelling system".

Unisurv Reports - S Series

S8-S15 Price (excluding postage): $5.00
S16 onwards Price (including surface mail postage): Individuals $18.00
Institutions $25.00

S8. A. Stolz, "Three-D Cartesian co-ordinates of part of the Australian geodetic network by the use of local astronomic vector systems", Unisurv Rep. S 8, 182 pp.

S9. H.L. Mitchell, "Relations between MSL & geodetic levelling in Australia", Unisurv Rep. S 9, 264 pp.

S10. A.J. Robinson, "Study of zero error & ground swing of the model MRA101 tellurometer", Unisurv Rep. S 10, 200 pp.

S12. G.J.F. Holden, "An evaluation of orthophotography in an integrated mapping system", Unisurv Rep. S 12, 232 pp.

S14. E.G. Anderson, "The Effect of Topography on Solutions of Stokes' Problem", Unisurv Rep. S 14, 252 pp.

S15. A.H.W. Kearsley, "The Computation of Deflections of the Vertical from Gravity Anomalies", Unisurv Rep. S 15, 181 pp.

S16. K. Bretreger, "Earth Tide Effects on Geodetic Observations", Unisurv S 16, 173 pp.

S17. C. Rizos, "The role of the gravity field in sea surface topography studies", Unisurv S 17, 299 pp.

S18. B.C. Forster, "Some measures of urban residual quality from LANDSAT multi-spectral data", Unisurv S 18, 223 pp.

S19. Richard Coleman, "A Geodetic Basis for recovering Ocean Dynamic Information from Satellite Altimetry", Unisurv S 19, 332 pp.

S20. Douglas R. Larden, "Monitoring the Earth's Rotation by Lunar Laser Ranging", Unisurv Report S 20, 280 pp.

S21. R. Patterson, "Approximation and Statistical Methods in Physical Geodesy", Unisurv Report S 21, 179 pp.

S22. J.M. Rueger, "Quartz Crystal Oscillators and their Effects on the Scale Stability and Standardization of Electronic Distance Meters", Unisurv Report S 22, 151 pp.

S23. I.P. Williamson, "A Modern Cadastre for New South Wales", Unisurv Report S 23, 250 pp.

S24. K.R. Bullock, "Design Principles for Land Information Systems", Unisurv Report S 24, 307 pp.

S25. E.G. Masters, "Applications of Satellite Geodesy to Geodynamics", Unisurv Report S25, 208 pp.

Proceedings

P.V. Angus-Leppan (Editor), "Proceedings of conference on refraction effects in geodesy & electronic distance measurement", 264 pp.
Price: $4.00*

R.S. Mather & P.V. Angus-Leppan (Eds), "Australian Academy of Science/International Association of Geodesy Symposium on Earth's Gravitational Field & Secular Variations in Position", 740 pp.
Price: $10.00*

I.P. Williamson (Editor), "Proceedings of Seminar on Land Information Systems for State and Local Government", 247 pp.
Price: $20.00*

Monographs

1. R.S. Mather, "The theory and geodetic use of some common projections", (2nd edition), 125 pp. Price: $ 6.00*

2. R.S. Mather, "The analysis of the earth's gravity field", 172 pp.
Price: $ 2.50*

3. G.G. Bennett, "Tables for prediction of daylight stars", 24 pp.
Price: $ 0.50*

4. G.G. Bennett, J.G. Freislich & M. Maughan, "Star prediction tables for the fixing of position", 200 pp. Price: $ 3.00*

5. M. Maughan, "Survey computations", 98 pp. Price: $ 5.00*

6. M. Maughan, "Adjustment of Observations by Least Squares", 61 pp.
Price: $ 4.00*

7. J.M. Rueger, "Introduction to Electronic Distance Measurement", (2nd Edition), 140 pp. Price: $ 10.00*

8. A.H.W. Kearsley, "Geodetic Surveying", 77pp. Price: $ 5.00*

*Note: Prices do not include postage.

OTHER PRICES for 1984 (Surface Mail Postage Inclusive)

1. Aust.J.Geod.Photo.Surv. (formerly Unisurv G), 2 issues annually of approximately 100 pages each issue.

   To Institutions $20 ; To Individuals $14

2. Special Series (Unisurv S)
   Research reports of 200 to 300 pages, published annually (on average).

   To Institutions $25 per copy ; To Individuals $18 per copy

To order, write to Publications Officer, School of Surveying, U.N.S.W.

Publications No Longer Available

G1. G.G. Bennett, "The discrimination of radio time signals in Australia", Uniciv Rep. D1, 88 pp.

G2. J.S. Allman, "A comparator for the accurate measurement of differential barometric pressure", Uniciv Rep. D3, 9 pp.

G4. R.S. Mather, "The extension of the gravity field in South Australia", Uniciv Rep. R-19, 26 pp.

G5. P.V. Angus-Leppan (Editor), "Control for mapping". (Proceedings of Conference, May 1967), Unisurv Rep. 7, 329 pp.

G6. G.G. Bennett & J.G. Freislich, "The teaching of field astronomy", Unisurv Rep. 8, 30 pp.

G7. J.C. Trinder, "Photogrammetric pointing accuracy as a function of properties of the visual image", Unisurv Rep. 9, 64 pp.

G8. P.V. Angus-Leppan, "An experimental determination of refraction over an icefield", Unisurv Rep. 10, 23 pp.

G9. R.S. Mather, "The non-regularised geoid and its relation to the telluroid and regularised geoids", Unisurv Rep. 11, 49 pp.

G10. G.G. Bennett, "The least squares adjustment of gyro-theodolite observations", Unisurv Rep. 12, 53 pp.

G11. R.S. Mather, "The free air geoid for Australia from gravity data available in 1968", Unisurv Rep. 13, 38 pp.

G12. R.S. Mather, "Verification of geoidal solutions by the adjustment of control networks using geocentric Cartesian co-ordinate systems", Unisurv Rep. 14, 42 pp.

G13. G.G. Bennett, "New methods of observation with the Wild GAKI gyro-theodolite", Unisurv Rep. 15, 68 pp.

J31. Aust.J.Geod.Photo.Surv. No. 31 (December, 1979), 177 pp.
(contribution to the XVII General Meeting of the IUGG, Canberra, 3-15 December, 1979):
Allman et al., "Readjustment of Australian geodetic survey";
Angus-Leppan, "Ratio method and meteorology", and
"Refraction in levelling;
Berlin, "Adjustment of continental networks";
Brunner, "Limiting factor to geodetic precision";
Coleman et al., "Sea surface slope along NE Australia";
Kahar & Kearsley, "Jawa geoid from altimetry and gravity";
Masters et al., "Tide models from GEOS-3 altimetry", and
Mather & Rizos, "Global mean sea level from altimetry".

S1. J.S. Allman, "An analysis of the reliability of barometric elevations", Unisurv Rep. 5, 335 pp.

S2. R.S. Mather, "The free air geoid for South Australia and its relation to the equipotential surfaces of the earth's gravitational field", Unisurv Rep. 6, 491 pp.

S3. G.G. Bennett, "Theoretical and practical study of a gyroscopic attachment for a theodolite", Unisurv Rep. 16, 343 pp.

S4. J.C. Trinder, "Accuracy of a monocular pointing to blurred photogrammetric signals", Unisurv Rep. 17, 231 pp.

S5. J.G. Fryer, "The effect of the geoid on the Australian geodetic network", Unisurv Rep. 20, 221 pp.

S6. G.F. Toft, "The registration and cadastral survey of native-held rural land in the Territory of Papua and New Guinea", Unisurv Rep. 21, 441 pp.

S7. A.H. Campbell, "The dynamics of temperature in surveying steel and invar measuring bands", Unisurv Rep. S 7, 195 pp.

S13. G.J. Hoar, "The analysis, precision and optimization of control surveys", Unisurv Rep. S 13, 200 pp.